Inhibition of nuclear factor kappa beta (NF-kβ) as therapeutic strategy for the treatment of IBD and cancer

A thesis presented to the Ulster University of Northern Ireland for the degree of Doctor of Philosophy in School of Pharmacy and Pharmaceutical Science

Faculty Life and Health Sciences
Ulster University, Coleraine

By

Mohammed Naeem Khan
Master in pharmaceutics
January 2018

Supervisors: Dr Murtaza M. Tambuwala
Professor Paul McCarron
Dr Paul Thompson

Head of School: Professor Paul McCarron

Declaration

I hereby declare that with effect from the date on which this thesis is deposited in the Research Office of the Ulster University, I permit the Librarian of the University to allow the thesis to be copied in whole or in part without reference to me on the understanding that such authority applies to the provision of single copies made for study purposes or for inclusion within the stock of another library. The thesis to be made available through the Ulster Institutional Repository and/or EThOS under the terms of the Ulster eThesis Deposit Agreement which I have signed. IT IS A CONDITION OF USE OF THIS THESIS THAT ANYONE WHO CONSULTS IT MUST RECOGNISE THAT THE COPYRIGHT RESTS WITH THE AUTHOR AND THAT NO QUOTATION FROM THE THESIS AND NO INFORMATION DERIVED FROM IT MAY BE PUBLISHED UNLESS THE SOURCE IS PROPERLY ACKNOWLEDGED.

Publications

Caffeic acid phenethyl ester is protective in experimental ulcerative colitis via reduction in levels of pro-inflammatory mediators and enhancement of epithelial barrier function
KHAN, M. N., LANE, M. E., MCCARRON, P. A. & TAMBUWALA, M. M. 2017. Inflammopharmacology, 20, 017-0364.

Polymeric nano-encapsulation of curcumin enhances its anti-cancer activity in breast (MDA-MB231) and lung (A549) cancer cells. KHAN, M. N., HAGGAG, Y. A., LANE, M. E., MCCARRON, P. A. & TAMBUWALA,M.M.2017
Curr Drug Deliv, 19**,** 1567201814666171019104002.

Manuscript under preparation

Enhanced anticancer potential of PIC loaded albumin nanoparticles in colorectal cancer cell lines KHAN, M. N., LANE, M. E., MCCARRON, P. A. & TAMBUWALA, M. M.

Enhanced anticancer potential of CAPE loaded albumin nanoparticles in colorectal cancer cell lines KHAN, M. N., LANE, M. E., MCCARRON, P. A. & TAMBUWALA, M. M.

Enhanced ant-inflammatory therapetics of PIC and CAPE nanoparticles of albumin in mouse model ulcerative colitis via inhibition of NF-kβ and HIF-1α
KHAN, M. N., LANE, M. E., MCCARRON, P. A. & TAMBUWALA, M. M.

Poster presentation

Abstract in at 37th All Ireland School of Pharmacy Conference "Polymeric Nanoparticle-encapsulation: a solubility enhancement and targeting strategy for Curcumin, March 2015, Belfast, Northern Ireland

Abstract in at 38th All Ireland School of Pharmacy Conference "Polymeric Nanoparticle-encapsulation: a solubility enhancement and targeting strategy for Curcumin, March 2016, Dublin, Ireland

Abstract

Ulcerative colitis and colorectal cancer are progressively spreading in developed and developing countries. However, the current therapeutics does not provide complete cure to these conditions. It has been reported that inflammatory cytokines, overstimulated NF-kβ and overexpressed HIF-1α play pivotal role in inflammation and colorectal cancer. The traditional method of treatment offers not only detrimental effects on health due to non-selectivity but also burdens financially. Additionally, in a chronic condition of ulcerative colitis and colorectal cancer patients undergo bowel surgery which makes the life difficult to live. Therefore, there is pressing need to utilize natural therapeutic compounds to treat ulcerative colitis and colorectal cancer. These natural compounds possess potent inhibition potential against inflammatory cytokines, NF-kβ and HIF-1α. These compounds treat the inflammatory condition and colorectal cancer with minimum or no side effects as documented in clinical trials. However, these natural compounds have limited solubility in aqueous media due to which therapeutic potential of natural compounds are compromised. Therefore, nanotechnology can be employed to overcome the solubility issue of these natural compounds.

In the current work, we have formulated nanoparticles of low soluble natural anti-inflammatory and anticancer agents such as curcumin, piceatannol and Caffeic acid phenethyl ester. Characterization and optimization have been performed to obtain suitable formation for the *in vitro* and *in vivo* experiment. Morphological studies were carried out by scanning electron microscopy. Significant increase in solubility has been confirmed in nanoparticles form. Cellular localization has been observed under phase contrast microscopy in MDA-MB-231, A549, HT-29 and CaCo-2 cells. Nanoparticles treated colon cancer cells has depicted the higher degree of

cytotoxicity, lower migration, less colony formation and decrease level of invasion than free drug in cancer cell lines. Nanoparticles treated cells have demonstrated low expression of inflammatory cytokines such as INF-γ, IL-6, IL-1β, TNF-α, and IL-10 in cancer cell lines. Stabilisation of nuclear proteins p65 and HIF-1α has been demonstrated significantly more in nanoparticles treated in lung cancer, breast cancer and colon cancer cell lines. The anti-inflammatory activity of these nanoparticles has been tested in mouse model of ulcerative colitis and it has been found that nanoparticles have higher therapeutic potential in inflammation than free drug.

Acknowledgements

I would like to appreciate and thanks for the constant support and guidance of my supervisors, Dr. Murtaza M. Tambuwala, Professor Paul McCarron and Professor Paul Thomson for their valuable advice and continuous support throughout my project. Also, I would like to thank staff members of the School of Pharmacy and Pharmaceutical Sciences, Ulster University, particularly Dr. Sukanta Kamila and Dr. Doherty, Bernadette. I would also like to thank my colleagues for their support, particularly Dr. Ankur Sharma, Dr. Dawood Khan, Dr. Annie Hasib, Dr. Sayed, Dr. Vidya and Luke Spears. Lastly, I would like to thank my parents, brothers and my wife for supporting me in every way throughout my Ph.D.

Abbreviations

IBD	inflammatory bowel disease
CD	crohn`s disease
UC	ulcerative colitis
NF-kβ	nuclear factor kappa beta
HIF	Hypoxia inducible factor
IL	interleukins
IFN	interferons
TNF	tumor necrosis factor
DSS	Dextran sodium sulphate
TNBS	Trinitrobenzenesulphonic acid
H & E	hematoxylin & eosin
MPS	mononuclear phagocytic system
NEMO	NF-kappa-B essential modulator
STAT	signal transducer and activator of transcription proteins
DNA	deoxyribonucleic acid
DMOG	dimethyloxalylglycine, n-(methoxyoxoacetyl)-glycine methyl ester
EPR	enhanced permeability and retention
MW	molecular weight
HPLC	high-performance liquid chromatography
$CHCL_3$	chloroform
KCl	potassium chloride
DAPI	4',6-diamidino-2-phenylindole
MTT	dimethylthiazol
FITC	fluorescein isothiocyanate
DAI	disease activity index
FIT	faecal immunochemical test
FDA	food and drug administration
NP	nanoparticles
cur	curcumin
CAPE	caffeic acid phenethyl ester
PIC	piceatannol
BSA	bovine serum album

mg	milligram
pg	picogram
µg	microgram
nm	nanometer
mV	millivolt
PDI	polydispersity index
ZP	zeta potential
SEM	standard error mean
EE	entrapment efficiency
PLGA	poly(lactic-co-glycolic) acid PLGA-PEG Poly(lactic-co-glycolic) acid- co poly (ethylene glycol)
PLA	polylactic acid
F	formulation
µl	microliter
PVA	poly (vinyl alcohol)
PBS	phosphate buffered saline
SEM	scanning electron microscopy
w/w	weight/weight
w/v	weight/volume
W	watt
DLS	dynamic light scattering
DMSO	dimethyl sulfoxide
DMEM	Dulbecco Modified Eagle Media
FBS	foetal bovine serum
CO_2	carbon dioxide
NMR	nuclear magnetic resonance
TMS	tetramethylsilane
UV	ultra violet
kDa	kilodalton
RPM	Revolution per minute

Contents Page no.

Chapter 1

Introduction

1.1 Inflammatory bowel disease

Inflammatory bowel disease (IBD) is an idiopathic disorder categorised chiefly as Crohn`s disease (CD) and ulcerative colitis (UC) (Xavier and Podolsky, 2007a., de Souza and Fiocchi, 2016). The characterization of IBD depends upon the location, depth and severity of the intestinal mucosa (Abraham and Cho, 2009). CD is linked with the small intestine and has complications such as stomach cramp, fever, diarrhoea, irregular ulceration strictures, abscesses and fistulas (Laass et al., 2014., de Souza and Fiocchi, 2016). UC is restricted to the large intestine. It instigates from the rectum and propagates to the superficial layer of bowel with inflammation, cryptitis and crypt abscesses (Neurath, 2014b., Pekow, 2015). CD and UC have common symptoms such as rectal bleeding, diarrhoea, abdominal pain, weight loss, fatigue and fever. Generally, both disorders exert long lasting and reverting inflammation (Strober et al., 2007). Although the main cause of IBD is still unclear, factors such as mucosal dysfunction, aberrant activation of NF-kβ, compromised immune system, environmental and genes have been linked to its pathogenesis (Fiocchi, 1998) (Danese et al., 2004., Zhang and Li, 2014). It has been documented that the alteration in the mucosa of the intestine is responsible for CD and UC (McCole, 2014., Dulai et al., 2015).

IBD has affected millions of people in the United States, Europe; and Asian countries (Engel and Neurath, 2010). The chronic nature of IBD involves a period of alternating remission thereby making it difficult for clinical investigation of active disease Current treatments used in IBD, such as immunomodulator, corticosteroids and antibiotics do not provide a permanent cure but instead produce side effects due to the non-selectivity and long-term exposure (Moura et al., 2015). Approximately 30-40% of patients need to undergo surgical removal of inflamed tissue in majority

of cases (Ferrari et al., 2016b) which is not only expensive but inconvenient to patients. Moreover, ulcerative colitis patients are prone to develop colorectal cancer in later stages (Kim and Chang, 2014). The current strategy for management of ulcerative colitis and colorectal cancer depends on suppressing inflammation but associated with no complete cure. The primary focus of the work in this thesis is to understand the disease mechanism of UC and associated colorectal cancer with the aim of developing novel therapeutics.

1.2 Ulcerative colitis

UC is an inflammatory condition of the colon and rectum, which damages the superficial layers of mucosa by forming granulomatous patches (Lunney and Leong, 2012). UC leads to weight loss, stomach ache, diarrhoea, blood in stool, loss of appetite, and fatigue (Conrad et al., 2014). In North America and Europe it is reported that 250 out of 10000 people suffer from UC (Danese and Fiocchi, 2011., Molodecky et al., 2012). In severe inflammatory conditions, patients undergo entire colon removal (Kornbluth and Sachar, 2010). It has been postulated that UC triggers an alteration in the mucosal layers and damages superficial mucosal protective layer (Qin, 2013) as presented in the Figure 1.1. Froslie and colleagues postulated that mucosal repair could present a potential cure for UC (Frøslie et al., 2007).

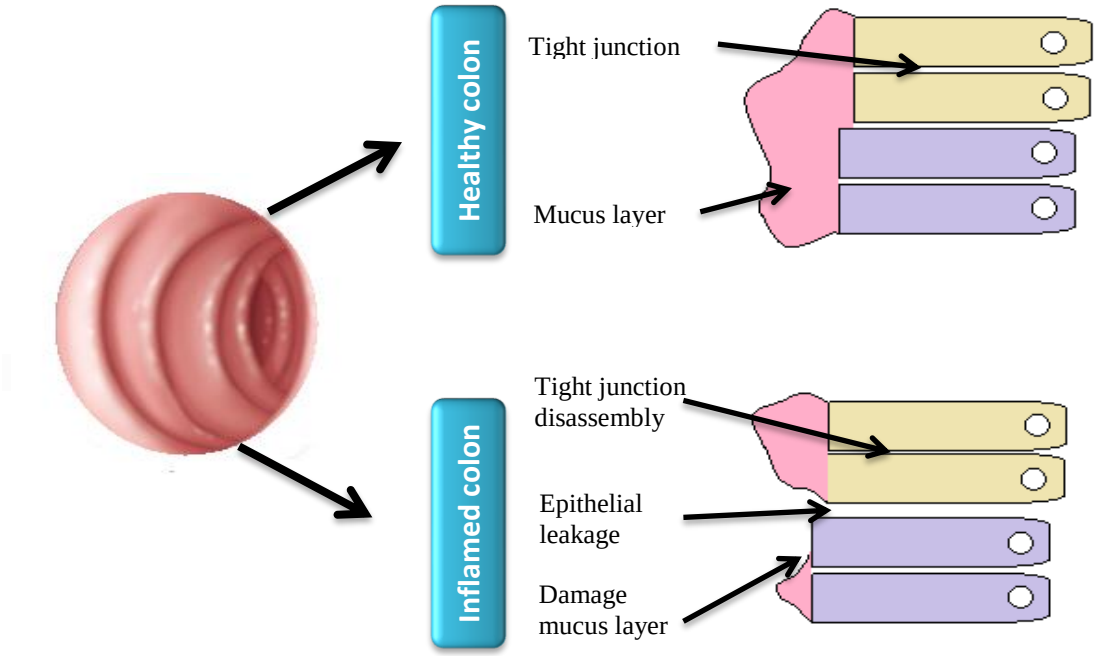

Figure 1.1: Representative diagram of healthy and inflamed colon. Tight junctions and the mucus layer are fully intact in healthy tissue, whereas in the inflamed colon this arrangement of tight junctions is disrupted giving rise to epithelial leakage and loss of the mucus layer.

1.3 Colorectal cancer

The prolonged inflammation of gastrointestinal tract results in colorectal cancer (Rubin et al., 2012). Colorectal cancer is a major health issue causing high mortality rates in cancer patients. It is the third most commonly diagnosed cancer and third leading cause of cancer death in the United States of America (Tariq and Ghias, 2016). Clinical investigations demonstrate that 110 out of 55000 UC patients develop colorectal cancer in 10 years and this trend increases to 440 and 990 after 20 and 30 years, respectively (Triantafillidis et al., 2009). The contribution of UC patients towards colorectal cancer is higher than CD patients (Grivennikov, 2013). The probability of developing colorectal cancer in Crohn's disease depends upon the stage of inflammation (Mellemkjaer et al., 2000). Ulcerative colitis patients are more prone to develop colon cancer which increases mortality rate in colorectal cancer patients (Bergmann et al., 2017., Abdalla et al., 2017). The event of colorectal cancer

will be higher in future, which will increase the death rate in patients (Kim and Chang, 2014). Sometimes the treatment used to cure IBD such as 5-aminosalicylic acid, azathioprine, sulfasalazine and 6-mercaptopurines produce adverse effect and worsen the condition. It also produces side effects such as organ depletion, hepatoxicity, bone marrow depletion and infertility (Connell et al., 1994., Dubinsky et al., 2000).

Millions of people suffer from IBD and colorectal cancer in United States. It has been stated that IBD and colorectal cancer are interrelated diseases because prolong IBD conditions results in colorectal cancer (Kimura et al., 2000., Triantafillidis et al., 2009). IBD and colorectal cancer are not only confined to these countries but is also spreading to Asian and Gulf countries (Kaplan, 2015). It hampers the quality of life of patients because they have to face the burden of long term treatment in term of hospitalization and surgery (Ananthakrishnan, 2015). The factors which govern IBD include genetic factors, environmental factors and alteration in mucosal barrier functions (Ponder and Long, 2013., Zhang and Li, 2014., Castaño-Rodríguez et al., 2015). However, the damaged intestinal mucosal layer promotes IBD and colorectal cancer with different stage of tumour development as shown in the Figure 1.2 (Wlodarska et al., 2015., Zeng et al., 2017). It has been estimated that occurrences of colorectal cancer may increases in future due to increase in IBD disease (Kim and Chang, 2014). The chronic inflammatory condition alters the microbes of the mucosal layer and results in colon cancer (Oke and Martin, 2017).

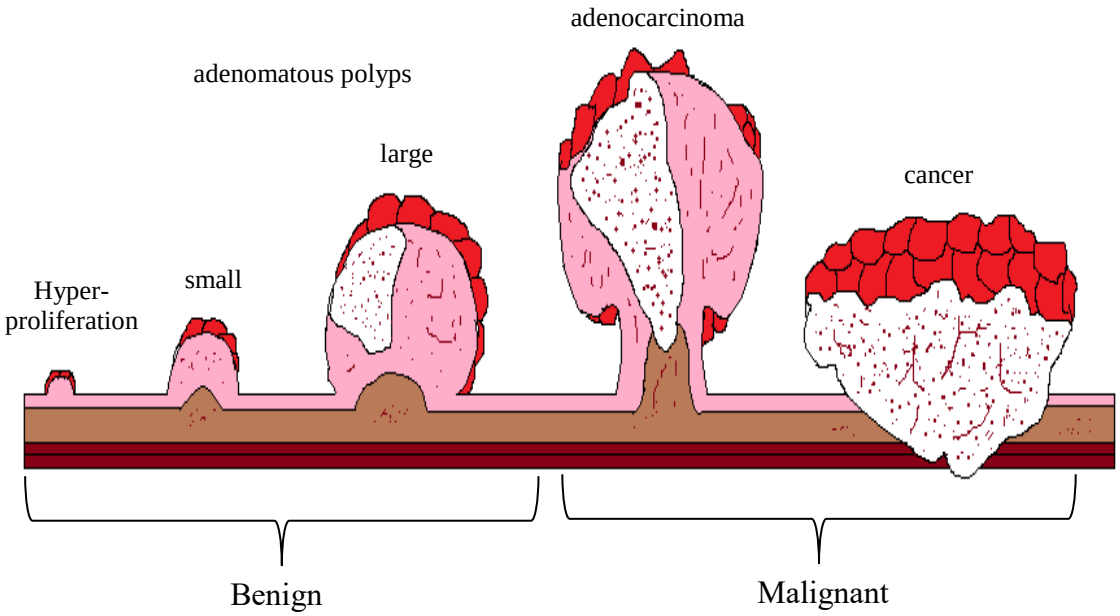

Figure 1.2: Representation of different stage of cancer development. It starts from the formation of harmless polyps to adenomatous polyps and later turns to malignant cancer.

1.4 Pathogenesis of ulcerative colitis and colorectal cancer

Colorectal cancer and ulcerative colitis share common factors, such as condition age, family history, hygiene, diet, cigarette smoking and obesity, which contributes to disease induction (Haggar and Boushey, 2009., Scarpa et al., 2014b). It has been scripted that factor such as compromised immune response, oxidative stress, hereditary and damage to intestinal mucosa are the key regulators of colorectal cancer and ulcerative colitis (Kim and Chang, 2014., Kim et al., 2017). However, mucosal damage plays pivotal role in the prognosis of colorectal cancer and ulcerative colitis (Tanaka et al., 2006., Meira et al., 2008). In both condition alteration and abscess have been documented to disrupt the mucosal barrier of intestine (Rogler, 2014., Rafa et al., 2017). This mucosal damage is a result of increased expression of pro-inflammatory cytokines such as TNF-α, interferons, interleukins and DNA damaging agents etc. in ulcerative colitis patients (Hassanzadeh, 2011., Klampfer, 2011., Műzes et al., 2012., Scarpa et al., 2014a.,

Francescone et al., 2015., Sreedhar et al., 2016). These over-triggered agents result into aberrant activation of nuclear factor kappa beta (NF-kβ) and HIF-1α which play the main role in maintaining the homeostasis of the mucosal layer (Pal et al., 2014., Manzat-Saplacan et al., 2015., Serra et al., 2017). Therefore, inhibition of overactivated pro-inflammatory cytokines may control the level of NF-kβ and HIF-1α and provide a therapeutic cure to colorectal cancer and ulcerative colitis.

1.5 Diagnosis of ulcerative colitis and colorectal cancer

Early detection of ulcerative colitis and colorectal cancer is the key for their control and prevention. Diagnostic tools such as information of patient's history and visual observation help in detecting the disease condition as mentioned in the table 1.1. In mild to moderate inflammatory condition, clinical investigation of body fluid and blood components is recommended. Sometime microbiological test of stool is also necessary to find out the strain of bacteria responsible for inflammation. The extent of colitis is also determined by microscopic imaging method.

Table 1.1 Modes of clinical diagnosis (Taghipour et al., 2016)

Sr. No.	Methods of diagnosis	Examples
1	**History**	Age of onset, Type of stool, lifestyle, previous bowel infection and medication, smoking.
2	**Visual observation**	Pulse, BP, temperature, weight, height, BMI, abdominal pain, rectal inspection, examination of eyes, skin, joints and muscles
3	**Clinical investigation**	Electrolytes, urea, creatinine, complete blood count, ESR, liver enzymes, bilirubin, alkaline phosphatase, transferrin, ferritin, vitamin B12, B folic acid, CRP, urinalysis
4	**Faecal investigation**	Stool testing for bacterial organisms
5	**Microscopic observation**	Endoscopy and colonoscopy
6	**Imaging**	Ultrasound and MRI

1.6 Inflammation and colorectal cancer therapeutics

Researchers are targeting receptors in colorectal cancer treatment, such as vascular endothelial growth factor, epidermal growth factor receptor and receptor tyrosine kinase (Moriarity et al., 2016). Monoclonal antibodies are approved by FDA to treat colorectal cancer such as Bevacizumab, Cetuximab, Trastuzumab, Panitumumab and Ramucirumab (Pileri et al., 2016). Some monoclonal antibodies are also prescribed in combination for the treatment of colorectal cancer at chronic stages of disease (Samant and Shevde, 2011). Recently, angiogenesis inhibitors have been suggested in the treatment of inflammation and colorectal cancer. These inhibitors are found in the human body, natural agents and synthetic compound etc. (Khan et al., 2017b). Proteasome inhibitors are another category of the anticancer agent used in

inflammation and colorectal cancer treatment which stimulate apoptosis and prevent overactivation of NF-kβ and HIF-1α (Hochwald et al., 2003).

1.7 Side effects of treatments prescribed in ulcerative colitis

Table 1.2, summarises the side effects due to longterm exposure and drug interaction of commonly prescribed ulcerative colitis drugs (Carter et al., 2004). These therapeutic require multiple longterm exposure which disturbs normal lifestyle. Ulcerative colitis patients fail to stick to these treatment because of the negative consequence of the therapeutics, which increases the possibility of disease remission, colon cancer and lead to colon surgery (Kane, 2006).

Table 1.2: Different treatment of ulcerative colitis with side effects

Treatment	Side effects	Reference
5-aminosalicylic acid	Headache, epigastric pain, diarrhoea, idiosyncratic reactions, Renal impairment	(Loftus et al., 2004., Van Staa et al., 2004)
Corticosteroids	mood disturbance, dyspepsia, glucose intolerance, posterior sub-capsular cataracts, osteoporosis, osteonecrosis of the femoral head, myopathy, and susceptibility to infection, adrenal insufficiency, myalgia, malaise, and arthralgia, raised intracranial pressure	
methotrexate	nausea, vomiting, diarrhoea, stomatitis, hepatotoxicity, and pneumonitis	(Te et al., 2000., Fraser, 2003),
Cyclosporine	tremor, paraesthesia, malaise, headache, abnormal liver function, gingival hyperplasia, and hirsutism, renal impairment, infections, and neurotoxicity	(D'Haens et al., 2001., Van Assche et al., 2003)
Infliximab	joint pain and stiffness, fever, myalgia, and malaise	(Ljung et al., 2004., Colombel et al., 2004)

1.8 Side effect of treatment prescribed in colorectal cancer

Conventional therapeutics fail to provide a cure for colorectal cancer because of non-selectivity, overdose due to frequent and combination therapy and systemic toxicity (Kemp et al., 2016). They also have serious side effects, such as nausea, vomiting, loss of appetite, decreased immunity, oral ulcers, sleep disorder, tiredness, depression, anxiety, infertility, bone marrow depletion, impairment of neuron and renal function (Denlinger and Barsevick, 2009). Compounds, like monoclonal antibodies have efficient therapeutic potential in colon cancer. Although they have adverse effects on patients such as papulopustular rash, mucosal toxicity, electrolyte

imbalances (notably hypomagnesemia), diarrhoea, acne-like rash, nail disorder, infusion reactions and pruritus (Hofheinz et al., 2017b). The angiogenesis inhibitors also exert an adverse effects on colorectal cancer patients such as hypertension, proteinuria, ruptured bowel, bleeding, fatigue, inflammation of mucous membrane and diarrhoea (Aalders et al., 2017). Proteasome inhibitors offer some disadvantages such as therapeutic failure in patients, resistance development for long term use, and induction of neuropathy (Dou and Zonder, 2014).

1.9 Disease models of ulcerative colitis

The preclinical animal studies play a pivotal role in providing preliminary data in drug discovery. They also help in finding factors responsible for the etiology or target particular factor involve in clinical disease (Low et al., 2013). Animal model of inflammatory bowel disease is already documented as given in the table 1.3 and have been used to detect novel sites for disease cure. It also use to evaluate the efficacy of different compounds (Maxwell et al., 2009). There are different method available to induce inflammatory condition which mimics either UC or CD such as gene knockout mice, transgenic mouse, spontaneous colitis model, induce colitis model and adoptive transfer model (Mizoguchi, 2012). However, it has been documented that the above models do not completely resemble human ulcerative colitis (Jurjus et al., 2004). However, chemically (dextran sodium sulphate) induce model of ulcerative colitis mimic the human ulcerative colitis more prominently (Maxwell et al., 2009., Low et al., 2013., Kiesler et al., 2015., Taghipour et al., 2016).

Dextran sodium sulfate (DSS) is a widely used chemical to mimic human UC with more common features of inflammation than any other methods (Okayasu et al., 1990). Additionally, DSS is readily available, cost effective and easy to induce inflammation as it can be orally administered through drinking water. Also, Dieleman and colleagues demonstrated the redevelopment of the colon after stopping DSS administration in few weeks periods (Dieleman et al., 1998). It alters mucosal layer of colon epithelium and uncovers submucosa and lamina propria to luminal antigens and mucosal bacteria as shown in Figure 1.3 (Yan et al., 2009). This alteration induces inflammation due increased expression of inflammatory markers (Hakansson et al., 2015). The injured epithelial layer produces similar symptoms of UC colitis, such as loss of weight, diarrhoea, bleeding, blood in faeces, abdominal pain, shortening of colon length, cryptic abscess and epithelial distortion (Randhawa et al., 2014). The acute and chronic inflammation depends on the dose of DSS, molecular weight of DSS, time period of DSS administration, strain and sex of animal use to induce inflammation (Okayasu et al., 1990., Chassaing et al., 2014a). Acute and chronic inflammation can be induced in mice (C57BL\6), hamsters or guinea-pigs upon administration of 1% to 5% DSS in drinking water for 6 to 7 days (Wirtz et al., 2007., Low et al., 2013).

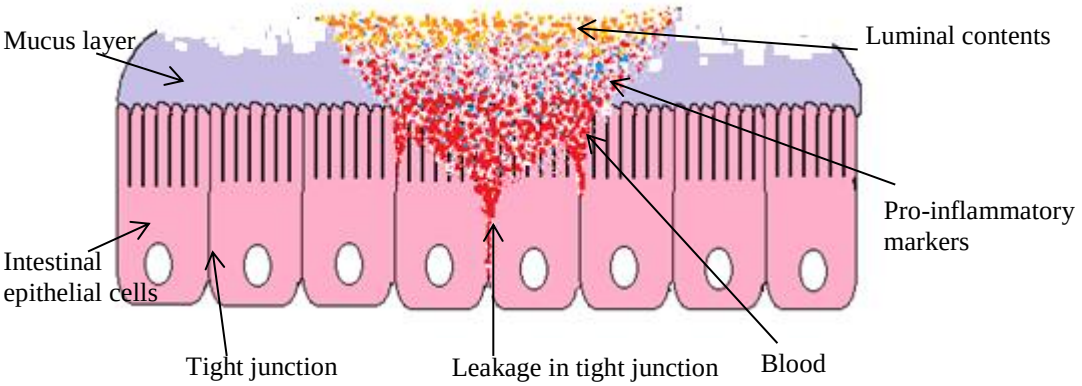

Figure 1.3: Schematic representation of acute colitis. The above image shows faeces (yellow dots) blood clot (red dots) and inflammatory markers (blue dots). This figure also demonstrates leakage in the epithelial layer and altered epithelial layer due administration of DSS in drinking water.

Table 1.3: Animal model of colitis (Low et al., 2013) ((Kanneganti et al., 2011)

Model of colitis	UC	CD
Gene knockout mice	IL-2 knockout mice, T cell receptor (TCR) mutant mice	IL-10 knockout mice, TNF-3, untranslated region (UTR), Trefoil factor receptor mice
Transgenic mouse and rat model	IL-7 transgenic mice, Signal transducer and activating transcription (STAT)-4 transgenic mice, HLA B27 transgenic mice	
Spontaneous colitis model	C3H/HejBir mice	SAMP1/Yit mice
Induce colitis model	Acetic acid induced colitis, TNBS induce colitis, Oxazalone colitis, DSS colitis, Peptidoglycan polysaccharide colitis	Indomethacin induced enterocolitis
Adaptive transfer model	Induction of colitis by heat shock protein, CD45RB transfer model	

1.10 Nuclear factor kappa beta (NF-kβ) in ulcerative colitis and colorectal cancer

Sen and Baltimore discovered NF-kβ in 1986 (Aggarwal, 2004). Dysregulation of NF-kβ is associated with clinical diseases such as cancer, asthma, alzheimers disease, AIDS, atherosclerosis diabetes, arthritis, heart attack, muscle fatigue and viral infections as shown in Figure 1.4 (Gupta et al., 2010b., Shih et al., 2015). Colonic specimens from ulcerative colitis and colorectal cancer patients have been reported to exhibit irregular overexpression of transcription factor nuclear factor kappa beta (NF-kβ) (Ardite et al., 1998., Atreya et al., 2008., Jani et al., 2010., Viennois et al., 2013).

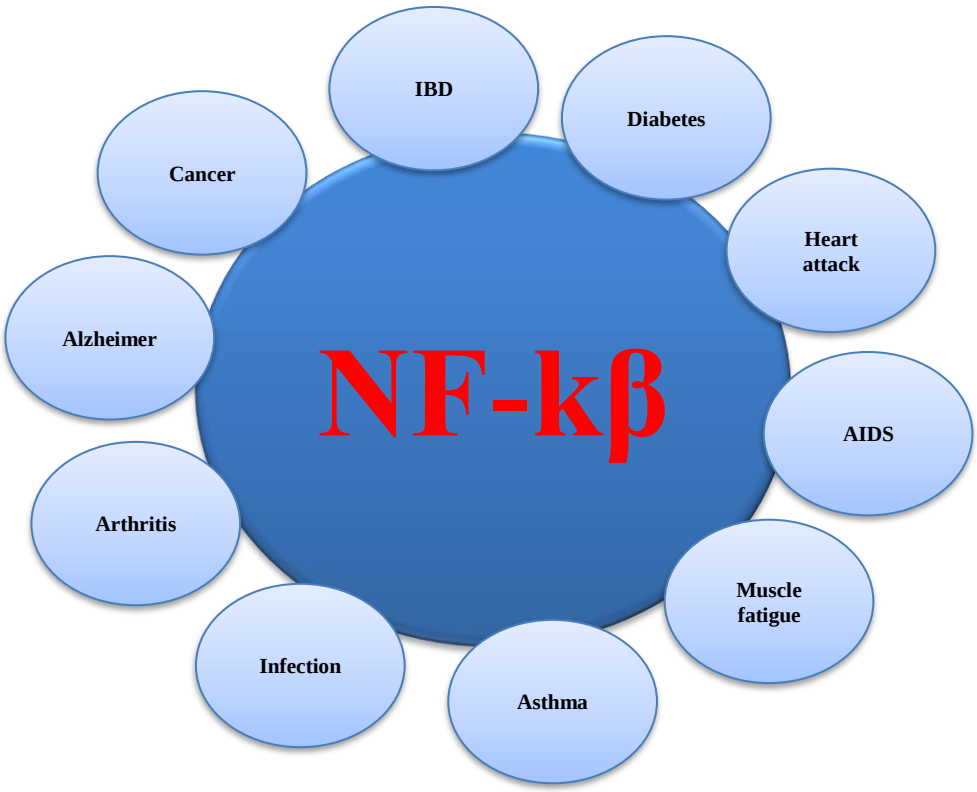

Figure 1.4: Pivotal role of NF-kβ in various disease conditions. The above figure shows that NF-kβ is overexpressed in number of human disease.

NF-kβ is upregulated by factors, such as smoking, free radicals, tumour necrosis factor (TNF-α), interleukin (IL), interferon, and chemokines, DNA damaging agent and bacterial cell wall components and lipopolysaccharide during chronic inflammatory condition as shown in Figure 1.5 (Xavier and Podolsky 2007., Atreya et al., 2008., Viennois et al., 2013., Serasanambati and Chilakapati, 2016).

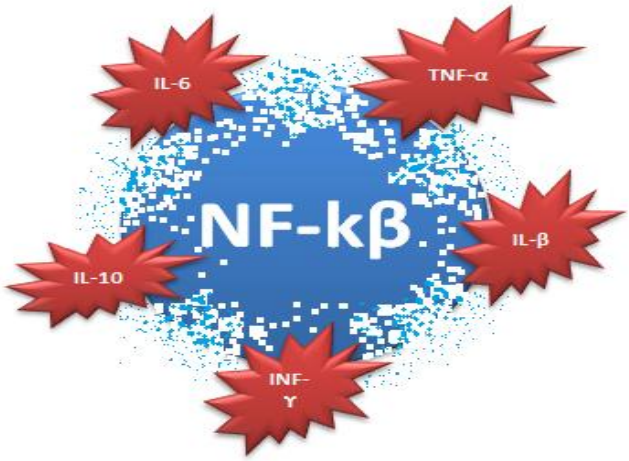

Figure 1.5: Stimulatory action of pro-inflammatory on NF-kβ. The inflammatory markers such as interleukins, interferons and TNF-α phosphorylates inhibitory molecules Ikβ and cause translocation of NF-κβ subunits from cytoplasm to nucleus.

NF-κβ regulates host inflammatory, immune responses and cellular growth properties by increasing the expression of specific cellular genes (Yamamoto and Gaynor, 2001., Baker et al., 2011). NF-kβ plays a vital role in immunity and cell maintenance (Zhang and Sun, 2015). It also contributes in the initiation of inflammation by producing inducible nitric oxide which generates nitric oxide and cyclooxygenase (COX-2) (Zhang and Sun, 2015). Inhibitors of NF-kβ, such as aspirin, 5 amino-salicylic acid, 5-fluorouracil, and oxaliplatin have been prescribed therapeutically in inflammation and cancer. Though side effects and the economic

burden makes these drug less effective (Hassanzadeh, 2011). Therefore, inhibition of NF-kβ is the novel research topic in the treatment of inflammation and cancer.

The NF-kβ is composed of five different protein molecules namely p50, p52, p65, RelB, and c-Rel (Tak and Firestein, 2001., Serasanambati and Chilakapati, 2016). NF-kβ is sequestered in the cytoplasm bound with inhibitory proteins called Ikβ. The inhibitory molecules Ikβ is degraded by inflammatory mediators which cause the nuclear location of NF-kβ as shown in Figure 5. The translocation of NF-kβ into the nucleus is mediated by classical and alternative pathways as shown in Figure 1.6 (Weber et al., 2000., Atreya et al., 2008). It has been found that NF-kβ is overactivated in intestinal mucosa of ulcerative colitis with increased subunits such as p50, p52 and p65 binds to DNA upon Ikβ phosphorylation (Andresen et al., 2005).

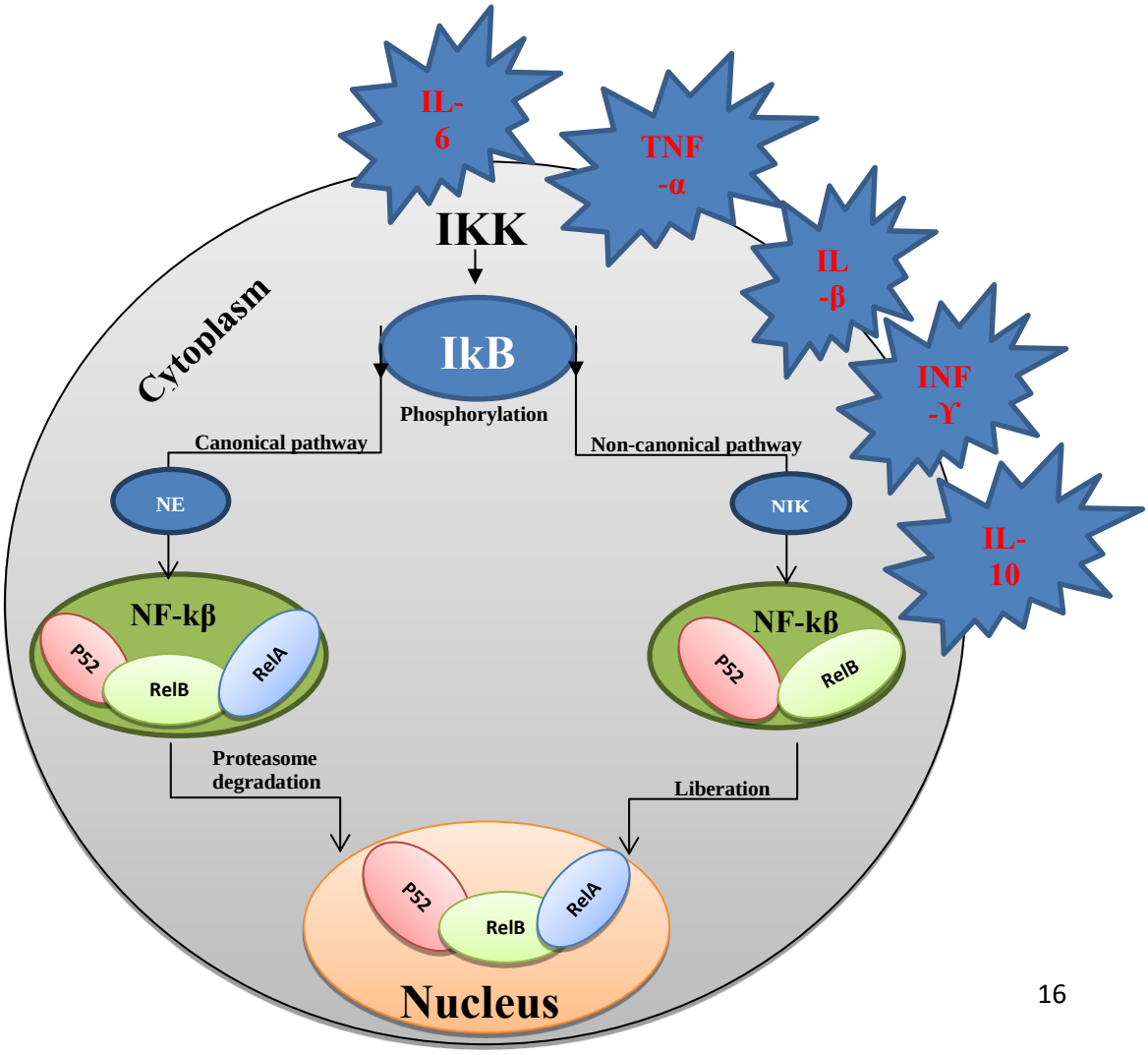

Figure 1.6: The NF-kβ sequestered in the cytoplasm with the inhibitory Ikβ molecule. The inflammatory agents cause translocation of NF-kβ by canonical and noncanonical pathways. In the canonical pathway, the inflammatory stimuli trigger overactivation of core NF-kβ element IKK complex, which causes phosphorylation of Ikβ through ubiquitin binding activity of NEMO. Phosphorylation of Ikβ further leads to proteasome degradation of Ikβ and translocate the molecules of NF-kβ such as p52, RelB and RelA into the nucleus. In non-canonical pathway, the inflammatory agents provoke activation of NF-kβ inducing kinase (NIK) which phosphorylates and activates IKK complex which in turn incite phosphorylation of Ikβ. Phosphorylation of Ikβ results in liberation of p52 and RelB molecules of NF-kβ into the nucleus. After NF-kβ molecules enter into nucleus it increases the expression of genes responsible for immune and inflammatory response ((Kumar et al., 2004., Aggarwal et al., 2004).

1.11 Hypoxia in ulcerative colitis and colorectal cancer

The small intestine was reported to contain 8% of oxygen, with the intestinal lumen containing 2% oxygen. Percentage of oxygen concentration changes based upon on the blood pressure, food intake, disease condition and intestinal cellular structure (Taylor and Colgan, 2007., Fisher et al., 2013). Hypoxia is produced in cells and tissue upon disease induction and is responsible for pathological process in diseases such as intestinal disease, colon cancer, arthritis and heart disease (Semenza, 2012) (Biddlestone et al., 2015a). Therefore, treating the hypoxic condition may provide therapeutics to cure cellular disease.

Colitis and colorectal cancer produced by inflammatory cytokines (Sanchez-Muñoz et al., 2008., Fang et al., 2013) increase the consumption of oxygen at site of inflamed epithelial tissue and leads to hypoxic condition (Colgan and Taylor, 2010., Wilson and Hay, 2011., Campbell et al., 2014).

1.12 Hypoxia inducible factor (HIF) in ulcerative colitis and colorectal cancer

HIF is a transcription factor, which plays a major role in the maintenance of oxygen homeostasis under hypoxic condition. Live cells in the body respond to this hypoxic condition via transcription factor hypoxia inducible factor 1 (HIF-1). HIF-1 consists of two subtypes HIF- 1α (oxygen and cellular hemostasis) and HIF- 1β (Ziello et al., 2007., Zeitouni et al., 2016). It has been reported that HIF exerts protective therapeutic action against chronic inflammation in TNBS induced and HIF-1 knockout mice (Karhausen et al., 2004., Robinson et al., 2008). Mucosal protective effect of HIF-1 has been documented via oxygen-sensing enzymes pan hydroxylate through DMOG (Cummins et al., 2008). However, HIF- 1α also provide oxygen to cancerous cells while its activation in hypoxic condition (Ziello et al., 2007). Induction of HIF-1α has been also reported in the mucosal tissue of inflamed bowel (Giatromanolaki et al., 2003). The HIF- 1α is hydroxylated at Pro 402 and Pro564 by prolyl hydroxylases in the presence of ferrous iron (Fe^{+3}) and catalyzed by 2-oxoglutarate. This hydroxylated HIF-1 α is a target for E3 ubiquitin degradation ligase von Hippel-Lindau (pVHL) which leads to the ubiquitin and proteasome degradation (Kaelin and Ratcliffe, 2008., Shah, 2016). HIF- 1α repair damaged epithelial layer in colitis through energy metabolism via initiation of energy metabolism and cell migration process through apoptosis (Furuta et al., 2001., Synnestvedt et al., 2002., Louis et al., 2005).

1.13 NF-kβ and HIF in ulcerative colitis and colorectal cancer

The inflammatory disease produces hypoxia and inflammation (Biddlestone et al., 2015b). Activation of HIF1-α has been reported in hypoxic condition and activation of NF-κB has been documented in inflammatory condition as illustrated in Figure 1.7 (Bandarra and Rocha, 2013). In another review, HIF-1α and NF-kβ have been postulated as interdependent on each other (Cummins et al., 2006., Culver et al., 2010).

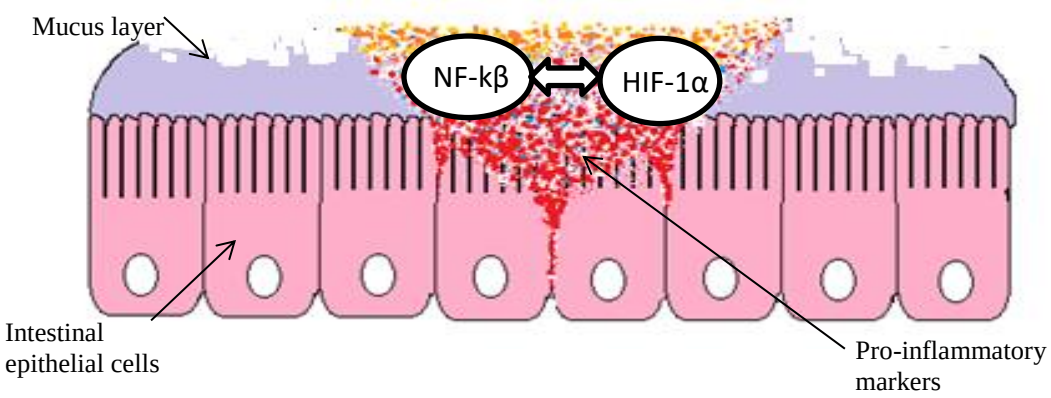

Figure 1.7: Overexpressed NF-kβ and HIF-1α in colonic tissue. The above image shows faeces (yellow dots) blood clot (red dots) and inflammatory markers (blue dots). This figure also demonstrates leakage in the epithelial layer and altered epithelial layer.

1.14 Natural compounds in ulcerative colitis and colorectal cancer

Based on the non specificity, side effects, drug resistance, ineffectiveness, inconvenience and high cost of conventional therapeutics, there is a urgent need of safe, effective and economical chemotherapeutics for inflammation and cancer care (Singh et al., 2017d., Schuster et al., 2017., Grosser et al., 2017). Colorectal cancer and ulcerative colitis treatments with natural compounds is an evolving approach in cancer therapeutics (Debnath et al., 2013., Xiao et al., 2016). Natural constituents have been recommended to possess therapeutic potential against inflammation and

cancer for many years as given in the table 1.4 (Miyata, 2007., Espin et al., 2007). These natural elements retain medicinal values against a number of disease with little or no side effects (Patel et al., 2010., Aung et al., 2017).

Table 1.4: Active therapeutic components in natural compounds

Sr. No.	Natural compounds	Active elements	Sr. No.	Natural compounds	Active elements
1	turmeric	curcumin	8	Green tea	polyphenols
2	garlic	diallyl sulfide	9	honeybee hives	CAPE
3	ginger	gingerol	10	vegetables	isothiocyanates
4	grapes	Resveratrol,	11	broccoli	sulforaphane
5	grapes	piceatannol	12	tomato	lycopene
6	milk	silymarin	13	rosemary	rosmarinic acid
7	soybean	genistein	18	parsley	apigenin

Administration of natural compound as a therapeutic agent in various diseases is limited due to inadequate solubility, low permeability and poor bioavailability. Therefore, nanotechnology is being applied to overcome the aforementioned therapeutic potential issues of natural compounds (Cragg and Pezzuto, 2016., Puglia et al., 2017).

1.15 Role of curcumin in ulcerative colitis and colorectal cancer

Curcumin is a natural polyphenolic compound derived from *Curcuma longa* as shown in the Figure 1.8. It has been used in a number of diseases such as cancer, inflammation, bacterial and viral infection, wounds and skin disease (Stanić, 2017., Nelson et al., 2017., Kunnumakkara et al., 2017b., Kunnumakkara et al., 2017a).

Curcumin has an affinity to regulate a number of faulty signaling molecules responsible for human disorder due to which it has been under clinical investigation for decades (Gupta et al., 2013). It normalizes triggered activation of NF-kβ, interleukins, TNF-α and interferons which play a pivotal role in the pathogenesis of various human disease (Gu et al., 2013., Karunaweera et al., 2015). It has been used either alone or in combination with conventional medicine such as sulfasalazine or mesalamine for the of treatment of colorectal cancer and UC (Patel et al., 2010., Taylor and Leonard, 2011., He et al., 2011., Garg et al., 2012).

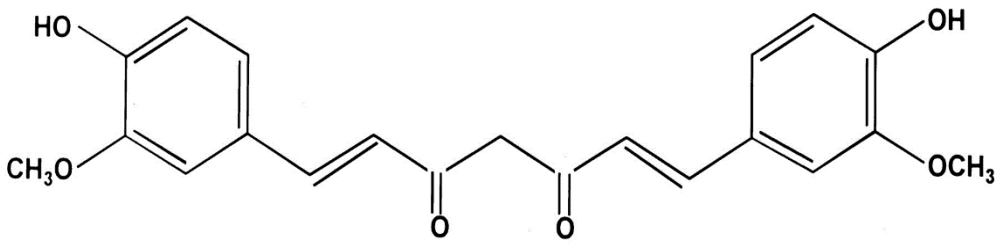

Figure 1.8: Chemical structure of curcumin.

1.16 Role of Caffeic acid phenethyl ester in ulcerative colitis and colorectal cancer

Caffiec acid phenethyl ester (CAPE) is a polyphenolic compound derived from honeybee hives as presented in Figure 1.9 (Tolba et al., 2016a). Anticancer, antibacterial, antioxidant, antiviral and anti-inflammatory property of CAPE has been documented in various human disease (Kuo et al., 2015, Khan et al., 2017c., Morin et al., 2017). Over stimulation of NF-kβ have been documented in colorectal cancer and ulcerative colitis aggravated by inflammatory medtaiors (Karin, 2009., Colotta et al., 2009a., Hoesel and Schmid, 2013., Rashidian et al., 2016., Marelli et al., 2017). CAPE inhibits overexpression of NF-kβ either by preventing translocation

of NF-kβ or interaction of NF-kβ-DNA binding in colorectal cancer and ulcerative colitis (Shepherd et al., 2018). It also reduces the stimulation of inflammatory mediators which provoke induction of NF-kβ and HIF-1α (Akyol et al., 2013., Murtaza et al., 2014a). It has not been used in clinical trials therefore, it will be worth investigating its potential efficacy in patients. It can also be administered with other convention anticancer and anti-inflammatory compounds to verify its combinatorial effects with traditional therapeutics.

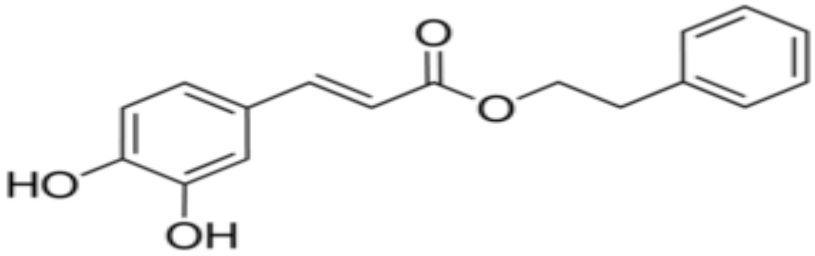

Figure 1.9: Chemical structure of CAPE.

1.17 Role of piceatannol in ulcerative colitis and colorectal cancer

Piceatannol is a natural polyphenolic constituents which has therapeutic potential in cancer, diabetes, heart disease and in inflammatory bowel disease documented (Tang and Chan, 2014., Seyed et al., 2016., Lu et al., 2017). Figure 1.10 shows different functional groups attached. Piceatannol is extracted from grapes, passion fruit, red wines, white tea tree, peanuts and sugar cane, (Lu et al., 2017). It arrests the unwanted growth of tumour cell in blood cancer, prostate cancer, breast cancer and rectal cancer (Piotrowska et al., 2012., Ko et al., 2012., Tang and Chan, 2014). Inhibition potential of piceatannol against NF-kβ and HIF-1α has been seen in different cancer cell lines (Piotrowska et al., 2012., Zhang et al., 2014., Seyed et al.,

2016). It has not been yet considered for clinical studies either in alone or in combination with other conventional medicine.

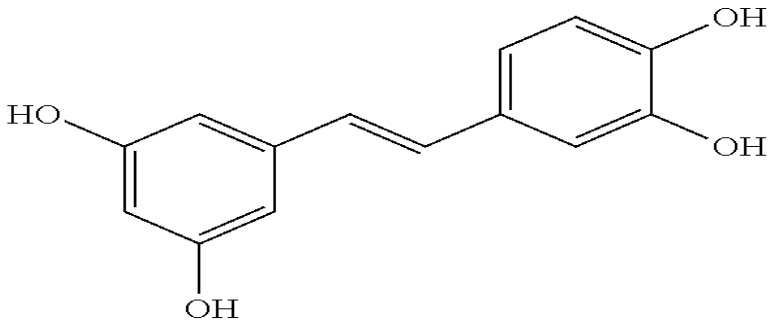

Figure 1.10: Chemical structure of PIC.

Apart from various medicinal values of curcumin, CAPE and PIC, they have limited solubility and bioavailability, which decreases the therapeutic activity of these natural compounds (Ketkar et al., 2016., Inagaki et al., 2016., Gómez-Estaca et al., 2017). Nanoparticles have been extensively employed to improve solubility, specificity for low soluble natural anticancer and anti-inflammatory agents (Bonferoni et al., 2017). Therefore, to improve its solubility nanotechnology or green technology is required to formulate nanoparticles of these natural compounds to maximise efficacy (Jahangirian et al., 2017).

1.18 Nanotechnology approach to improve solubility of natural compounds

Pharmaceutical industry started fabricating nanoparticles from last 30 years to overcome the solubility issue of hydrophobic drugs and nanoparticle technology has

been used in different fields such as microscopic imaging, tissue architect, biopathogens detections, protein and gene targeting etc (Salata, 2004., Muller et al., 2011., Zaman et al., 2014). Advectus Life Sciences, Alnis Biosciences, and Argonide are some examples of a pharmaceutical company which are involved in formulation and marketing of nanoparticles in a different field (Salata, 2004).

As active constituents such as curcumin, CAPE and piceatannol have limited solubility. Due to the difficulties arisisng from the poor solubility of natural compounds, it is problemtic to achieve maximum therapeutic benefits. Therefore, to resolve this issue fabrication of nanoparticles of these compounds increases the solubility with decrease in particle size.

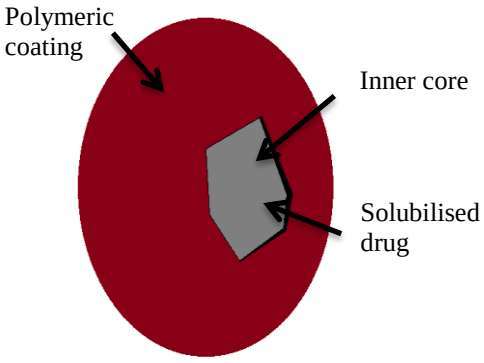

Figure 1.11: Schematic view of polymeric encapsulated nanoparticles. The inner core of polymer encapsulate the nanosize drug particle which provide targetd efficeincy in drug delivery.

These nanosized particles can be delivered to mucusal layer of the desired site (Jafari and McClements, 2017). The nanoparticulate delivery increases the efficacy via an increase in bioavailability and decreases the cytotoxicity (Yameen et al., 2014). Nanoparticles of specific size bypass the interaction with kidney or liver which decrease the pressure on these organs (Bobo et al., 2016). Nanoparticles delivery prevents drug degradations, increase residence time and improves cellular uptake at the diseased site (Wang et al., 2014). Solvent evaporation, salting-out, dialysis and

supercritical fluid technology are the methods employed to formulate solid nanosphere etc (Soppimath et al., 2001., Rao and Geckeler, 2011). Solvent evaporation method was the first and most widely used techniques to formulae nanoparticles by the pharmaceutical industry and research institute for polymeric nanoparticles (Rao and Geckeler, 2011). Solvent evaporation methods can be used for both hydrophilic as well as hydrophobic drugs (Kilicay et al., 2011). In solvent evaporation method, the polymer of choice is dissolved in organic solvents such as dichloromethane, chloroform or ethyl acetate. The drug is dissolved or dispersed either in polymeric organic solution or an aqueous solution of stabilizer depending on the hydrophilic or hydrophobic nature of the drug. This polymeric organic solution is then emulsified into an aqueous solution of a surfactant such as gelatin, polyvinyl alcohol or polysorbate. The stable emulsion is then stirred to remove organic solvent and it leads to solid nanoparticles formulation after lyophilzation as shown in Figure 1.11 (Sahoo et al., 2002., Hans and Lowman, 2002). Formulation parameter such as, sonication or homogenization speed and time, type and amount of organic solvent, concentration of surfactant, concentration of drug, type and amount of polymers have an impact on particle size and zeta potential (Sharma et al., 2016., Sheikholeslami et al., 2017). Polymer used in the formulation of nanoparticles such as, PLGA, chitosan and PLA are well-accepted and biodegradable (Kumari et al., 2010b).

1.19 Nanoparticles delivery in inflammation and cancer

Nanoparticles have been widely accepted possessing diagnostic and therapeutic potential (Revia and Zhang, 2016., Kang et al., 2017). They deliver chemical agents

to the tumour site, reduce the detrimental effects on healthy tissues and enhance the accumulation of active compound at desired site due to its nanosize (Baetke et al., 2015., Chen et al., 2016., Torrice, 2016). The nanomaterial is extensively used to study the pathogenesis of various diseases, biodistribution of drug, and mechanism of action of chemical compound (Bae et al., 2011., Baetke et al., 2015). Some of the nanoparticles are successfully used in inflammation and cancer treatment. Nanoparticles of a therapeutic agents such as doxorubicin, paclitaxel, and docetaxel are under preclinical and clinical investigation (Baetke et al., 2015., Rafiei and Haddadi, 2017). Nanotechnology also enhances stability and can be used for co-delivery with other pharmaceutical ingredients (Shi et al., 2017). Natural agents from plants sources have been extensively applied in treatment and management of cancer (Xiao et al., 2016., Sapio et al., 2017., Singh et al., 2017d). However, limited solubility hinders its pharmacological property to utilize in inflammation and cancer disease. Nanotechnology has been broadly employed to increase the solubility of natural compounds so that medicinal value can be improved in cancer treatment (Bharali et al., 2011., Watkins et al., 2015b). These natural compounds formulated as nanoparticles with a polymer such as PLGA, PLA, albumin, gelatin, polycaprolactone, and chitosan increase the solubility and offer controlled release of active pharmaceutical agents (Kumari et al., 2010b.,Watkins et al., 2015a). Polymeric nanoparticles do not interact with mononuclear phagocytic system due to the small size and bypass first pass effect (Khan et al., 2013). These polymeric nanoparticles aggregate at the desired site due to enhanced permeability and retention effect (Wang et al., 2017). The repository of nanoparticles aggregates at tumour site and release the drug in a controlled fashion for an extended period (Singh and Lillard, 2009).

1.20 PLGA nanoparticles of natural anti-inflammatory and anticancer compounds

Poly(lactic-co-glycolic acid) (PLGA) is one of the extensively used biodegradable polymer employed in fabrication of a number of natural and synthetic compounds for cancer treatment (Dinarvand et al., 2011., Khan et al., 2016). The safety of PLGA has been documented by US FDA to use in drug delivery systems due to controlled and sustained- release behavior, low toxicity, and biocompatibility with tissue and cells (Rafiei and Haddadi, 2017). PLGA nanoparticles is not recognize by mononuclear phagocytic system and deposit at cancer site due to EPR effects as shown in Figure 1.12 (Chen et al., 2015). Upon hydrolysis, PLGA breaks into lactic acid and glycolic acid which is metabolized in the body by Krebs cycle (Danhier et al., 2009., Kumari et al., 2010a).

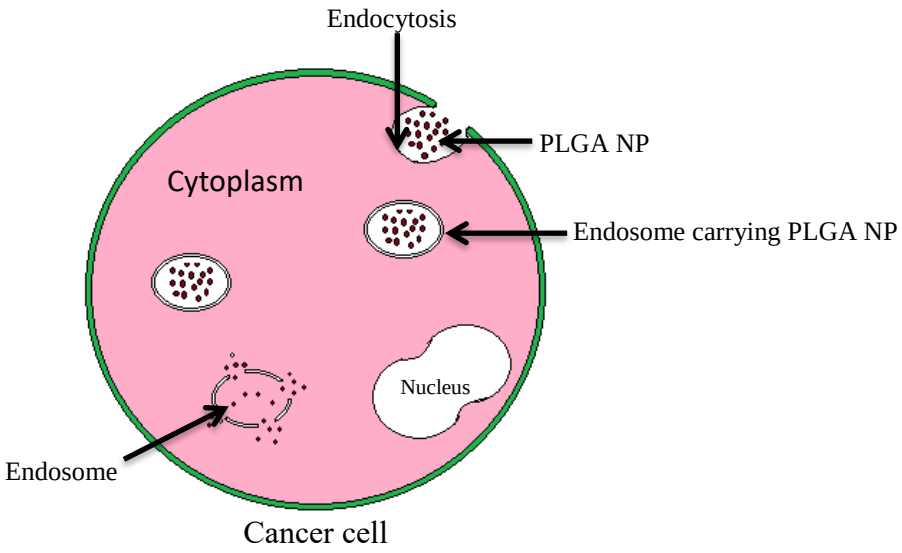

Figure 1.12: Mode of action of PLGA nanoparticles. The PLGA nanoparticles were taken by endocytosis into cytoplasm. Due to the nanosize of drug and polymeric encapsulation the active releases into nucleus and avoid reticuloendopasmic monosystem (RES).

1.21 Albumin nanoparticles of natural anti-inflammatory and anticancer compounds

Desovation method is the most widely used technique in the fabrication of albumin nanoparticles (Li et al., 2015b., Tarhini et al., 2017., Singh et al., 2017b., Singh et al., 2017c). Protein polymers such human serum albumin, bovine serum albumin, polypeptide, collagen, casein, silk protein, soya protein, gelatin and gliadin have been extensively using in nanoparticles fabrication for targeted delivery (Akash et al., 2016., Tarhini et al., 2017). Protein polymer easily networks with drug and solvent use in nanoparticle formulation (Lohcharoenkal et al., 2014). Therefore, albumin has been used in the current work due to its nontoxicity, nonimmunogenicity and biodegradability etc (Fallacara et al., 2017., Liu et al., 2017., Louage et al., 2017). It has been demonstrated that albumin can be used as a carrier for hydrophobic drug to improve pharmacokinetic profile and increase residence time at the target site (Dennis et al., 2002). Firstly, albumins attracts towards overexpressed interleukins to provide amino acids at inflammed and tumour sites, which provides targeted delivery of anti-inflammatory and anticancer agents as shown in Figure 1.13 (Jiang et al., 2017). Secondly, albumin holds several binding sites for ligands. It binds to a receptor to induce transcytosis (Larsen et al., 2016). Therefore, based on the accumulating evidence fabrication of nanoparticles of natural compounds with albumin as a polymer will improve solubility, bioavailability, efficacy and targeting potential of nanoparticles by desolvation method.

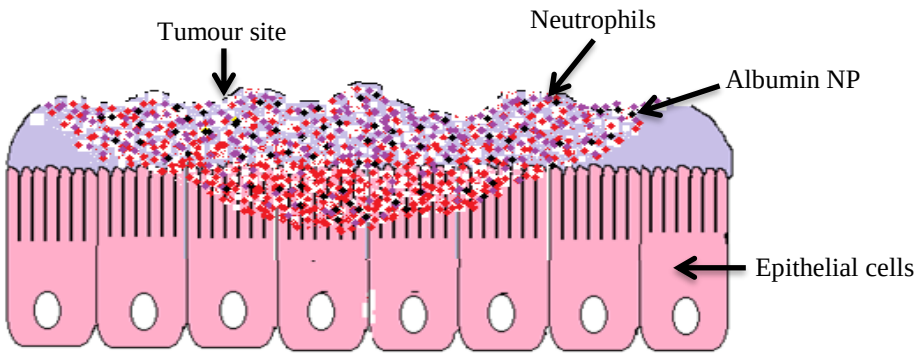

Figure 1.13: Mode of action of albumin nanoparticles. The albumin gets attratced towards neutrophils because of release of amino acid during dissociation. It also targets tumour cells due to gp60 membrane protein.

1.22 Conclusion

UC and colorectal cancer are serious human disorders. The associated side effect and nonspecificity of the current treatment fail to provide permanent cure to these disease. Therfore, there is need to use effective therapeutics with minimum or no side effects. Natural compounds exhibit medicinal value against number disease. However, limited solubility and low permieability compromised its efficacy. This solubility and permeability issue can be resolve by employing nanotechnology. Therfore, in the current thesis nanoparticles of natural anti-inflammatory and anticancer natural comound were fabricated. PLGA and albumin were used as polymer. The anticancer activities of these nanoparticles were studies on cancer cell lines. Anti-inflammatory efficacy of these nanoparticlers were evaluated in mouse (C57BL\6) model of colitis.

1.23 Hypothesis

In the thesis, we hypothesize that the reduction in particle size will enhance the solubility and increase anticancer and anti-inflammatory activities of nanoparticles of natural compounds PIC and CAPE.

1.24 Aims and objectives

- Formulation of PLGA nanopartciles of natural compounds
- Formulation of albumin nanoparticles of natural compounds
- Characterisation of PLGA and albumin nanoparticles of natural compounds
- Evaluation of anticancer activity of PLGA and albumin nanoparticles of natural compounds
- Evaluation of anti-inflammatory activity of PIC/CAPE-loaded albumin nanoparticles in ulcerative model of colitis

Chapter 2

Material and methods

2.1 Materials

Poly (lactic-co-glycolic acid) PLGA (50:50 lactide-glycolide ratio; with an average molecular weight of 7000-17000kDa), poly (vinyl alcohol) (PVA) 87-89% hydrolysed (MW 31.000-50.000), curcumin (log no. 78246, purity≥99.5%, sigma), Caffeic acid phenethyl ester (CAPE) (Cat no: -C8221, purity>97%, Sigma) and dichloromethane (HPLC grade) were purchased from Sigma Chemical Co. (St. Louis, USA). piceatannol (PIC) (Cat no: -P1928, purity->98%, CAS: -10083-24-6) was purchased from Tokyo Chemical Industry. Dextran sodium sulphate (DSS) (Cat no: -160110, lot no: -M2356, MW: -36000-50000) was obtained from MP Biomedicals. Bovine serum albumin (BSA) (Cat no: -A2153, Lot no-049k1585), Glutaraldehyde solution (Cat no: -G5882) was ordered from Sigma. Ethanol (HPLC grade, Ulster University) and all other reagents were of analytical grade or higher purity. Milli-Q-water was used throughout the study.

2.2 Preparation of PLGA nanoparticles

Curcumin loaded nanospheres was optimised as shown in the table 2.1. NP was formulated using solvent evaporation technique. Briefly, PLGA was dissolved in 2 ml chloroform. Free curcumin was added to the PLGA/chloroform solution and sonicated at 55 W for 3 minutes in a Branson Sonifier model W-350 (Branson, Danbury, CT, USA) to produce the s/o primary emulsion. This emulsion was then added to a solution of 1.5% PVA and again sonicated at 55 W for 3 minutes to form the final s/o/w emulsion. The final s/o/w emulsion was kept for overnight stirring and then centrifuged at 1345×g for 30 minutes to assist the removal of residual solvents. The nanospheres thus obtained were washed three times with deionized

distilled water. They were then freeze dried and lyophilized for 48 hours on an ATR FD 3.0 system (ATR Inc., St. Louis, MO, USA). Lyophilized nanoparticles were stored at 4˚C until further use (Mukerjee and Vishwanatha, 2009).

Table 2.1: Formulation code for PLGA loaded nanoparticles

Formulation Code	Amount of drug (mg)	Amount of Polymer (mg)	Conc. of PVA (%w/v)
F1	25	-	-
F2	50	-	-
F3	75	-	-
F4	-	30	-
F5	-	60	-
F6	-	90	-
F7	-	-	1.5
F8	-	-	2.5
F9	-	-	3.5
F10			
F11			
F12			

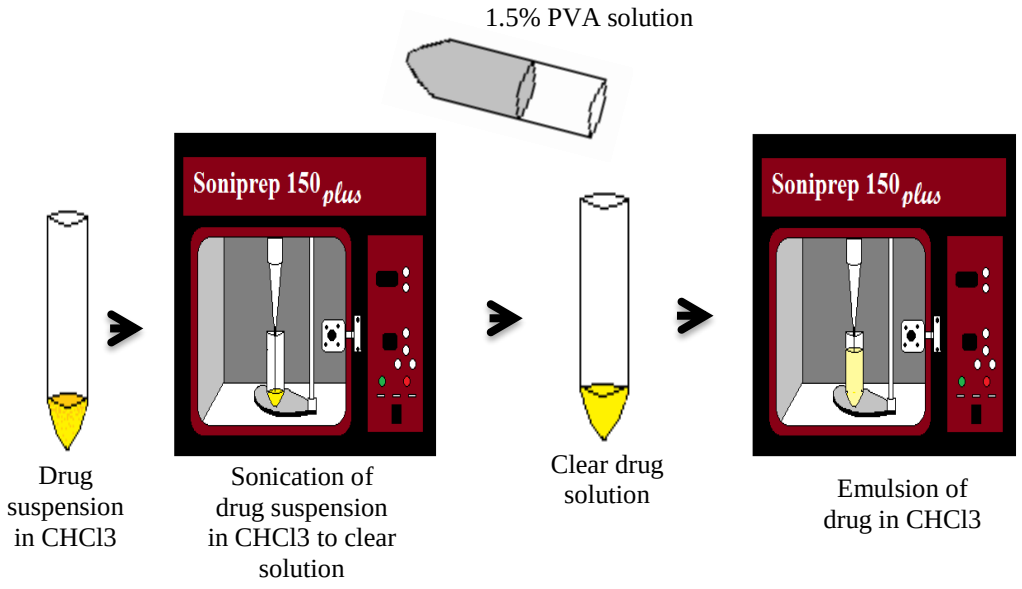

Figure 2.1: Schematic diagram of solvent evaporation method

2.3 Preparation of albumin nanoparticles

Drug albumin nanoparticle was optimised as shown in the table 2.2. NP was fabricated by desolvation method as described by Chen et al., 2017 with slight modification (Li et al., 2015a). Briefly, the drug was dissolved in ethanol. The drug solution then added to BSA solution dropwise under constant magnetic stirring which leads to the formation of coacervates. Crosslinking agent, glutaraldehyde was added after co-acervate formation. This co-acervates were stirred overnight to remove the organic solvent. Later, the resultant colloidal suspension was centrifuged to remove the organic solvent and washed with ultra-purified water. After centrifugation, the albumin nanoparticles were freeze dried and store at 4°C.

Table 2.2: Formulation code for albumin loaded nanoparticles

Formulation Code	Amount of ethanol (ml)	Conc. of albumin	Conc. of Glutaraldehyde	Amount of drug (mg)
F1	4	-	-	-
F2	8	-	-	-
F3	12	-	-	-
F4	-	0.5%	-	-
F5	-	2%	-	-
F6	-	3.5%	-	-
F7	-	-	4%	-
F8	-	-	8%	-
F9	-	-	12%	-
F10	-	-	-	10
F11	-	-	-	20
F12	-	-	-	30

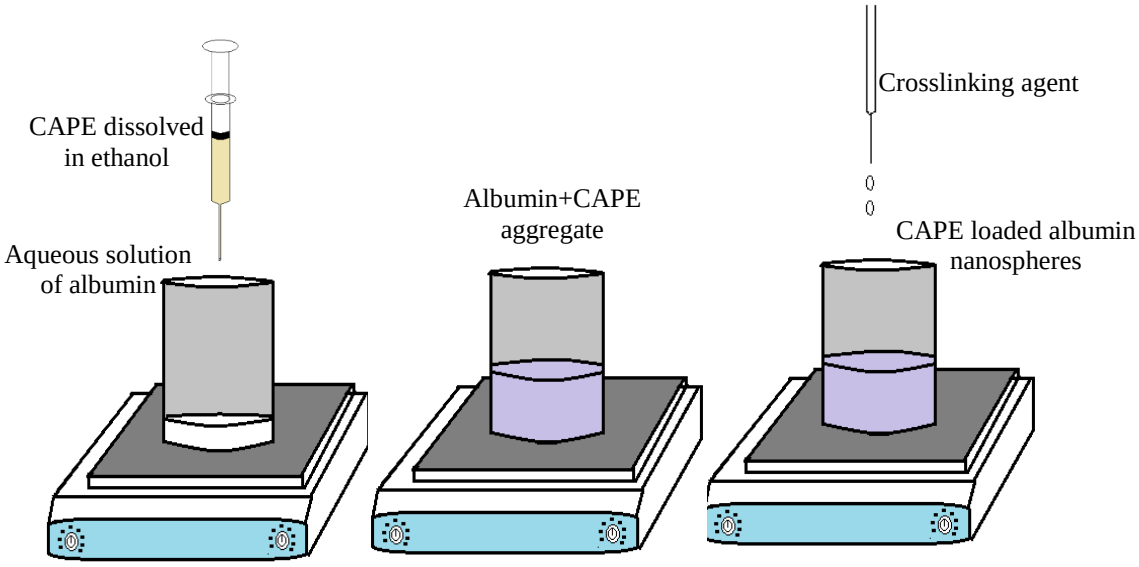

Figure 2.2: Schematic diagram of conservation method

2.4 Characterisation of particle size and zeta potential

The particle size and distribution of nanoparticles was determined by using Zetasizer (Zetasizer 5000, Malvern Instruments, Malvern, UK) based on dynamic light scattering principle technique. A sample of nanoparticle suspension (5 mg/ml) was vortexed for 5 minutes. An aliquot from this suspension was diluted by ultrapure water and utilized to measure particles size in triplicate. A zetasizer was used to measure the zeta potential of nanoparticles. 0.001 M KCl solutions with an adjusted conductivity were used to prepare diluted nanoparticle suspension. The principle of electrophoretic mobility under an electric field was used to measure the zeta potential values. The average of 3 measurements was reported (Haggag et al., 2016).

2.5 NMR spectra of nanoparticles

NMR spectra were run on a 500 MHz Bruker AVANCE DRX instrument using a broadband probe equipped with a z-gradient coil (Bruker-Biospin, Freemont, CA). All NMR samples were 600 íL and run in standard 5 mm NMR tubes at 25 °C. Pulse programs used were standard sequences taken from the Bruker XWINNMR pulse sequence library. NMR experiments were set up and processed generally using the parameters suggested in 200 and More NMR Experiments: A Practical Course. The pulse programs selected for the 2D COSY, HMQC, and HMBC experiments employed z gradients for coherence pathway selection. 1H and 13C chemical shifts were calibrated relative to the solvents and TMS (Payton et al., 2007).

2.6 Determination of entrapment efficiency

Entrapment efficiency of drugs in nanoparticles was calculated by the indirect method to determine drugs content in the supernatant. The concentration of non-encapsulated drug in the supernatant was measured by a UV spectrophotometer at 430 nm, as described earlier (Bisht et al., 2007). A standard plot of drug was prepared under identical conditions. The amount of entrapped drugs inside the NP was calculated by the difference between the initial amount of drug added and the measured non-encapsulated drug remaining in the external aqueous phase after NP fabrication. All measurements were assayed in triplicate and the average of each sample was recorded as the percentage curcumin encapsulation efficiency.

$$\text{Entrapment efficiency (EE)} = \frac{\text{Experimental drug loading}}{\text{Practical drug loading}} \times 100 \ldots\ldots(1)$$

2.7 Determination of percentage yield

Percentage yield is calculated as mentioned by Feng Li. et al., where the weight of the nanoparticles was divided by the total weight of drug and polymer used in the formulation as described below in the equation (Li et al., 2008b).

$$\text{Percentage yield} = \frac{\text{Total weight of the nanoparticles}}{\text{Weight of drug+Weight of polymer}} \times 100 \ldots\ldots.(2)$$

2.8 *In-vitro* release

The *in-vitro* release of drug from NP was carried out in phosphate buffer saline (pH 7.4, containing 0.1% w/v Tween-80). Briefly, 5 mg of NP was placed in a dialysis membrane (17kD) and suspended in 1ml PBS solution The sample pouches were incubated at a temperature of 37 °C and speed of 100 rpm in a reciprocal shaker water bath (Yallapu et al., 2010). The release samples from dialysis membrane were taken at predetermined time intervals of 0 minutes, 15 minutes, 30 minutes, 1 hour, 2 hours, 3 hours, 6 hours, 12 hours, 24 hours, 48 hours, 72hour, 96hour, 120 hours, 144 hours and 168 hours. The collected samples were centrifuged for 5 minutes at 10,000 rpm. Each experiment was performed in triplicate.

2.9 Determination of water solubility

Water solubility of nanoparticles was determined by dissolving NP and equivalent amount of free drug in distilled water. The mixtures were kept for stirring overnight and centrifuged at 13450RPM for 10 minutes. The absorbance of the supernatant was measured by UV-spectroscopy (Kim et al., 2011).

2.10 Scanning electron microscopy of nanoparticles

Nanoparticle's surface morphology was characterized by the aid of scanning electron microscopy (SEM) on a FEI Quanta 400 FEG (FEI Company). A sample of NP was mounted on carbon tape and sputter-coated with gold under vacuum in an argon atmosphere prior to imaging under SEM.

2.11 Cell culture

MDA-MB-231 cells (metastatic breast cancer cell line) and A549 cells (metastatic lung cancer cell line), CaCo-2 and HT-29 (metastatic colon cancer cell line) were generously provided by Keith Thomas, Ulster University These cells were maintained as monolayer cultures in Dulbecco's Modified Eagle's Medium–High Glucose (DMEM-Hi) medium (Gibco BRL, Grand Island, NY) and McCoy's media supplemented with 10% fetal bovine serum (Gibco BRL, Grand Island, NY) and 1% penicillin–streptomycin (Gibco BRL, Grand Island, NY) at 37 °C in a humidified atmosphere (5% CO_2).

2.12 Cellular uptake of nanoparticles

Cellular uptake of NP was investigated by seeding 1×10^5 of A549, MDA-MB-231, HT-29 and CaCo-2 cells on chamber slide in 6 well plates. After incubation for 24 hours, cells were washed 3 times with PBS. Cells were treated with 200µg/ml of NP then incubated for 3 hours. After 3 hours incubation, the cell was washed with PBS to remove the excess NP from well and fixed with 4% paraformaldehyde for 15 minutes. The nucleus of cells was stained with 5 µg DAPI in 1 ml normal media and

incubated for 15 minutes (Lamichhane et al., 2015). The fluorescence images of different groups were obtained from phase contrast microscopy.

2.13 *In-vitro* cytotoxicity assay

Cytotoxicity assays were performed as previously reported by (Kumar et al., 2014) with minor modifications. MDA-MB-231, A549, HT-29 and CaCo-2 cells ($5x10^4$ cells/well in 500 µl media) were seeded in 24-well plates. The following day, cells were treated with the free drug and an equivalent amount of nanoparticles in Optimem® media. The cytotoxic effect of free drug and nanoparticles was determined every 24 hours using MTT assay to assess the viability of cancer cells. The treated cells were washed with 500 µL PBS, and 500 µL of 15% MTT dye solution in complete media was added to each well. The plates were incubated at 37°C and 5% CO_2 for an additional 3 hours. The supernatant was discarded and formazan crystals were solubilized by adding 500 µL of DMSO and the solution was vigorously mixed to dissolve the precipitate. The colour intensity was measured at 570 nm (reference wavelength 630 nm) in a microplate reader (Fluostar Omega, BMG Lab Tech GMBH, Germany). The anti-proliferative effect of the free drug and nanoparticles treatment was calculated as a percentage of cell growth with respect to the DMSO and blank NP controls. The absorbance of the untreated cells was set at 100%. All the experiments were repeated three times.

2.14 Migration assay

Migration assay was performed through wound scratch assay as previously described by (Liang et al., 2007). MDA-MB-231, A549, HT-29 and CaCo-2 cells were seeded ($7.5x10^5$/well) into each well of 6-well plates. The cells were pipetted drop by drop around the edge of each well and shaken gently to evenly distribute the cells in each well. The plates were placed in an incubator to allow cells to grow to confluence. A wound was introduced to confluent cells by using the yellow pipette tip by carefully scraping the tip down the center of each well. Old media was removed and 2 ml of fresh media with PLGA, albumin NP and an equivalent amount of free drug were transfected into respective wells. Medium containing equivalent amounts of blank PLGA and albumin NP was used as the control. A photograph for each wound at 0 hrs was then taken and recorded. A photograph was taken at the same time of day at 24 hours, 48 hours and 72 hours. To quantify the results from the photographs, image J software was used to measure the width of the wound. The width of the wound was measured at 3 different points in the photograph and the average was recorded. The degree of wound closure over 72 hours was calculated in all the treatment and compared with control and blank NP. All the experiments were repeated three times.

2.15 Colony formation assay

For colony formation assay, 500 cells of MDA-MB-231, A549, HT-29 and CaCo-2 cells were seeded in 2 ml media in 6-well plates and allowed 2 days to attach and initiate colony formation (Yallapu et al., 2010). These cells were treated with PLGA NP, albumin NP and the same amount of free drugs suspended in Optimem® media

over a period of 7 days. The plates were washed twice with PBS, fixed in chilled methanol, stained with Crystal Violet, washed with water and air dried. The number of colonies was counted by using a magnifying lens. The percent of colony formation was calculated by dividing the number of colonies formed in treatment by the number of colonies formed in blank NP.

2.16 Invasion assay

An invasion assay was performed as previously reported (Yuen et al., 2013). This was conducted to investigate the effect of nanoparticles and free drug treatment on the ability of MDA-MB231, A549, HT-29 and CaCo-2 cells to invade a Matrigel-coated membrane. A number of 8 µm membrane transwell inserts were inserted into the well of 12-well plate (BD Bioscience, San Jose, CA). The membrane transwell was coated with Matrigel before seeding the cancer cells. Matrigel was placed on ice and left to thaw at 4°C then diluted 1:1 with water and 135 µl of the solution was placed carefully into the required number of inserts. The inserts were shaken gently to ensure the Matrigel solution spread evenly on the membrane. The whole plates were left in the laminar flow hood to dry for 60 minutes. $4x10^4$ cells were seeded into each insert in a suspension of 200 µl of serum free media. Next 100 µl containing nanoparticles of drug and equivalent amount of free drug was treated into corresponding wells. The same volume of 100 µl containing equivalent amounts of blank NP was used as the control. Finally, 700 µl of DMEM media containing 10% FBS was added to each well to bath the outer membrane surface and act as chemoattractant. The next day, to new 12-well plates, 500 µl of methanol was added to the corresponding number of wells used. The media in both chambers were

removed and cotton wool scrubbers were used to clean off any remaining cells or Matrigel layer. The inserts were placed into methanol for 10 minutes for fixation. Once fixation has completed the inserts were left to dry. Using a scalpel the membrane was cut out and placed with the original outer surface facing upwards in wells of a new 12-well plate. 250 µl of Crystal Violet was then added to each well to stain up the cells that invaded through the membrane pores. The plates were left to be shaken for 20 minutes. Afterwards, the Crystal Violet solution was pipetted out and the membranes were washed thoroughly in their wells with Milli-Q water. The membranes were left to air dry for 60 minutes. 250 µl of 70% ethanol was added to each membrane in each well and shaken for 30 minutes. Finally, 200 µl was pipetted out from each well and placed into the wells of 96-well plate. Absorbance at 590 nm was measured using a microplate reader (Fluostar Omega, BMG Lab Tech GMBH, Germany). The effect of the free drug and an equivalent amount of nanoparticles treatments was calculated as a percentage of cell invasions with respect to blank NP controls. The absorbance of the untreated cells was set at 100%. All the experiments were repeated three times.

2.17 Immunostaining for cells

A sterile glass coverslip was placed in six-well plates. MDA-MB-231, A549, HT-29 and CaCo-2 cell was seeded at 1.9×10^5 cell density in six-well plates. The plates were incubated for 24 hours. Next day, plates were washed with sterile PBS to remove the dead cells from each well. 7.5 µg/ml of free drug and nanoparticles were transfected for 24 hours. Blank nanoparticles were taken as control. Next day the wells were washed with sterile PBS for 5 minutes twice. The cells were fixed with

4% paraformaldehyde solution for 30 minutes. Later the cells were permeabilized with 0.25% Triton-X for 15 minutes and washed with PBS two times for 5 minutes. The blocking was carried out with 2% albumin in PBS for 30 minutes. After binding, the cells were incubated with primary antibody 50 µl/ml overnight at 4°C. Next day cells were washed with PBS two times for 5 minutes. Later it was incubated with anti-rabbit secondary antibody for 1 hour at room temperature. After incubation with secondary antibody, it was stained with DAPI for 15 minutes. The cover clip then transferred to a glass slide and nail polish was applied to the edges of the coverslip to prevent it from drying (Váradi et al., 2017).

2.18 Quantification of p65 and HIF-1α

MDA-MB-231, A549, CaCo-2 and HT-29 cells (pre-treated for 12 hours with 10% oxygen) were treated with free drugs, PLGA nanoparticles and albumin loaded nanoparticles for 6 hours. Whole cell lysates were prepared and assayed for HIF-1α and p65 levels using Invitrogen HIF1a Human ELISA Kit (EHIF1A) and NF-kβ p65 (Total) Human ELISA Kit (KHO0371) and used according to the manufacturer's instructions at 450 nm, using a BioTek optical plate reader. Optical density was converted to concentration (pg ml-1247) using the standard calibration curve provided in the manufacturer's protocol.

2.19 Induction of dextran sodium sulphate model of colitis

For DSS colitis-induced experiments, 12-week old C57BL/6 female mice were used (Charles River U.K.). All procedures described were approved by the Ulster

University Animal Research Ethics Committee and UK Home Office, under Project license (PL2768). Colitis was induced by administering 2.5% w/v DSS in drinking water over a period of 6 days. The mice were divided into groups such as healthy, DSS, free drug and nanoparticles. These groups also received 2.5% DSS in drinking water. The DAI score was used to record morphological changes, such as weight loss, stool consistency and presence of blood in faeces as explained in the table 2.3.

Table 2.3: Scoring of disease activity index

Score	Weight loss	Stool consistency	Faecal blood
0	None	Normal	None
1	1-5%		
2	5-10%	Loose	Hemoccult+
3	10-20%		
4	>20%	Diarrhoea	Gross bleeding

On termination of the experiment, mice were sacrificed by cervical dislocation (Okayasu et al., 1990., Egger et al., 2000).The isolated colon was excised, washed in PBS and laid flat on the moist tissue to measure its length. Sections, approximately 1.0 cm, of excised colonic tissue were fixed in 10% paraformaldehyde (pH, 7.4; phosphate-buffered saline) and embedded in paraffin. Sections (4 μm) were cut and stained with haematoxylin and eosin. Histologic assessment and scoring of colon tissue sections against inflammation were carried out in a blinded fashion based on defined parameters such as severity of inflammation, the extent of inflammation, crypt damage and percentage involvement as highlighted in the table 2.4 (Sutherland et al., 1987). All tissue slides were imaged using light microscopy.

Table 2.4: Scoring of the severity of histological damage**.**

feature	Score	Description
Severity of inflammation	0	None
	1	Mild
	2	Moderate
	3	severe
Extent of inflammation	0	None
	1	Mucosa
	2	Mucosa and submucosa
	3	Transdermal
Crypt damage	1	1/3 damaged
	2	2/3 damaged
	3	Crypt lost, surface epithelium present
	4	Crypt lost, surface epithelium lost
Percentage involvement	0	0%
	1	1-25%
	2	26-50%
	3	51-75%
	4	76-100%

2.20 Quantification of cytokines and myeloperoxidases in colonic tissues

Post-mortem colon tissue was homogenized using a method adapted from processing lung tissue (Mangan et al., 2006). Levels of pro-inflammatory cytokines, such as Interferon gamma (INF-γ), IL-6, IL-1β, TNF-α and IL-10 were detected using V-Plex Assay Plates (Meso Scale Diagnostics; Rockville, MD) and assayed as per the manufacturer's protocol. Myeloperoxidases (MPO) activity was detected using o-phenylenediamine dihydrochloride as substrate and the data was interpolated from an

MPO standard curve (Sigma). Levels of cytokines and MPO were expressed as pg per mg or U per mg, respectively, relative to colon protein (Cummins et al., 2008).

2.21 *In-vivo* intestinal permeability measurements

Mice were exposed to 7 days of DSS treatment before oral administration of 0.6 mg per gram of body weight fluorescein isothiocyanate (FITC)–labelled dextran (4 kDa) by standard oral gavage. Mice were euthanized 4 hours later and blood removed by cardiac puncture. Plasma was separated and FITC levels in plasma determined by fluorimeter (Tambuwala et al., 2010).

2.22 Immunohistochemistry

Colon tissues was stored in formalin and embedded into paraffin. 5 μm of paraffin molded colonic tissues was sectioned under microtome. The sectioned then placed on a superfrost glass slide. The paraffin colonic segments were immersed (10 minutes twice) in xylene jar to remove the paraffin and rehydrated in decreasing concentration of ethanol such as 100%, 95% and 75% each for 5 minutes. It was then submerged in a glass jar filled with boiled sodium citrate buffer (95°C, pH6) for 20 minutes to break the bond formed during tissue processing due to paraffin in hot water bath at 100°C. After heating for 20 minutes, it was taken out and kept to cool down at room temperature for 20 minutes. The slide was then washed in PBS twice for 5 minutes and blocking was carried out in 5% BSA solution for one hour at room temperature. The slide was washed again for 5 minutes twice. After washing, the section was incubated with secondary antibody for one hour at room temperature.

The tissue section was then stained with DAPI for 15 minutes and antifade was applied to laid the coverslip. The sectioned was observed under a microscope (Nuñez-Sánchez et al., 2017).

2.23 Statistical analysis

Results were expressed as mean ± standard error of the mean (SEM) for a series of experiments. Data were assumed to be normally distributed and statistical analyses were carried out using Prizm GraphPad V6 software (GraphPad, San Diego, CA, USA). A paired t test was used for comparisons of paired treatments between two groups, unpaired t tests for comparisons of unpaired treatments between two groups, and one-way ANOVA using Bonferroni multiple comparisons tests for treatments of three groups or more. P values ≤ 0.05 were considered to be significant.

Chapter 3

Caffeic acid phenethyl ester is protective in experimental ulcerative colitis via reduction in levels of pro-inflammatory mediators and enhancement of epithelial barrier function

3.1 Introduction

Inflammatory bowel disease (IBD) is an idiopathic disorder, generally categorized as either Crohn`s disease (CD) or ulcerative colitis (UC) (Ford et al., 2011., Neurath, 2014a). There is no therapeutic cure for IBD and the current disease management strategies possess challenging drawbacks. For example, immunomodulatory agents, such as azathioprine and 6-mercaptopurine, causes bone marrow depletion and damage to both white blood cell and hepatic cell populations. Furthermore, results from recent clinical trials confirm that azathioprine is ineffective in UC (Ardizzone et al., 2006., O'Connor et al., 2010., Kamath et al., 2016). Sulfasalazine causes ruptures in liver tissue and decreases platelets count in blood (Rubin, 1994., de Abajo et al., 2004). Pulmonary disorders are reported in IBD patients treated with chimeric monoclonal antibodies, such as infliximab (Patel et al., 2016). The clinical symptoms of IBD range from episodes of relapse and remission, mild inflammation and discomfort to a chronic ulcerative disease requiring surgical removal of the inflamed gut. The current therapeutic strategies for IBD are limited, but recent clinical advancement has occurred in the area of immunotherapy with monoclonal antibodies, which are directed against inflammatory mediators, such as TNF-α (Targan, 2006., .,Subramanian et al., 2017., Gecse and Lakatos, 2017., Chan and Ng, 2017). However, these biologicals are not only expensive but have resulted in severe side effects and life threatening complication (Cote-Daigneault et al., 2015., Blonski and Lichtenstein, 2006., Cohen and Thomas, 2006., Clarke and Regueiro, 2012., Côté-Daigneault et al., 2015) Hence, there is an urgent need in the field of IBD therapy to develop new therapeutics which are effective, safe and economical. We strongly believe that one way to achieving this goal is by exploring natural anti-inflammatory compounds and understanding their mechanism of action during IBD.

Lack of specificity and the encumbrance of severe side effects necessitates a further investigation into effective and safer options for treatment of this chronic inflammatory disease (Pichai and Ferguson). This is the issue address in the current study.

Colonic specimens from UC patients have been shown to overexpress transcription factor nuclear factor kappa beta (NF-kβ) (Atreya et al., 2008). NF-kβ is upregulated by TNF-α, interleukin (IL), interferon, and chemokines, DNA damaging agents bacterial cell wall components, lipopolysaccharide, during inflammatory condition (Xavier and Podolsky, 2007b., Lawrence, 2009). In UC, the inflammatory mediators such as TNF-α, interleukins, and interferons levels increase due to the over stimulation of NF-kβ during inflammation (Schreiber et al., 1998). It is feasible, that inhibition of NF-kβ may be of therapeutic benefit in UC, which forms the hypothesis of our current work.

Although there are several novel pharmacological inhibitors of NF-kβ currently available these compounds suffer from toxic/side effects in humans. Hence, in this work, caffeic acid phenethyl ester (CAPE) is used as a phenolic constituent derived from honeybee propolis with no known toxic/side effects (Figure 1) (Liao et al., 2003., Tolba et al., 2016a). CAPE possesses anti-inflammatory properties and is a selective inhibitor of NF-kβ (Ozturk et al., 2012., Lin et al., 2013). CAPE represses translocation of NF-kβ, either by inhibition of Ikβ degradation or by blocking of NF-kβ and DNA binding (Wang et al., 2010b., Bezerra et al., 2012). It has been reported that inflammatory markers, such as INF-γ, IL-6, IL-1β, TNF-α and IL-10 cause degradation of Ikβ, which results in induced overexpression of NF-kβ (Lang et al., 2004). CAPE has the potential to inhibit this overexpression of NF-kβ via prevention of degradation of Ikβ (Liao et al., 2003., Lee et al., 2008., Wang et al., 2010a).

3.2 Summary

Therefore, as per the detrimental effect of IBD and allied adverse effects of conventional therapeutics, there is pressing need to practice novel and natural anti-inflammatory agent in the treatment and control of IBD. As per the control action of CAPE on factor responsible for the progression of UC such as over induction of NF-kβ, HIF-1α and pro-inflammatory markers, it will provide a better understanding of the mechanism of action of CAPE in a mouse model of ulcerative colitis.

3.3 Hypothesis

In this chapter, we hypothesize that the natural anti-inflammatory compound CAPE will mitigate inflammatory condition during UC.

3.4 Aims and objective

- To study the effects of free CAPE on macroscopic level such weight loss, and DAI and change in colon length in UC.
- To study effects of free CAPE on mucosal layer in UC
- Effect of induced level of NF-kβ, HIF-1α and pro-inflammatory markers in UC.

3.5 Results

3.5.1 CAPE ameliorates weight loss and DAI in DSS-induced colitis

Colitis was induced as described in section 2.19. It has been reported by us and several researchers mentioned that colitis is the collection of symptoms such as weight loss, diarrhoea, blood in faeces collectively known as disease activity index (DAI) and shortening of colon length (Ogawa et al., 2004., Chen et al., 2007., Chassaing et al., 2014b., Taghipour et al., 2016). To study the protective effect of CAPE on mice with DSS-induced colitis, we recorded the weight of each mouse in all groups daily for seven days. The graph in the Figure 3.1A shows lowered weight loss in DSS + CAPE treated mice when compared to the DSS-only group. Similarly, Figure 3.1B shows that mice in the DSS-alone group had the highest DAI score, which confirmed the development of colitis. Mice treated with CAPE showed a lower DAI score when the comparison is made to the DSS-only group. This finding suggests that CAPE was protecting the mice against weight loss and the occurrence of diarrhoea and appearance of blood in faeces during DSS-induced colitis.

3.5.2 Change in colon length

Shortening of the colon is one of the clinical sign of colitis (Tambuwala et al., 2015). Figure 3.2A shows a representative image from the colon of a healthy mouse which shows well-formed stool pellets. In contrast, there were no formed stools and blood observed in the colon of mice treated with DSS alone. However, semi-formed stools and no blood were visible in the colon of mouse treated with CAPE. A graphical presentation of the average colon length of each group is shown in Figure 3.2B. It is observed that there was a significant reduction in colon length in mice treated with

DSS alone when compared to the healthy control and DSS+CAPE treated mice. Thus, CAPE treatment profoundly attenuated the impact of DSS on colon length reduction and also helps in the formation of stool.

3.5.3 Histological observation of mucosal layer

Colon H and E staining were performed as stated in the section 2.19. Histological examination of colon tissue confirmed that DSS treatment caused extensive colonic damage with lose of epithelium and collapse of crypt structure. This was accompanied by oedema and infiltration of inflammatory neutrophils as shown in the Figure 3.3A. In contrast, there was a marked reduction in severity of DSS-induced colon injury in CAPE-treated mice. The crypt architecture showed no ulceration or evidence of oedema lesser degree of infiltration of inflammatory cells and neutrophils were observed in the colon histology of mice receiving CAPE treatment as depicted in the Figure 3.3A. The blinded histological scoring of colon tissue histology revealed a significant reduction of damage in the colon of CAPE-treated mice relative to healthy control mice ($P<0.001$) as shown in the Figure 3.3B.

3.5.4 Quantification of inflammatory markers

Quantitative analysis was carried out as discribed in section 2.20. investigation of CAPE on the expression of markers of colonic inflammation that are increased in mice exposed to DSS was performed. DSS alone control mice showed a significant increase in MPO activity, a marker for inflammation and leukocyte infiltration; Figure 3.4A. However, exposure of CAPE-treated mice to DSS did not result in

increased colon MPO levels as shon in the Figure 3.4A. It was also noted that colonic levels of pro-inflammatory cytokines, such as INF-γ, IL6, IL-1β, TNF-α and IL-10 as shown in the Figure 3.4(B, C, D, E and F) were significantly increased in mice with DSS-induced colitis ($P< 0.001$). Co-administration of CAPE resulted in small increases in INF-γ, IL6, IL-1β, TNF-α and IL-10, which were not significantly different from that of the healthy control. Thus, the DSS-induced increase in MPO, INF-γ, IL-6, IL-1β, TNF-α and IL-10 all were diminished significantly in CAPE-treated mice ($P<0.001$). Furthermore, treatment of mice with CAPE alone had no effects on MPO, INF-γ, IL-6, IL-1β, TNF-α and IL-10 levels in the colon of healthy mice (data not shown).

3.5.5 Enhanced epithelial barrier function in mice treated with CAPE

Intestinal permeability was measured as stated in section 2.21. To investigate the effect of CAPE treatment on the intestinal epithelial integrity, the *in-vivo* barrier function was measured in healthy mice, mice exposed to DSS and mice co-treated with CAPE and DSS. An oral dose of FITC-dextran was administered to mice on the last day of DSS exposure. Four hours later, FITC levels in plasma were determined as a measure of intestinal permeability. The DSS-only group of mice exhibited a significant increase in intestinal permeability, which was reflected by an increased appearance of FITC in plasma. This effect was markedly diminished in mice treated with CAPE as depicted in the Figure 3.5, indicating that co-treatment with CAPE during DSS-induced colitis reduces the leakiness of the colon and maintains the epithelial barrier function.

3.5.1 CAPE ameliorates weight loss and DAI in DSS-induced colitis

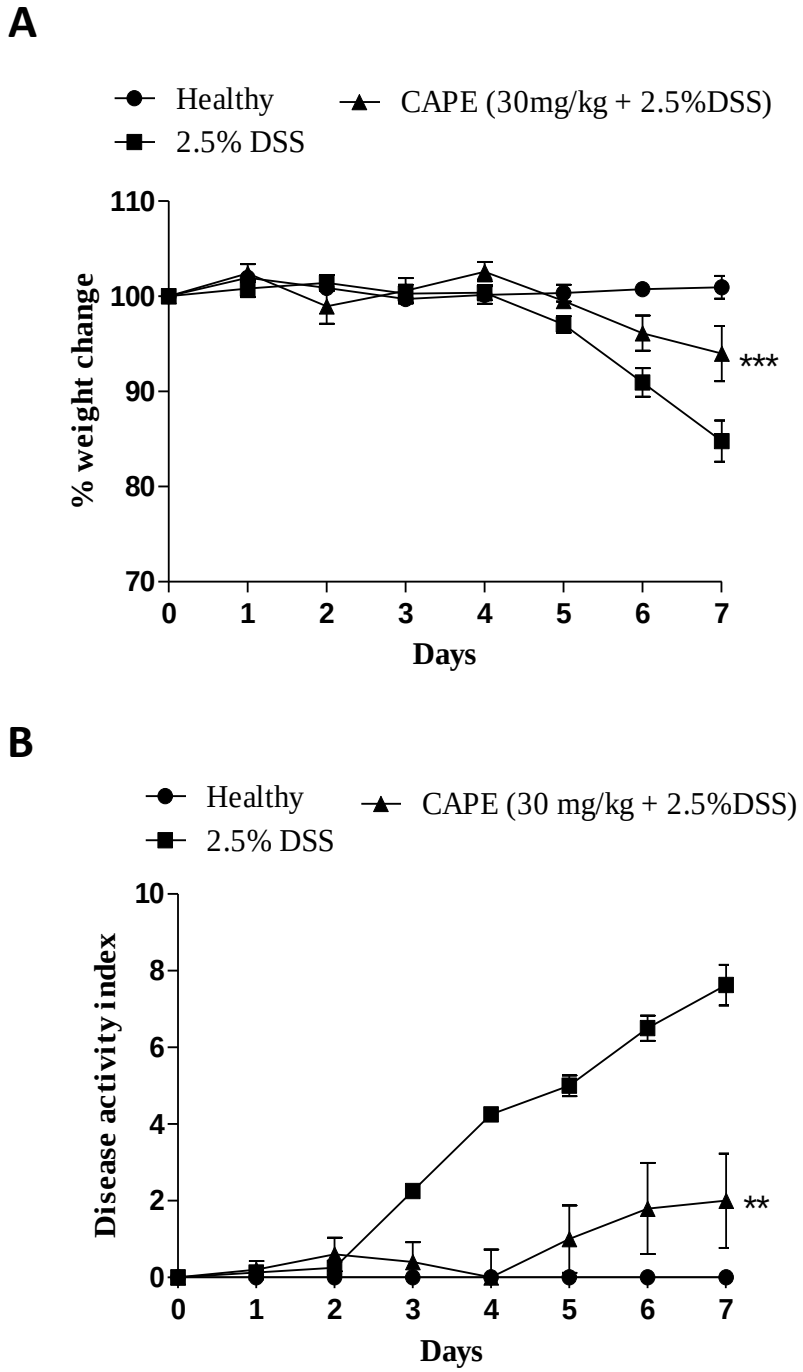

Figure 3.1: Lowered percentage weight loss (A) and DAI (B) score in mice treated with CAPE during DSS-induced colitis.(A) Percentage weight loss was assessed in mice treated with DSS-alone, DSS and CAPE and no DSS healthy mice . (B) Disease activity index was assessed in mice treated with DSS-alone , DSS and CAPE and no DSS healthy mice over 7 days. N=5-6 individual mice. **P<0.01 and ***P<0.001

3.5.2 Change in colon length after treatment with free CAPE

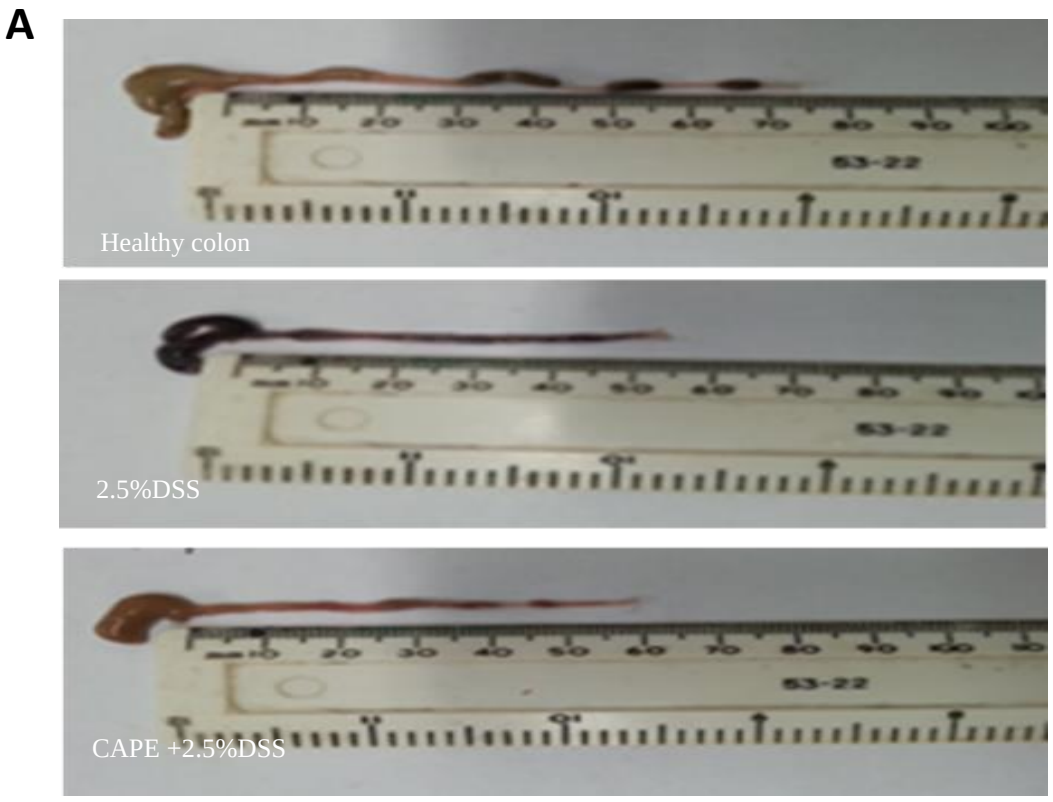

Figure 3.2: CAPE treatment is effective in protecting gross anatomy and colon length. (A) Gross appearance of the colonic anatomy shows the effect of CAPE on DSS-induced colon shortening and formation of fecal pellets. (B) Colon length was measured at post-mortem autopsy. N = 5-6 mice per group. ***P<0.001.

3.5.3 Histological observation of mucosal layer

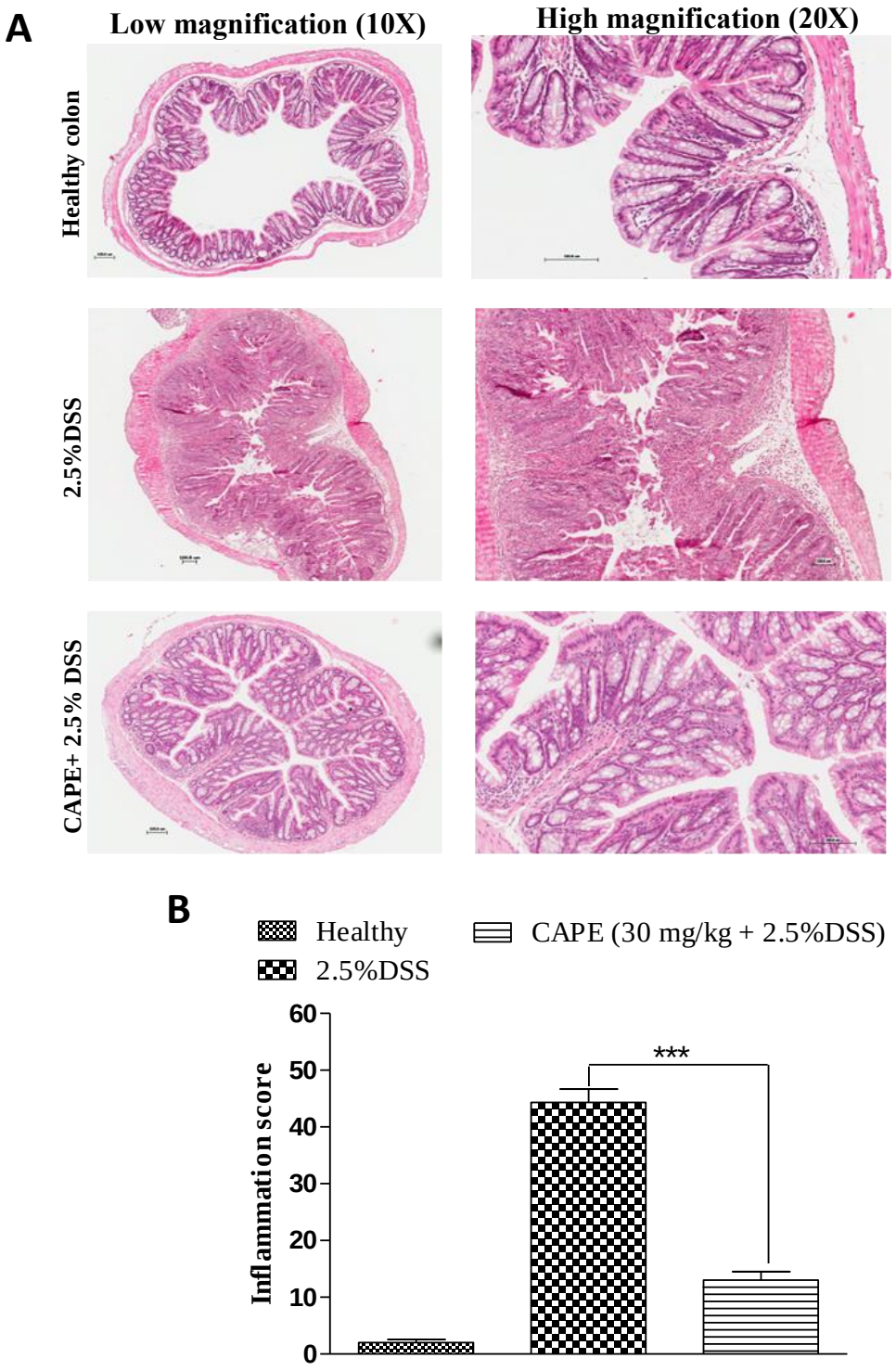

Figure 3.3: Improved colon histological outcome in mice treated with CAPE. (A) Representative histological images of colonic tissue showing the effect of CAPE treatment (H&E staning). (B) Histological scores of sections scored blinded. N = 5-6 mice per group. ***P<0.001.

3.5.4 Quantification of inflammatory markers

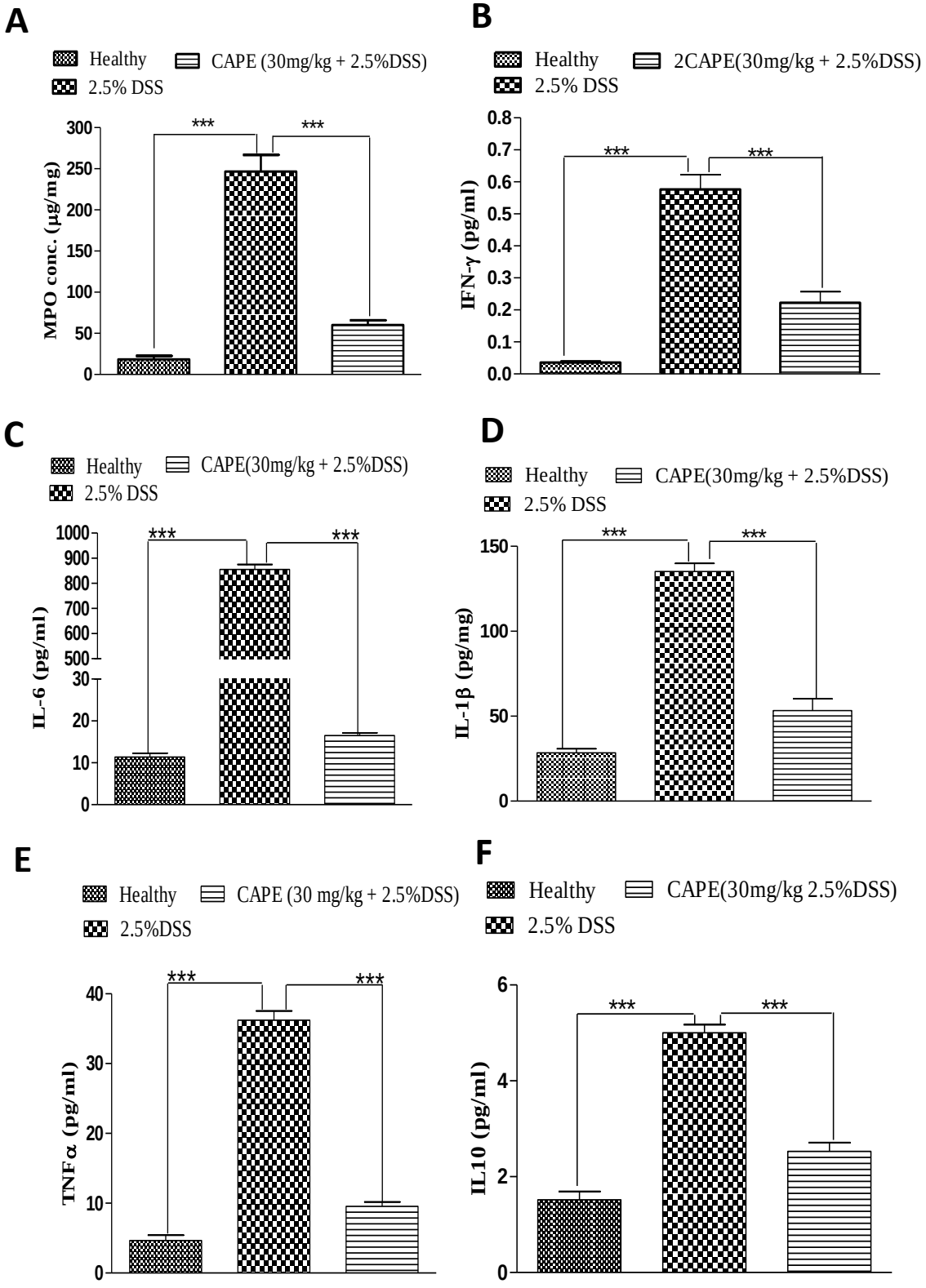

Figure 3.4: Effect of CAPE on the expression of pro-inflammatory mediators. The colon tissue homogenates analyzed for (A) MPO, (B) INF-γ, (C) IL-6, (D) IL-1β, (E) TNF-α and (F) IL-10. N = 5-6 mice per group. ***P<0.001.

3.5.5 Enhanced epithelial barrier function in mice treated with CAPE

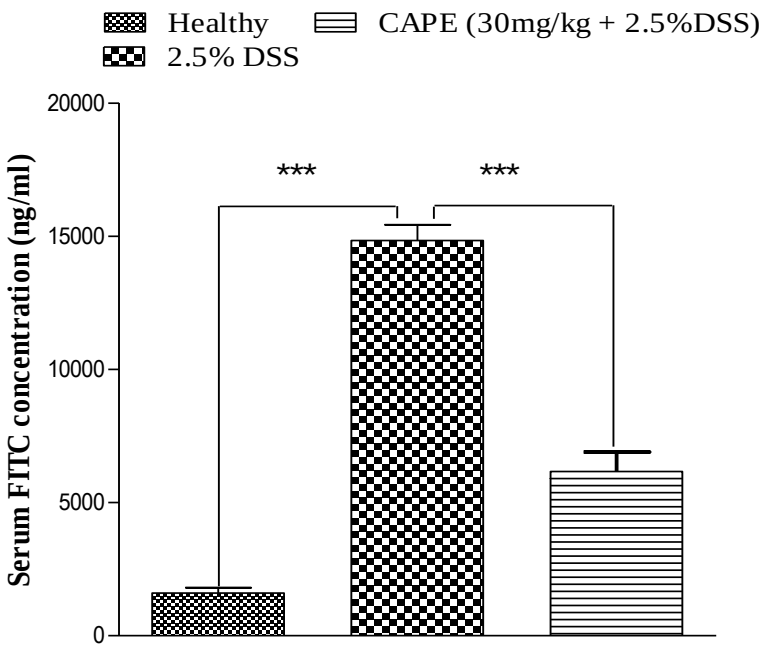

Figure 3.5: Reduced epithelial permeability in mice treated with CAPE. Mice treated with DSS with or without CAPE (30mg/kg) IP and healthy mice were administered 4 kDa-FITC-labeled dextran orally and serum levels of FITC were assessed. N=5-6 mice. ***P<0.001.

3.6 Discussion

Previous studies have indicated that CAPE is an effective inhibitor of NF-kβ and related cytokines *in-vitro*, and also has the ability induce apoptosis in inflammatory cells (Fitzpatrick et al., 2001). In our current study, we have shown for the first time that CAPE significantly ameliorates the severity of the disease in a mouse model of UC.

One of the initial events which occur during the onset of IBD is disruption of the intestinal epithelial barrier function. This epithelial dysfunction leads to compromised epithelial barrier resulting in unwanted movement of luminal antigenic material into the lamina propria leading to the activation of mucosal immune cells to trigger off an inflammatory response. It has been suggested that one of the critical events in the development of inflammation in the intestine could be the regulation of intestinal epithelial cell apoptosis (Cummins et al., 2008., Tambuwala et al., 2010). In case of chronic inflammation during IBD constant intestinal epithelial cell apoptosis could lead the loss of the epithelial barrier which will result in spread of inflammation resulting in increased severity of the disease creating an imbalance in the innate and adaptive immunity of our gut (Nenci et al., 2007., Zaph et al., 2007).

Several researchers have indicated that NF-kβ pathway plays an important role during intestinal inflammation ((Fitzpatrick et al., 2001, Lawrence, 2009., Wei and Feng, 2010., Buhrmann et al., 2011) and inhibition of this pathway targets pro-inflammatory cytokines such as interferons and TNF-α which are known to play key role during ulcerative colitis (Bishop et al., 2014., Baird et al., 2016., Ferrari et al., 2016a).

In the present work, we have shown for the first time that CAPE a potent inhibitor NF-kβ is profoundly protective in an *in-vivo* mouse model of acute colonic inflammation. Although it was hypothesized that the protective effects of CAPE are mediated through the inhibition of the over activation of the NF-kβ pathway, we cannot exclude the possibility of NF-kβ independent mechanism of action such as inhibition of hydroxylases and activation of hypoxia inducible pathway (Cummins et al., 2008). CAPE treatment significantly ameliorated the severity of disease after acute DSS exposure in all parameters studied, including weight loss (Figure 3.1A), clinical DAI score (Figure 3.1B), reduction of colon length, appearance of blood in faeces (Figure 3.2A & B), and a marked improvement in colon histology was observed (Figure 3.3A) along with improved blinded inflammation scores (Figure 3.3B). In the murine model of DSS induced colitis, the increase in MPO and pro-inflammatory cytokines occurred after the disruption of the intestinal barrier; that CAPE treated mice did not have increased MPO (Figure 4A) and only small increase in other pro-inflammatory cytokines as shown in thr Figure 3.4(B, C, D, E, & F) suggests that CAPE treatment prevented the damage to colon epithelial cells caused by DSS, which is evident by reduced permeability of FITC in mice treated with CAPE as demonstrated in the Figure 3.5.

However, whether improved epithelial barrier function or indeed cytokine expression is the cause or consequence of the protective effects of CAPE remains to be elucidated. This critical question will be the topic of further investigations.

In mice treated with CAPE, in the absence of DSS exposure, there were no alterations in MPO or cytokines in the colon and no alterations in colon histology or length. This confirms that in the acute 6-day treatment regimen used in this study CAPE did not alter physiologic inflammation in normal tissue, but instead

suppressed inflammation in the colon when occurred due to DSS induced disruption of the barrier function.

In this study, it showed that CAPE is therapeutic in a mouse model of ulcerative colitis. Since CAPE is a natural compound, with no known toxic/side effects (Tambuwala, 2016) it would be highly desirable therapeutic over other novel compounds with pro-tumorigenic effects; such as DMOG which have shown to be protective in experimental colitis (Cummins et al., 2008). The findings of this work indicate that CAPE can be used an effective add on treatment for a patient with UC to improve their intestinal barrier function and halt the progression of the disease while promoting mucosal healing. The next stage of our study will focus on the development of nanoparticle based colonic drug delivery of CAPE which could allow for local delivery of the drug to the inflamed tissue to ensure effective therapeutic outcome using a lower dose.

3.7 Conclusion

The data obtained after studying the anti-inflammatory activity of free CAPE in colitis induce mice reveals that free CAPE able to control the loss in weight produced by DSS. The mucosal layer of mice treated with CAPE was protected against inflammation. CAPE successfully lowers the primary factor responsible for ulcerative colitis such as overstimulated level of NF-kβ, HIF-1α and inflammatory cytokine. Therefore, furhter comparative investigation of anti-inflammatory therapeutic of free CAPE and CAPE nanoparticles in colitis induce mice will be the future study because this natural compound has limited solubility in aqueous media.

Chapter 4

Formulation and *in-vitro* evaluation of the anticancer properties of PIC-loaded albumin NP in colorectal cancer cell lines

4.1 Introduction

Cancer of colon ranks third among all type of cancer diagnosed in humans (Tosi et al., 2017., dos Reis et al., 2017). The exact cause of the malignancy has not yet been documented. However, it is believed that genetic mutation, environment, living habits and previous existence of UC are the pivotal factor of colorectal cancer (Aune et al., 2011., Favoriti et al., 2016., Broderick et al., 2017., Turner and Lloyd, 2017). Stomach ache, rectal bleeding, bowel obstruction, nausea, loss of appetite, weight loss, rectal pain, and lethargy are the early sign of colorectal cancer (Leiva et al., 2017). Colonoscopy screening is the widely used approached to detect colorectal cancer (Porté et al., 2017). However, this method is painful and difficult to perform in patients. Therefore, other techniques such as faecal occult blood tests, faecal immunochemical test (FIT) and stool DNA (sDNA) testing are some other effective method to diagnose colorectal cancer. These methods are inexpensive, non-invasive and easily operable (Martin et al., 2017). Chemotherapy (5-fluorouracil, paclitaxel, methotrexate, doxorubicin, and cyclophosphamide), immunotherapy (monoclonal antibodies, cytokine therapy,) radiation therapy and nutrition supplement based therapy (vitamins, minerals, proteins) are the mostly prescribed therapeutics in colorectal cancer (Hébuterne et al., 2014., Sathyanarayanan and Neelapu, 2015., Gustavsson et al., 2015., Wallis et al., 2016., Porté et al., 2017). These chemotherapies cause fatigue, vomiting, hair fall, infertility, anorexia, stomach cramp, bowel obstruction, bone marrow depletion and peripheral neuropathy (Saxena et al., 2016., (Hofheinz et al., 2017a). Monoclonal antibody prescribed in colorectal cancer damage mucosal layer. It also causes electrolyte disturbance, diarrhoea, skin rash, nail disorder and pruritus (Costa et al., 2017). Moreover, exposure to high dose of radiation (0.125 cGy/min) causes impairment to DNA in

healthy tissue (Rödel et al., 2015). These anticancer agents effect lifestyle and cause a burden on the financial condition of patients. The chronic mucosal inflammation is the common factor involved in both ulcerative colitis and colorectal cancer (Ma et al., 2017b., Guo et al., 2017). Overexpressed pro-inflammatory cytokines responsible for over induction of transcription factor nuclear factor kappa beta (NF-kβ) and hypoxia inducible factor-1α (HIF-1α) (Colotta et al., 2009b., Eissa et al., 2017). Due to overactivation of NF-kβ and HIF-1α, the event of proliferation, migration and invasion increases at the tumour site (Chaudary and Hill, 2007., Gupta et al., 2010a., Ben-Neriah and Karin, 2011). Additionally, pro-inflammatory cytokines have been documented to overexpress in ulcerative colitis and colorectal cancer patients which triggered aberrant activation of NF-kβ and HIF-1α (Herfarth et al., 2000., Malicki et al., 2009., Hegazy and El-Bedewy, 2010., Nathke and Rocha, 2011). The accumulation of NF-kβ and HIF-1α was reported in colorectal cancer cell line such as HT-29 and CaCo-2 (Tammali et al., 2011., Mastropietro et al., 2015., Ge et al., 2016., Owczarek et al., 2017). Therefore, inhibition of overstimulated NF-kβ and HIF-1α by natural compound may provide therapeutic cure in colorectal cancer and ulcerative colitis. Piceatannol is the natural compound which has anticancer and anti-inflammatory properties documented by several researchers (Seyed et al., 2016., Lu et al., 2017). Piceatannol exists in grapes, passion fruit, red wines and white tea (Lu et al., 2017). It arrests the unwanted growth of tumour cell in blood cancer, prostate cancer, breast cancer and rectal cancer (Piotrowska et al., 2012). Inhibition potential of PIC against NF-kβ and HIF-1α has been seen in different cancer cell lines (Piotrowska et al., 2012., Zhang et al., 2014., Song et al., 2015., Seyed et al., 2016). However, PIC is low soluble in water and less absorbable in the intestine which alters its therapeutic potential (Kwon et al., 2012., Inagaki et al., 2016). Therefore,

fabrication of PIC-loaded albumin nanoparticle was carried out to overcome the limited solubility and absorption to facilitate the efficacy of PIC. Desolvation method has been employed to formulate albumin nanoparticles of PIC. This method has been widely used to fabricate nanoparticles of natural polyphenolic compound (Elzoghby et al., 2012b., Tarhini et al., 2017). Albumin has been incorporated in the formulation of PIC nanoparticles due its low toxic, low immunogenisity and biodegradable nature (Fallacara et al., 2017., Liu et al., 2017., Louage et al., 2017). It increases the gastric residence time and enhance the accumulation of hydrophobic drug at the tumour site (Dennis et al., 2002). Albumin is attracted to inflammatory markers and supply amino acid at tumour site which provide a target delivery to anticancer compound (Larsen et al., 2016., Jiang et al., 2017).

Therefore, based on the accumulating evidence PIC nanoparticles was fabricated using albumin to improve solubility, bioavailability, efficacy and targeting potential of PIC nanoparticles by desolvation method.

4.2 Summary

Based on the severity of colorectal cancer and associated side effects with commonly prescribed therapeutics, there is a significant urgency to utilize natural compound for the treatment and management of colorectal cancer. The natural compound PIC needs to reduce particle size to attain higher therapeutic value by increasing the solubility. Therefore, nanotechnology can be employed with aid of natural polymer to provide targeted delivery of natural nanoparticles.

4.3 Hypothesis

In the current chapter, we hypothesize that the reductions of particle size of natural compound PIC will improve the anticancer property to a higher extent than the free PIC.

4.4 Aims and objectives

- Formulation of PIC-loaded albumin nanoparticles
- Optimisation of PIC-loaded albumin nanoparticles
- Evaluation of anticancer properties of PIC-loaded albumin nanoparticles in CaCo-2 and HT-29 cell lines

4.5 Results

4.5.1Calibration of PIC

Calibration curve of PIC was plotted as shown in the Figure 4.1 in methanol (1:9) and absorbance was measured at 325 nm.

4.5.2 Effect of ethanol amount

PIC-loaded albumin NP was fabricated by the method described in section 2.3. The effects of physiochemical factor such as the amount of ethanol were evaluated. PIC-loaded albumin NP was fabricated with 4 ml, 8 ml and 12 ml of ethanol. However, increase in ethanol amount has no effect on particle size (Figure 4.2A) as well as the polydispersity index (Figure 4.2B). A similar pattern of observation was also documented by Langer et al (Langer et al., 2003b). The particle size was found to be in the range 227 nm to 238 nm and the polydispersity index was in the range of 0.154 to 0.172. Though, zeta potential (Figure 4.2C) shows a slight decrease in value from -13 mV to -18 mV. (Ardani et al.).

4.5.3 Effect of albumin concentration

Albumin attracts to neutrophils, provides amino acid to tumour cells, easily digest by serum and does not yield any detrimental effect (Abbasi et al., 2012., Elzoghby et al., 2012a., Zhao et al., 2017). PIC-loaded albumin NP was formulated with a different concentration of albumin to observe its effect on parameters such as particle size, polydispersity and zeta potential. A significant increase in particle size (Figure 4.3A) was reported with an increase in albumin content in the formulation. Similarly,

June et al also documented an increase in particle size with increase in albumin concentration (Jun et al., 2011). The formulation batches show a significant increase in particle size from 211 nm to 252 ($P<0.01$) when albumin content increases from 0.5% to 2%. It further increases significantly to 294 ($P<0.001$) as the concentration of albumin increases to 3.5%. Similarly, polydispersity index (Figure 4.3B) increases significantly from 0.11 to .27 ($P<0.001$) with an increase in albumin ratio. Additionally, zeta potential (Figure 4.3C) also increases from -19 mV to -12 mV upon increasing the albumin content.

4.5.4 Effect of Glutaraldehyde concentration

Increasing amount of crosslinking agent (glutaraldehyde) was used from 4% to 12% to study its effect on particle size, polydispersity index and zeta potential. As depicted in Figure 4.4, increase in the concentration of glutaraldehyde increases particle size (Figure 4.4A). Rajith et al., 2014 also demonstrated the same pattern of increase in particle size as glutaraldehyde concentration increases (Rajith and Ravindran, 2014). Particle size increases significantly ($P<0.05$) from 225 nm to 257 nm and from ($P<0.001$) 257nm to 391nm. Though, an increase in glutaraldehyde concentration had an inverse effect on polydispersity index (Figure 4.4B), also documented by (Langer et al., 2003b). Polydispersity index decreases significantly ($P<0.001$) from 0.20 to 0.14 but it slightly changes with a further increase in glutaraldehyde concentration. However, zeta potential (Figure 4.4C) shows significant ($P<0.01$) decrease from -13 mV to -18 mV as glutaraldehyde concentration increases. Li et al also stated the similar effect of glutaraldehyde increase on zeta potential (Li et al., 2008a).

4.5.5 Effect of drug content

The effect of drug content was studied on particle size, polydispersity index and zeta potential. PIC-loaded albumin NP was formulated with 10 mg, 20 mg and 30 mg of PIC. A significant increase in particle size (Figure 4.5A) was detected upon increasing the drug amount. This increase in particles size may arise due to increase amount of drug which increases the viscosity of drug solution. Halayqa et al documented the increase in particle size as the drug amount increases due increase in viscosity of solvent (Halayqa and Domańska, 2014). The Figure 4.5A shows significant ($P<0.001$) increased in particle size from to 210 nm to 257 nm as the amount of drug increased from 10 mg to 20 mg. Similarly, particle size significantly ($P<0.05$) increased to 288 when drug content increased to 30 mg. The polydispersity index significantly ($P<0.01$) increased from 0.11 to 0.18 as drug amount increases as shown in the Figure 4.5B. Likewise, zeta potential (Figure 4.5C) significantly ($P<0.001$) increases from -20 mV -8 mV to with increased PIC amount in the formulation.

4.5.6 NMR spectra of PIC-loaded albumin NP

The 1H NMR study (in DMSO-d6) of PIC in albumin nanoparticles revealed that the signal due four hydroxyl groups appeared as a broad spectrum (brs) around 9.1 ppm whereas the two trans olefinic protons a and b resonates at around 6.87 and 6.75 ppm respectively. The four singlet aromatic protons (d,f,g,h) appears at around 6.96, 6.71, and 6.11 respectively. These data confirmed the PIC in albumin nanoparticles structure as shown in Figure 4.6.

4.5.7 Entrapment efficiency

Entrapment efficiency was determined by the procedure given in section 2.6. The influence of albumin concentration and drug content was studied on entrapment efficiency. Figure 7 represents the pattern of entrapment efficiency of PIC-loaded albumin NP which shows significant ($P<0.01$) increase in entrapment efficiency as the concentration of albumin increases as shown in Figure 4.7A. A similar trend of increase in entrapment was reported by (Ganesh et al., 2015)**.** Significant ($P<0.01$) increase in entrapment efficiency (approximately 65%) was seen of as the albumin content increases from 0.5% to 2%. However, it was found to be 64% when albumin concentration increases to 3.5%. Figure 4.7B demonstrates significant ($P<0.01$) decrease in entrapment efficiency from 60% to 39% as the content of drug increases to 30 mg (approximately 39%). This implies that an increase in drug amount decreases the entrapment efficiency because the higher amount of drug requires more amount of albumin to encapsulate. The similar pattern of entrapment was reported by (Sebak et al., 2010).

4.5.8 Percentage yield

Percentage yield was calculated from the equation given in section 2.7. The effect of albumin concentration and drug content was evaluated on percentage yield. Figure 4.8A represents an increase in percentage yield upon an increase in albumin content in the formulation. Percentage yield increased significantly ($P<0.05$) from 50% to 64% when albumin concentration increased from 0.5% to 2%. However, there is a slight increase in yield as the albumin concentration increased in the formulation to 3.5%. This increase in percentage yield may be due to the availability of more

amount of albumin for the same amount of PIC. A similar trend of percentage yield can be seen in the Figure 4.8B where percentage yield increase ($P<0.05$) from 42% to 67% when drug amount increases. It slightly increases to 68% when amount of drug increases to 30 mg. Kılıçarslan and Baykara also reported the same pattern of percentage yield on increasing amount of drug (Kılıçarslan and Baykara, 2003).

4.5.9 In-vitro release

The release study of PIC nanoparticles was as carried out as described in section 2.8. PIC nanoparticles were formulated with a 0.5%, 2% and 3.5% concentration of albumin. These batches show burst release of PIC from nanoparticles after 24 hours as shown in the Figure 4.9A. It was noted that increase amount of albumin decreases the release of PIC from nanoparticles. The release of 34%, 29% and 22% was documented after 24 hours in these batches. Moreover, 70%, 62% and 55% release of PIC was reported after 168 hours. Increase in particles size may cause a decrease in release due to increase in albumin content. Increase in albumin concentration contributes to decrease in the *in-vitro* release of drug was also demonstrated by (Jenita et al., 2014). The effect of the increased amount of PIC from 10 to 30 mg on release profile was evaluated. Burst release of PIC from nanoparticle was noticed as expressed in the Figure 4.9B. After 24 hours 50%, 37% and 32% release of PIC was reported. After 168 hours the PIC release was 77%, 63% and 50% in batches formulated with 10 mg, 20 mg and 30 mg of PIC. A similar trend of release was documented by (Azizi et al., 2017). Rapid dissolution of PIC present on the surface of albumin may cause the burst release in the dissolution media.

4.5.10 Solubility of PIC-loaded albumin NP

The solubility of PIC-loaded albumin NP was determined by the method given in section 2.9. The apparent water solubility of PIC in both free and encapsulated form was determined by UV-spectroscopy at 325 nm. The vials in Figure 4.10A depict the enhanced solubility of PIC when formulated as PIC-loaded albumin NP vs free PIC (10B) in water. It is evident from the figures that tube A produces a uniform dispersion of PIC-loaded albumin NP as shown in Figure 4.10A, whereas free PIC was sparingly soluble as shown in Figure 4.10B. The tube B in the Figure 4.10 shows turbidity and particles whereas tube A shows the clear solution. The solubility of the free PIC was 17.87 µg/ml, whereas that of PIC-loaded albumin NP was 29.26 µg/ml, which represented an approximate increase in aqueous solubility of PIC-loaded albumin NP double as compared to the free PIC as shown in 4.10B absorbance spectra of PIC-loaded albumin NP and free PIC.

4.5.11 Scanning electron microscopy

The sample for SEM was prepared by the method mentioned in the section 2.10. Figure 4.11 represents the SEM images of the free PIC and different batches of nanoparticles such as F1 (PIC 10 mg), F2 (PIC 20 mg) and F3 (PIC 30 mg). The free PIC represents the random and solid structure of drug whereas as the nanoparticles images shows spherical and smooth surface. Image F1 demonstrate monodisperse and smooth textured appearance in the Figure 4.11. However, image F2 and F3 show larger particle size and partially disperse texture in the Figure 4.11. Therefore, from the above SEM images, it can be concluded that increase in drug content increases

the particle size of nanoparticles. Thus, to achieve intracellular targeting smaller particle size ranging from 0.1µ to 100nm is desirable (De Jong and Borm, 2008).

4.5.12 Cellular uptake of PIC-loaded albumin NP

The HT-29 and CaCo-2 cell were incubated with PIC-loaded albumin NP for cellular uptake as described in the section 2.12. The nucleus image of cell and uptake of nanoparticle was taken under phase contrast microscope for CaCo-2 and HT-29 cells. Image F1 in the Figure 4.12(A and B) represent CaCo-2 and HT-29 cells with no treatment. Image F2 in the Figure 4.12(A and B) shows CaCo-2 and HT-29 cells treated with Nile Red coated PIC-loaded albumin NP. The images in F1 depicts nucleus without any treatment, however, images in F2 exhibit nanoparticles labeled with Nile Red observed under the microscope in both the Figure 4.12(A and B). The merged images in F1 as shown in the Figure 4.12(A and B) represent nucleus only although fluorescent nanoparticles can be seen around the nucleus in F2 of Figure 4.12(A and B) of both the merged images.

4.5.13 In-vitro cytotoxicity assay

The cytotoxicity study was performed by methods as described in the section 2.13. The cytotoxic assay was executed to evaluate cell viability as described by (Kumar et al., 2014) for free PIC and PIC-loaded albumin NP. The assay was done by MTT dye for a period of 24, 48, 72, and 96 hours. The blank nanoparticles had no cytotoxicity in colorectal cancer cell lines such as CaCo-2 and HT-29 as evident from the Figure 4.13(A and B). The graphs in Figure 4.13(A and B) exhibit dose

dependent response to cytotoxicity. The cell viability was reported to be low (65%) in PIC-loaded albumin NP than the free PIC (74%) in CaCo-2 after 24 hours of incubation at dose of 7.5 μg/ml. Similarly, cell viability was found to be 35% in PIC-loaded albumin NP and 52% in free PIC after 96 hours of treatment at same dose. Moreover, cell viability was noticed to be 57% in PIC-loaded albumin NP and 75% in free PIC after 24 hours in HT-29 cells at dose of 7.5 μg/ml. Similarly, it was 32% in PIC-loaded albumin NP and 42% in free PIC after 96 hours of treatment in HT-29 at same dose.

PIC-loaded albumin NP sustained the cytotoxic action of the free drug due to the enhanced penetration and retention effect inside the colorectal cells (Patil et al., 2009) (Chavanpatil et al., 2006). It also enhanced the solubility which in turn enhances the half-life and bioavailability (Mittal et al., 2007., Anand et al., 2010) due to a reduction in particle size of PIC. Therefore, based on the above data it can be concluded that PIC-loaded albumin NP improves the cytotoxicity potential due to a reduction in particle size, which suggest that albumin nano-particulate formulation enhances the biological therapeutic efficacy of PIC over the free PIC.

4.5.14 Migration assay

The migration study was carried out in CaCo-2 and HT-29 as stated in the section 2.14. Like other tumour cells, colon cancer cells also migrate from one side to another (Friedl and Wolf, 2003., Qi et al., 2015). Thus, anti-migration potential of free PIC and PIC-loaded albumin NP was assessed in CaCo-2 and HT-29. These cell lines were transfected with 7.5 μg/ml free PIC and PIC-loaded albumin NP. Figure 4.14 and 4.15 display the evaluation of the degree of wound closure in CaCo-2 and

HT-29 cells. The PIC-loaded albumin NP treated groups in microscopic Figures 4.14A and 4.15A show greater void space than free PIC treated cells. About 77% ($p<0.001$) of void space was reported in CaCo-2 upon treatment with 7.5 µg/ml of PIC-loaded albumin NP compare to control. Although, 80% ($p<0.01$) of void space was observed when treated with free PIC closure as shown in Figure 4.14B. Likewise, PIC-loaded albumin NP shows a significant reduction in wound closure when transfected with the same amount of nanoparticles as compare to free drug in HT-29. Approximately, 74% ($p<0.001$) of clear space was noticed when HT-29 treated with PIC-loaded albumin NP whereas, free PIC demonstrates only 78% of wound opening as shown in Figure 4.15B of the graph. Thus PIC-loaded albumin NP shows strong inhibition of migration of the tumour cells in both cell lines, but the free PIC has less efficiency against migration of cancer cell in both cell lines. Therefore, albumin nanoparticles have high efficiency against migration of cancer cells to prevent metastasis of colon cancer cell lines.

4.5.15 Colony formation assay

The colony formation assay was performed according to procedure stated in Section 2.15. A colony formation study was performed to determine and compare the long-term anticancer activity of free PIC and PIC-loaded albumin NP as reported previously (Yeung et al., 2010) in CaCo-2 and HT-29 cells. The cells were transfected with 7.5 µg/ml of PIC-loaded albumin NP and same amount of free PIC. After 7 days the number colonies form were measured in control, blank NP, free PIC and PIC-loaded albumin NP treated group under stereo zoom Nikon microscopy as shown in Figure 4.16A and 4.17A. The colony formed in healthy cells and cells

treated with blank nanoparticles do not have any significant difference as shown in the microscopic image. The number of colonies grown in cell treated with 7.5 µg/ml of PIC-loaded albumin NP (10) was significantly ($P<0.01$) less as compare to the free PIC (27) in CaCo-2 cells as depicted in the graph 4.16B. Similarly, a total number of colonies were found to be significantly less (15) upon transfection with PIC-loaded albumin NP than an equivalent amount of free PIC (41) in HT-29 cells as represented in the graph 4.17B.

4.5.16 Invasion assay

The protocol for invasion assay was followed as stated in the 2.16. The effect of PIC-loaded albumin NP on invasion activity of colorectal cancer cell lines such as CaCo-2 and HT-29 was assessed as reported by (Yuen et al., 2013). Both the colorectal cancer cell line was transfected with 7. 5 µg/ml of PIC-loaded albumin NP and the corresponding amount of free PIC. The efficiency of PIC-loaded albumin NP was significantly ($p<0.01$) greater than free PIC as illustrated in the microscopic images of Figure 4.18A) and Figure 4.19A in both cell lines. The inhibition of invasion was significantly ($p<0.001$) lesser (38 %) when CaCo-2 cells transfected with PIC-loaded albumin NP as compare to the free PIC (51%) as shown in the graph of Figure 4.18B. Additionally, PIC-loaded albumin NP depicts increase efficiency against invasion than the free PIC in HT-29 as presented in the graph of Figure 4.19B. Cell invasion was reported to significantly less ($p<0.05$) in PIC-loaded albumin NP group (34%) than the free PIC (57%) in HT-29 cells. Thus, according to the above data PIC-loaded albumin NP is more effective against the invasion of

CaCo-2 and HT-29 because PIC-loaded albumin NP restored and enhanced the anti-invasion therapeutic efficiency.

4.5.17 Immunostaining of p65

The fluorescent images of CaCo-2 (20A) and HT-29 (21A) were captured under bright field microscopy after staining cells with p65 antibody as stated in the Section 2.17. Both the cell line was treated with 7.5 µg/ml dose of PIC-loaded albumin NP and an equivalent amount of free PIC. The induced level of NF-kβ such as p65 can be noticed in the control and blank NP as shown in the microscopic images of Figure 4.20A and Figure 4.21A. However, the group was treated with free PIC and PIC-loaded albumin NP shows a noticeable difference in the level of p65 in the Figure 4.20B and Figure 4.21B. The graphs in the Figure 4.20B (CaCo-2) and Figure 4.21B (HT-29) demonstrate a higher level of p65 in control and blank NP groups. PIC-loaded albumin NP depicts the significantly low level of p65 protein than blank nanoparticles. The expression of p65 in PIC-loaded albumin NP transfected cells was significantly ($P<0.01$) lower than a free PIC transfected cell in CaCo-2 (C). Similarly, PIC loaded nanoparticles decrease the p65 expression significantly ($P<0.001$) than free PIC in HT-29 (D).

4.5.18 Immunostaining of HIF-1α

The Caco-2 (A) and HT-29 (B) were stained with HIF-1α antibody and observed under bright field microscopy to study the effect of PIC treatment as stated in section 2.17. The CaCo-2 and HT-29 cell line were treated with 7.5 µg/ml dose of PIC-

loaded albumin NP and an equivalent amount of free PIC. The plates were incubated for 24 hours and the level of HIF-1α was observed under a microscope. The increased expression of HIF-1α was reported as shown in images of Figure 4.22A (CaCo-2) and Figure 4.22B (HT-29). The overstimulated expression of HIF-1α was found in control and cells transfected with blank NP in both cell lines as depicted in the Figure 22A and 22B. Also, the group was treated with free PIC and PIC-loaded albumin NP show a noticeable difference in the level of HIF-1α as represented in Figure 4.22(A and B).

4.5.1Calibration of PIC

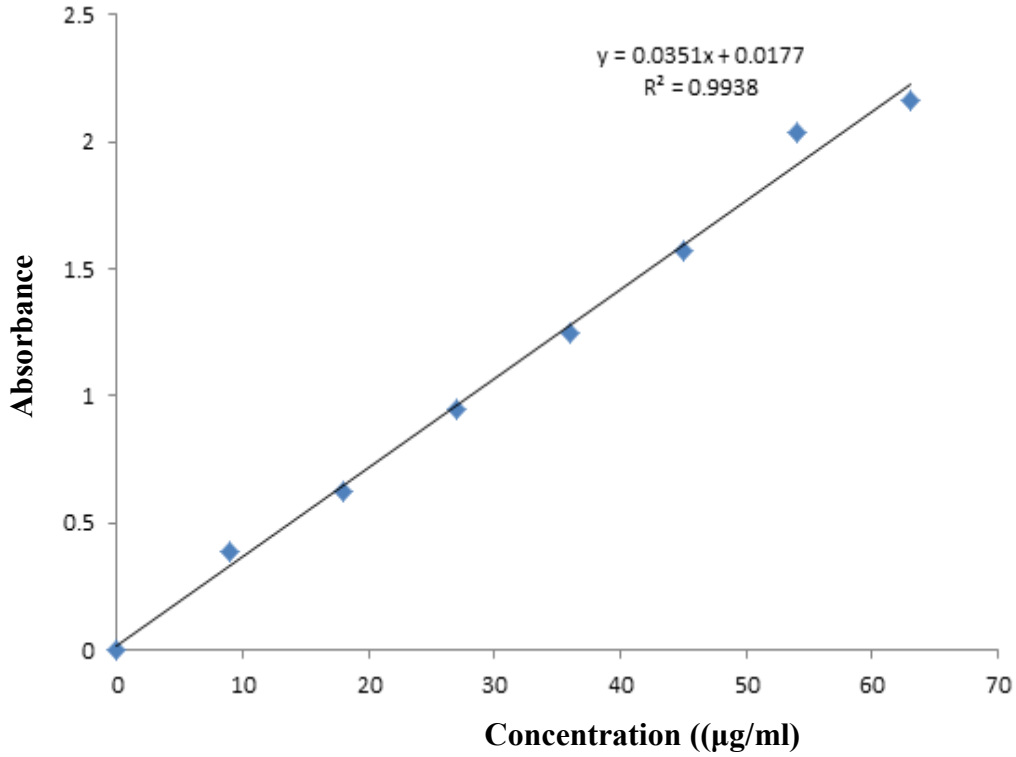

Figure 4.1: Calibration curve of PIC

4.5.2 Effect of ethanol amount

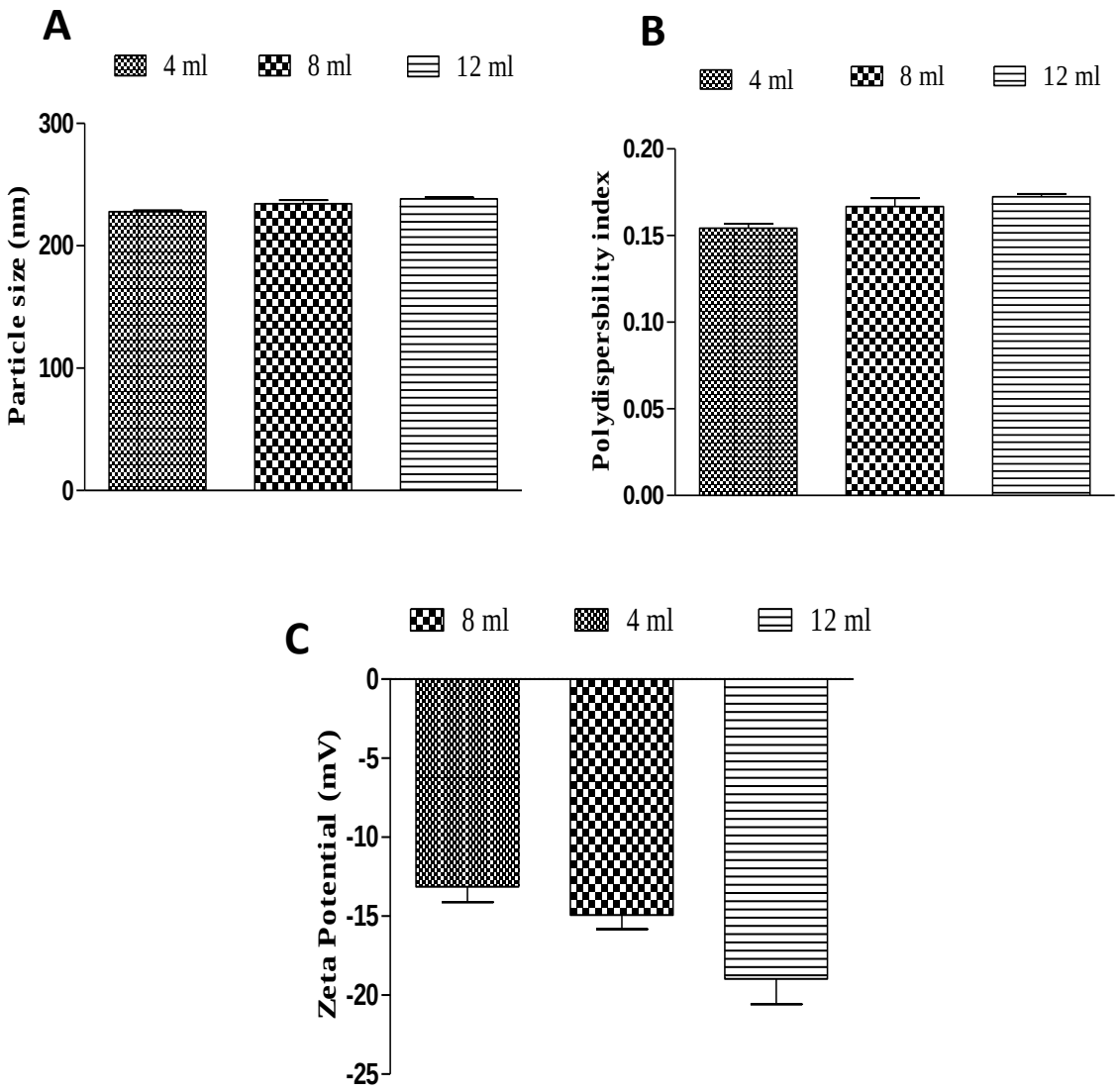

Figure 4.2: Effect of ethanol amount on particle size (A), polydispersity index (B) and zeta potential (C). The above graph shows the effect of ethanol amount on Particle size (A), polydispersity index (B) and zeta potential (C). It was reported that ethanol amount does not have any significant effect on particle size, polydispersity index and zeta potential. Values are mean ± SEM (n = 3).

4.5.3 Effect of albumin concentration

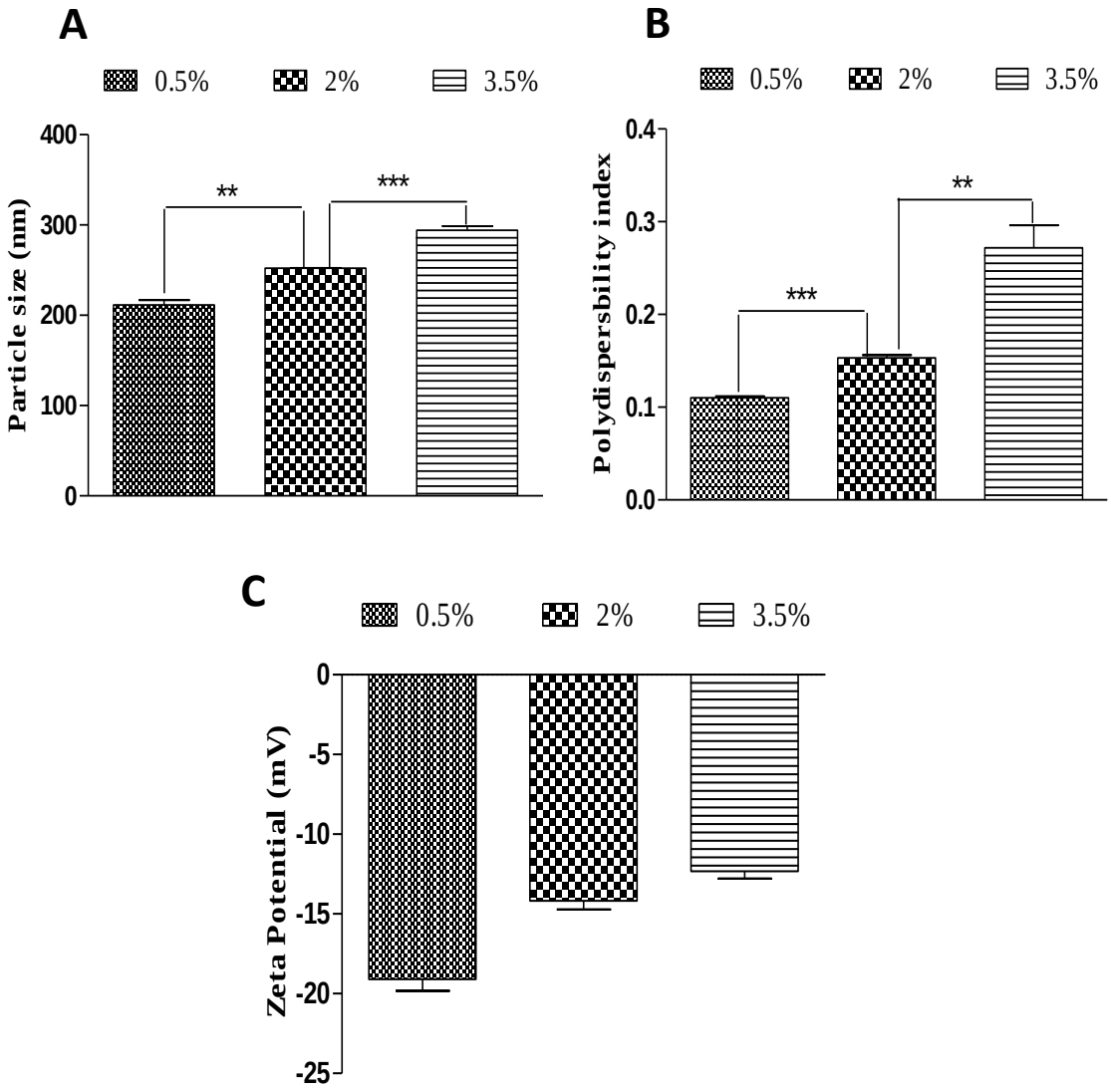

Figure 4.3: Effect of albumin concentration on particle size (A), polydispersity index (B) and zeta potential (C). The above graph represents the effect of increasing albumin concentration on Particle size (A), polydispersity index (B) and zeta potential (C). It was demonstrated that increase in albumin concentration leads to increase in particles size (A) as well as the polydispersity index (B) significantly ($P<0.001$). Polydispersity increases significantly when albumin concentration increases from 0.5% to 2%. However, it does not have any significant effect on zeta potential. Values are mean ± SEM (n = 3), **$P<0.01$ and ***$P<0.001$.

4.5.4 Effect of Glutaraldehyde concentration

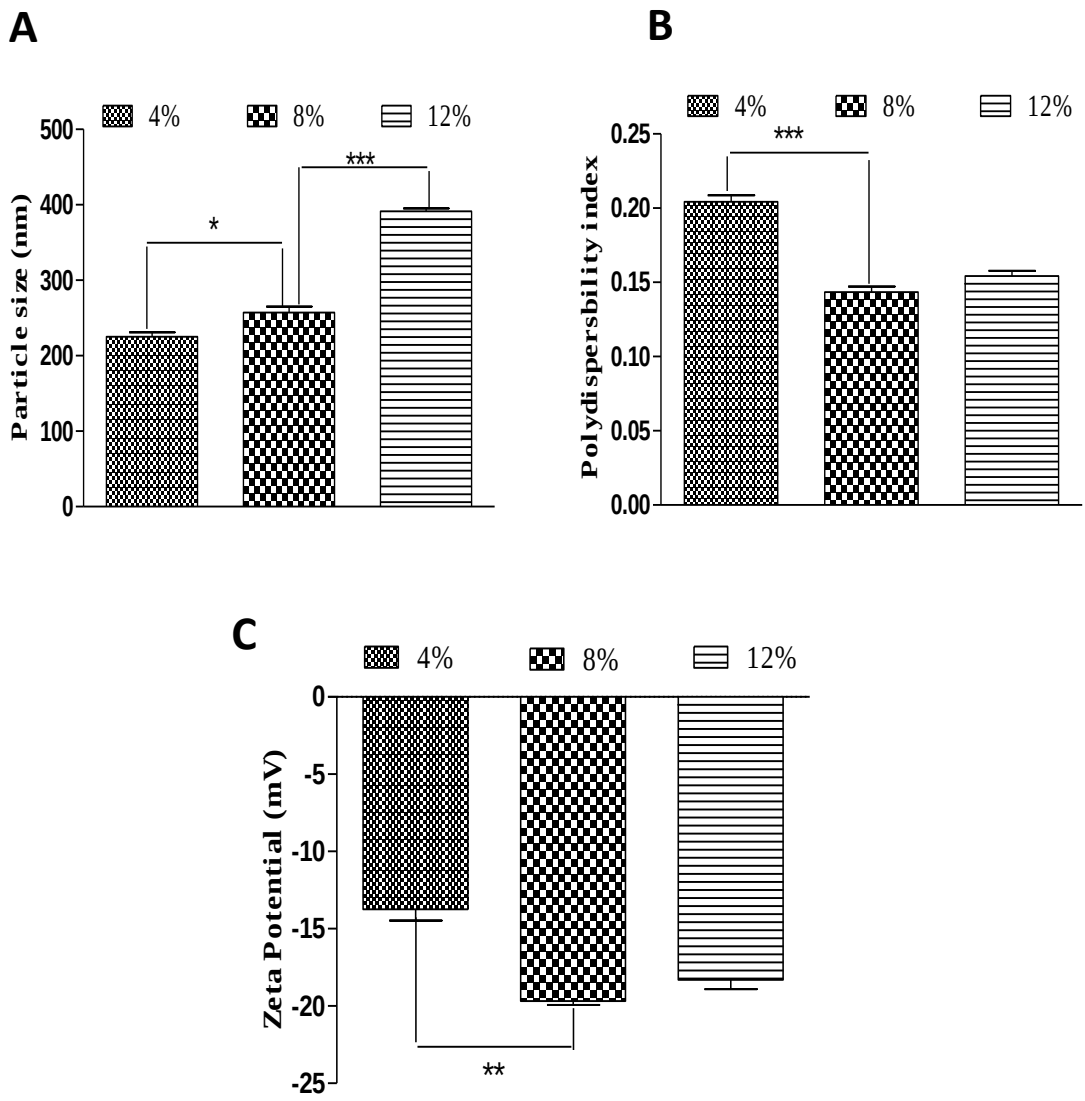

Figure 4.4: Effect of increasing concentration of glutaraldehyde on particle size (A), polydispersity index (B) and zeta potential (C). The above graph represents the effect of an increase in glutaraldehyde concentration on Particle size (A), polydispersity index (B) and zeta potential (C). It was evident from the graph that glutaraldehyde concentration increases particle size significantly ($P<0.001$) when it increases from 4% to 12%. However, polydispersity index decreases significantly ($P<0.001$) upon an increase in glutaraldehyde concentration but later it does not have any effect on PDI. Similarly, increase in glutaraldehyde concentration causes a significant ($P<0.01$) decrease in zeta potential initially. Values are mean ± SEM (n = 3). *$P<0.05$, **$P<0.01$, and ***$P<0.001$.

4.5.5 Effect of drug content

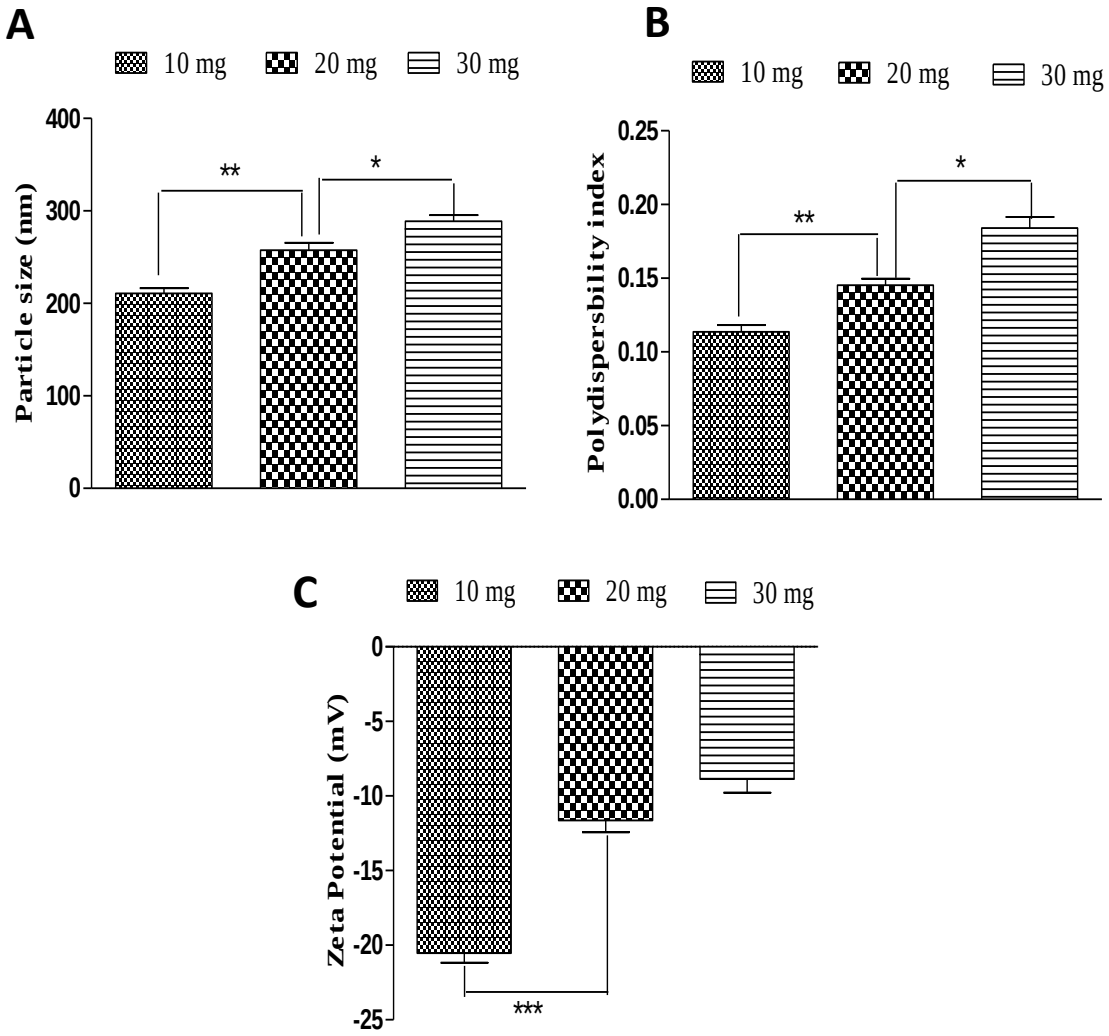

Figure 4.5: Effect of increase in drug amount on particle size (A), polydispersity index (B) and zeta potential (C). The above graph shows the effect of drug amount on Particle size (A), polydispersity index (B) and zeta potential (C). It is evident from the above graph that increases in PIC amount significantly ($P<0.01$) increase the particle size and PDI. Similarly, zeta potential increases significantly ($P<0.001$) upon an increase in PIC amount. Values are mean ± SEM (n = 3). *$P<0.05$, **$P<0.01$ and ***$P< 0.001$.

4.5.6 NMR spectra of PIC-loaded albumin NP

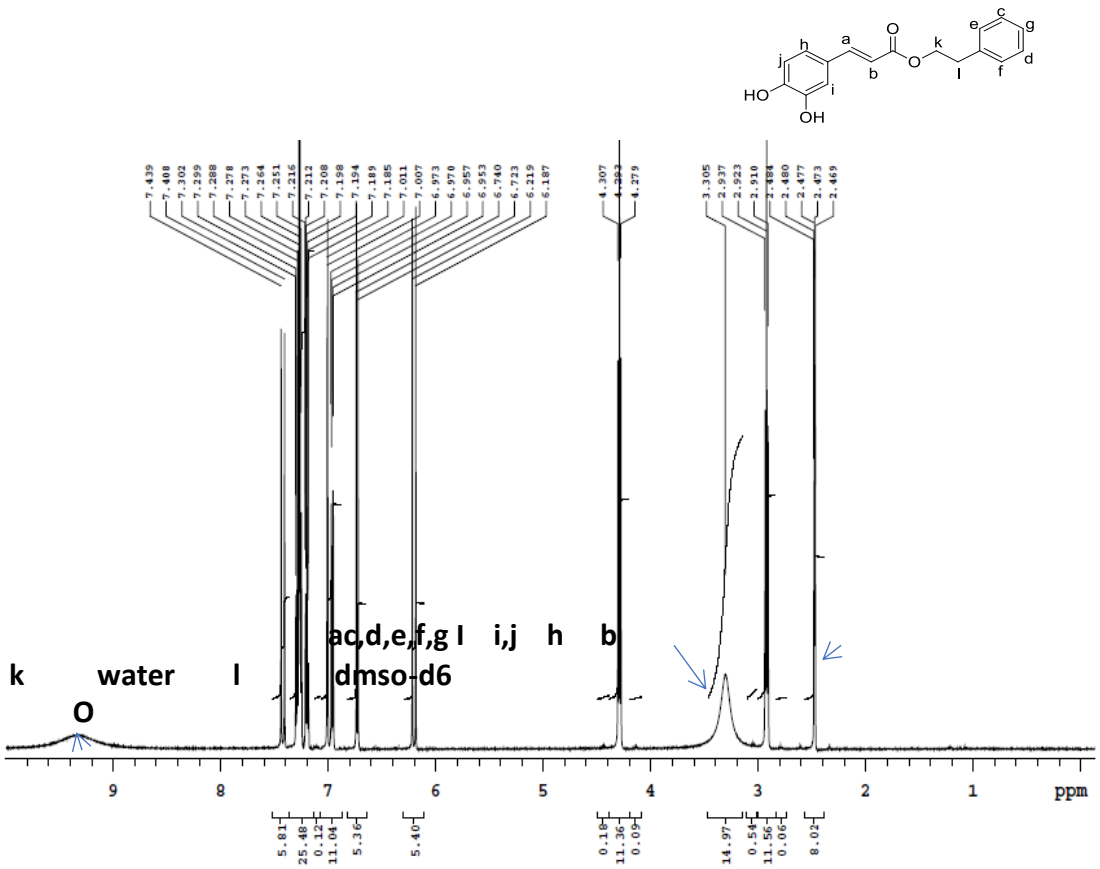

Figure 4.6: H NMR of piceatannol pf albumin nanoparticles. The above H NMR confirms the piceatannol stucture in the nanoparticle form.

4.5.7 Entrapment efficiency

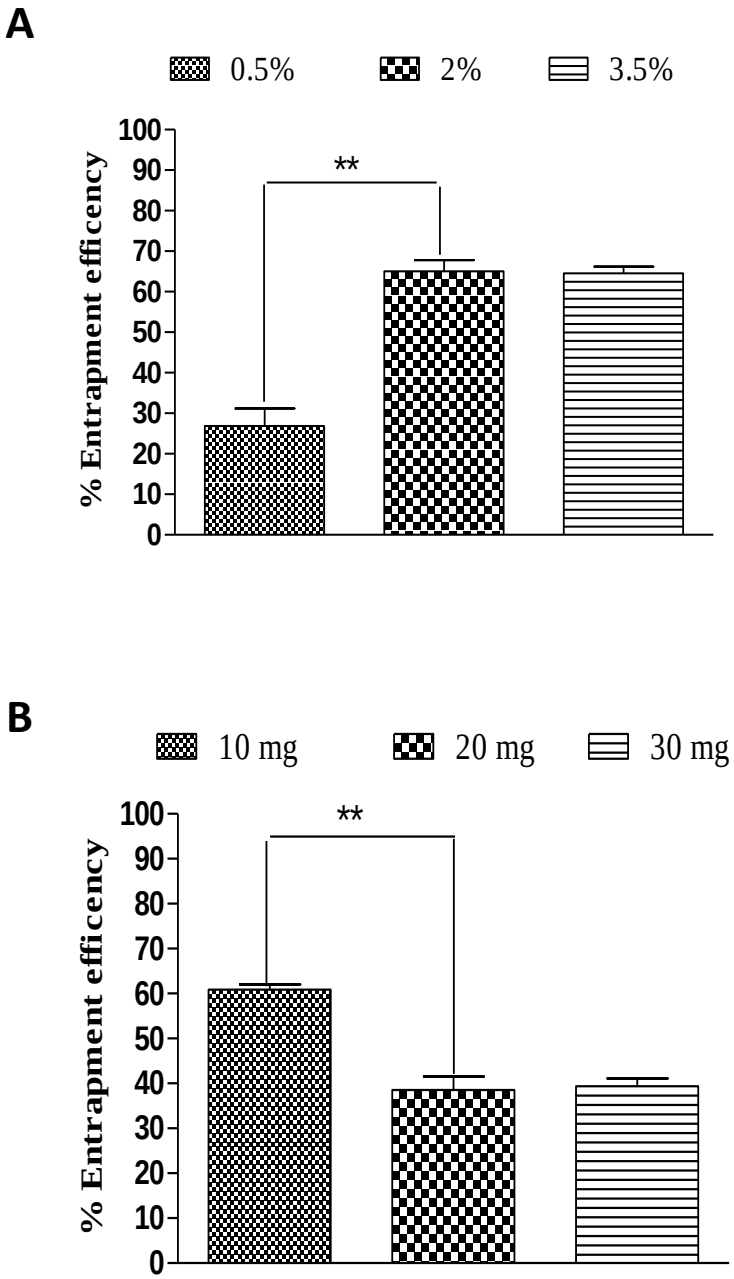

Figure 4.7: Effect of albumin concentration (A) and drug amount (B) on entrapment efficiency. The above graph demonstrates effect albumin concentration (A) and drug content (B) on entrapment efficiency. Figure 4.7A in the above graph show a significant difference ($P<0.01$) when albumin concentration increases from 0.5% to 2%, however, entrapment efficiency slightly increase upon further increase in albumin concentration. Figure 4.7B in the above graph illustrates the significant decrease in entrapment efficiency ($p<0.01$) as the drug amount increases from 10 mg to 20 mg but it does not have any significant effect when further increases to 30 mg. Values are mean ± SEM (n = 3). **P<0.01.

4.5.8 Percentage yield

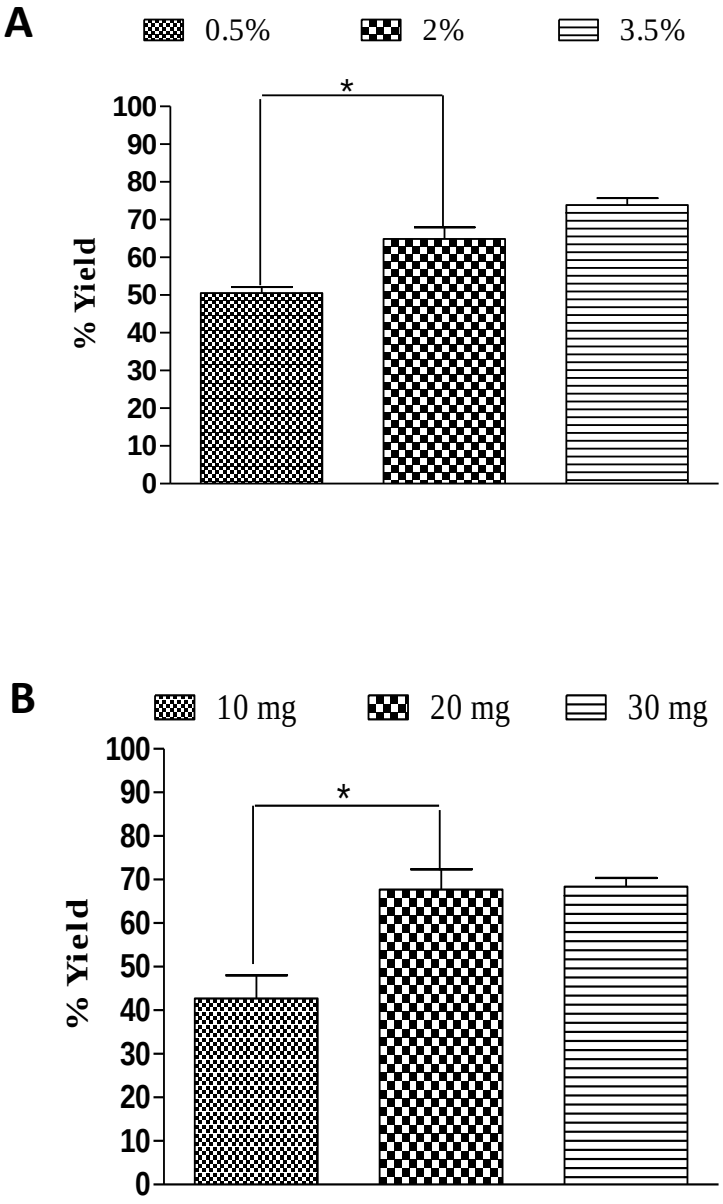

Figure 4.8: Effect of albumin concentration (A) and drug amount (B) on percentage yield. The above graph represents effect albumin concentration (A) and drug content (B) on percentage yield. Figure 4.8A in the above graph reveal a significant difference ($P<0.05$) when albumin concentration increases from 0.5% to 2% although percentage yield slightly increases upon further increase in albumin concentration. Figure 4.8B in the above graph express no significant difference ($P<0.05$) as the amount of drug increases. Values are mean ± SEM (n = 3). *$P< 0.05$.

4.5.9 In-vitro release

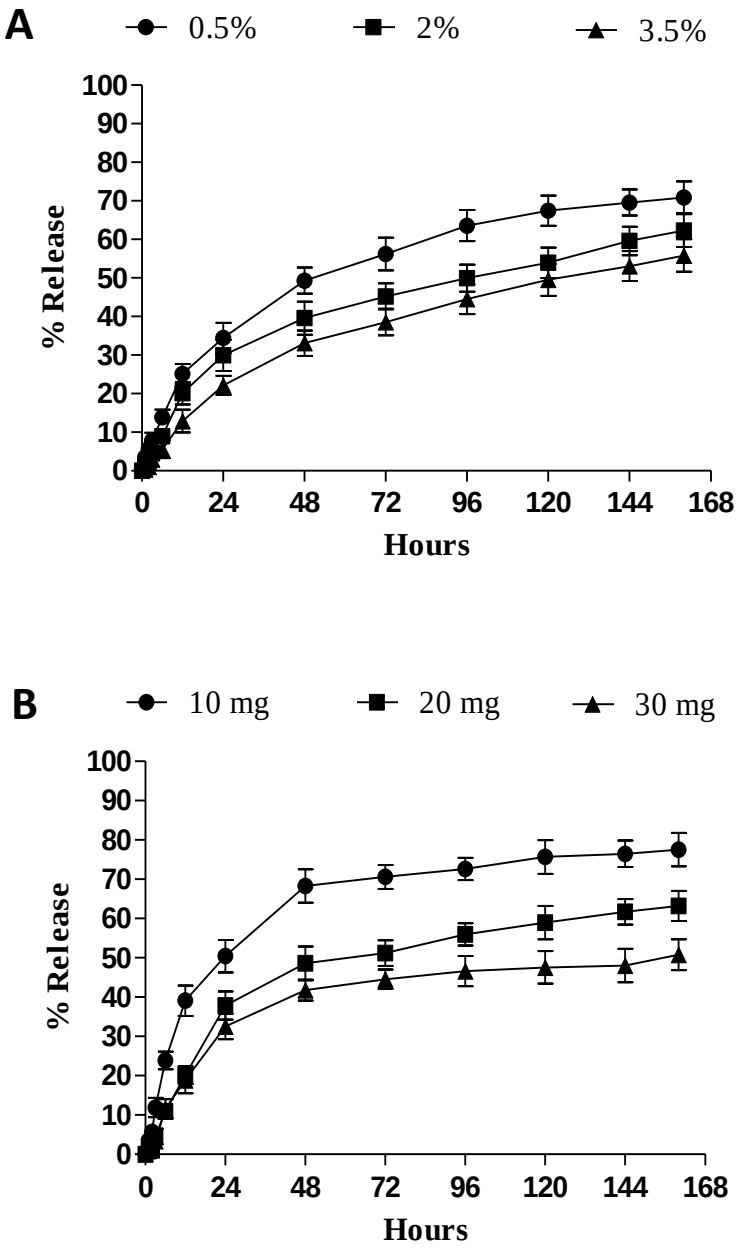

Figure 4.9: effect of albumin concentration (A) and drug amount (B) on *In-vitro* release profile. The above graph illustrates burst release after 24. The above graph depicts that increase in albumin and drug concentration leads to decrease the *in-vitro* of PIC release from the formulation. Values are mean ± SEM (n = 3).

4.5.10 Solubility of PIC-loaded albumin NP

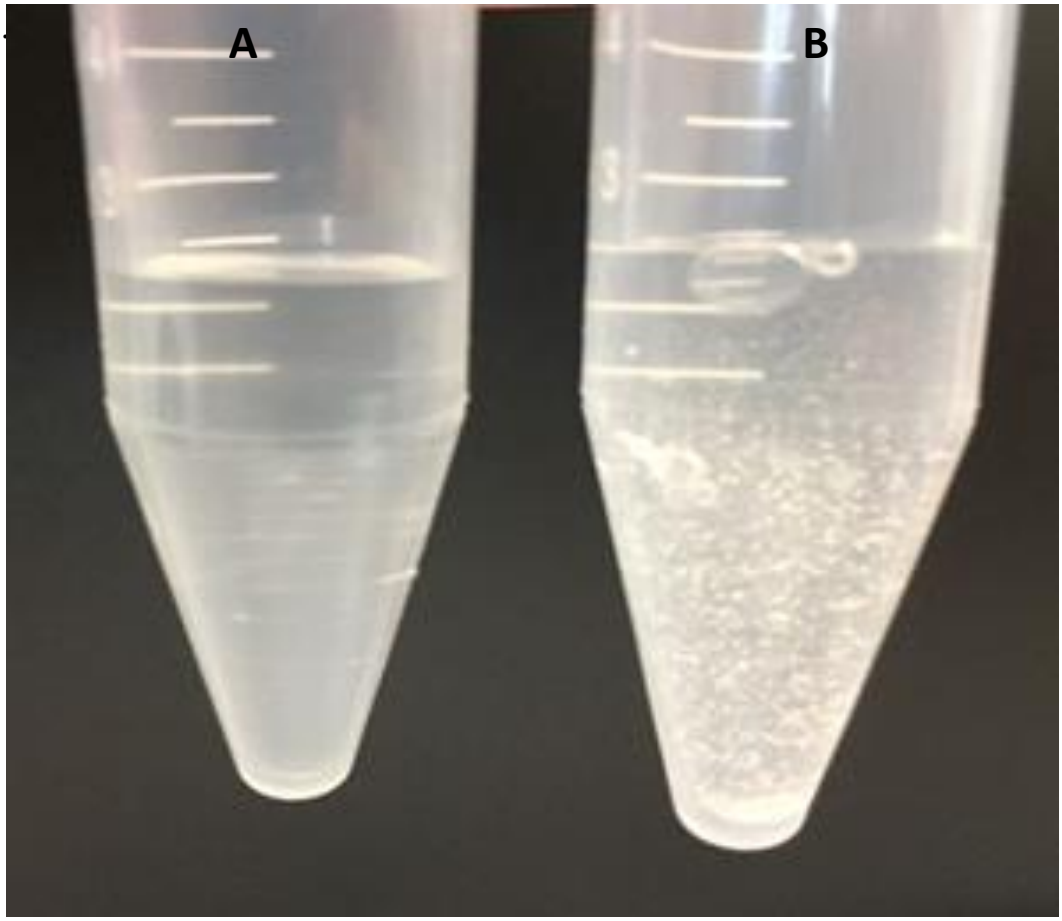

Figure 4.10: water solubility of PIC-loaded albumin NP (A) and free PIC (B). The vials in the Figure 4.10(A and B) show the solubility of PIC-loaded albumin NP and free PIC, respectively. A Clear solution of PIC-loaded albumin NP in Figure A and turbid free PIC in Figure 10B can be observed above. Figure 10A indicates enhance in solubility of PIC-loaded albumin NP.

4.5.11 Scanning electron microscopy

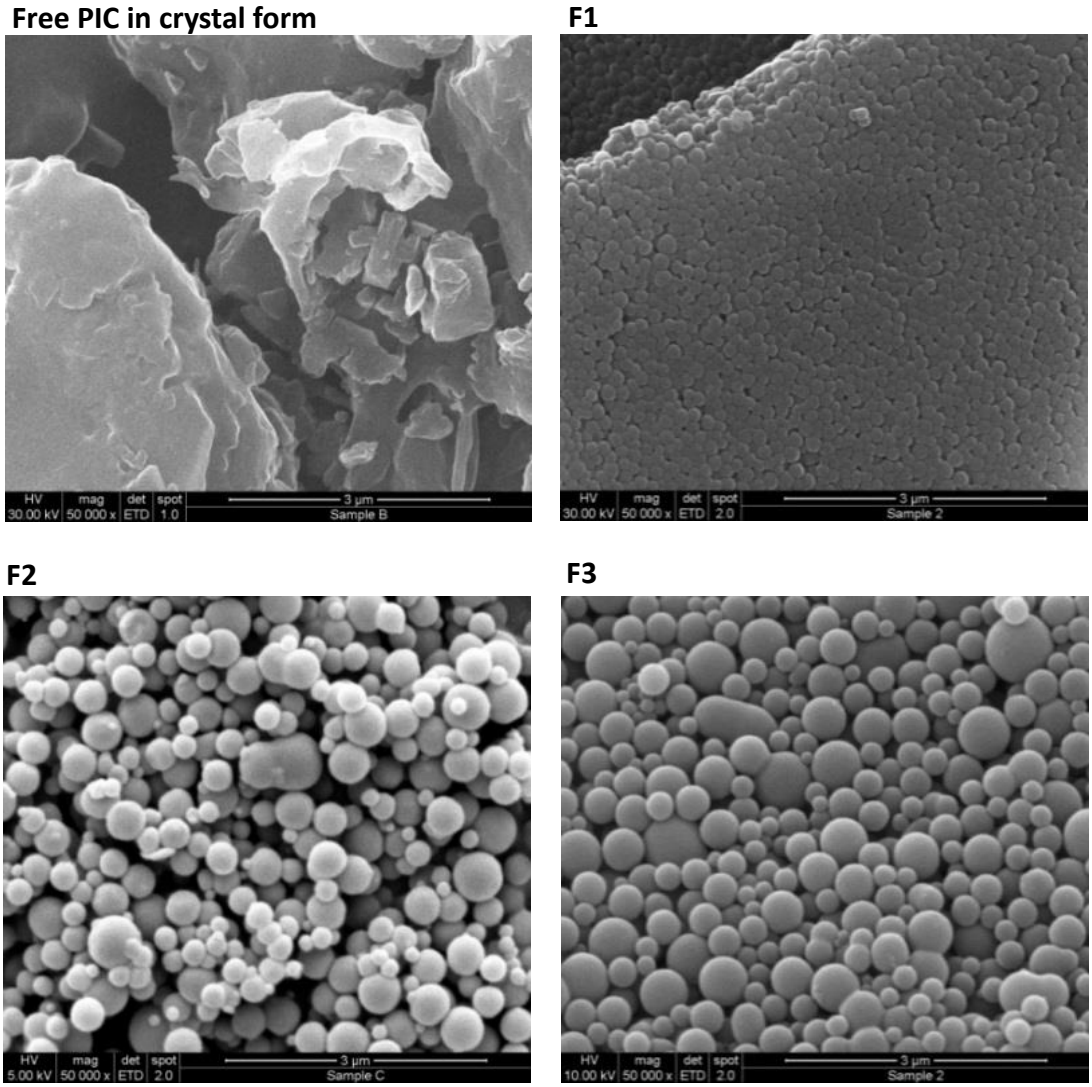

Figure 4.11: Scanning electron microscopy of different batches of nanoparticles. The above Figure 4.11 represents SEM imaging of free PIC, the batch containing 10 mg (F1), 20 mg (F2), and 30 mg (F3) of PIC used in the formulation. Batch formulated with 10 mg PIC represents smaller particles size whereas batch fabricated with 30 mg PIC shows larger particle size. F1 also demonstrate uniformity in size although F2 and F3 exhibit partial uniformity.

4.5.12 Cellular uptake of PIC-loaded albumin NP

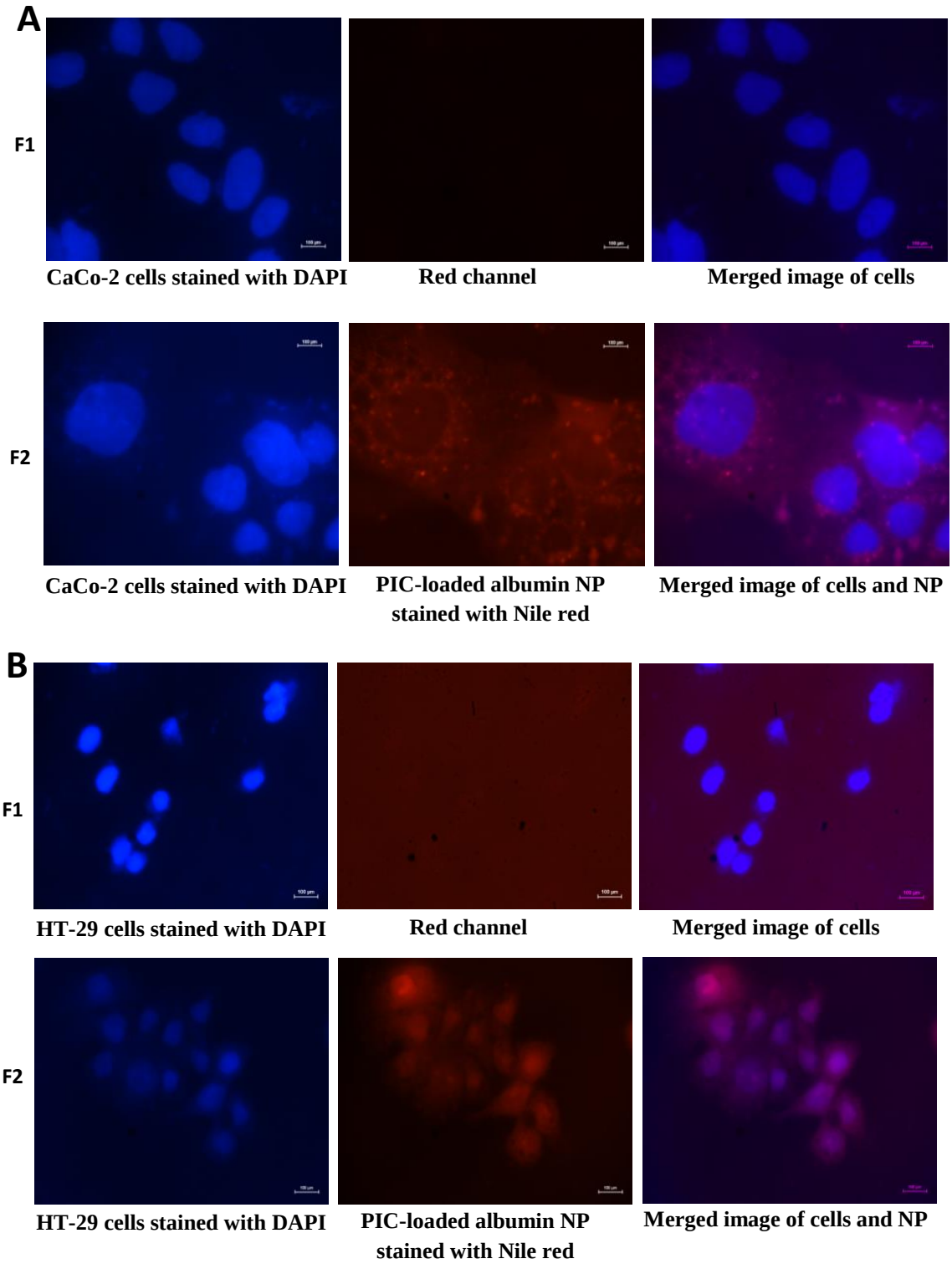

Figure 4.12: Cellular Uptake of optimised PIC-loaded albumin NP in CaCo-2 and HT-29 cells at 100X. Cellular localization of Nile red-coated PIC-loaded albumin NP was observed in CaCo-2 (A) and HT-29 (B) cells and visualized by overlapping under fluorescent microscopy. The red fluorescent can be observed in the microscopic images F2 in the Figure 4.12(A and B).

4.5.13 In-vitro cytotoxicity assay

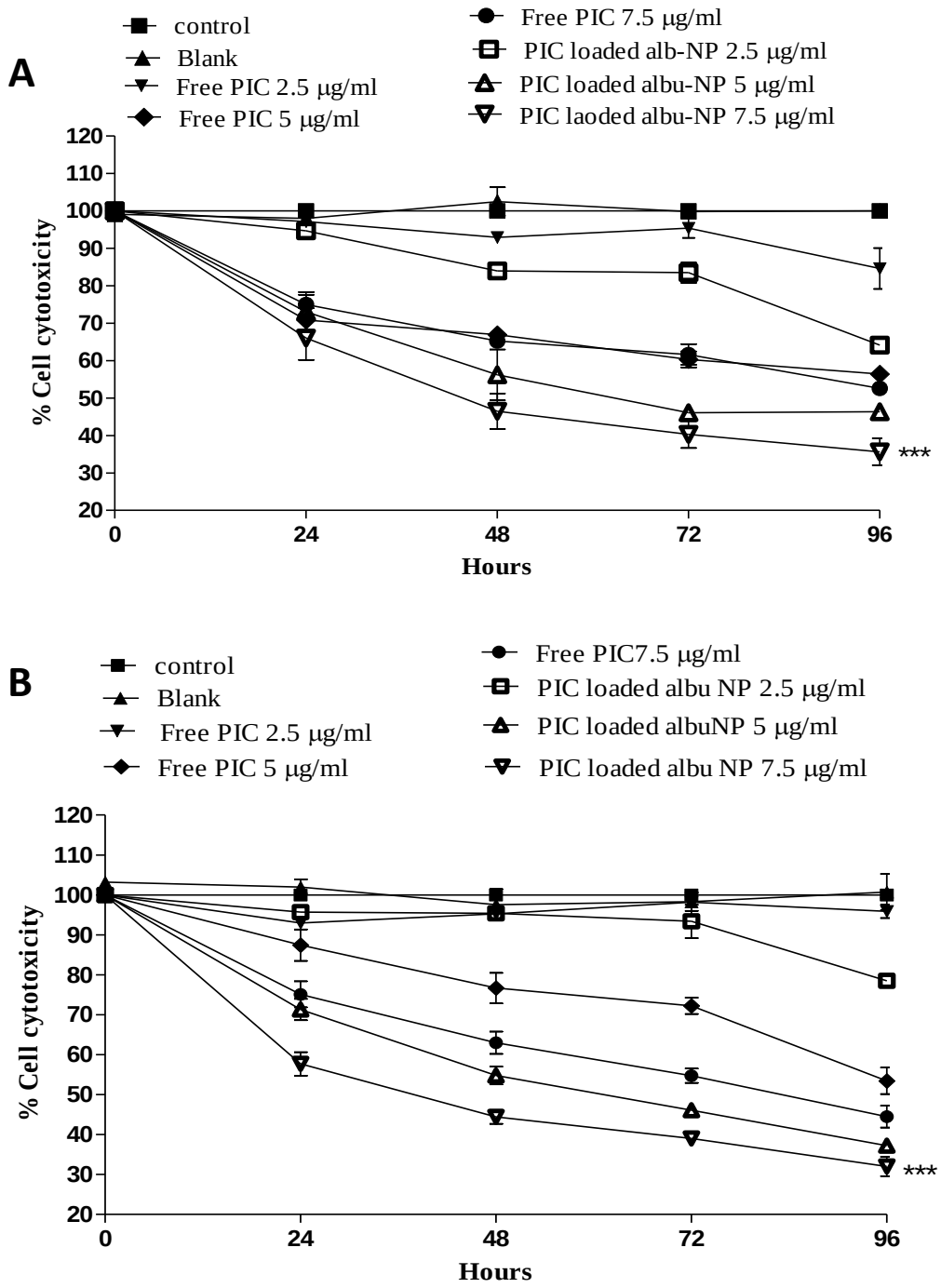

Figure 4.13: Effect of PIC-loaded albumin NP and free PIC on cytotoxicity of CaCo-2 (A) and HT-29 (B) cell lines. The cytotoxicity assay was evaluated on CaCo-2 (A) and HT-29 (B) cell lines. 40×10^4 cells were seeded on 24 well plates and treated with 2.5 µg/ml, 5 µg/ml and 7.5 µg/ml of PIC-loaded albumin NP and an equivalent amount of free PIC. The absorbance was calculated after 24 hours, 48 hours, 72 hours and 96 hours. PIC-loaded albumin NP shows higher cell cytotoxicity as compared to the free PIC. Values are mean ± SEM with n = 3. ***P<0.001 compared with same amount of free drug.

4.5.14 Migration assay in CaCo-2

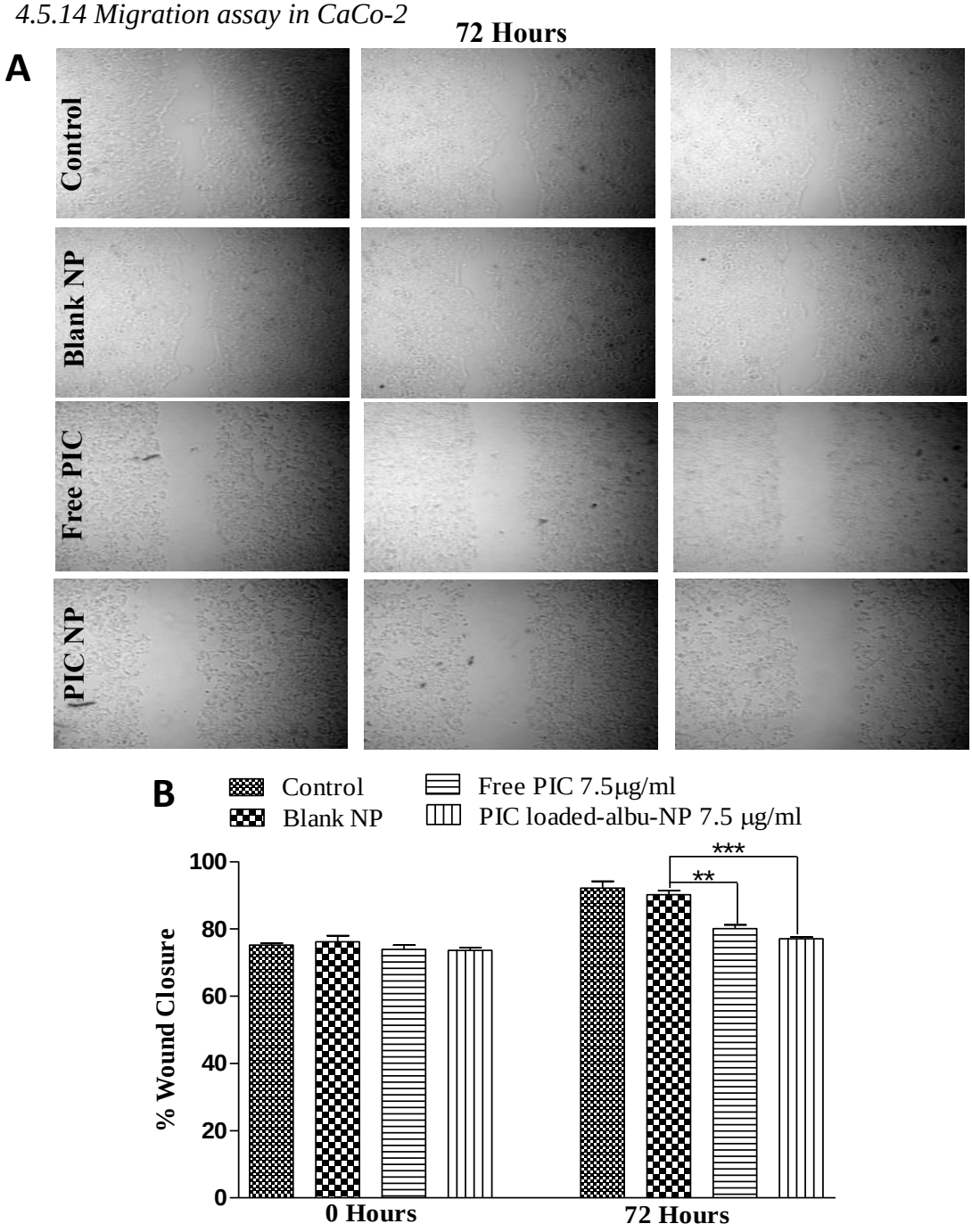

Figure 4.14: Effect of PIC-loaded albumin NP and free PIC on migration potential of CaCo-2 cell lines. The above image in the Figure 4.14 A (CaCo-2) demonstrate the effect of free PIC and PIC-loaded albumin NP on wound closure after 72 hours of treatment. PIC-loaded albumin NP demonstrate more void space than the free PIC in wound scratch of cell line as compare to control and blank NP. The graph B (CaCo-2) depicts a significant variation of anti-migration activity of free PIC ($P<0.01$) and PIC-loaded albumin NP ($P<0.001$) after 72 hours of treatment at equal dose. Values are mean ± SEM with n=3. **$P<0.01$, ***$P<0.001$ compared with blank NP.

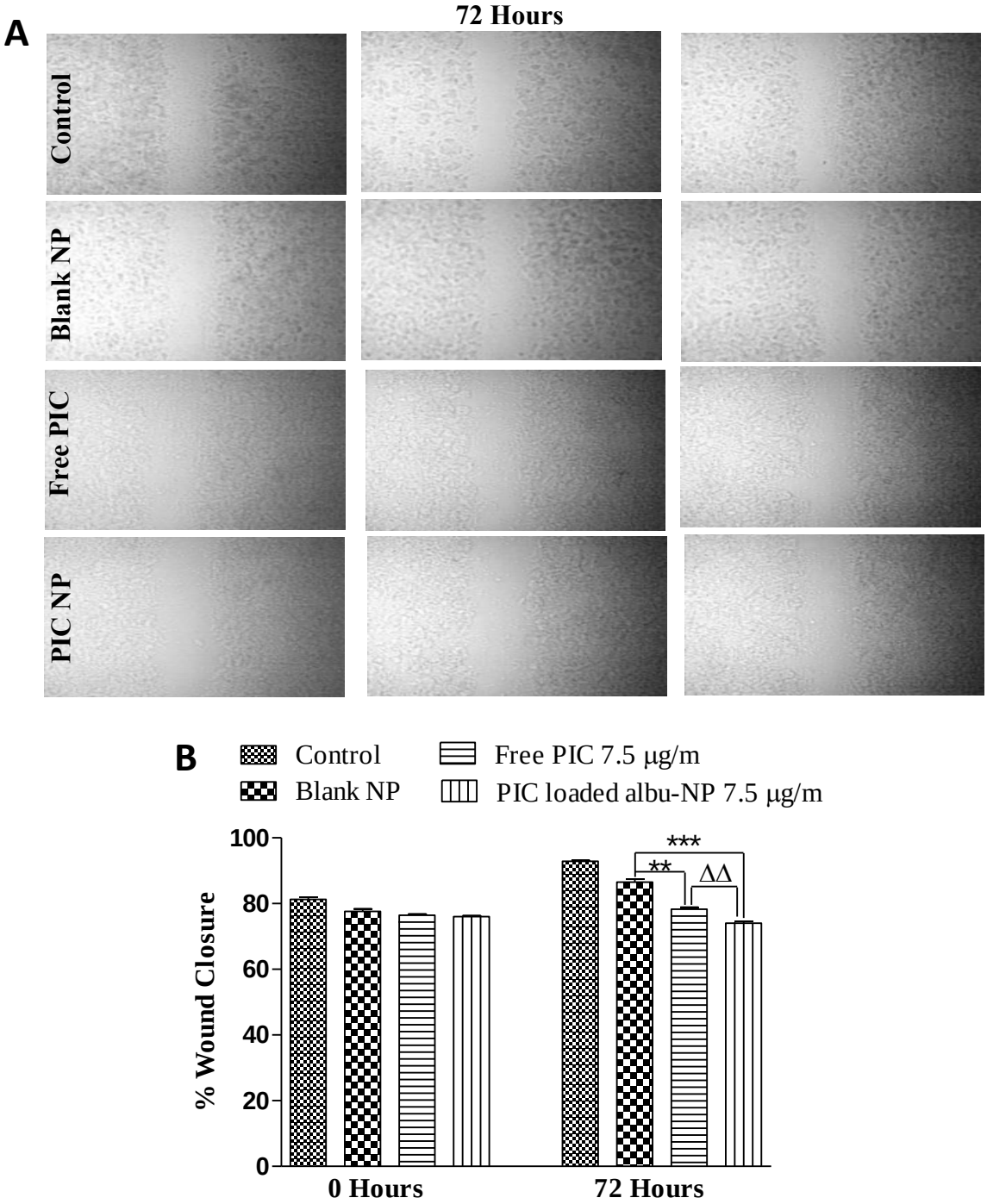

Figure 4.15: Effect of PIC-loaded albumin NP and free PIC on migration potential of HT-29 cell lines. The above images in the Figure 4.15A (HT-29) demonstrate the effect of free PIC and PIC-loaded albumin NP on wound closure after 72 hours of treatment. PIC-loaded albumin NP demonstrate more void space than the free PIC in wound scratch of cell line as compare to control and blank NP. The graph 15B (HT-29) shows a significant variation of anti-migration activity of free PIC ($P<0.01$) and PIC-loaded albumin NP ($P<0.001$) after 72 hours of treatment at equal dose. Values are mean ± SEM with n=3. **$P<0.01$, ***$P<0.001$ compared with blank NP and $^{\Delta\Delta}P<0.01$ compared with the same dose of the free PIC.

4.5.15 Colony formation assay in CaCo-2

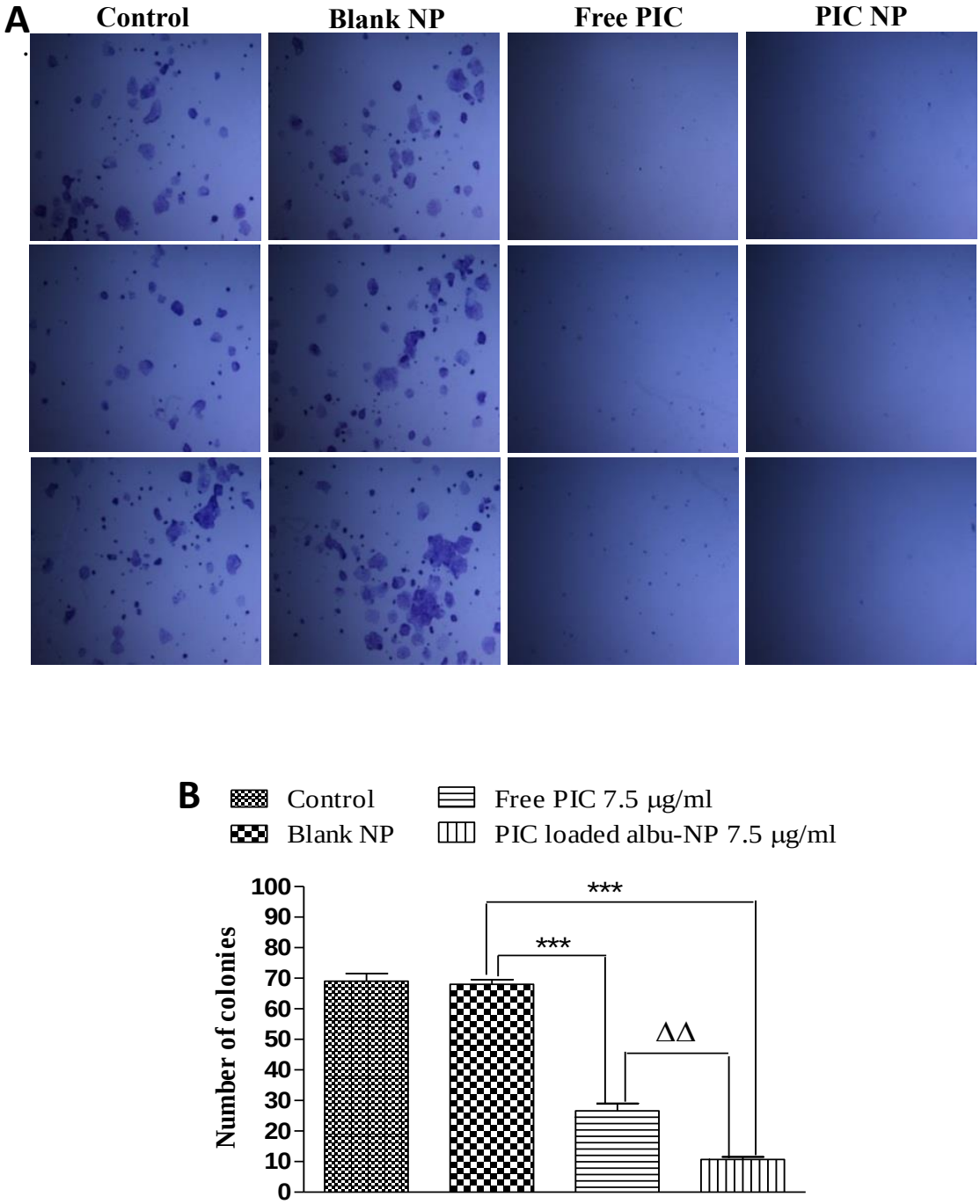

Figure 4.16: Effect of PIC-loaded albumin NP and free PIC on colony formation ability of CaCo-2 cell lines. The above images in the Figure 4.16A (CaCo-2) demonstrate a pattern of colon formation in control, blank NP, free PIC and PIC-loaded albumin NP treated the group as demonstrated in the microscopic images. The graph B (CaCo-2, $P<0.01$) represents significant variation in colony formation upon treatment with free PIC and PIC-loaded albumin NP. It is evident from the figure that PIC-loaded albumin NP shows significant less number of colonies than the free PIC. Values are mean ± SEM with n=3. ***$P<0.001$ compared with blank NP. $^{\Delta\Delta}P<0.01$ compared with the same dose of the free PIC.

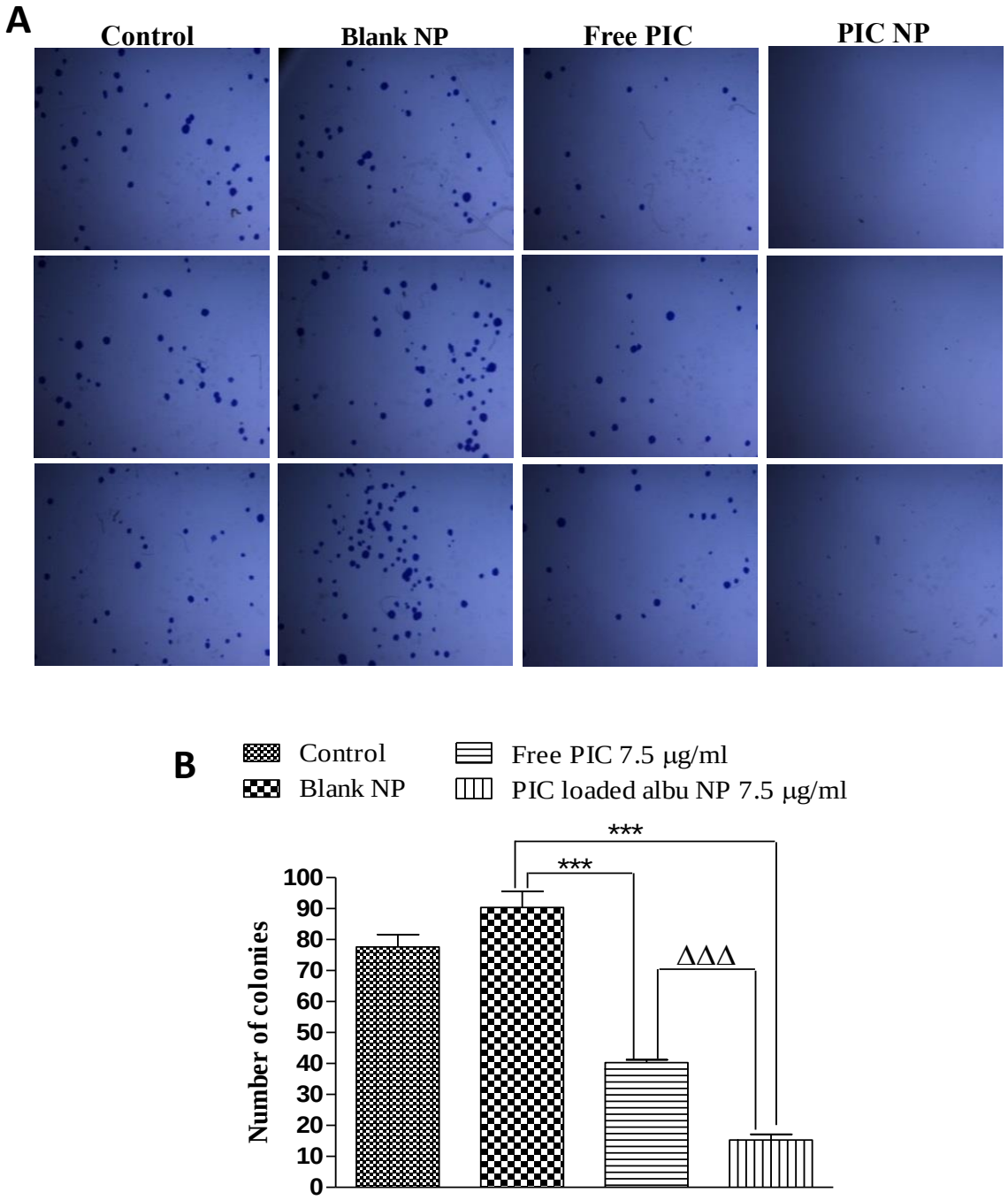

Figure 4.17: Effect of PIC-loaded albumin NP and free PIC on colony formation ability of HT-29 cell lines. The above images in the Figure 4.17A (HT-29) exhibit a pattern of colon formation in control, blank NP, free PIC and PIC-loaded albumin NP treated the group as demonstrated in the microscopic images. The graph B (HT-29, $P<0.001$) represents significant variation in colony formation upon treatment with free PIC and PIC-loaded albumin NP. The above figures revealed that PIC-loaded albumin NP shows significant less number of colonies than the free PIC. Values are mean ± SEM with n=3. ***$P<0.001$ compared with blank NP. $^{\Delta\Delta\Delta}P<0.001$ compared with the same dose of the free PIC.

4.5.16 Invasion assay in CaCo-2

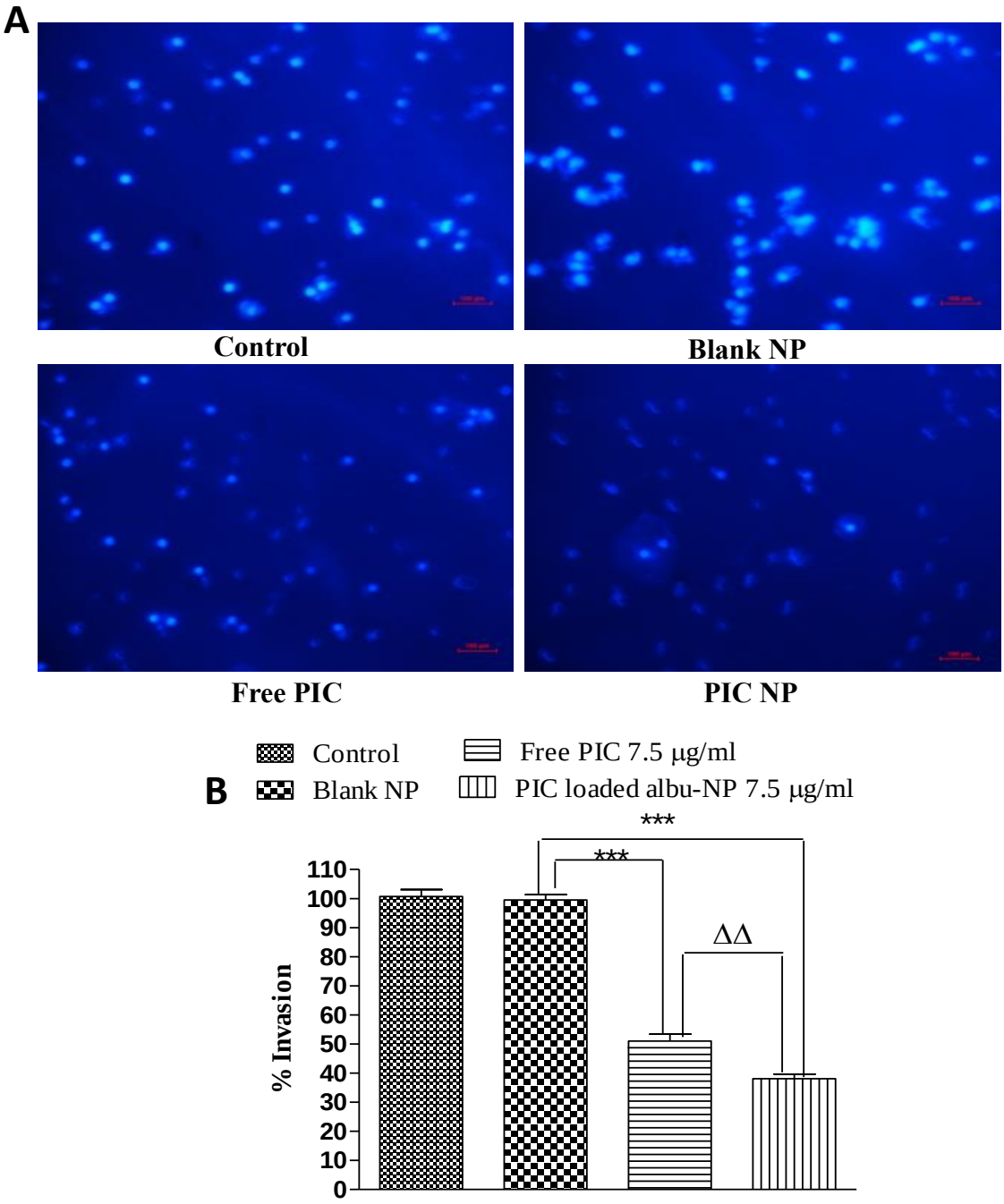

Figure 4.18: Effect of PIC-loaded albumin NP and free PIC on invasion potential of CaCo-2 cell lines. The above microscopic images in the Figure 4.18A (Caco-2) represents anti-invasive activity of free PIC and PIC-loaded albumin NP after treatment. The cells which appear bright are the one which invaded through the membrane. PIC-loaded albumin NP ($P<0.01$) shows significantly less percentage of invasion than the free PIC. The graph B shows that PIC nanoparticles represent significant less invasion than the free PIC in CaCo-2 ($P<0.01$). Values are mean ± SEM with n=3. ***$P<0.001$ compared with blank NP. $^{\Delta\Delta}P<0.01$ compared with the same dose of the free PIC.

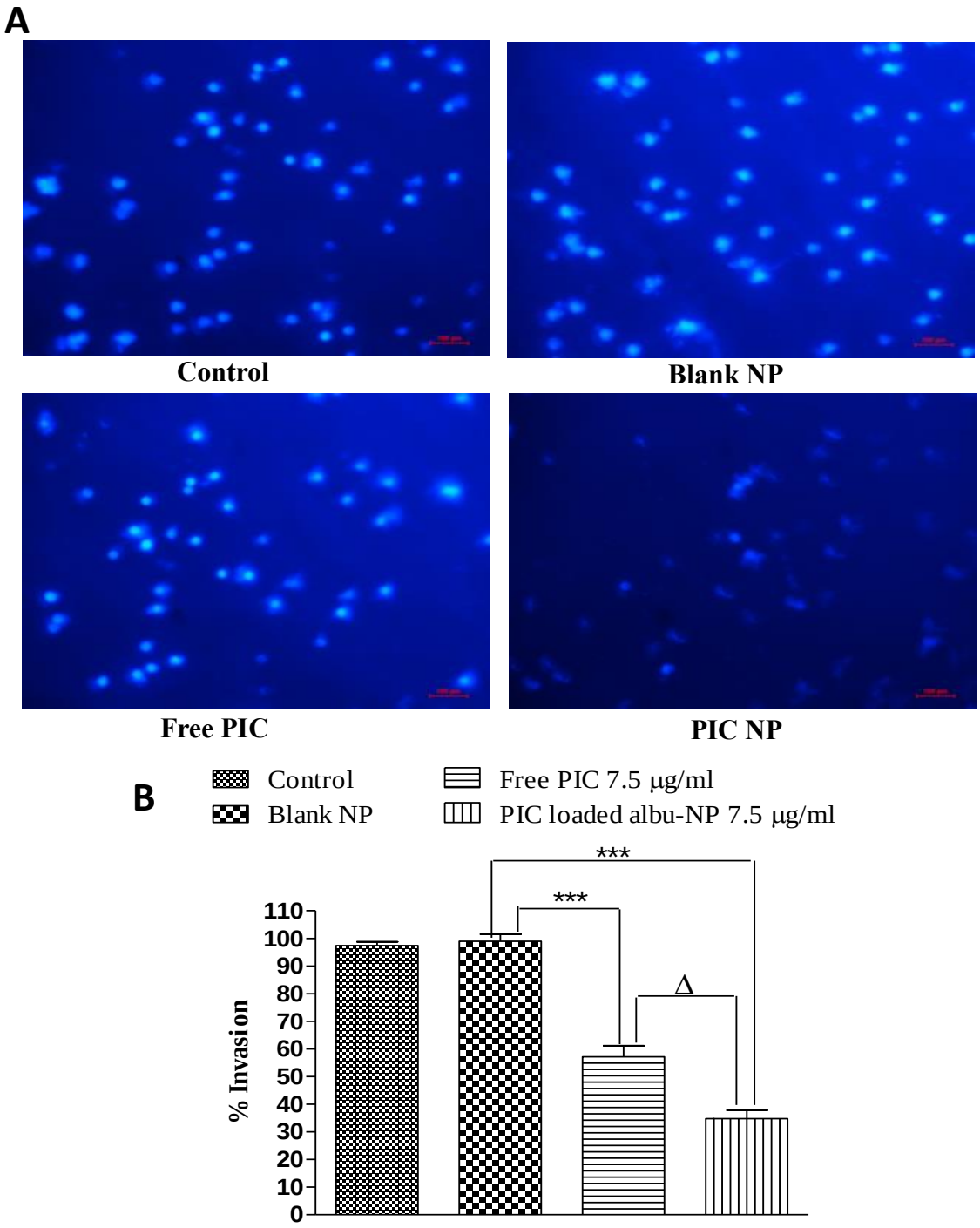

Figure 4.19: Effect of PIC-loaded albumin NP and free PIC on invasion potential of HT-29 cell lines. The above microscopic images in the Figure 4.19A (HT-29) represents anti-invasive activity of free PIC and PIC-loaded albumin NP after treatment. The cells which appear bright are the one which invaded through the membrane. PIC-loaded albumin NP ($P<0.05$) shows significantly less percentage of invasion than the free PIC. The graph B shows that the PIC nanoparticles have significant less invasion than the free PIC in HT-29 ($P<0.05$). Values are mean ± SEM with n=3. ***$P<0.001$ compared with blank NP. $^{\Delta}P<0.05$ compared with the same dose of the free PIC.

4.5.17 Immunostaining of p65 in CaCo-2

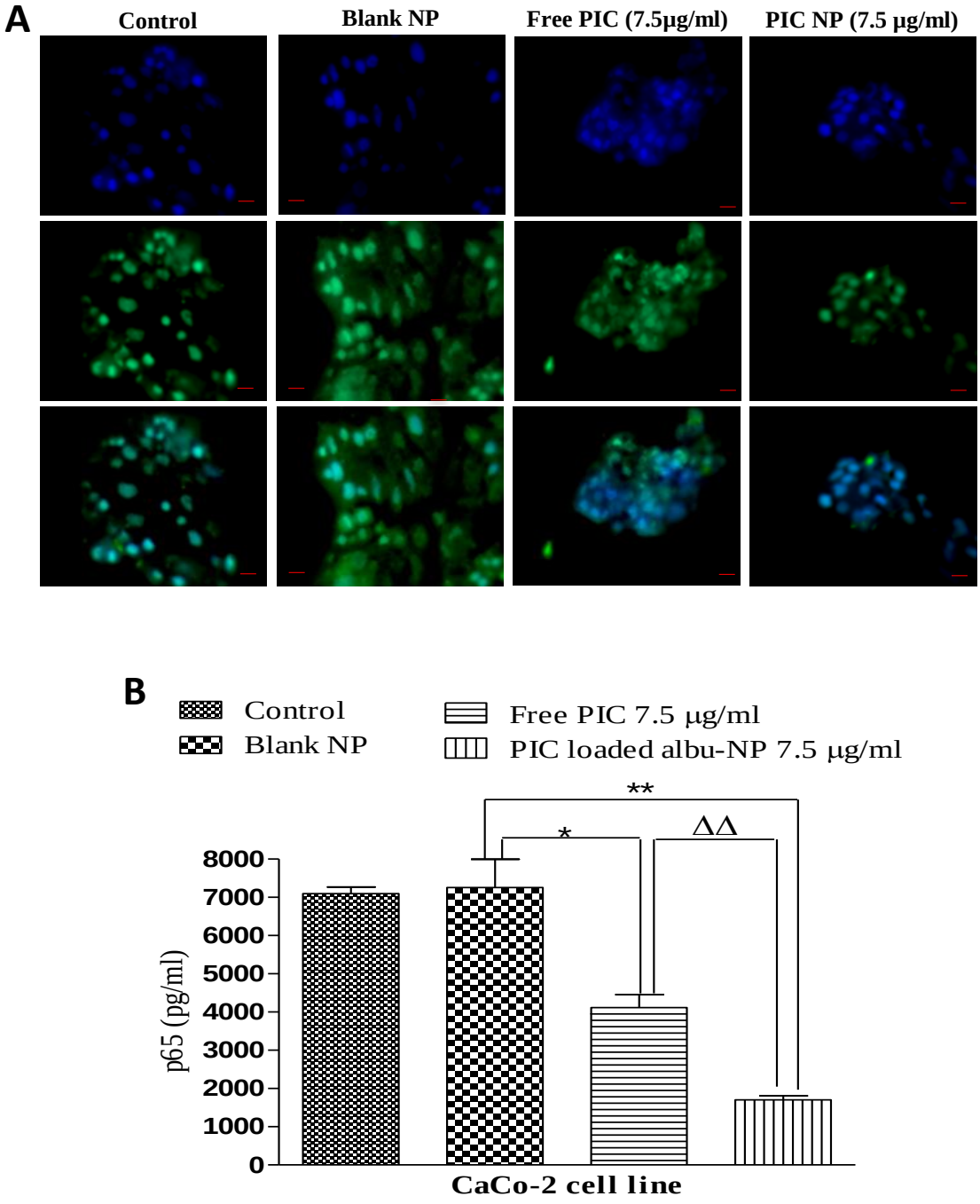

Figure 4.20: Effect of PIC-loaded albumin NP and free PIC on expression of p65 in CaCo-2 at 40X. The above images in the Figure 4.20A (CaCo-2) were taken under bright field microscopy. Control and blank images show induction of p65 whereas images under the free PIC and PIC-loaded albumin NP show a reduced level of p65. The graph B demonstrate significant reduction in the level of p65 in CaCo-2 ($P<0.01$). Values are mean ± SEM (n = 3). *$P<0.05$ and **$P<0.01$ as compare to control. $^{\Delta\Delta}P<0.01$ compared to same amount of free PIC.

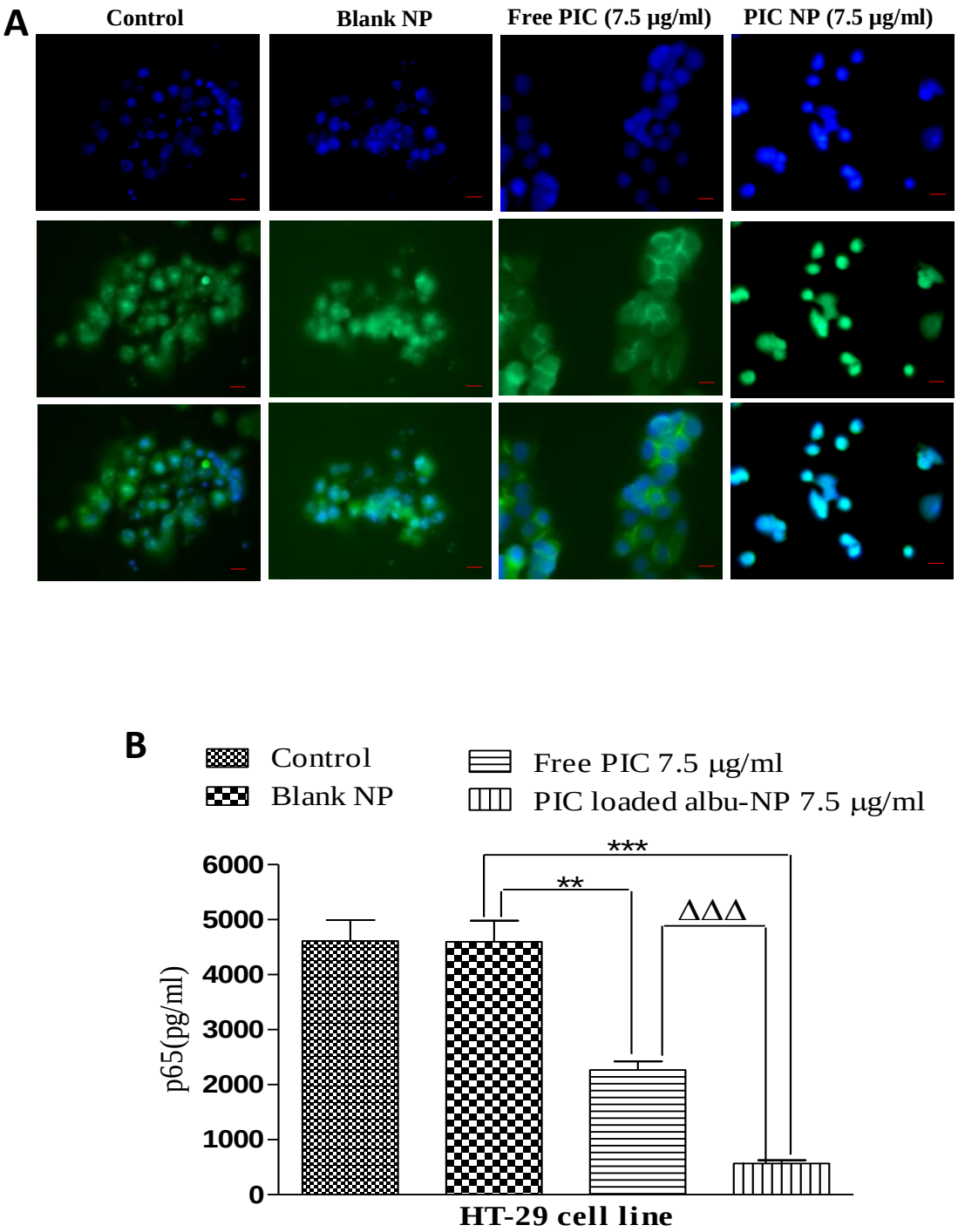

Figure 4.21: Effect of PIC-loaded albumin NP and free PIC on expression of p65 in HT-29 at 40X. The above images in the Figure 4.21A (HT-29) were taken under bright field microscopy. Control and blank images show induction of p65 whereas images under the free PIC and PIC-loaded albumin NP show a reduced level of p65. The graph B reveals significant reduction in the level of p65 in HT-29. Values are mean ± SEM (n = 3). **P<0.01 and ***P<0.001 as compare to control. $^{\Delta\Delta\Delta}$P<0.001 compared to same amount of free PIC.

4.5.18 Immunostaining of HIF-1α

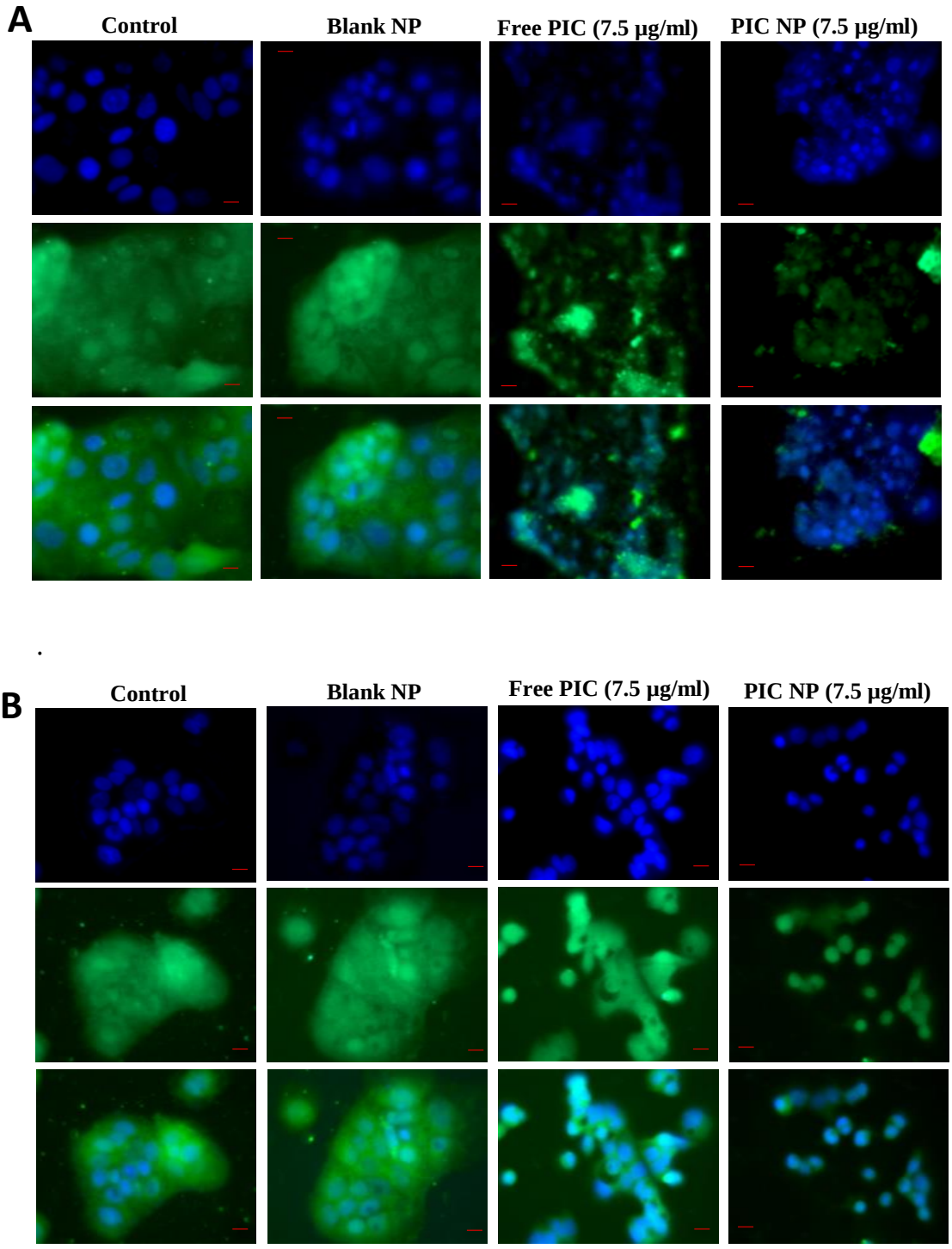

Figure 4.22: Effect of PIC-loaded albumin NP and free PIC on expression HIF-1α in CaCo-2 (A) and HT-29 (B) at 40X. The above images in Figure 4.22 show induction of HIF-1α in control and blank transfected group, whereas images under the free PIC and PIC-loaded albumin NP shows a reduced level of HIF-1α.

4.6 Discussion

Effects of solvent concentration, albumin concentration, glutaraldehyde and amount of drug on particle size, zeta potential and polydispersity were studied. Increase concentration of desolvating agent ethanol has no significant effects on particle size, polydispersity index and zeta potential also reported by (Langer et al., 2003b). Nanoparticle prepared with the different concentration of albumin shows an increase in the particle size, polydispersity index and zeta potential significantly as confirmed in Figure 4.3 with an increase in albumin concentration. Higher concentration of albumin produces dense aqueous albumin solution which results an increase of physicochemical properties of nanoparticles. Same trend of increase in particle size was reported by (Jun et al., 2011). Higher concentration of glutaraldehyde increases the particle size significantly and reduces the polydispersity index as reported by (Rajith and Ravindran, 2014). However, it has no significant effect on zeta potential as shown in Figure 4.4. Increase in drug amount increases the particle size significantly, polydispersity index and zeta potential. The increase in particle size result due to increase in viscosity of drug solution as the amount of drug increases as visible in Figure 4.5. The effect of higher amount of drug on particle size was demonstrated by (Halayqa and Domańska, 2014). We have confirmed the purity of PIC in nanoparticles through NMR study as shown in Figure 4.6. Figure 4.7A show increase in entrapment efficiency when albumin concentration and PIC amount increases. Likewise, Figure 4.8A shows increase in percentage yield as albumin concentration and PIC amount increase in the formulation. This increase in entrapment efficiency and percentage yield was due to the accessibility of more amount of albumin to enclose the same amount of CAPE in the formulation. On the other hand entrapment efficiency and percentage yield decrease when the amount of

PIC increases as shown in the Figure 4.7B and Figure 4.8B. Effect of higher albumin concentration and amount of PIC was studied on *in-vitro* release behaviour as shown in the Figure 4.9. The graph show decrease in *in-vitro* release as the albumin concentration and PIC amount increases due to larger particles size of nanoparticles. Solubility study reveals that PIC loaded albumin (Figure 4.10A) exhibit clear aqueous solution than the free PIC (Figure 4.10B), which testifies increase in solubility of PIC loaded albumin as compared to the free PIC. Morphological evaluation of free PIC and PIC-loaded albumin NP was done by scanning electron microscopy. Rough and solid structure of free PIC can be observed in Figure 4.11. However, images F1, F2 and F3 show spherical and smooth architecture of nanoparticles in the Figure 4.11. However, increase in particle size can be seen as the PIC amount increase in formulation, which also confirm that increase in drug amount leads to increase in particle size. CaCo-2 and HT-29 were stained with DAPI and observed under a fluorescent microscope as evident in the images F1 of Figure 4.12(A and B). Images F2 in the Figure 4.12(A and B) Nile Red coated PIC-loaded albumin NP can be noticed around the cells. This confirms accessibility of PIC nanoparticles to cancer cells. *In-vitro* cytotoxicity graph in the Figure 4.13(A and B) describes dose-dependent effect on cell proliferation CaCo-2 and HT-29. The lower rate of cell proliferation was noted in PIC-loaded albumin NP than the free PIC in cancer cells. Decrease percentage of cell migration was reported in PIC-loaded albumin NP treated cells than free PIC as illustrated in microscopic images of Figure 4.14A (CaCo-2) and Figure 4.15A (HT-29) after 72 hours. Graph in Figure 4.14B (CaCo-2) and Figure 4.15B (HT-29) revealed significant declines in the migration of cancer cell after 72 hours. Figure 4.16A (CaCo-2) and Figure 4.17A (HT-29) represent a microscopic depiction of colony formation. Where PIC-loaded albumin

NP transfected cells in the Figure 4.16A (CaCo-2) and Figure 4.17A (HT-29) shows less colonies as compare to free PIC, blank NP and control group. Similarly, graph in the Figure 4.16B (CaCo-2) and 17B (HT-29) confirm the significant reduction in colony formation in PIC-loaded albumin NP. Fluorescent microscopic images show less number invaded cell upon treatment with PIC-loaded albumin NP as compare to free PIC, blank NP and control group in the Figure 4.18A (CaCo-2) and 19A (HT-29). Significant low invasion rate was reported with PIC-loaded albumin NP treated cells than the free PIC in CaCo-2 and HT-29 as depicted in graph of Figure 4.18B and Figure 4.19B. Induction of p65 was recognised in control and blank NP group in CaCo-2 and HT-29 under bright field microscopy as shown in the Figure 4.20A and Figure 4.21A. Although a low level of p65 can be noticed in PIC-loaded albumin NP than free PIC. Similarly, low expression of HIF-1α protein was depicted in cells treated with PIC-loaded albumin NP as shown in the Figure 4.22(A and B). Hence decrease in particle size results in higher solubility of low soluble natural compound PIC in nanoparticle form. This nanoparticle down-regulate over activation of p65 (RelA) and HIF-1α levels to a higher extent than free PIC in colon cancer cell lines. Thus PIC nanoparticles increase therapeutic value of the natural anticancer agent via suppression of overactivated HIF and NF-kβ pathways during cancer. Hence the findings from our work conclude that nanotechnology could be an effective tool to enhance the anticancer activity of several natural and/or novel anticancer compounds, which are currently not in clinical use due to their limited solubility and/or poor bioavailability.

4.7 Conclusion

The data from this chapter reveals that PIC nanoparticles can be formulated by desolvation method. Optimisation of nanoparticles assists to dispense suitable formulation to carry out the *in-vitro* characterization in cancer cells. The cell proliferation assay established the relation of dose relationship with proliferation in CaCo-2 and HT-29 cells and proves that PIC-loaded albumin NP has less cell proliferation than the free PIC. PIC enhances anticancer properties which can be confirmed from an experiment such as migration, colony formation, and invasion assays in nanoparticles form than the free PIC. PIC-loaded albumin NP inhibits overestimated levels of p65 and HIF-1α higher extent than free PIC. Therefore, delivery of PIC-loaded albumin NP may provide a therapeutic cure in cancer treatment.

Chapter 5

Formulation and *in-vitro* evaluation of the anticancer properties of CAPE-loaded albumin NP in colorectal cancer cell lines

5.1 Introduction

Colorectal cancer is the most common of tumour after breast and prostate cancer worldwide (Gadaleta et al., 2017., Klaver et al., 2017., Siegel et al., 2017). The main etiology of the disease is not been confirmed. However, it is hypothesized that genetic factors, hereditary, lifestyle and prevalence of ulcerative colitis are the key regulators of colorectal cancer (Adami et al., 2016., Khan et al., 2017a., Carrat et al., 2017). Symptoms such as abdominal pain, constipation, diarrhoea, rectal bleeding, and excessive weight loss may be the early sign of colorectal cancer (Mitchell et al., 2008). Colonoscopy is the most widely used technique in the diagnosis of colorectal cancer (Martin et al., 2017). However, colonoscopy causes discomfort in colorectal cancer patients. Therefore, other techniques like Faecal occult blood tests, faecal immunochemical test (FIT) and stool DNA (sDNA) testing are commonly employed by a medical practitioner (Janz et al., 2016). Clinical therapeutics such as chemotherapy (5-fluorouracil, paclitaxel, methotrexate and cyclophosphamide), immunotherapy (monoclonal antibodies, cytokine therapy,) radiation therapy and nutrition supplement based therapy (vitamins, minerals, proteins) are current first line of treatment (Mishra et al., 2013., Mirnezami et al., 2013., Lynch and Murphy, 2016., Staff et al., 2017., Cuhls et al., 2017). However, these chemotherapeutics causes peripheral neuropathy, vomiting, fatigue, anorexia, hair fall, infertility, bone marrow depletion, stomach pain, bowel discomfort, impairment of neuron and renal function (Denlinger and Barsevick, 2009., Lorusso et al., 2017). Immunotherapy casues papulopustular rash, mucosal toxicity, electrolyte imbalances, diarrhoea, acne-like rash, nail disorder, infusion reactions and pruritus (Hofheinz et al., 2017b). High dose of radiation more than 0.125 cGy/min may cause damage to healthy tissue in radiation therapy (Kim et al., 2016). These treatments alter lifestyle and burden

financial condition of colorectal cancer patients. It has been reported that chronic inflammation produces in ulcerative colitis is the main cause of colorectal cancer (Lasry et al., 2016). The chronic inflammation triggers over activation of pro-inflammatory mediators. These mediators of inflammation induces overstimulation of nuclear factor kappa beta (NF-kβ) and hypoxia-inducible factor (HIF-1α) and results into colorectal cancer (Karin, 2009., Nathke and Rocha, 2011., Biddlestone et al., 2015a., Fan et al., 2016). The over-expressed NF-kβ and HIF-1α causes cancer cells to proliferate, migrate and invade at the tumour site (Chaudary and Hill, 2007., Jana et al., 2017). Overstimulation of inflammatory mediators (TNFα, IL-8, IL-6, NF-kβ and HIF-1α) was documented in colorectal cancer patients during a clinical trial. (Klampfer, 2011., Hassanzadeh, 2011., Tan et al., 2017b). The potential role of overexpressed NF-kβ and HIF-1α were reported in HT-29 and CaCo-2 colorectal cancer cell lines via proliferation, migration and invasion nature of tumour cells (Voboril and Weberova-Voborilova, 2006., Sakamoto et al., 2009., Tammali et al., 2011., Jana et al., 2017). Therefore, inhibition may provide a therapeutic cure for colorectal cancer.

Therefore, to inhibit the overexpression of NF-kβ and HIF-1α there is a pressing need to develop novel and natural anticancer agents that have no side effects and can bring about specific drug delivery. It has been documented that cafiec acid phenethyl ester (CAPE) posses medicinal value against cancer and inflammation (Murtaza et al., 2014b., Murtaza et al., 2015., Tolba et al., 2016b). CAPE is derived from honeybee hives and rich in phenolic constituents (Yang et al., 2017). CAPE has an affinity to inhibit over stimulated NF-kβ and HIF-1α in clinical patients, mice and cancer cell lines (Borthakur et al., 2008., Choi et al., 2010., Wang et al., 2010b., DeDiego et al., 2014). CAPE inhibits overactivation of NF-kβ and HIF-1α

responsible for inflammation and colorectal cancer. It also prevents the translocation of Ikβ, and phosphorylation of subunit of NF-kβ (p65) (Toyoda et al., 2009., Akyol et al., 2013., Murtaza et al., 2014a). However, the low solubility and low bioavailability of CAPE limit its therapeutic potential (Tolba et al., 2016b).

In the current chapter, CAPE-loaded albumin nanoparticles were fabricated. We employed desolvation method to fabricate albumin nanoparticles loaded with CAPE. As this method has been widely used in the formulation of albumin nanoparticles in cancer delivery (Tarhini et al., 2017). Albumin has been used as polymer in the nanoparticles formulationdue to its nontoxicity, immunogenisity and biodegradability (Fallacara et al., 2017., Liu et al., 2017., Louage et al., 2017). It enhances pharmacokinetic properties of hydrophobic drugs and increases residence time at the tumour site (Dennis et al., 2002). Albumins has an affinity towards inflammatory markers and offer amino acid at the tumour site. This affinity of albumin helps in targeted delivery of anticancer compounds (Larsen et al., 2016., Jiang et al., 2017).

Based on the accumulating evidence, CAPE nanoparticles were fabricated using albumin as a polymer to improve solubility, bioavailability, efficacy and targeting potential of CAPE nanoparticles by desolvation method.

5.2 Summary

Therefore, given the severity of colorectal cancer and the affiliated adverse effects of conventional therapeutics, there is pressing need to use novel and natural anticancer agents in the treatment and control of colorectal cancer. However, reduction in

particle size by nanotechnology may overcome the poor solubility of CAPE. Also, the use of albumin as a polymer will serve targeted delivery to the nanoparticles.

5.3 Hypothesis

In this chapter, we hypothesize that the reduction of particle size will improve the anticancer property of CAPE at a higher extent than free CAPE.

5.4 Aims and objectives

- Formulation of CAPE-loaded albumin nanoparticles
- Optimisation of CAPE-loaded albumin nanoparticles
- Evaluation of anticancer properties of CAPE-loaded albumin nanoparticles in CaCo-2 and HT-29 cell line

5.5 Results

5.5.1 Calibration of CAPE

Calibration curve of CAPE was plotted as shown in the Figure 5.1 in methanol (1:9) and absorbance was measured at 425 nm.

5.5.2 Effect of ethanol

CAPE-loaded albumin NP was fabricated by the method stated in Section 2.3. Effect of ethanol amount on particle size was studied by varying the amount of ethanol from 4 ml to 12 ml. It was found that increase in the ethanol amount has no significant effect on particle size as shown in the graph (Figure 5.2A). The particle size was found to be in the range of from 266 nm to 279 nm. A similar observation was also documented by Langer et al (Langer et al., 2003b). In addition polydispersity index (Figure 5.2B) also shows no significant difference in an increase in ethanol amount. The polydispersity index was reported in the range of 0.144 to 0.164. Although, zeta potential (Figure 5.2C) decreases slightly from -14 mV to -18 mV with an increase in ethanol amount.

5.5.3 Concentration of albumin

Albumin has a tendency to attach to neutrophils, well accepted in the serum and does not produce any undesired effect (Abbasi et al., 2012., Elzoghby et al., 2012a). Jun et al reported an increase in particle size with increasing concentration of albumin (Jun et al., 2011). Moreover, increase in the particle size (Figure 5.3A) was reported in the current work. Particle size increases significantly ($P<0.001$) from 222 nm to 277

nm with increase albumin centration. Similarly, polydispersity index (Figure 4.3B) also increases significantly ($P<0.01$) from 0.05 to 0.27 with an increase in albumin concentration. Likewise, zeta potential (Figure 5.3C) slightly increases from -17 mV to -13 mV as albumin concentration increases.

5.5.4 Effect of Glutaraldehyde concentration

The effect of the crosslinking agent on the size of nanoparticles was evaluated with varying concentration of glutaraldehyde from 4% to 12%. Increasing concentration of glutaraldehyde increases the particle size significantly ($P<0.001$) from 230 nm to 394 nm as shown in the graph (Figure 5.4A). Similar trend of particle size was also demonstrated by Rajith and Ravindran, 2014. Although increasing concentration of glutaraldehyde decreases polydispersity index from 0.23 to 0.18 (Figure 5.4B). Decrease polydispersity index pattern was also reported by langer et al, upon increase concentration of glutaraldehyde (Langer et al., 2003a). However, increasing the concentration of glutaraldehyde shows no significant effect on zeta potential (Figure 5.4C) as documented by Li et al., 2008a.

5.5.5 Amount of drug

The effect of drug amount on particle size, polydispersity index and zeta potential was evaluated by using an increasing amount of CAPE in the formulation. It observed that increase amount of CAPE increases the particle size (Figure 5.5A) of nanoparticles. This increase in particle size may cause increase in CAPE amount which increase viscosity of drug solution (Halayqa and Domańska, 2014). Particle

size very slightly increases from 245 to 274 nm when CAPE amount increase from 10 mg to 30 mg. Similarly, polydispersity index (Figure 5.5B) also increases slightly with an increase in CAPE amount. The polydispersity index increase from 0.139 to 0.179. Similarly, increase in CAPE amount increases the Zeta potential from 15 mV to -9 mV (Figure 5.5C) significantly ($P<0.01$).

5.5.6 NMR spectra of CAPE-loaded albumin NP

The 1H NMR study (in DMSO-d6) of CAPE in albumin nanoparticles revealed that the signal due two hydroxyl groups appears as a broad spectrum (brs) around 9.5 ppm, whereas the two trans olefinic protons a and b resonates at around 7.43 and 6.18 ppm respectively. The signals due to eight aromatic protons appear as multi plate stating from 7.28 to 7.07 ppm. A strong peak around 4.29 ppm and 2.92 ppm indicates the -OCH_2 group and benzylic protons respectively. These data confirmed the CAPE structure in albumin nanoparticles as shown in Figure 5.6.

5.5.7 Entrapment efficiency

The entrapment efficiency of CAPE in nanoparticles was calculated from the equation given in section 2.6. The impact of albumin concentration and drug content were demonstrated on entrapment efficiency. Figure 5.7A represents the pattern of entrapment efficiency of CAPE-loaded albumin NP. Entrapment efficiency increases as the concentration of albumin increases in the formulation. A similar trend of increase in entrapment was reported by Ganesh et al., 2015**.** Significant ($P<0.001$) increase in entrapment efficiency from 18% to 61% was reported as the albumin

content increases from 0.5% to 2%. However, it shows no change in entrapment when albumin concentration increases to 3.5%. Figure 5.7B also demonstrates significantly ($P<0.01$) decrease in entrapment efficiency from 56% to 43% as the content of drug increases. This implies an increase in drug amount decreases the entrapment efficiency because the higher amount of drug requires more amount of albumin for encapsulation. Due to which the drug makes a loose hollow structure which might get disperse in the supernatant while washing. The similar pattern of entrapment was reported by (Peltonen et al., 2004., Sebak et al., 2010).

5.5.8 Percentage yield

The percentage yield was measured by the equation given the section 2.7. The effect of albumin concentration and drug content was assessed on percentage yield. Figure 5.8A represents an increase in percentage yield upon an increase in albumin content in the formulation. At 2% albumin concentration, the percentage yield was 67.5% shows significant ($P<0.001$) increase in nanoparticle yield. However, there is a slight increase in yield as the albumin concentration increases in the formulation to 3.5%. This increase in percentage yield may be due to the availability of more amount of albumin for the same amount of CAPE. A similar trend of percentage yield can be seen in the Figure 5.8B where percentage yield increase slightly from 53% to 60 % when drug amount increases. It further increases to 64% as the amount of drug increases to 30 mg. The amount of albumin here plays a key role in nanoparticles yield. Kılıçarslan and Baykara also reported the same pattern of percentage yield on increasing amount of drug (Kılıçarslan and Baykara, 2003)

5.5.9 In-vitro release

In-vitro release study was performed by methods mentioned in section 2.8. CAPE nanoparticles were formulated with 0.5%, 2% and 3.5% of albumin. These batches show burst release of albumin nanoparticles after 24 hours. It was noted that increase amount of albumin decreases the release of CAPE from nanoparticles as illustrated in the Figure 5.9A. The release of 44%, 42% and 38% was documented after 24 hours in these batches. After 168 hours 79%, 66% and 57% release of CAPE was reported in three batches. Increase in particles size may cause decreases in *in vitro* release of CAPE when formulated with different concentration of albumin. Increase in albumin concentration contributes to decrease in the *in-vitro* release was also demonstrated by (Jenita et al., 2014). The effect of the increased amount of drug on release profile was evaluated and burst release of CAPE from nanoparticle was noticed as shown in the Figure 5.9B. After 24 hours 51%, 34% and 31% release of CAPE from nanoparticles was reported. After 168 hours the CAPE release was 72%, 56% and 51% in the batches formulated with 10 mg, 20 mg and 30 mg of CAPE. A similar trend of release was documented by (Azizi et al., 2017). Rapid dissolution of CAPE present on the surface of albumin may cause the burst release in the dissolution media.

5.5.10 Solubility of CAPE-loaded albumin NP

The solubility of CAPE-loaded albumin NP and was determined by the method given in section 2.9. The apparent water solubility of CAPE in both free and encapsulated form was determined by UV-spectroscopy at 425 nm. The vials in Figure 5.10A depict shows the enhanced solubility of CAPE when formulated as

CAPE-loaded albumin NP vs free CAPE as shown in Figure 5.10B. It is evident from the figures that CAPE-loaded albumin NP (Figure 5.10A) produces a uniform clear dispersion throughout the tube, whereas free CAPE (Figure 5.10B) was sparingly soluble and produces turbidity throughout. The solubility of free CAPE was 256.72 µg/ml, CAPE-loaded albumin NP was 435.50 µg/ml, which represented an approximately two-fold increase in aqueous solubility as compared to free CAPE.

5.5.11 Scanning electron microscopy

The sample for SEM was prepared by the method as mentioned in the section 2.10. The morphological study of nanoparticles was done by scanning electron microscopy. The size, shape and texture of optimized CAPE-loaded albumin NP was observed under 50000X magnification as shown in Figure 5.11. Average particle size was found to be 157 nm. The images in the Figure 5.11 represents the SEM images of free CAPE, F1 nanoparticles with 10 mg CAPE, F2 nanoparticles with 20 mg CAPE and F3 nanoparticles formulated with 30 mg CAPE. The free drug represents the random and solid structure of drug whereas the nanoparticles images shows spherical and smooth surface. Image F1 demonstrate monodisperse and smooth textured appearance in the Figure 5.11. However, images F2 and F3 show larger particle size and partially disperse texture in the Figure 5.11. Therefore, from the SEM images, it can be concluded that increase in drug content increases the particle size of nanoparticles. Thus, to achieve intracellular targeting smaller particle size ranging from 0.1µ to 100 nm is desirable (De Jong and Borm, 2008).

5.5.12 Cellular uptake of CAPE-loaded albumin NP

The CaCo-2 and HT-29 cell were incubated with CAPE-loaded albumin NP as described in the section 2.12 for cellular uptake study. The nucleus image of cell and uptake of nanoparticle was taken under phase contrast microscope for CaCo-2 and HT-29 cells. Image F1 in the Figure 5.12(A and B) represent CaCo-2 and HT-29 cells with no treatment. Image F2 in the Figure 5.12(A and B) shows CaCo-2 and HT-29 cells treated with Nile red-coated CAPE-loaded albumin NP. The images in F1 depicts nucleus without any treatment, however, images in F2 exhibit nanoparticles labeled with Nile Red observed under the microscope in both the Figure 5.12(A and B). The merged images in F1 represent nucleus only although fluorescent nanoparticles can be seen around the nucleus in F2 of both the merged images.

5.5.13 In-vitro cytotoxicity assay

The cytotoxicity study was performed by methods as described in Section 2.13. The cytotoxic potential of free CAPE and CAPE-loaded albumin NP was evaluated by method demonstrated by (Kumar et al., 2014). The cytotoxic study of free CAPE and CAPE-loaded albumin NP was carried by MTT assay for a period of 24, 48, 72 and 96 hours. The data showed that the blank NP had no cytotoxic action on colorectal cell lines within the concentration used. Free CAPE and CAPE-loaded albumin NP demonstrate dose dependent response to cytotoxicity. The cell death has been observed after the first day in CaCo-2 and HT-29 cells upon treatment with free CAPE and CAPE-loaded albumin NP. However, the cytotoxic activity was reported more in CAPE-loaded albumin NP treated cells as shown in the Figure 5.13(A and

B). The cytotoxic activity of CAPE-loaded albumin NP was significantly increased as compared to free CAPE in both cell lines after 96 hours of treatment. The cell viability was found to be 88% and 85% when CaCo-2 cells treated with free CAPE and CAPE-loaded albumin NP respectively after 24 hours of treatment at highest concentration i.e. 7.5µg/ml. Similarly, the viability of cell was reported to be 56% and 46% at same concentration after 96 hours respectively. Moreover, cell viability in HT-29 was demonstrated to be 91% and 75% upon treatment with free CAPE and CAPE-loaded albumin NP at 7.5µg/ml concentration after 24 hours respectively. Likewise, the viability of HT-29 was decreased to 57% and 41% at same concentration after 96 hours respectively.

CAPE-loaded albumin NP sustained the cytotoxic action of the free drug due to the enhanced penetration and retention effect inside the colorectal cells (Patil et al., 2009., Chavanpatil et al., 2006). It also improved the solubility which in turn enhances the half-life and bioavailability (Mittal et al., 2007., Anand et al., 2010) due to reducing the particle size of CAPE. Therefore, based on the above data it can be concluded that CAPE-loaded albumin NP enhances the cytotoxicity potential due to a reduction in particle size, which suggest that albumin nano-particulate formulation enhances the biological therapeutic efficacy of CAPE over free CAPE.

5.5.14 Migration assay

The migration study was carried out in CaCo-2 and HT-29 as stated in Section 2.14. A cancer cell has potential to migrate from one tumour site to another (Friedl and Wolf, 2003). Both the cell lines were treated with 7.5 µg/ml of CAPE-loaded albumin NP and same amount of free CAPE for 72 hours. Figure 5.14 and Figure

5.15 shows the evaluation of the degree of wound closure in CaCo-2 and HT-29 cells. CAPE-loaded albumin NP treated cells have greater void space ($P<0.05$) than free CAPE treated cells as shown in the Figure 5.14A and Figure 5.15A after 72 hours of treatment. Approximately 76% wound closure was observed when CaCo-2 cells were treated with 7.5 µg/ml of CAPE-loaded albumin NP. However, it was 81% of wound closure in an equivalent amount of free CAPE as depicted in the graph of Figure 5.14B. Similarly, CAPE-loaded albumin NP also exhibits a significant difference ($P<0.01$) in wound closure as compared to free CAPE in HT-29. Approximately 72% of wound closure was depicted by CAPE-loaded albumin NP but free CAPE illustrates 79% of wound closure in HT-29 cells at an equivalent dose as illustrated in the graph of Figure 5.15B. Therefore, CAPE-loaded albumin NP illustrates the significantly higher percentage of inhibition of migration potential in both cell lines. Whereas, free CAPE demonstrate the lower percentage of anti-migration potential as compared to control and blank NP at the same dose. Hence, albumin nanoparticulate form sustained and improved the anti-migration capacity of CAPE which is essential to prevent metastasis of invasive colon cancer cells.

5.5.15 Colony formation assay

The colony formation assay was carried out as mentioned in section 2.15. Colony formation assay was carried out to determine and compare the long term anticancer activity of free CAPE and CAPE-loaded albumin NP as described by (Yeung et al., 2010) in CaCo-2 and HT-29 cells. The colorectal cell lines were treated with 7.5 µg/ml of CAPE-loaded albumin NP and free CAPE at equal concentration. The number of colonies formed after 7 days was calculated in control, blank NP, free

CAPE and CAPE-loaded albumin NP treatment under stereo zoom Nikon microscopy as shown in Figure 5.16A and Figure 5.17A. The colonies in healthy and blank NP treated group were found to be almost equal in both cell lines as shown in Figure 5.16A and Figure 5.17A. The number of colonies was significantly reduced when CaCo-2 cells treated with 7.5 µg/ml CAPE-loaded albumin NP ($P<0.001$) and an equivalent amount of free CAPE ($P<0.01$) compare to colonies in control and blank NP treated cells as shown in the graph of Figure 5.16B. An average number of colonies were found to be 29 when CaCo-2 cells treated with free CAPE whereas it was only 14 colonies observed in CAPE-loaded albumin NP treatment in CaCo-2 cells. Likewise, the number of colonies was significantly reduced when HT-29 cells treated with 7.5 µg/ml of CAPE-loaded albumin NP ($P<0.001$) an equivalent amount of free CAPE ($P<0.001$) compare to colonies in control and blank NP treatment as shown in the graph of Figure 5.17B. The average number of colonies was reported to be 29 in free CAPE treatment whereas it the average number of colonies was 10 in CAPE-loaded albumin NP treatment in HT-29 cells as shown in the figure.

5.5.16 Invasion assay

The procedure for invasion assay was described in Section 2.16. Anti-invasive activity of CAPE-loaded albumin NP and free CAPE was evaluated on colorectal cancer cell lines such as CaCo-2 and HT-29 as describe by (Yuen et al., 2013). Colon cancer cells were treated with 7. 5 µg/ml of CAPE-loaded albumin NP and an equivalent amount of free CAPE. The anti-invasive potential of CAPE-loaded albumin NP was higher than free CAPE treatment in both cell lines as shown in Figure 5.18B and Figure 5.19B. CAPE-loaded albumin NP show significant

($p<0.05$) reduction in invasion potential (36%) than free CAPE (55%) in CaCo-2 cells as demonstrated in graph of Figure 5.18B. Similarly, CAPE-loaded albumin NP show significantly ($p<0.01$) lower degree of invasion inhibition (33 %) than free CAPE (61%) in HT-29 cells as shown in Figure 5.19B. The above data demonstrate that CAPE-loaded albumin NP inhibit the invasion capacity of invasive colon cancer cells. CAPE-loaded albumin NP sustained and improved the anti-invasive power of CAPE which is essential to inhibit metastasis of invasive colorectal cancer cells.

5.5.17 Quantification of p65

The cell lysates were analyzed for p65 as described in Section 2.17. The fluorescent images of CaCo-2 (Figure 5.20A) and HT-29 (Figure 5.21A) were captured under bright field microscope after staining the cells with p65 antibody. Both the cell line was treated with 7.5 µg/ml dose of CAPE-loaded albumin NP and an equivalent amount of free CAPE. The induced level of NF-kβ such as p65 can be noticed in the control and blank NP as shown in the microscopic images in Figure 5.20A and Figure 5.21A. However, the group was treated with free CAPE and CAPE-loaded albumin NP show a noticeable difference in the level of p65. Additionally, CaCo-2(Figure 5.20B) and HT-29 (Figure 5.21B) treated with CAPE-loaded albumin NP show significantly low expression of p65 than free CAPE. The graphs in the Figure 5.20B (CaCo-2) and Figure 5.21B (HT-29) demonstrate a higher level of p65 in control and blank NP groups. CAPE-loaded albumin NP ($P<0.01$) depicts the low level of p65 protein than blank nanoparticles. The expression of p65 was significantly ($P<0.001$) lower than a free CAPE transfected cell in CaCo-2 as shown in the Figure 5.20B. Similarly, CAPE loaded nanoparticles decrease the p65

expression significantly ($P<0.05$) than free CAPE in HT-29 as represented in the Figure 5.21B.

5.5.18 Quantification of HIF-1α

The CaCo-2(Figure 5.22A) and HT-29 (Figure 5.22B) were stained with HIF-1α antibody and observed under bright field microscope to study the effect of PIC treatment as shown in the Figure 5.22. The CaCo-2 and HT-29 cell line were treated with 7.5 µg/ml dose of CAPE-loaded albumin NP and an equivalent amount of free CAPE. The plates were incubated for 24 hours and the level of HIF-1α was observed under a microscope. The increased expression of HIF-1α was reported as shown in the images of Figure 5.22A (CaCo-2) and Figure 5.22B (HT-29). The overstimulated expression of HIF-1α was found in control and cells transfected with blank NP in both cell lines as depicted in the Figure 5.22(A and B). Though the group was treated with free CAPE and CAPE-loaded albumin NP show a noticeable difference in the level of HIF-1α in the Figure 5.22(A and B). Furthermore, CaCo-2(Figure 5.22A) and HT-29 (Figure 5.22B) treated with CAPE-loaded albumin NP show significantly low expression of HIF-1α than free CAPE.

5.5.1 Calibration of CAPE.

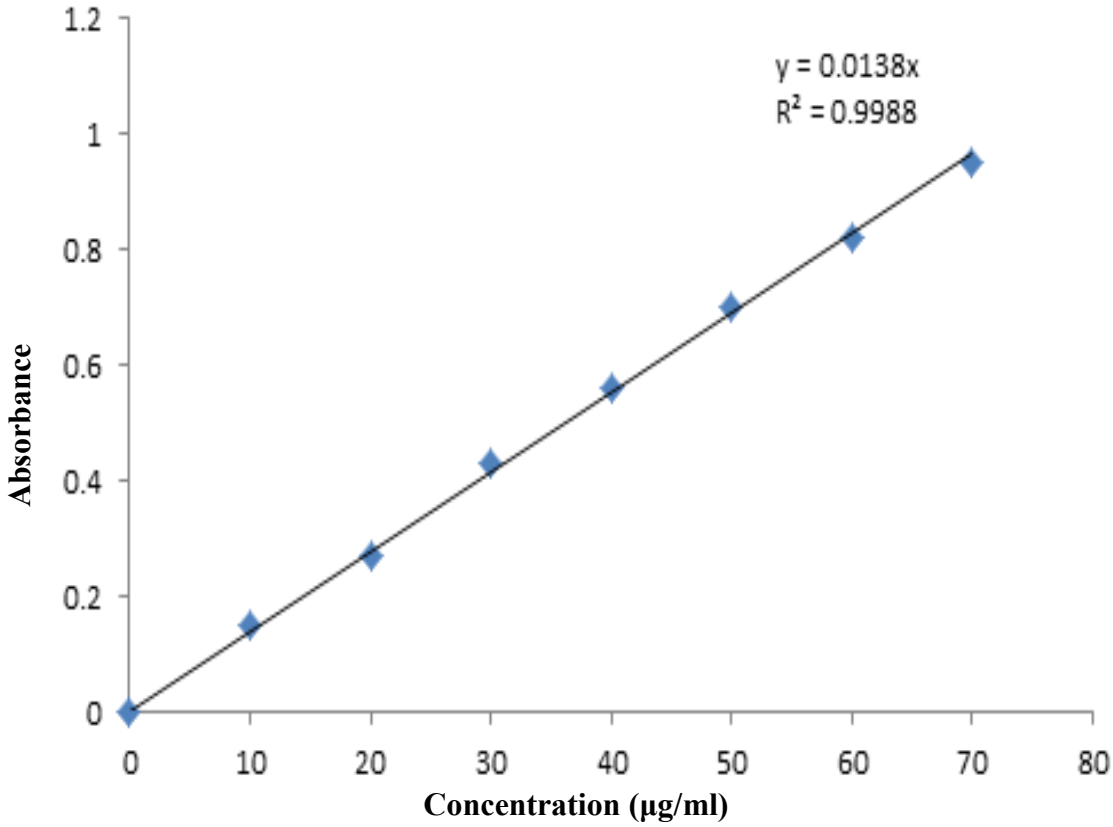

Figure 5.1: Calibration curve of CAPE

5.5.2 Effect of ethanol

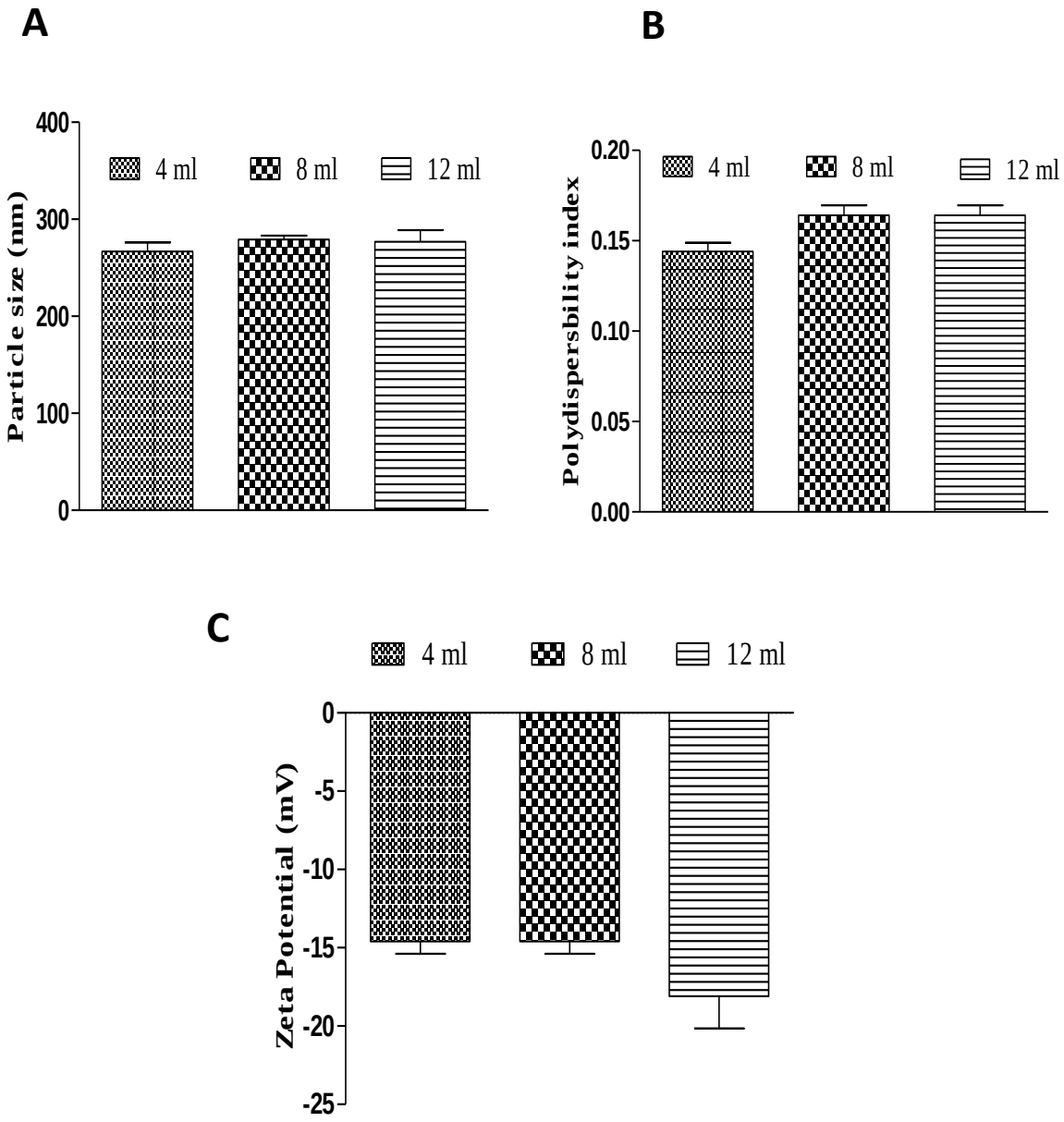

Figure 5.2: Effect of ethanol amount on particle size (A), polydispersity index (B) and zeta potential (C). The above graph shows the effect of ethanol amount on Particle size (A), polydispersity index (B) and zeta potential (C). It was reported that ethanol amount does not have any significant effect on particle size, polydispersity index and zeta potential. Values are mean ± SEM (n = 3).

5.5.3 Concentration of albumin

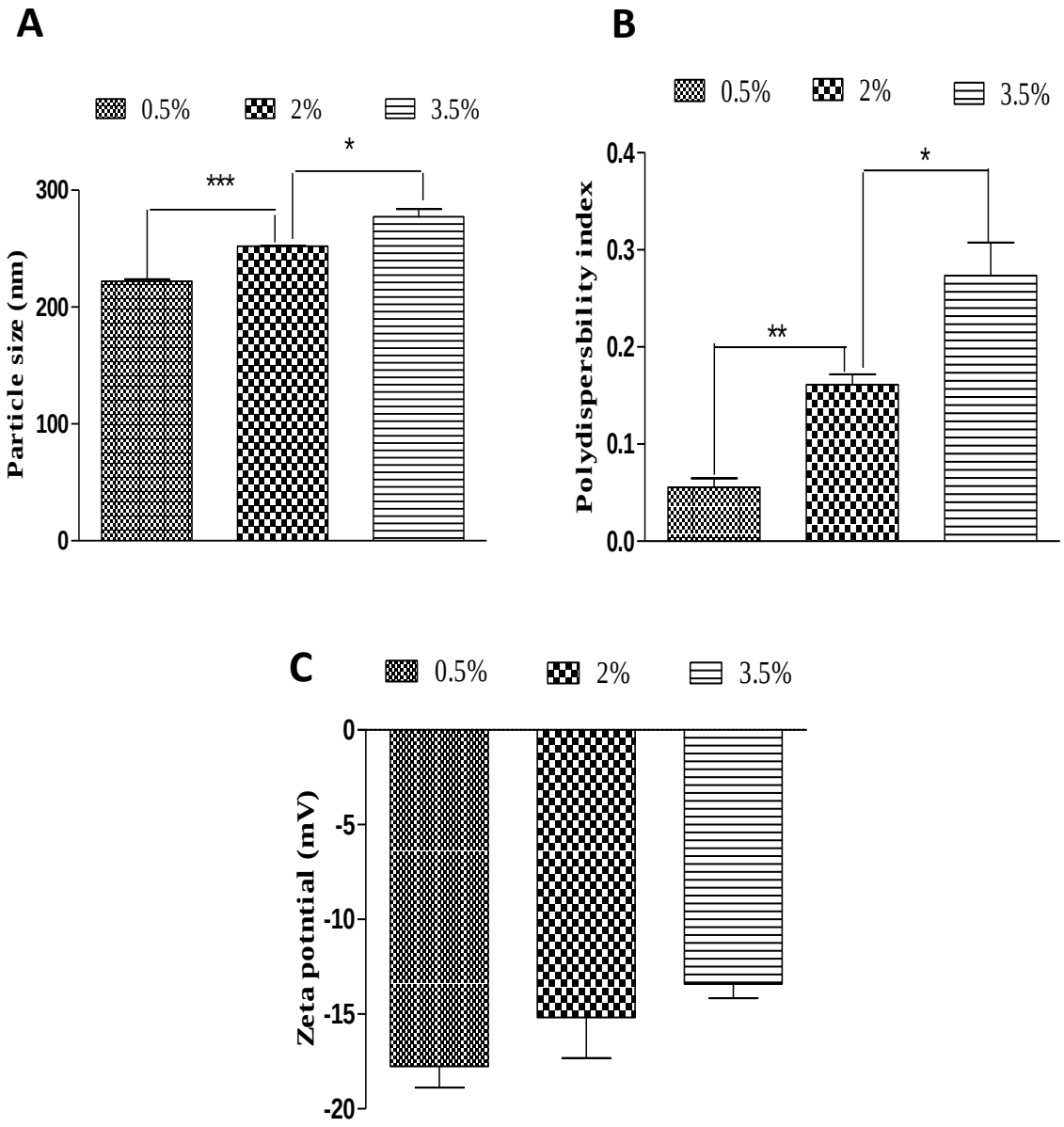

Figure 5.3: Effect of albumin concentration on particle size (A), polydispersity index (B) and zeta potential (C). The above graph represents the effect of increasing albumin concentration on Particle size (A), polydispersity index (B) and zeta potential (C). It was demonstrated that increase in albumin concentration leads to increase in particles size as well as polydispersity index significantly. It increases significantly ($P<0.001$) when albumin concentration increases from 0.5% to 2%. However, it does not have any significant effect on zeta potential. Values are mean ± SEM (n = 3). *$P<0.05$, **$P<0.01$ and ***$P<0.001$ compared with 2% albumin concentration.

5.5.4 Effect of Glutaraldehyde concentration

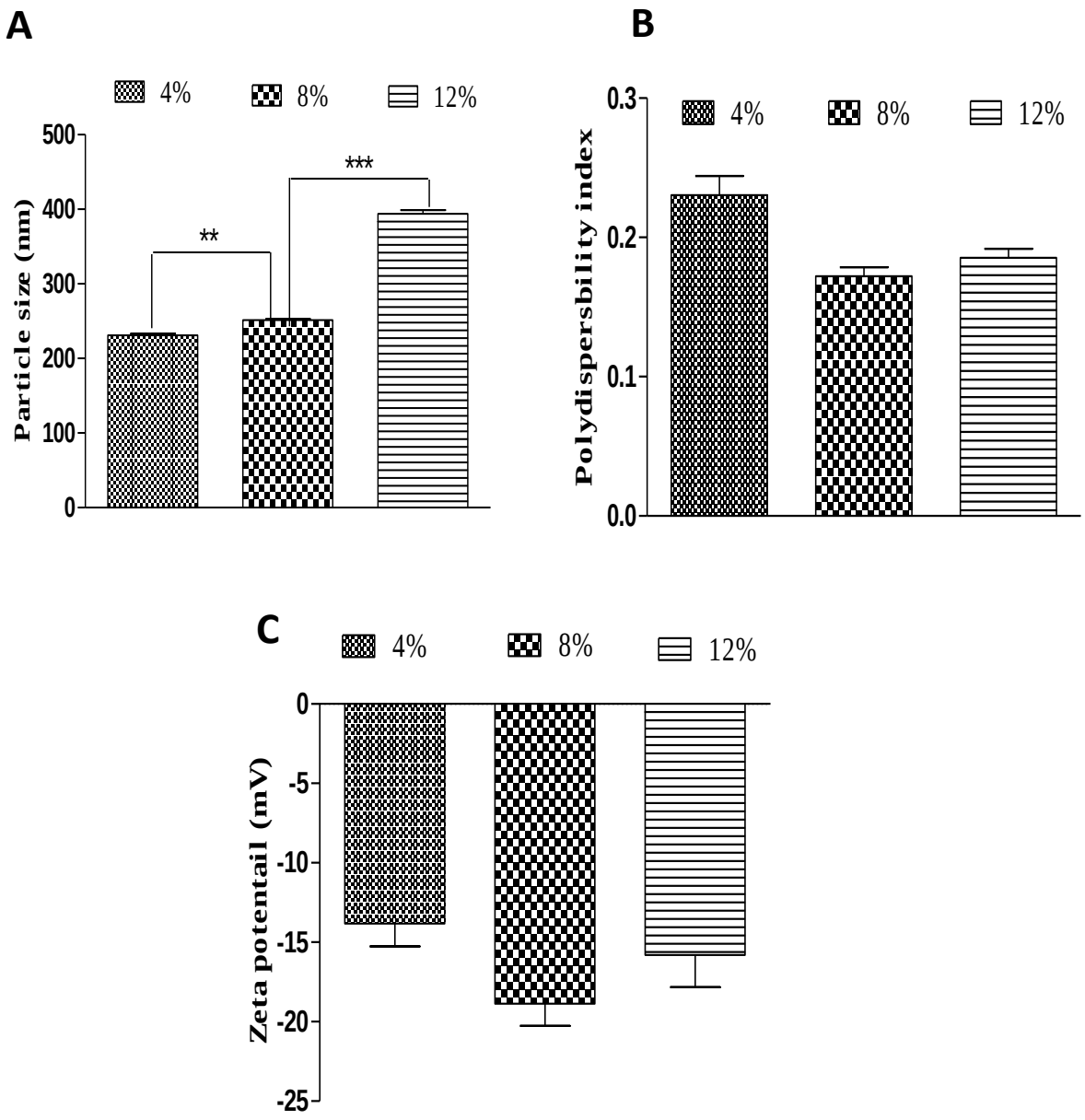

Figure 5.4: Effect of increasing concentration of crosslinking agent on particle size (A), polydispersity index (B) and zeta potential (C). The above graph represents the effect of an increase in glutaraldehyde concentration on Particle size (A), polydispersity index (B) and zeta potential (C). Increase in glutaraldehyde concentration leads to significant ($P<0.001$) increases in particle size). However, polydispersity index decreases upon an increase in glutaraldehyde concentration. Similarly, increasing concentration of glutaraldehyde does not have any significant effect on zeta potential. Values are mean ± SEM (n = 3). **$P<0.01$ and ***$P<0.001$ compared with 8% glutaraldehyde concentration.

5.5.5 Amount of drug

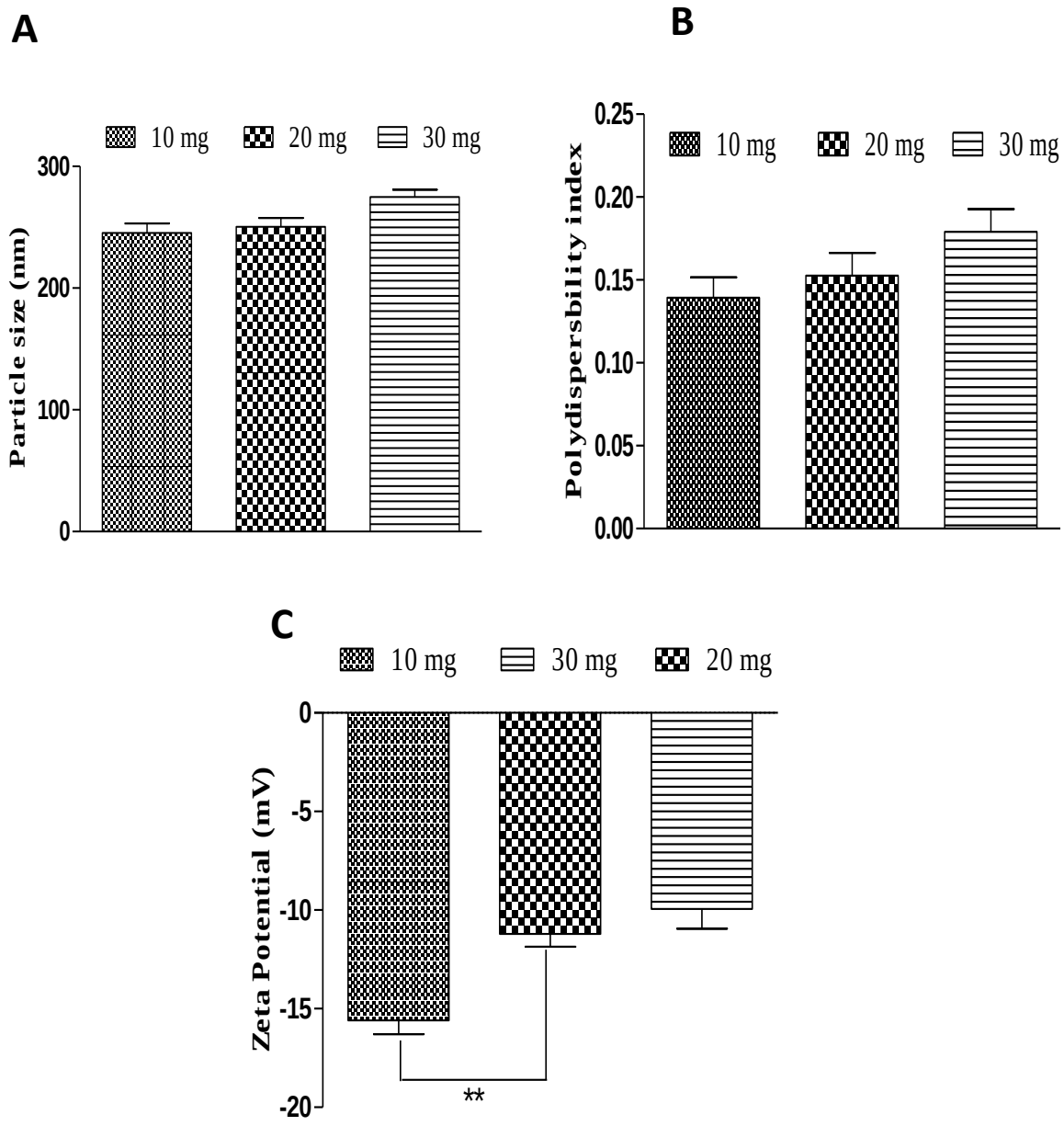

Figure 5.5: Effect of increase in drug amount on particle size (A), polydispersity index (B) and zeta potential (C). The above graph shows the effect of drug amount on Particle size (A), polydispersity index (B) and zeta potential (C). It is evident from the above graph that increases in CAPE amount slightly increase the particle size and PDI. Zeta potential increases upon an increase in CAPE amount although show significant increase ($P<0.01$). Values are mean ± SEM (n = 3). **$P<0.01$.

5.5.6 NMR spectra of CAPE-loaded albumin NP

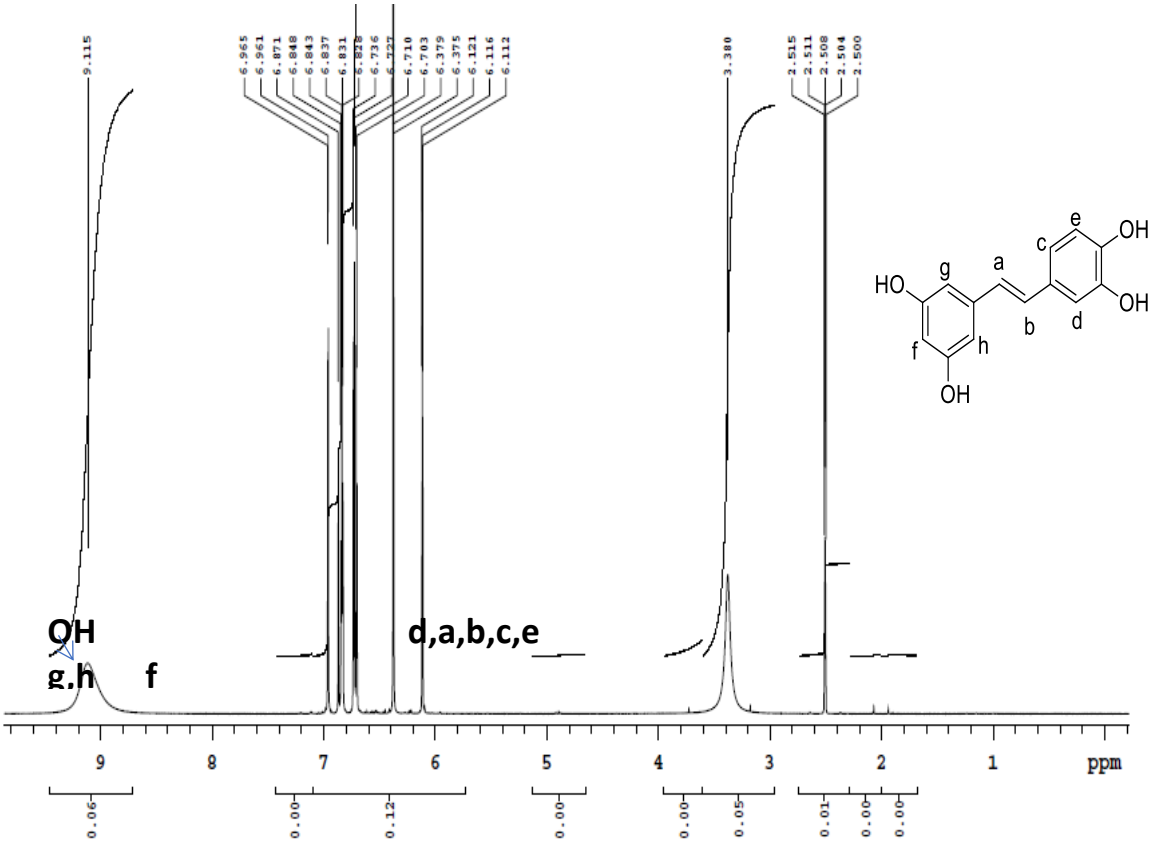

Figure 5.6: H NMR of CAPE in albumin nanoparticles. The above H NMR confirms the CAPE stucture in the nanoparticle form.

5.5.7 Entrapment efficiency

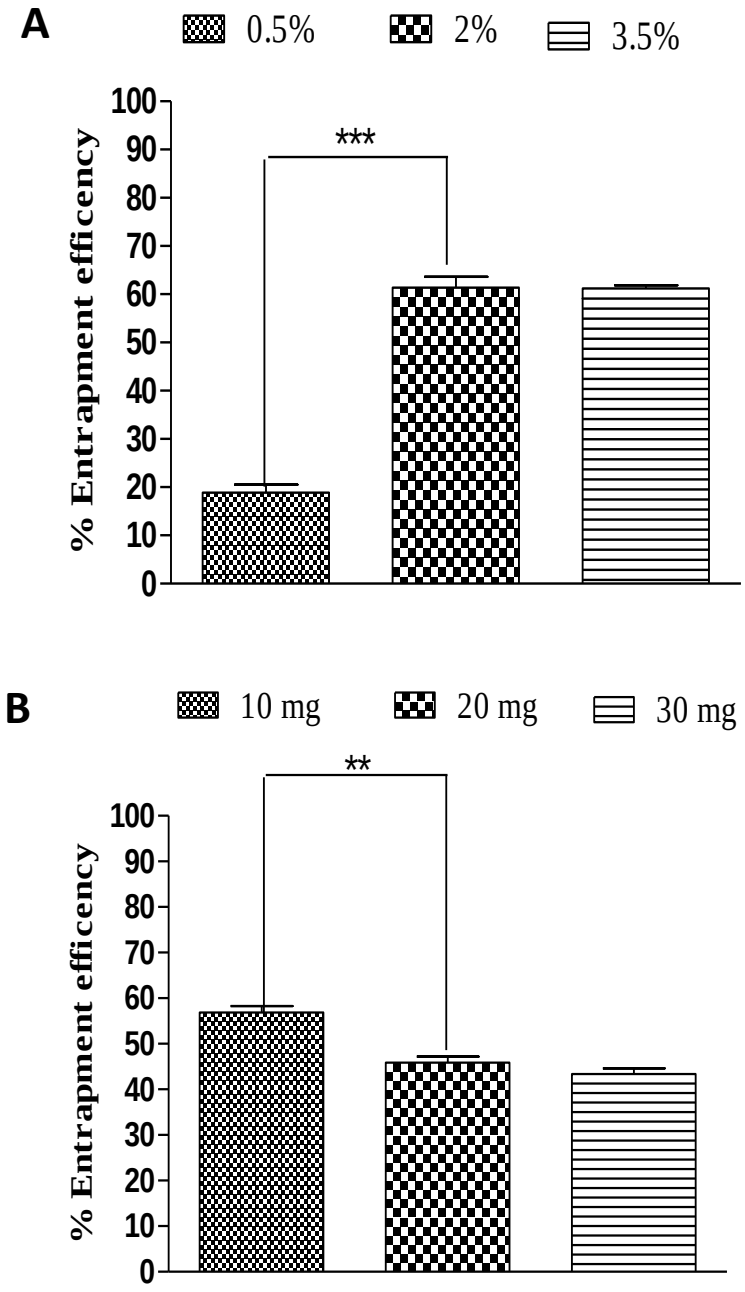

Figure 5.7: Effect of albumin concentration (A) and drug amount (B) on entrapment efficiency. The above graph illustrates effect albumin concentration (A) and drug content (B) on entrapment efficiency. Figure 5.7A in the above graph exhibit significant difference ($P<0.001$) when albumin concentration increases from 0.5% to 2%, however, entrapment does not exhibit any change upon further increase in albumin concentration. Figure 5.7B in the above graph illustrates the significant decrease in entrapment efficiency ($p<0.01$) as the drug amount increases from 10 mg to 20 mg but it does not have any significant effect when further increases to 30 mg. Values are mean ± SEM (n = 3). **P<0.01 and ***P<0.001

5.5.8 Percentage yield

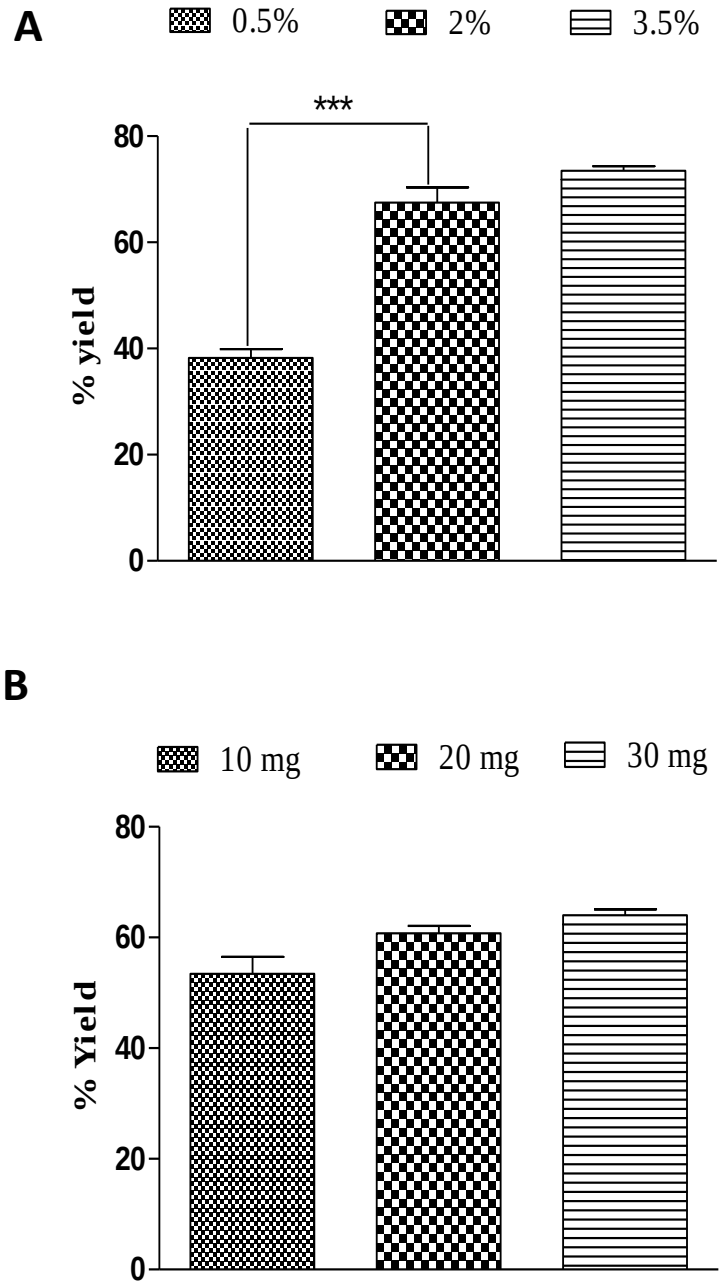

Figure 5.8: Effect of albumin concentration (A) and drug amount (B) on percentage yield. The above graph depicts effect albumin concentration (A) and drug content (B) on percentage yield. Figure 5.8A in the above graph demonstrates a significant difference ($P<0.001$) in percentage yield when albumin concentration increases from 0.5% to 2%, however, percentage yield slightly increases upon further increase in albumin concentration. Figure 5.8B in the above graph shows no significant difference as the amount of drug increases. Values are mean ± SEM (n = 3). ***$P<0.001$

5.5.9 In-vitro release

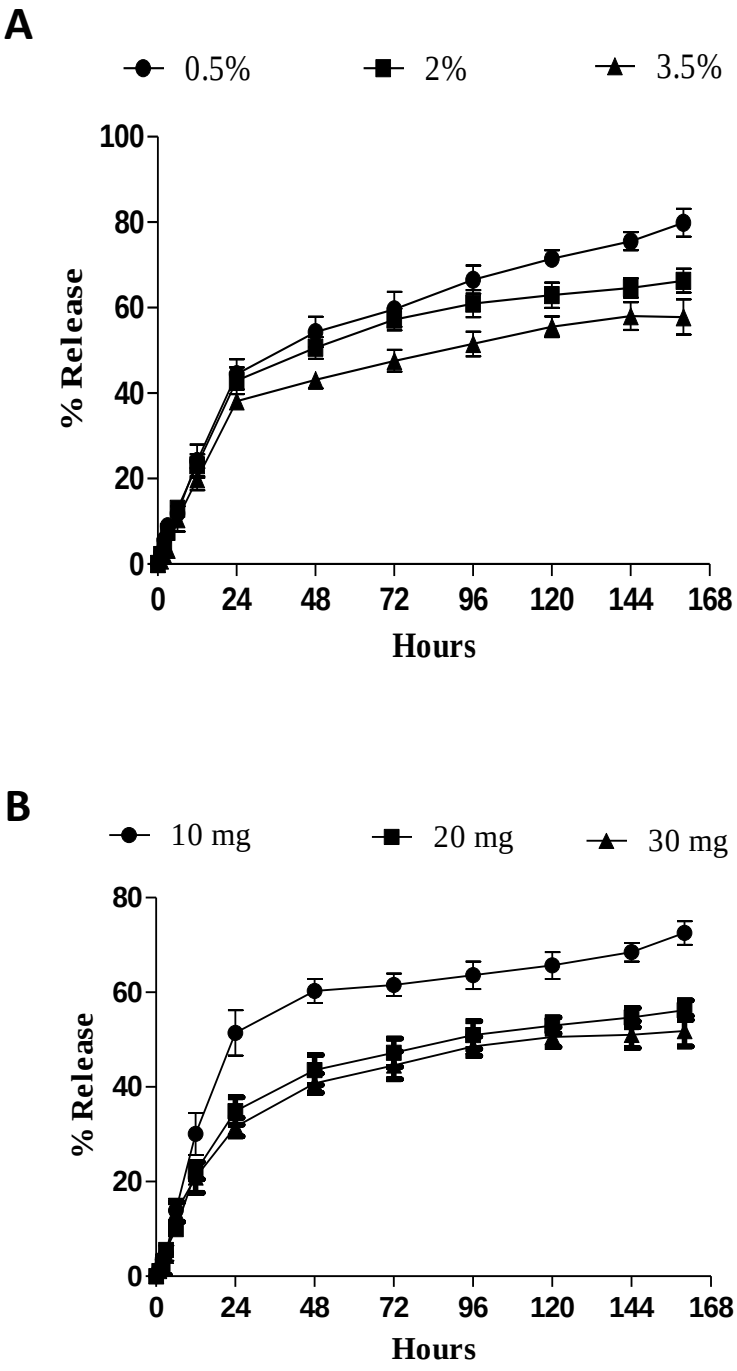

Figure 5.9: Effect of albumin concentration (A) and drug amount (B) on *in-vitro* release profile. The above graph illustrates burst release after 24. The above graph depicts that increase in albumin and drug concentration leads to decrease the *in-vitro* of CAPE release from the formulation. Values are mean ± SEM (n = 3).

5.5.10 Solubility of CAPE-loaded albumin NP

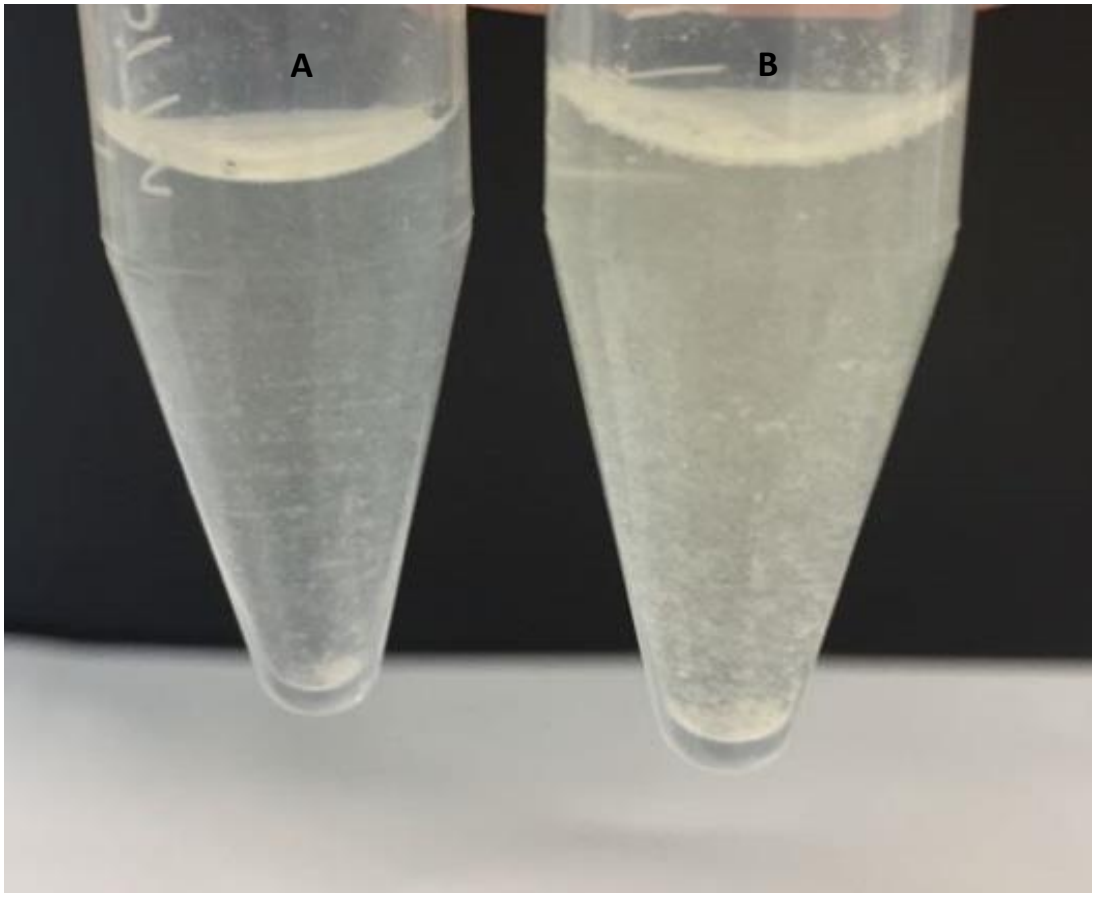

Figure 5.10: Water solubility of CAPE-loaded albumin NP (A) and free CAPE (B). The vials in Figure 5.10A and Figure 5.10B show the solubility of CAPE-loaded albumin NP and free CAPE, respectively. A Clear solution of CAPE-loaded albumin NP in Figure 5.10A and turbid free CAPE in Figure 5.10B can be observed.

5.5.11 Scanning electron microscopy

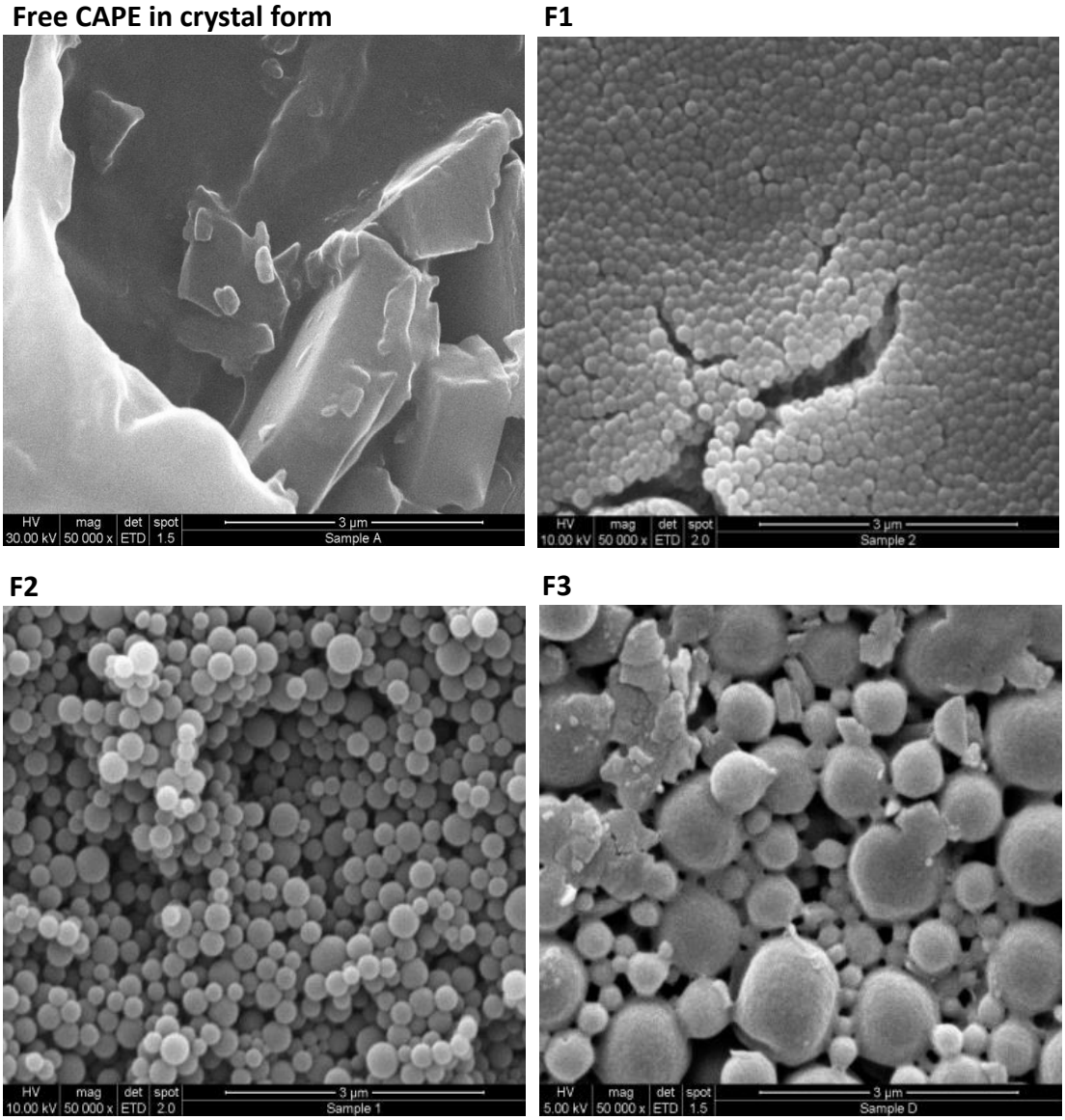

Figure 5.11: Scanning Electron Microscopy of CAPE-loaded albumin NP. The above Figure 5.11 represents SEM imaging of free CAPE, the batch containing 10 mg (F1), 20 mg (F2), and 30 mg (F3) of CAPE in the formulation. Batch formulated with 10 mg CAPE represents smaller particles size whereas batch fabricated with 30 mg CAPE shows larger particle size. F1 also demonstrate uniformity in size although F2 and F3 exhibit partial uniformity.

5.5.12 Cellular uptake of CAPE-loaded albumin NP

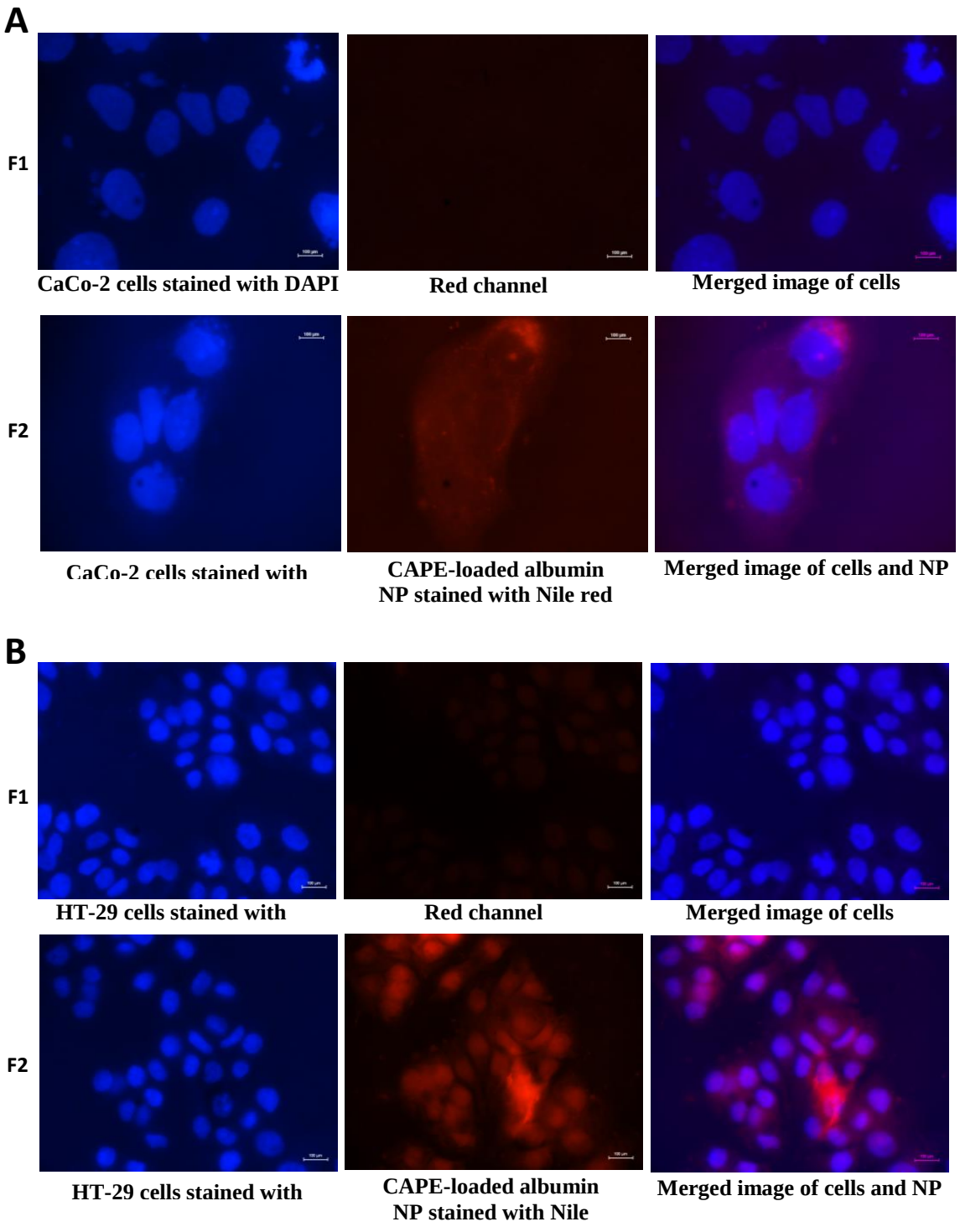

Figure 5.12: Cellular uptake of optimised CAPE-loaded albumin NP in CaCo-2 and HT-29 cells 100X. Cellular localization of Nile red-coated CAPE-loaded albumin NP was observed in CaCo-2 (A) and HT-29 (B) cells and visualized by overlapping under fluorescent microscopy.

5.5.13 In-vitro cytotoxicity assay

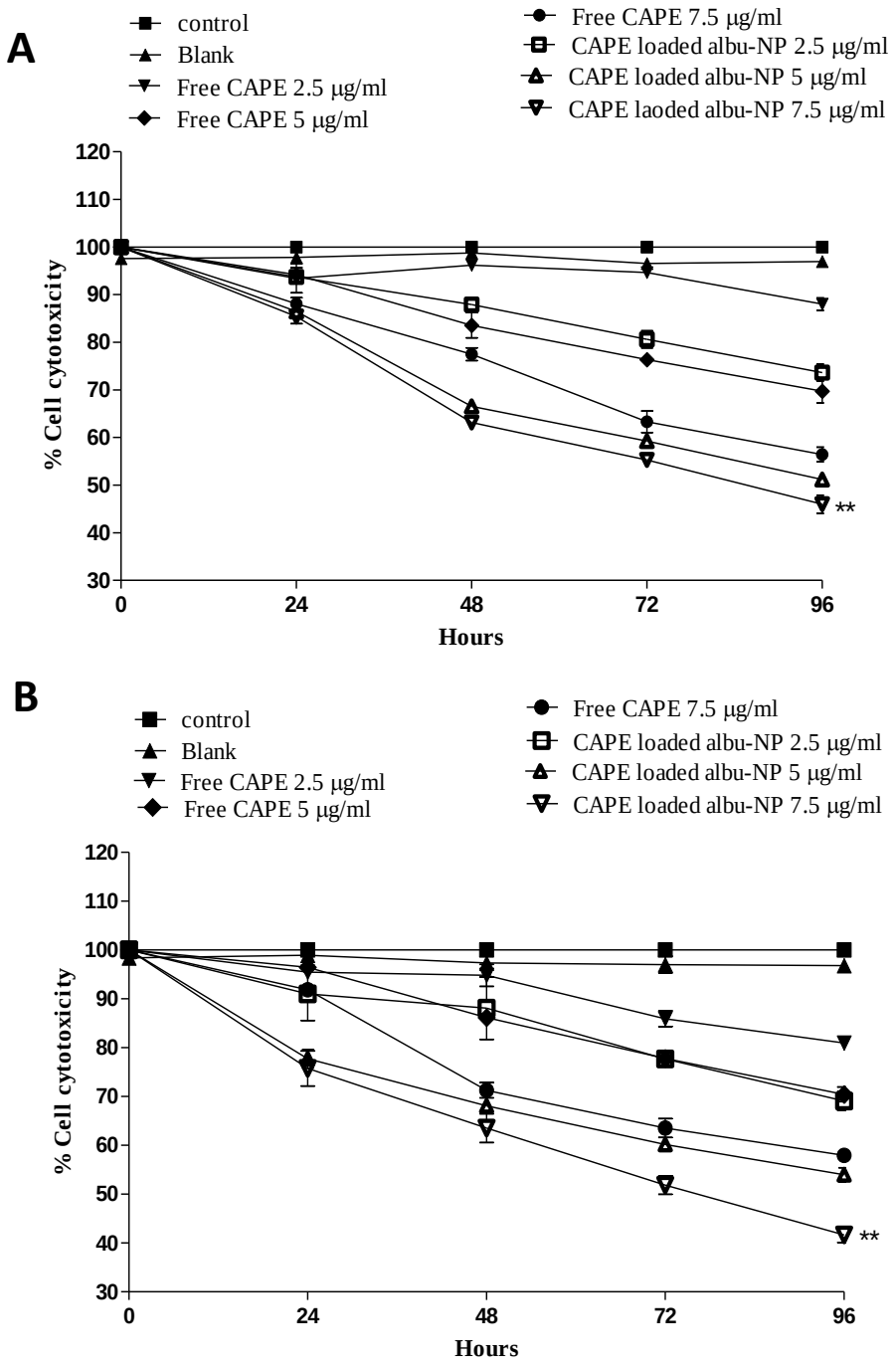

Figure 5.13: Effect of CAPE-loaded albumin NP and free CAPE on cytotoxicity of CaCo-2 (A) and HT-29 (B) cell lines. The cytotoxicity assay was performed on CaCo-2 (A) and HT-29 (B) cell lines. 40×104 cells were seeded on 24 well plates and treated with 2.5 µg/ml, 5 µg/ml and 7.5 µg/ml of CAPE-loaded albumin NP and an equivalent amount of free CAPE. The absorbance was measured after 24 hours, 48 hours, 72 hours and 96 hours. CAPE-loaded albumin NP shows higher cell cytotoxicity as compare to free CAPE. Values are mean ± SEM (n = 3). . **P<0.01 compared with same amount of free drug

5.5.14 Migration assay

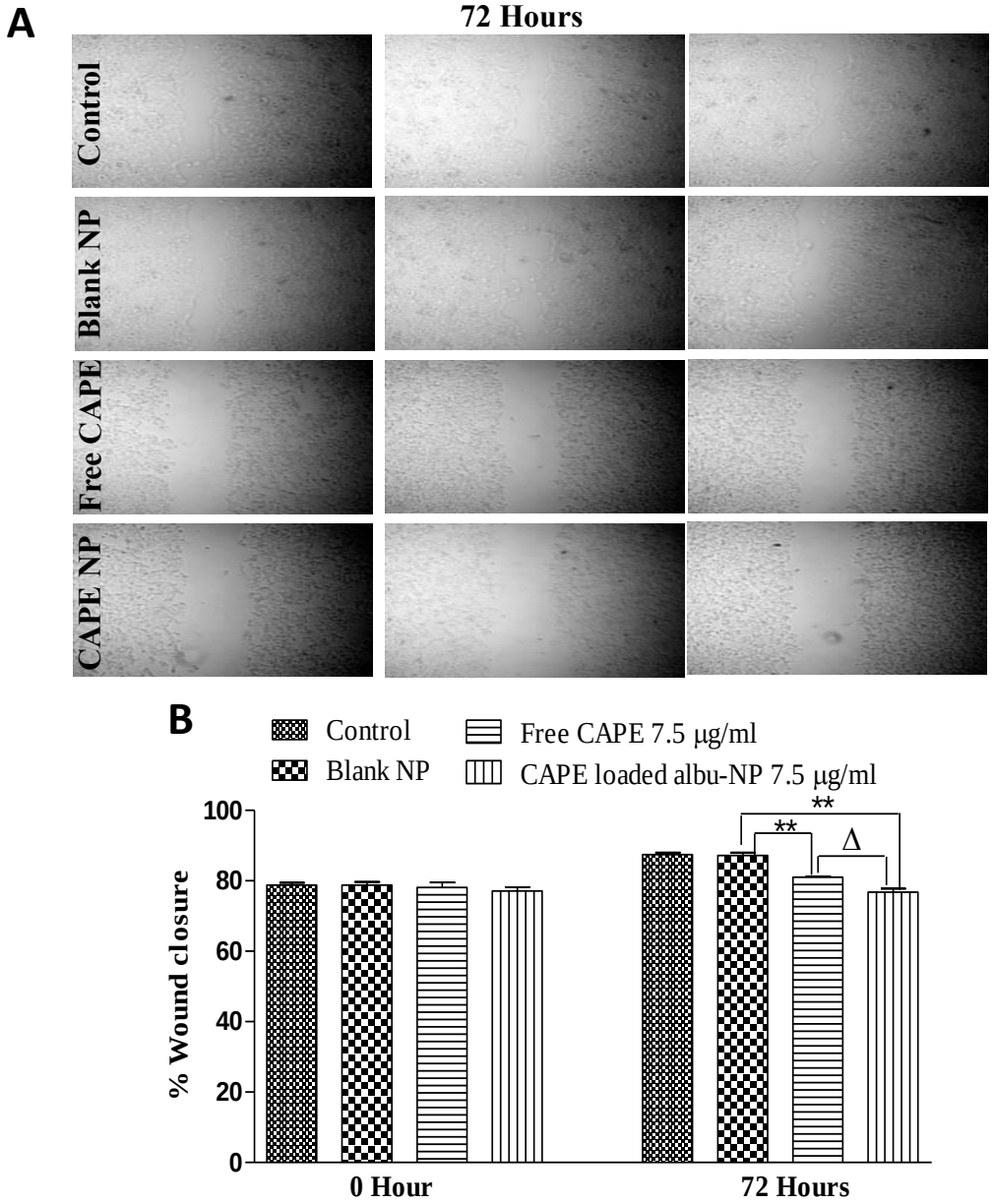

Figure 5.14: Effect of CAPE-loaded albumin NP and free CAPE on migration potential of CaCo-2 cell lines. The above images in the Figure 5.14A (CaCo-2) demonstrate the effect of free CAPE and CAPE-loaded albumin NP on wound closure after 72 hours of treatment. CAPE-loaded albumin NP demonstrate more void space than free CAPE in wound scratch of both cell line as compare to control and blank NP. The graph 5.14B (CaCo-2) depicts a significant variation of anti-migration activity of free CAPE and CAPE-loaded albumin NP after 72 hours of treatment at equal dose. CAPE-loaded albumin NP demonstrate significant low migration rate in CaCo-2 $P<0.01$) than control. Furthermore, CAPE-loaded albumin NP has less migration rate in CaCo-2 ($P<0.05$) than free CAPE. Values are mean ± SEM with n=3. **$P<0.01$ compared with blank NP. $^{\Delta}P<0.05$ compared with the same dose of the free PIC.

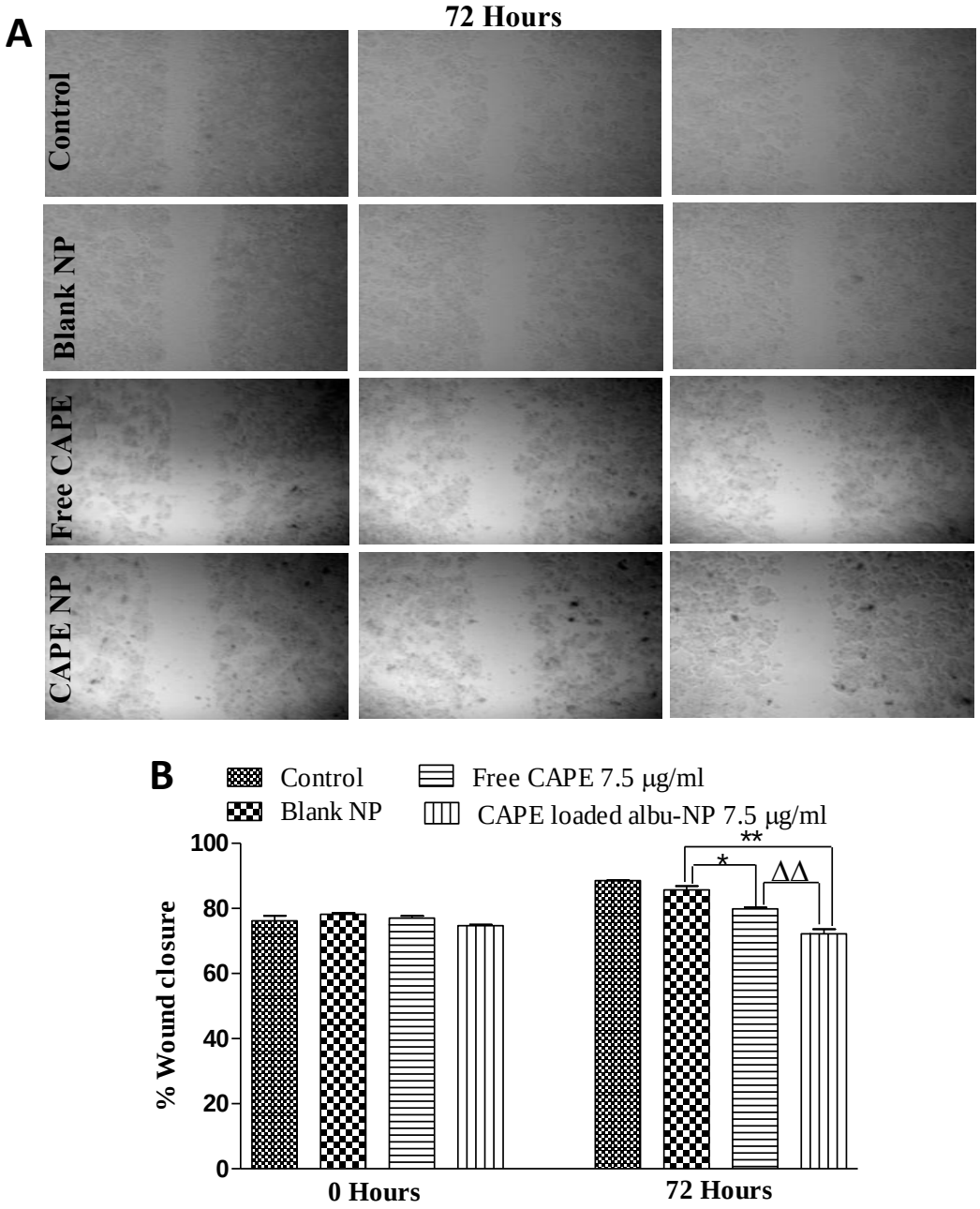

Figure 5.15: Effect of CAPE-loaded albumin NP and free CAPE on migration potential of HT-29 cell lines. The above images in the Figure 5.15A (HT-29) illustrate the effect of free CAPE and CAPE-loaded albumin NP on wound closure after 72 hours of treatment. CAPE-loaded albumin NP demonstrate more void space than free CAPE in wound scratch of both cell line as compare to control and blank NP. The graph 5.15B (HT-29) depicts a significant variation of anti-migration activity of free CAPE and CAPE-loaded albumin NP after 72 hours of treatment at equal dose. CAPE-loaded albumin NP demonstrate significant low migration rate in HT-29($P<0.01$) than control. Furthermore, CAPE-loaded albumin NP has less migration rate in HT-29($P<0.01$) than free CAPE. Values are mean ± SEM with n=3. *$P<0.05$ and **$P<0.01$ compared with blank NP. $^{\Delta\Delta}P<0.01$ compared with the same dose of the free PIC.

5.5.15 Colony formation assay

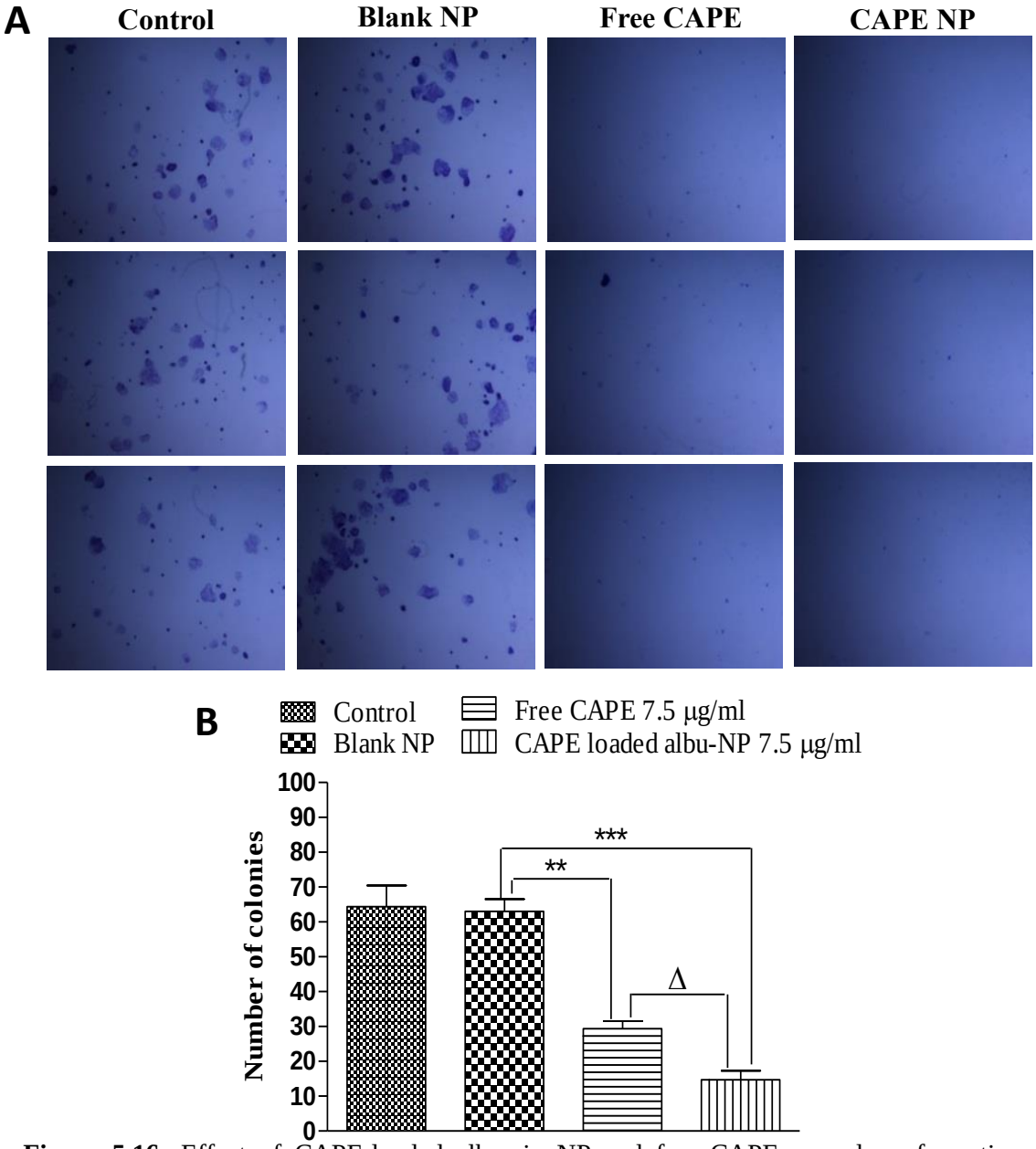

Figure 5.16: Effect of CAPE-loaded albumin NP and free CAPE on colony formation ability of CaCo-2 cell lines. The above images in the Figure 5.16A (CaCo-2) demonstrate a pattern of colon formation in control, blank NP, free CAPE and CAPE-loaded albumin NP treated the group as demonstrated in the microscopic image. It is evident from the images that CAPE-loaded albumin NP shows significant less number of colonies than the control group in CaCo-2. The graph 5.16B (CaCo-2) represents significant variation in colony formation upon treatment CAPE-loaded albumin NP than the control group in CaCo-2 ($P<0.001$). It can be seen from the above graph that CAPE-loaded albumin NP shows less number of colonies than free CAPE in CaCo-2 ($P<0.05$). Values are mean ± SEM with n=3. **$P<0.01$ and ***$P<0.001$ compared with blank NP. $^{\Delta}P<0.05$ compared with the same dose of the free PIC.

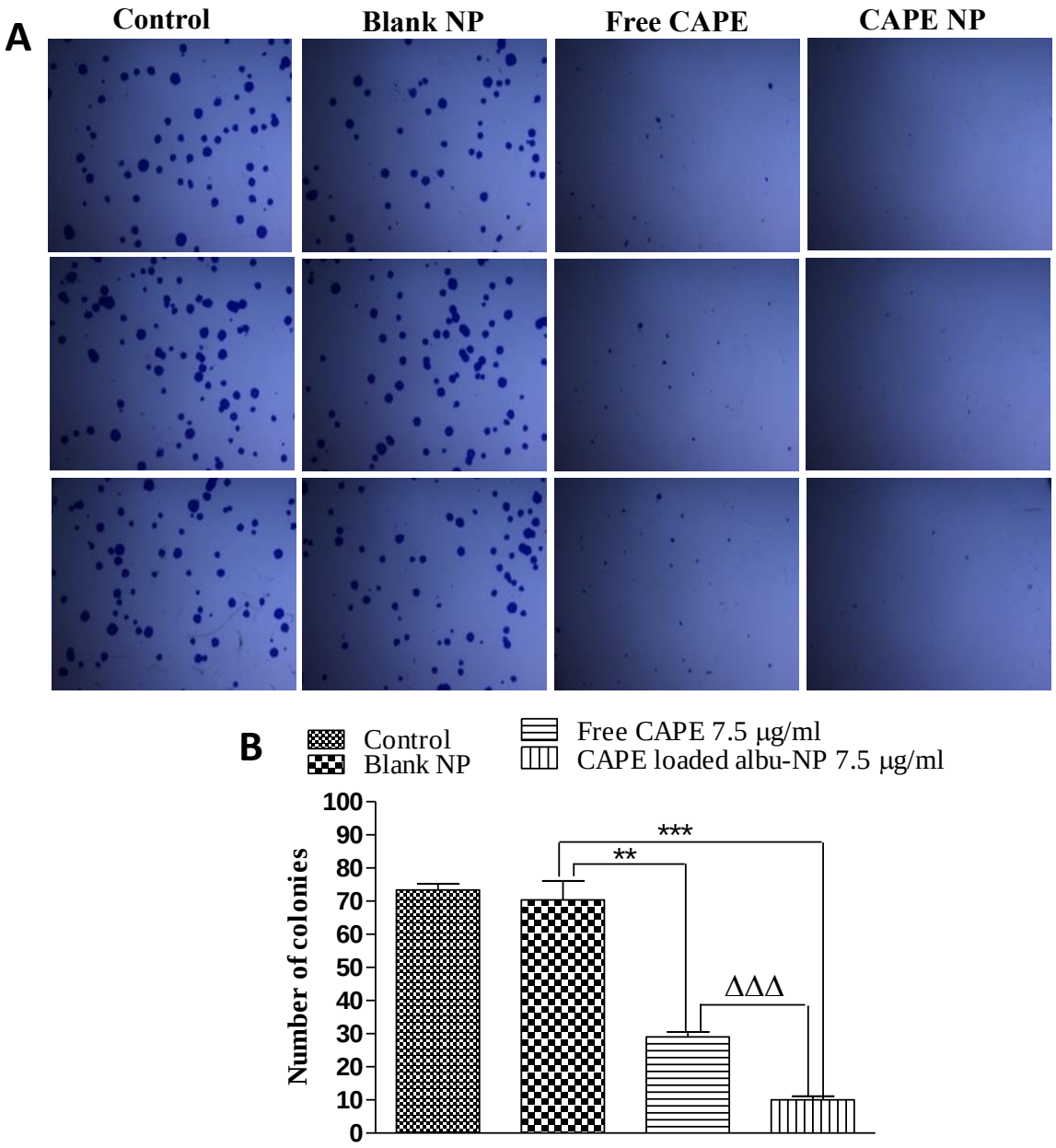

Figure 5.17: Effect of CAPE-loaded albumin NP and free CAPE on colony formation ability HT-29 cell lines. The above images in the Figure 5.17A (HT-29) demonstrate a pattern of colon formation in control, blank NP, free CAPE and CAPE-loaded albumin NP treated the group as demonstrated in the microscopic image. It is evident from the images that CAPE-loaded albumin NP shows significant less number of colonies than the control group in HT-29. The graph 5.17B (HT-29) represents significant variation in colony formation upon treatment CAPE-loaded albumin NP than the control group in HT-29 ($P<0.001$). It can be seen from the above graph that CAPE-loaded albumin NP shows less number of colonies than free CAPE in HT-29 ($P<0.001$). Values are mean ± SEM with n=3. **$P<0.01$ and ***$P<0.001$ compared with blank NP. $^{\Delta\Delta\Delta}P<0.001$ compared with the same dose of the free PIC.

5.5.16 Invasion assay

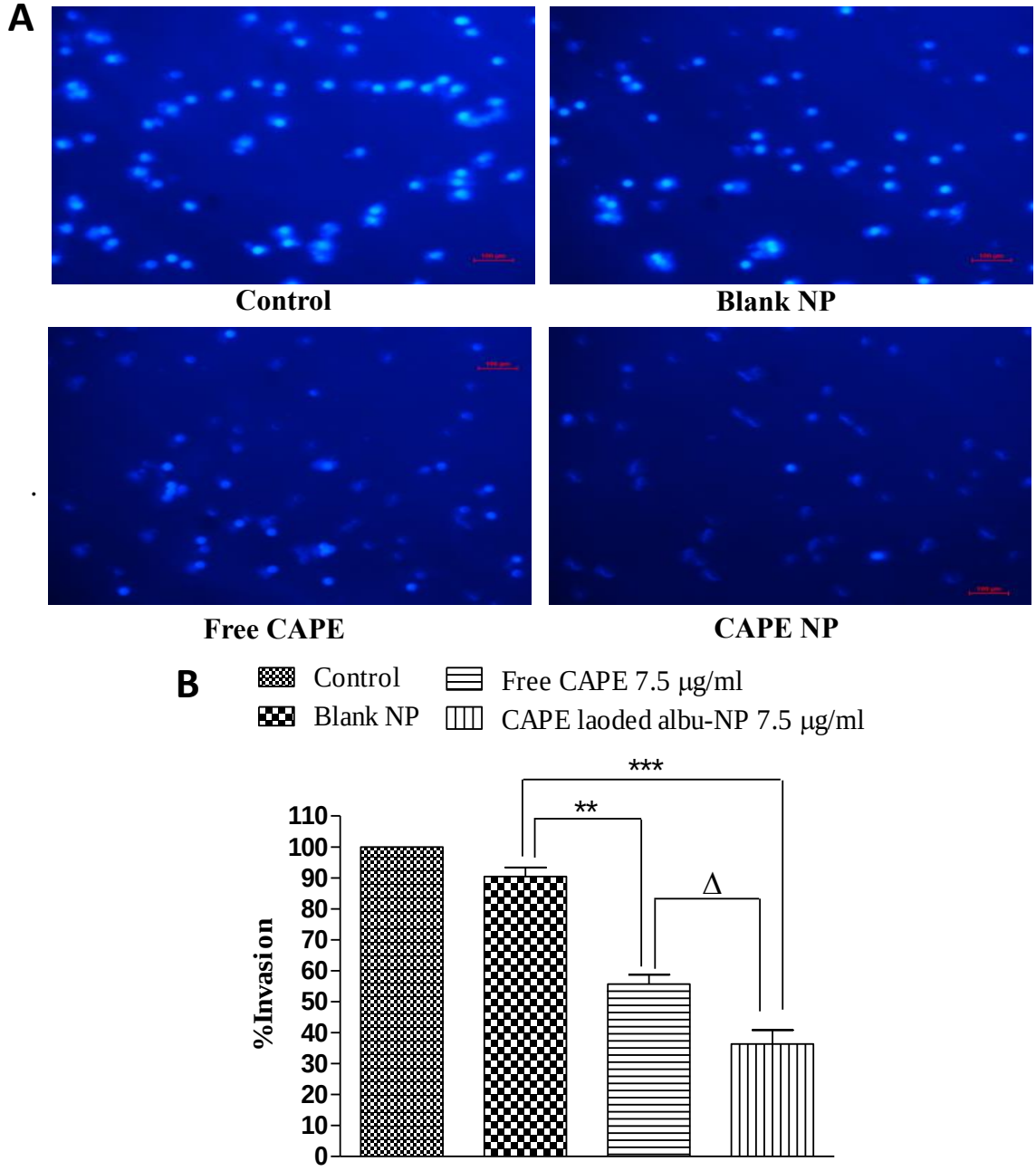

Figure 5.18: Effect of CAPE-loaded albumin NP and free CAPE on invasion potential of CaCo-2 cell lines. The above images in the Figure 5.18A (CaCo-2) represents a microscopic depiction of anti-invasive activity of free CAPE and CAPE-loaded albumin NP after of treatment. CAPE-loaded albumin NP ($P<0.05$) shows significantly less percentage of invasion than free CAPE ($P<0.001$). CAPE loaded NP reduced the percentage of invasion potential significantly in CaCo-2 ($P<0.05$) than free CAPE as shown in the graph 5.18B. The cells which appear bright are the one which invaded through the membrane. Values are mean ± SEM with n=3. **$P<0.01$ and ***$P<0.001$ compared with blank NP. $^{\Delta}P<0.05$ compared with the same dose of the free CAPE.

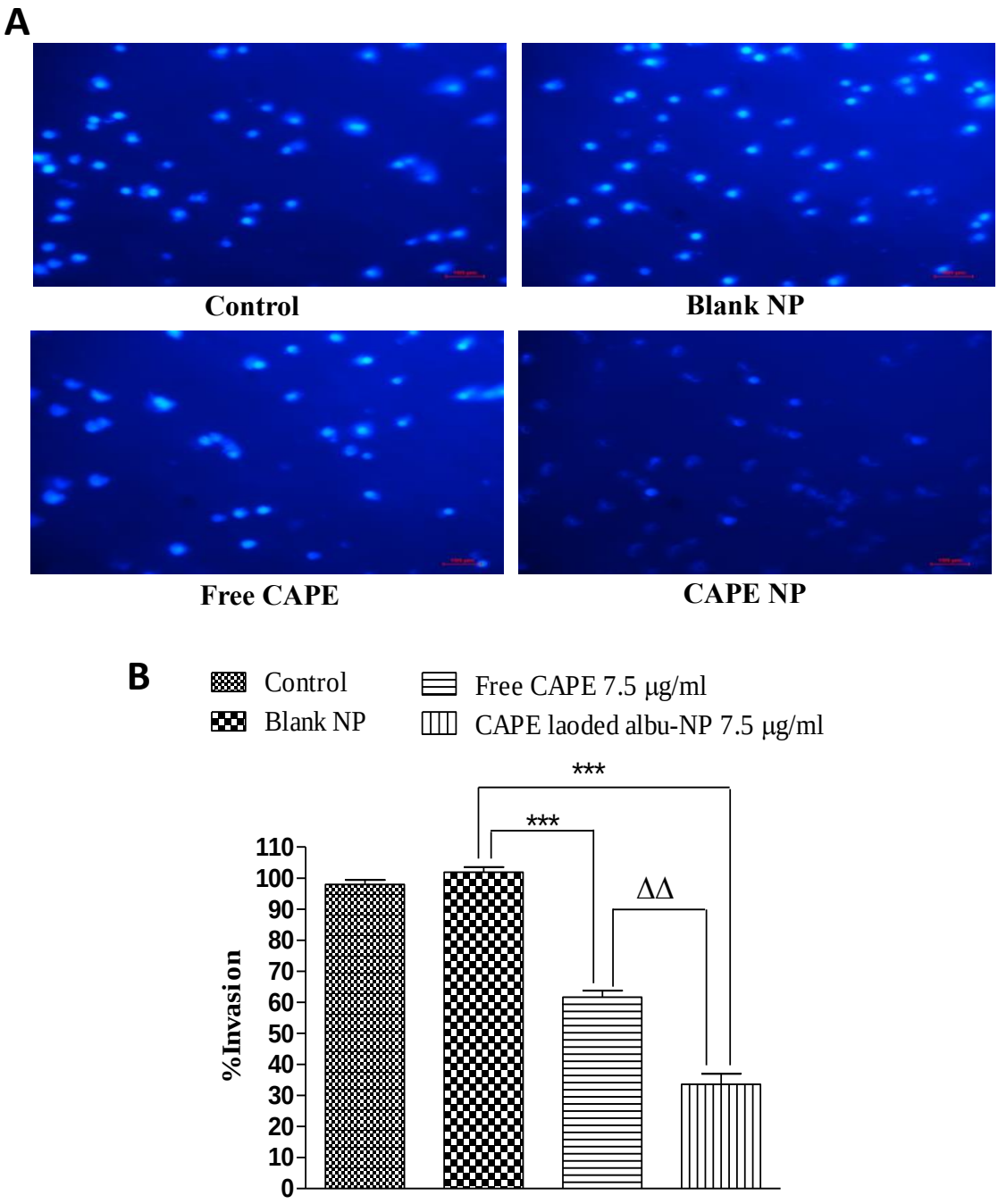

Figure 5.19: Effect of CAPE-loaded albumin NP and free CAPE on invasion potential of HT-29 cell lines. The above images in the Figure 19A (HT-29) represents a microscopic depiction of anti-invasive activity of free CAPE and CAPE-loaded albumin NP after of treatment. CAPE loaded NP reduced the percentage of invasion potential significantly in HT-29 ($P<0.01$) than free CAPE as shown in the graph 5.19B. The cells which appear bright are the one which invaded through the membrane. Values are mean ± SEM with n=3. ***$P<0.001$ compared with blank NP. $^{\Delta\Delta}$ $P<0.01$ compared with the same dose of the free CAPE.

5.5.17 Quantification of p65

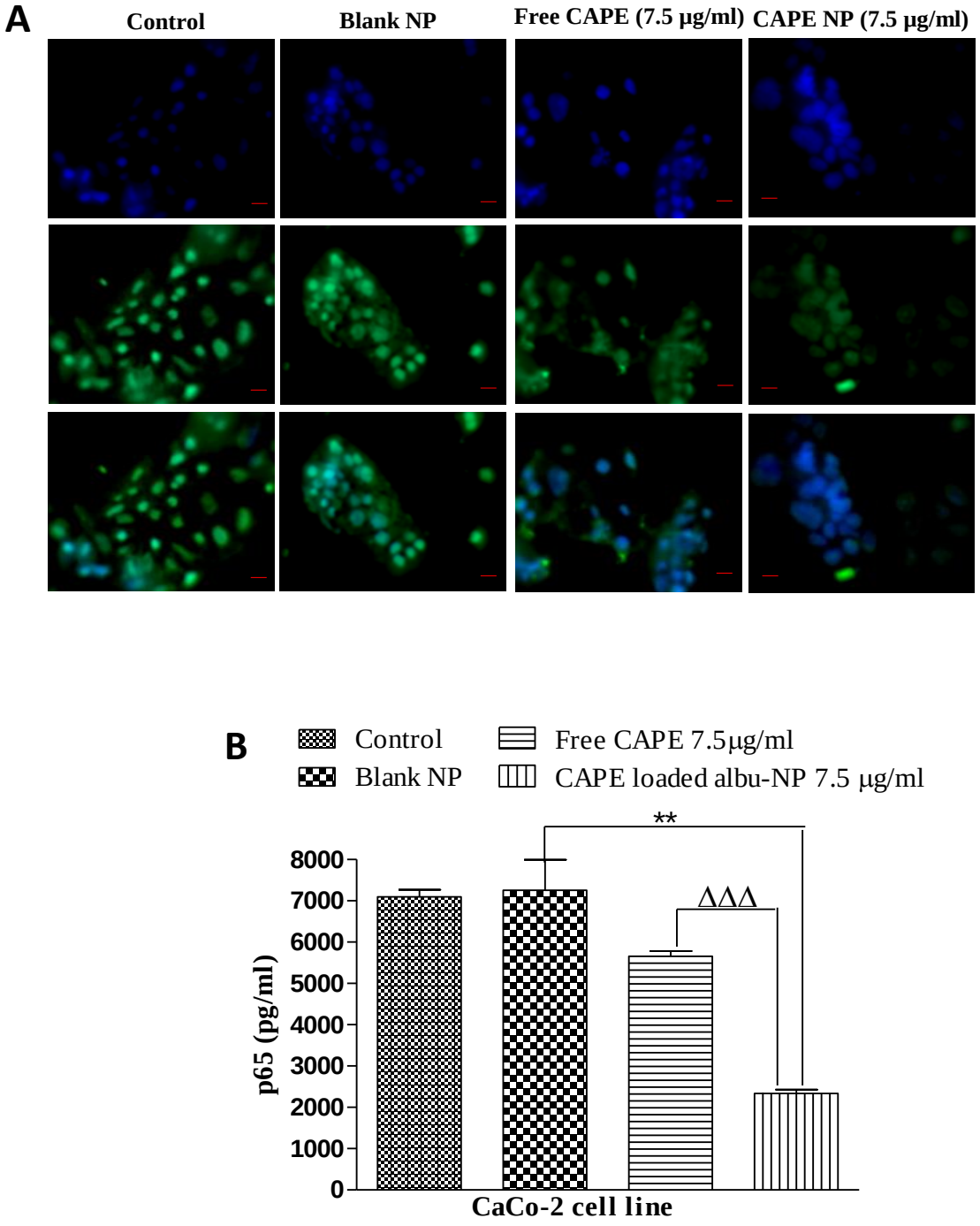

Figure 5.20: Effect of CAPE-loaded albumin NP and free CAPE on expression p65 in CaCo-2 at 40X. The above image in the Figure 5.20A (CaCo-2) was taken under bright field microscope. Control and blank images show induction of p65 whereas image under the free CAPE and CAPE-loaded albumin NP show a reduced level of p65. Figure 5.20B demonstrate a significant reduced level of p65 in CaCo-2 ($P<0.01$)) as compare to control. CAPE-loaded albumin NP also illustrate the significant low level of p65 in CaCo-2(**$P<0.01$) than free CAPE. Values are mean ± SEM with n=3. **$P<0.01$ compared to equal amount of free CAPE. $^{\Delta\Delta\Delta}P<0.001$ compared to the same amount of free CAPE.

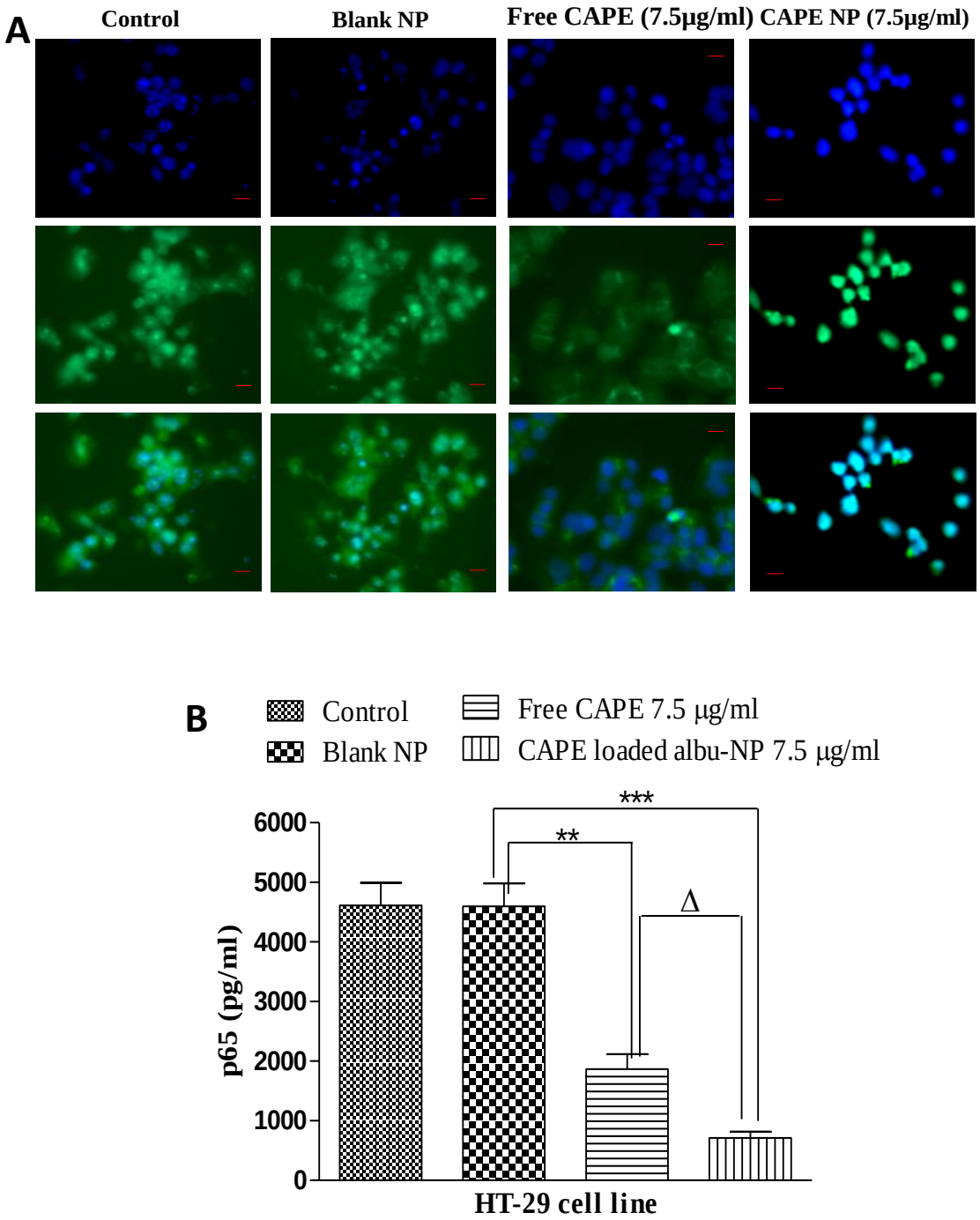

Figure 5.21: Effect of CAPE-loaded albumin NP and free CAPE on expression p65 in HT-29 at 40X. The above image in the Figure 5.21A (HT-29) was captured under bright field microscope. Control and blank images show induction of p65 whereas image under the free CAPE and CAPE-loaded albumin NP show a reduced level of p65. Figure 5.21B demonstrate a significant reduced level of p65 in HT-29 ($P<0.001$) as compare to control. CAPE-loaded albumin NP also illustrate the significant low level of p65 in HT-29 ($P<0.05$) than free CAPE. Values are mean ± SEM with n=3. **$P<0.01$ and ***$P<0.001$ compared to equal amount of free CAPE. $^{\Delta}P<0.05$ compared to the same amount of free CAPE.

5.5.18 Quantification of HIF-1α

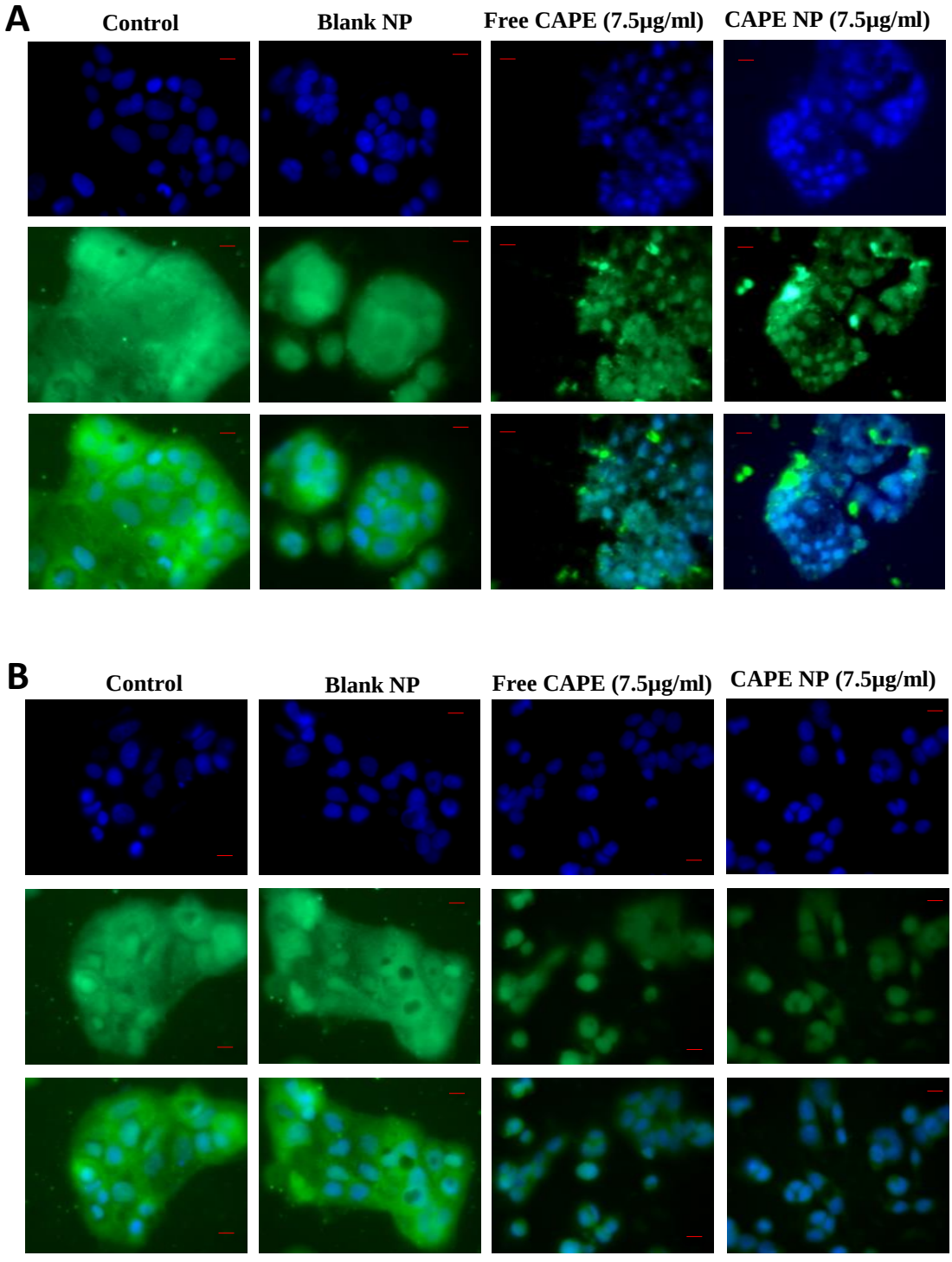

Figure 5.22: Effect of CAPE-loaded albumin NP and free CAPE on expression HIF-1α in CaCo-2 (Figure 5.22A) and HT-29 (Figure 5.22B) at 40X. The above control and blank images show induction of HIF-1α whereas images under free CAPE and CAPE-loaded albumin NP show a reduced level of HIF-1α.

5.6 Discussion

Effect of solvent concentration, albumin concentration, glutaraldehyde and amount of drug on as particle size, zeta potential, and polydispersity were observed. Increase concentration of ethanol has no significant effects on particle size, polydispersity index and zeta potential. Formulation of nanoparticles with increase concentration albumin depicts an increase in particle size, polydispersity index and zeta potential significantly as demonstrated in Figure 5.3. Increase in density of albumin solution upon increasing the albumin concentration may responsible for the increase in particle size of nanoparticles. Higher concentration of glutaraldehyde has a similar effect as the albumin centration on nanoparticles as represented in Figure 5.4. Particle size increases significantly with increase in concertation of the crosslinking agent. However, it does not have any significant effect on polydispersity and zeta potential. Nanoparticles shows an increase in particle size with increase drug amount in the formulation as exhibited in Figure 5.5. Although it does not depicts any significant difference in particle size, zeta potential and polydispersity index. Increase in viscosity of drug solution due to increase in the drug amount play vital role in increasing the particle size of nanoparticles. We have done NMR spectroscopy of CAPE to confirm the purity of drug in nanoparticles as illustrated in Figure 5.6. We have also evaluated the effect of albumin concentration and CAPE amount on entrapment efficiency and percentage yield as shown in Figure 5.7 (A and B) and Figure 5.8 (A and B). The entrapment efficiency and percentage yield increase significantly as the amount of albumin increases. This because the availability of more amount of albumin to encapsulate the same amount of CAPE in the formulation. Similarly, effect of albumin concentration and CAPE amount on *in-vitro* release was reported as illustrated in the Figure 5.9 (A and B). The data

obtained elucidate increase in *in-vitro* release pattern upon increasing albumin concentration and CAPE amount due to larger particles of nanoparticles.

Figure 5.10 express comparison of solubility of CAPE-loaded albumin NP (A) and free CAPE (B). Figure 5.10A shows the clear solution of CAPE-loaded albumin NP which is due to increase in solubility. Whereas, Figure 5.10B represents the turbid solution of free CAPE in water. Twofold increase in aqueous solubility in CAPE-loaded albumin NP was documented as compare to free CAPE. The morphology of free CAPE and nanoparticles of CAPE was evaluated by SEM as shown in the Figure 5.11. Solid crystal and large structure of free CAPE was reported by SEM imaging. However, spherical and smooth appearance of the nanoparticle was found under SEM. Though, increase in particle size can be observed as the CAPE amount increases.

Images F1 in the Figure 5.12(A and B) display CaCo-2 and HT-29 stained with DAPI whereas image F2 exhibit localization of CAPE-loaded albumin NP labeled with Nile Red in CaCo-2 and HT-29 under a fluorescent microscope. The anticipation of Nile Red labeled CAPE-loaded albumin NP in CaCo-2 and HT-29 establish that nanoparticles are easily taken by cells. Figure 5.13 interpret the effect of different dose of free CAPE and CAPE-loaded albumin NP in CaCo-2 (A) and HT-29 (B) cells. Decrease event of proliferation was noted with CAPE-loaded albumin NP as compare to free CAPE in colorectal cancer cell.

Figure 5.14A and Figure 5.15A shows microscopic images of migrating cancer cells at 0 hours and 72 hours. Both the microscopic appearance shows a decline in migration after treatment with CAPE-loaded albumin NP in CaCo-2 and HT-29 as compare to free CAPE at 72 hours. Graph in the Figure 5.14A and Figure 5.15A in

shows significant reductions in the migration of cancer cell after 72 hours. Figure 5.16A and Figure 5.17A also represent a microscopic picture of colony formation of control, blank NP, free CAPE and CAPE-loaded albumin NP groups in CaCo-2 and HT-29 cells. A number of the colony was found to be higher in control, blank NP group in both cell lines. However, decrease in colonies can be seen in CAPE-loaded albumin NP as compare to free CAPE in both cell line. Graph in the Figure 5.16B and 5.17B also confirmed significant reductions in colony formation for CaCo-2 and HT-29 cancer cells.

Figure 5.18A and Figure 5.19A are the representative images from invasion assay in CaCo-2 and HT-29 cells captured under a fluorescent microscope. The more number of fluorescent cells can be monitored in control and blank NP group as visible in Figure 5.18A and Figure 5.19A. However, very few bright cells detected in CAPE-loaded albumin NP as compare to free CAPE. A significant decrease in invasion was reported with CAPE-loaded albumin NP treated cells than free CAPE in CaCo-2 and HT-29 as depicted in graph of Figure 5.18B and Figure 5.19B.

Induction of p65 can be recognized in control and blank NP group in CaCo-2 and HT-29 as shown in the Figure 5.20A and Figure 5.21A under a bright field microscope. Although a low level of p65 was be observed in CAPE-loaded albumin NP than free CAPE in both cell line as represented in the graph of Figure 5.20B and Figure 5.21B. Similarly, low expression of HIF-1α was monitored in cells treated with CAPE-loaded albumin NP as shown in the Figure 5.22(A and B).

Hence the reduction in particle size has increases the solubility of low soluble natural compound CAPE in nanoparticle form. Nanoparticles down-regulate over activation of p65 (RelA) and HIF-1α levels to a higher extent than free CAPE in colorectal

cancer cell lines. Thus, CAPE nanoparticles increased the therapeutic value of the natural anticancer agent via suppression of overactivation of NF-kβ and HIF pathways during cancer.

Hence, the findings from this work conclude that nanotechnology could be an effective tool to enhance the anticancer activity of several natural and/or novel anticancer compounds, which are currently not in clinical use due to their low solubility and/or poor bioavailability.

5.7 Conclusion

The findings from this chapter show that PIC-loaded albumin nanoparticles can be fabricated by desolvation technique. Final and optimised batch of NPs were selected by optimization and characterization processes to carry out an *in-vitro* evaluation in cancer cell lines. Result from cell proliferation assay showed a dose-dependent relationship with proliferation in CaCo-2 and HT-29 cells and ascertained that CAPE-loaded albumin NP resulted in less cell proliferation than free CAPE in cancer cells lines. CAPE-loaded albumin NP controls migration, colony formation and invasion in cancer cells more effectively than free CAPE. CAPE loaded albumin reduces the overexpressed level of p65 and HIF-1α higher extent that free CAPE. Therefore, CAPE-loaded albumin NP delivery may be of therapeutic potential in cancer treatment.

Chapter 6

Albumin nanoparticles loaded with PIC/CAPE are protective in experimentally induced colitis via modulation of p65 and HIF-1α

6.1 Introduction

Ulcerative colitis (UC) and Crohn's disease (CD) are gastrointestinal ailments termed as inflammatory bowel disease (IBD) with no specific treatment (Ma et al., 2017a., Deiana et al., 2017., Karreman et al., 2017). UC and CD have common symptoms such as weight loss, diarrhoea, rectal bleeding, and abdominal cramp (Peyrin-Biroulet et al., 2010., Jordan et al., 2016). However, both disorders differ in location, UC is sequestered in the large intestine (Sullivan et al., 2017) and CD may occur anywhere in the gastrointestinal tract(Vezza et al., 2016). Both disease cause a cryptic abscess and alteration in mucosal layer (Vezza et al., 2016). The exact etiology of IBD is not clear but factors such as aberrant immunity, environmental factor, genetic disorder and dysregulation of the mucosal layer are responsible for colitis (Nitzan et al., 2016., Lane et al., 2017).These factors result in mucosal layer hypoxia and cause overactivation of hypoxia-inducible factor 1 (HIF-1α) and nuclear factor kappa beta (NF-kβ) (Taylor and Colgan, 2007., Taylor and Cummins, 2009). Moreover, an elevated level of HIF-1α and NF-kβ has been documented in human colitis (Ma et al., 2016).

More than 50% of IBD patients develop ulcerative colitis (Tan et al., 2017a). The associated healthcare cost is a major burdens for IBD patients in countries like USA, Europe, and Asian countries (Singh et al., 2017a., Savani et al., 2017) (Davies et al., 2017., Dan et al., 2017., Wilson et al., 2017., de et al., 2017). Damaged mucosal layer is the main cause of ulcerative colitis (Boal Carvalho and Cotter, 2017., Capaldo et al., 2017). The predominant therapies used in the management of ulcerative colitis such as amino-salicylic acid, corticosteroids, 6-mercaptopurines, azathioprine, cyclosporine, infliximab have several side effects on skin, eyes, muscle etc. (Taylor and Gibson, 2017., Danese et al., 2017). These therapeutics also induce

bone marrow depletion, lung disorders, liver and pancreas disease (Chumanevich et al., 2017., Khan et al., 2017c). Additionally, these treatments are not only non-selective but also impair lifestyle due to repeated use for a long time (Xiao et al., 2017., Larussa et al., 2017). Therefore, these therapeutics are not effective in treating ulcerative colitis due to which patients have to bear invasive surgeries in chronic conditions to prevent further complication such as colon cancer (Abdalla et al., 2017).

Novel agents, such as monoclonal antibodies, protease inhibitors, and anti-TNF-α compounds have been widely used in the treatment of ulcerative colitis (Vergnolle, 2016., Martelli et al., 2017). However, these agents also have limitation due to side effects, like liver damage, heart disease, infectious disease, skin disease and degenerative disorder. (Moćko et al., 2016., Larussa et al., 2017). Therefore, the existing treatment option does not offer a permanent cure for ulcerative colitis. The associated side effects make it less favourable and non-selectivity reduces the efficacy of these treatments. The cost of disease management further violates the financial condition of patients (Chumanevich et al., 2017).

Therefore, there is an urgent need for alternative therapeutics to treat ulcerative colitis which provide better healing, increased specificity, reduce side effect, are cost effective and patient friendly. A number of natural compounds such as curcumin, CAPE and PIC have been recently evaluated for their therapeutic potential against ulcerative colitis (Khan et al., 2017c., Chen et al., 2017., Shen et al., 2017). These natural compounds possess antioxidant property, stabilize free radicals, control inflammation and inhibit over stimulation of NF-kβ and HIF-1α (Yum et al., 2015., Alves de Almeida et al., 2017., Kocaadam and Şanlier, 2017). These natural compounds modulate overexpression of NF-kβ by inhibiting pro-inflammatory

mediators in colitis (Li et al., 2017., Rafa et al., 2017). They prevent the binding of NF-kβ with DNA or inhibition of Ikβ in the cytoplasm (Gu et al., 2017).

The natural compound are effective against a number of diseases however, low solubility and poor permeability limit the efficacy of these compounds (A Aljuffali et al., 2016., Namdari et al., 2017., Loureiro et al., 2017). The phenolic nature of herbal compound is responsible for their therapeutic efficacy against several disease (Huang et al., 2010). However, it has been documented that phenolic compound is poorly soluble in aqueous media thereby limiting their efficacy. (Queimada et al., 2009). Therefore, application of nanotechnology may enhance solubility, bioavailability and therapeutic effectiveness of natural compound. In the current research, nanoparticles of PIC CAPE were formulated. Albumin was used as nano-carrier to deliver PIC and CAPE because of its ability stabilizes plasma pH, alleviate osmotic pressure, and efficient delivery of proteins to cells (Singh et al., 2017c). Albumin nanoparticle is easily taken by damaged tissues due to inflammation at the mucosal site (Kinoshita et al., 2017., Jiang et al., 2017).

Based on the accumulating evidence, effect of albumin nanoparticles on mouse model of colitis has not been studying till date. Therefore, in the present work we have demonstrated and measured effect of albumin nanoparticles of PIC, CAPE and free drugs in mouse (C57BL\6) model of colitis.

6.2 Summary

Based on the detrimental effect of ulcerative colitis and to avoid side effects of current treatments, there is demand to utilize natural and novel anti-inflammatory

compounds such, as PIC and CAPE, to treat ulcerative colitis. Although these compounds have limited solubility in aqueous media, the use of nanotechnology can enhance the solubility of these natural anti-inflammatory compounds. Coacervation methods will be employed to formulate NPs loaded with PIC and CAPE using albumin as a polymer. These albumin NPs will be tested in colitis induced C57BL\6 mice.

6.3 Hypothesis

In this chapter, we hypothesize that the reduction of particle size of the natural anticancer compound will improve the anti-inflammatory property of PIC and CAPE at a higher extent than free PIC and CAPE.

6.4 Aims and objectives

- Formulation of PIC and CAPE loaded albumin nanoparticles
- Optimisation of PIC and CAPE loaded albumin nanoparticles
- Evaluation of anti-inflammatory properties of PIC and CAPE loaded albumin nanoparticles in colitis induce C57BL\6 mice

6.5 Results

6.5.1 PIC and CAPE-loaded albumin NP alleviate weight loss and DAI induced by DSS

Mice were assigned to four groups, comprising healthy subjects, DSS treated, free drug treated (PIC and CAPE) and NP treated (PIC and CAPE-loaded albumin NPs). Colitis was induced with 2.5% DSS as mentioned in section 2.19. Intraperitoneal injection of 20 mg/kg of free drug (PIC and CAPE) and equivalent amount of NP was administered in distilled water to mice. The mice under free and NP controls also received 2.5% DSS in drinking water. The symptoms of colitis such as diarrhoea, weight loss and blood in faeces were reported as composite score of disease activity index (DAI). After dissection weight and shortening in the colon was observed (Ogawa et al., 2004., Taghipour et al., 2016., Chassaing et al., 2014b., Chen et al., 2007).

Comparative defense activity of nanoparticles (PIC and CAPE) and free drugs (PIC and CAPE) was studied on C57BL\6 mice for six days. Documentation of weight of each mouse in all the group were carried out. PIC and CAPE-loaded albumin NP+DSS group demonstrate significantly ($P<0.001$) less weight loss as compared to free PIC+DSS, free CAPE+DSS and DSS alone groups as depicted in the percentage weight loss graph in Figure 6.1A and 6.2A.

Additionally, PIC and CAPE-loaded albumin NP+DSS group exhibit significant ($P<0.05$) lower DAI score than free PIC+DSS, free CAPE+DSS and DSS alone group as represented in the DAI graph in the Figure 6.1B and 6.2B.

The above finding suggests that PIC and CAPE-loaded albumin NP improve the inflammatory symptoms such as diarrhoea, weight loss and blood in faeces compared to free PIC and CAPE.

6.5.2 Change in colon length

Shortening of colon length and alteration in colon structure are other characteristics of human colitis and DSS induced colitis in mice (Randhawa et al., 2014). In the current study, effect of free drugs (PIC and CAPE) and NP (PIC and CAPE) on colon length was observed as shown in Figure 6.3 and Figure 6.4. It was reported that colon length of mice treated with PIC and CAPE-loaded albumin NP was significantly ($P<0.001$) longer as compare to free PIC and CAPE treated group as shown in the Figure 6.3A and 6.4A. The stool in the healthy group appeared to be normal. The stool in PIC and CAPE loaded NP was found to be semi solid and free form a blood clot. However, loose stool with a blood clot was found in the colon of the free PIC and CAPE, although colitis induced by DSS in mice showed blood clot and shorter colon length. PIC-loaded albumin NP illustrates significant ($P<0.01$) higher colon length than free PIC in Figure 6.3B. Similarly, CAPE-loaded albumin NP depicts significant ($P<0.05$) longer colon than free CAPE in Figure 6.4B. Therefore, above data propose that PIC and CAPE-loaded albumin NP prevents shortening of the colon more efficiently as compared to the free PIC and CAPE.

6.5.3 Wight of colon

DSS, free PIC and free CAPE treated group exhibited approximately equal amount of weight of colon, however, PIC-loaded albumin NP showed significant low weight loss as compared to DSS ($P<0.01$) and free PIC ($P<0.05$) treated mice as shown in the Figure 6.5A. A similar finding was reported by CAPE-loaded albumin NP treated mice. CAPE-loaded albumin NP demonstrated less weight loss as compared to DSS ($p<0.01$) and free CAPE ($p<0.05$) as illustrated in the Figure 6.5B.

6.5.4 Histological investigation

Staining of colonic tissue (haematoxylin and eosin) was performed as mentioned in section 2.19. Histological investigation of colonic epithelia treated with DSS demonstrated an alteration in structural integrity along with permeation of inflammatory markers inside the distorted epithelial layer. However, the degree of cryptic epithelial damage and infiltration of inflammatory cells was very low in PIC-loaded albumin NP as compared to free PIC and DSS group as depicted in the Figure 6.6A. A similar observation was reported in Figure 6.7A, where CAPE-loaded albumin NP treated mice showed less extent of epithelial damage and infiltration of neutrophils than DSS and free CAPE treated mice. The blinded tissue inflammation scores of colon tissue histology demonstrate a significant ($P<0.001$) reduction of colon damage in PIC and CAPE-loaded albumin NP treated mice relative to healthy control and free drugs mice as shown in Figure 6.6B and 6.7B.

6.5.5 Level of p65 in PIC and CAPE-loaded albumin NP tissue

The colonic tissue was stained for p65 antibody to express the effect of NP (PIC and CAPE) and free drugs (PIC and CAPE) in colonic tissue as discussed in section 2.22. This protein was observed under bright field microscopy. The overstimulation of p65 was reported in DSS treated mice as shown in the Figure 6.8(A and B). However, level of this proteins was reported to be low in PIC and CAPE-loaded albumin NP than the free drugs as depicted in Figure 6.8(A and B).

6.5.6 Level of HIF-1α in PIC and CAPE-loaded albumin NP treated tissue

The colonic tissue from mice was stained for HIF-1α antibody. High concentration of HIF-1α can be noticed in free drugs (PIC and CAPE) colonic tissue. However, tissues under NP (PIC and CAPE) exhibit low level of HIF-1α as observed in the Figure 6.9(A and B).

6.5.1.1 PIC -loaded albumin NP alleviate weight loss and DAI induced by DSS

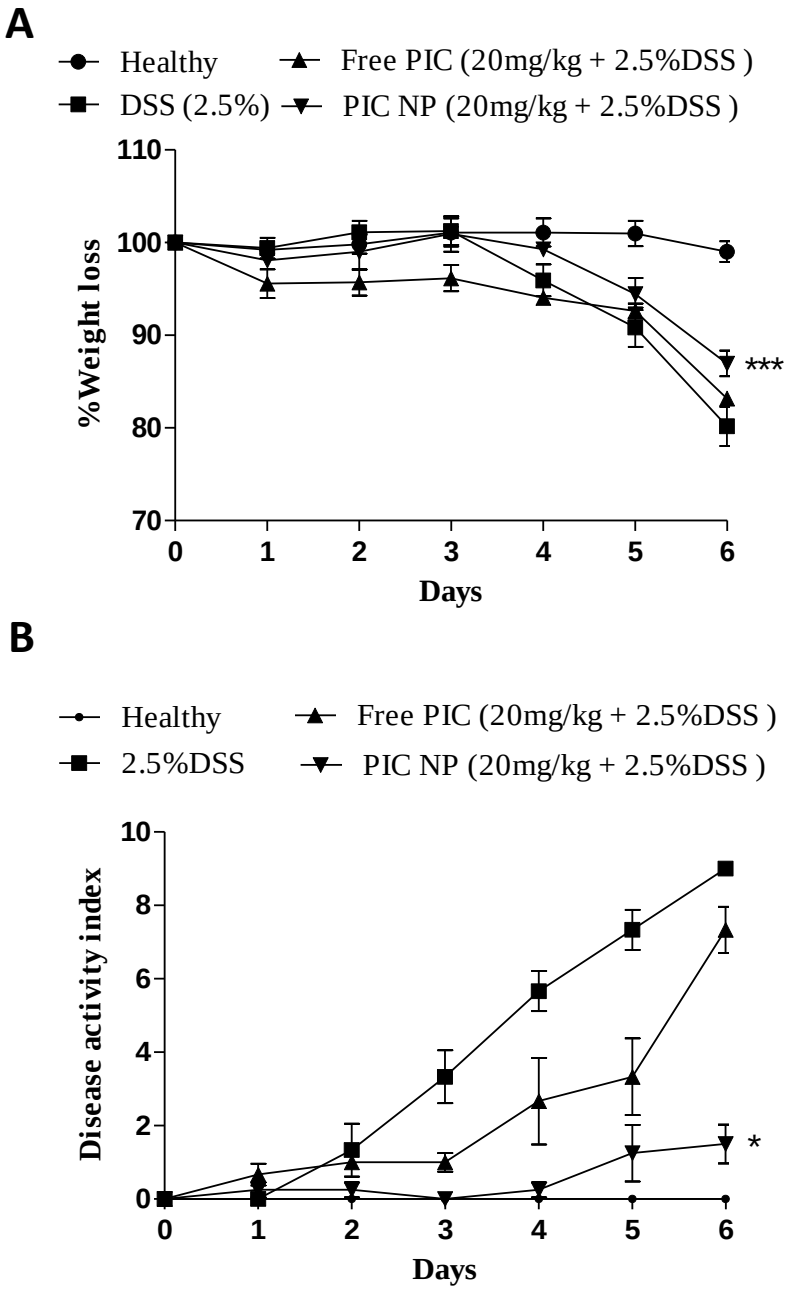

Figure 6.1: Lowered percentage weight loss (A) and DAI score (B) in mice treated with PIC-loaded albumin NP+DSS during DSS-induced colitis. PIC-loaded albumin NP treated group depicts low percentage in weight loss as compared to the free PIC. DAI of PIC-loaded albumin NP was found to be very low than to free PIC. N = 5-6 mice per group. *P<0.05 and ***P<0.001

6.5.1.2 CAPE -loaded albumin NP alleviate weight loss and DAI induced by DSS

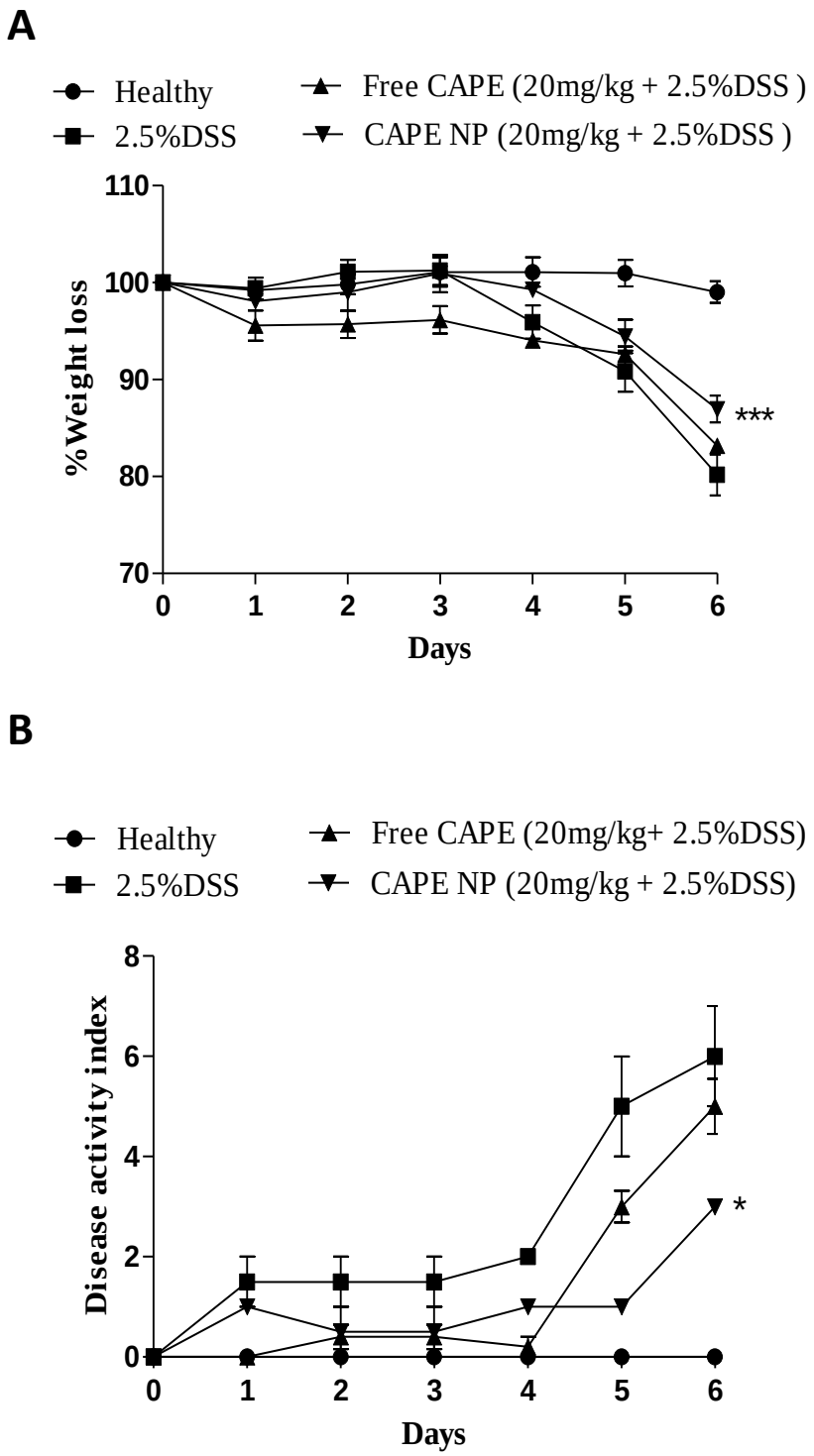

Figure 6.2: Lowered percentage weight loss (A) and DAI score (B) in mice treated with CAPE-loaded albumin NP+DSS during DSS-induced colitis. CAPE-loaded albumin NP treated group depicts low percentage in weight loss as compared to the free CAPE. DAI of CAPE-loaded albumin NP was found to be very low than to free CAPE. N = 5-6 mice per group. *P<0.05 and ***P<0.001

6.5.2.1 Change in colon length after treatment of PIC-loaded albumin NP

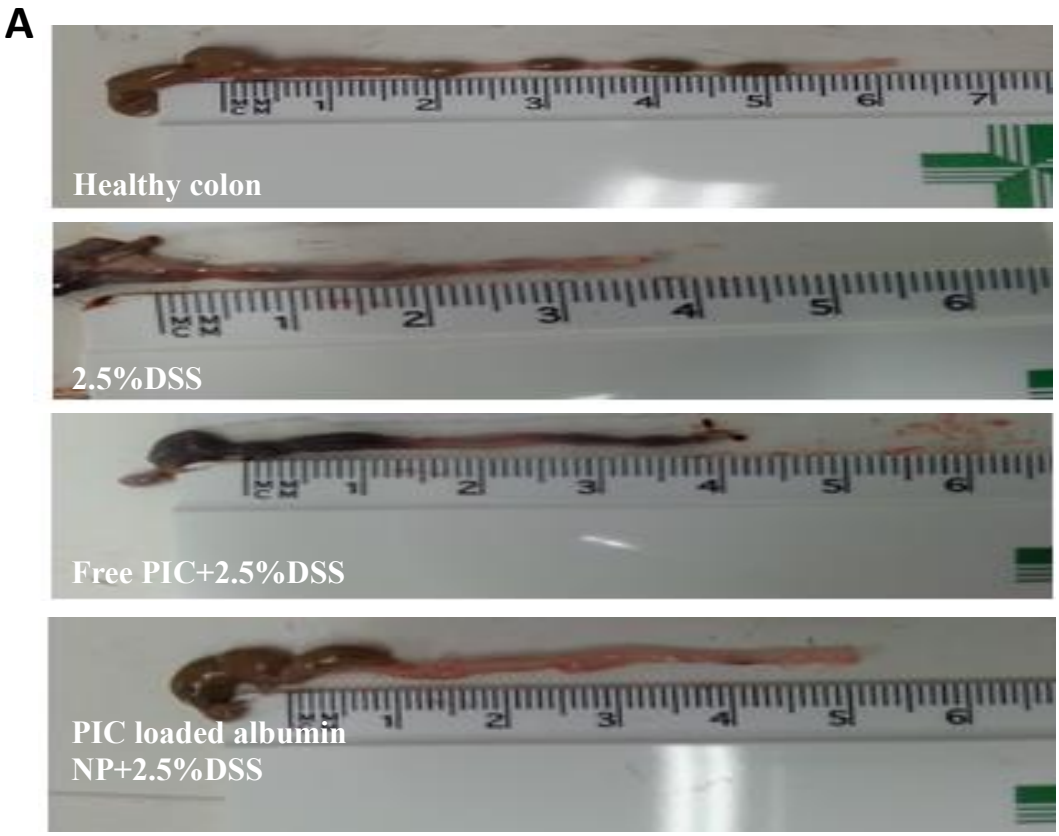

Figure 6.3: PIC-loaded albumin NP+DSS treatment is effective in protecting gross anatomy and colon length as compared to DSS group and free PIC. Gross appearance of the colonic anatomy shows the effect of PIC-loaded albumin NP+DSS, free PIC and DSS alone groups on colon shortening and formation of faecal pellets as shown in the Figure 6.3A. The colon of mice treated with PIC nanoparticles closely resembles colon of the healthy group. However, free PIC shows loose stool, blood in faeces and shorter colon length same as DSS treated group. N = 5-6 mice per group. *P<0.05 and ***P<0.001. $^{\Delta\Delta}$P<0.01.

6.5.2.1 Change in colon length after treatment of CAPE-loaded albumin NP

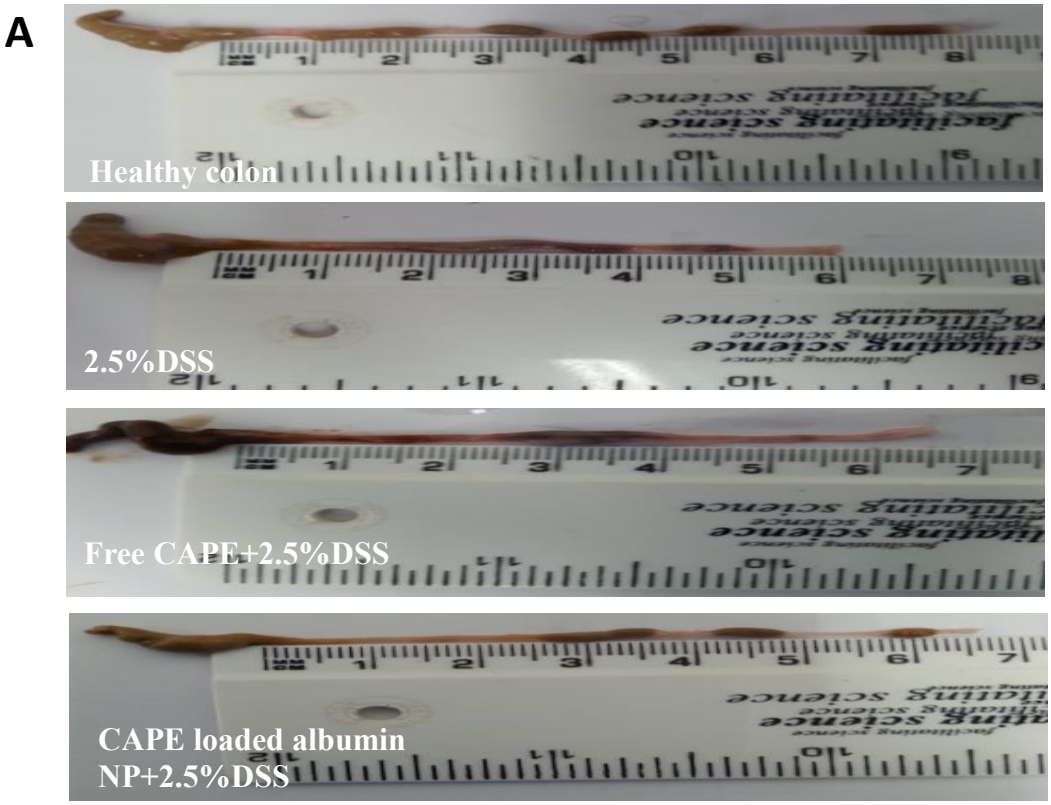

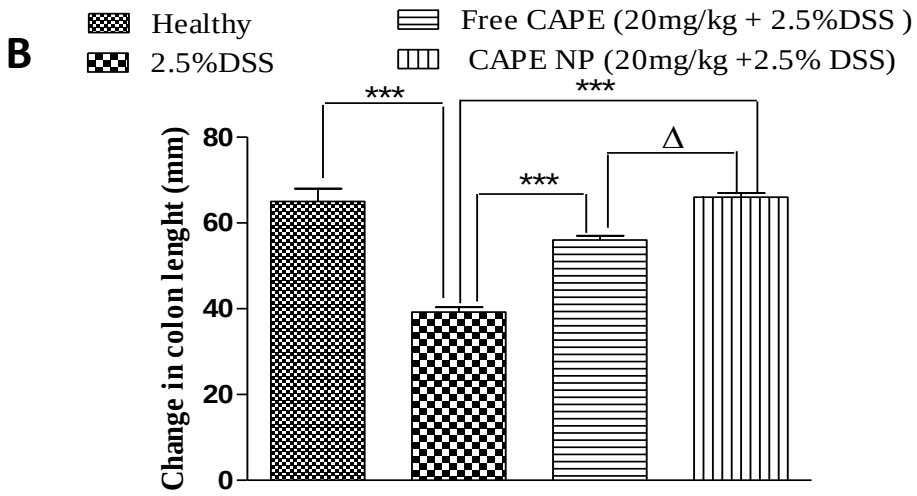

Figure 6.4: CAPE-loaded albumin NP+DSS treatment is effective in protecting gross anatomy and colon length as compared to DSS group and free PIC and CAPE group. Gross appearance of the colonic anatomy shows the effect of CAPE-loaded albumin NP+DSS, free CAPE and DSS alone groups on colon shortening and formation of faecal pellets as shown in the Figure 6.4A. The colon of mice treated with CAPE nanoparticles closely resembles colon of the healthy group. However, CAPE shows loose stool, blood in faeces and shorter colon length same as DSS treated group. Colon length was measured at post-mortem autopsy. N = 5-6 mice per group. ***P<0.001. $^{\Delta}$P<0.05.

6.5.3 Change in colon weight after treatment of PIC and CAPE-loaded albumin NP

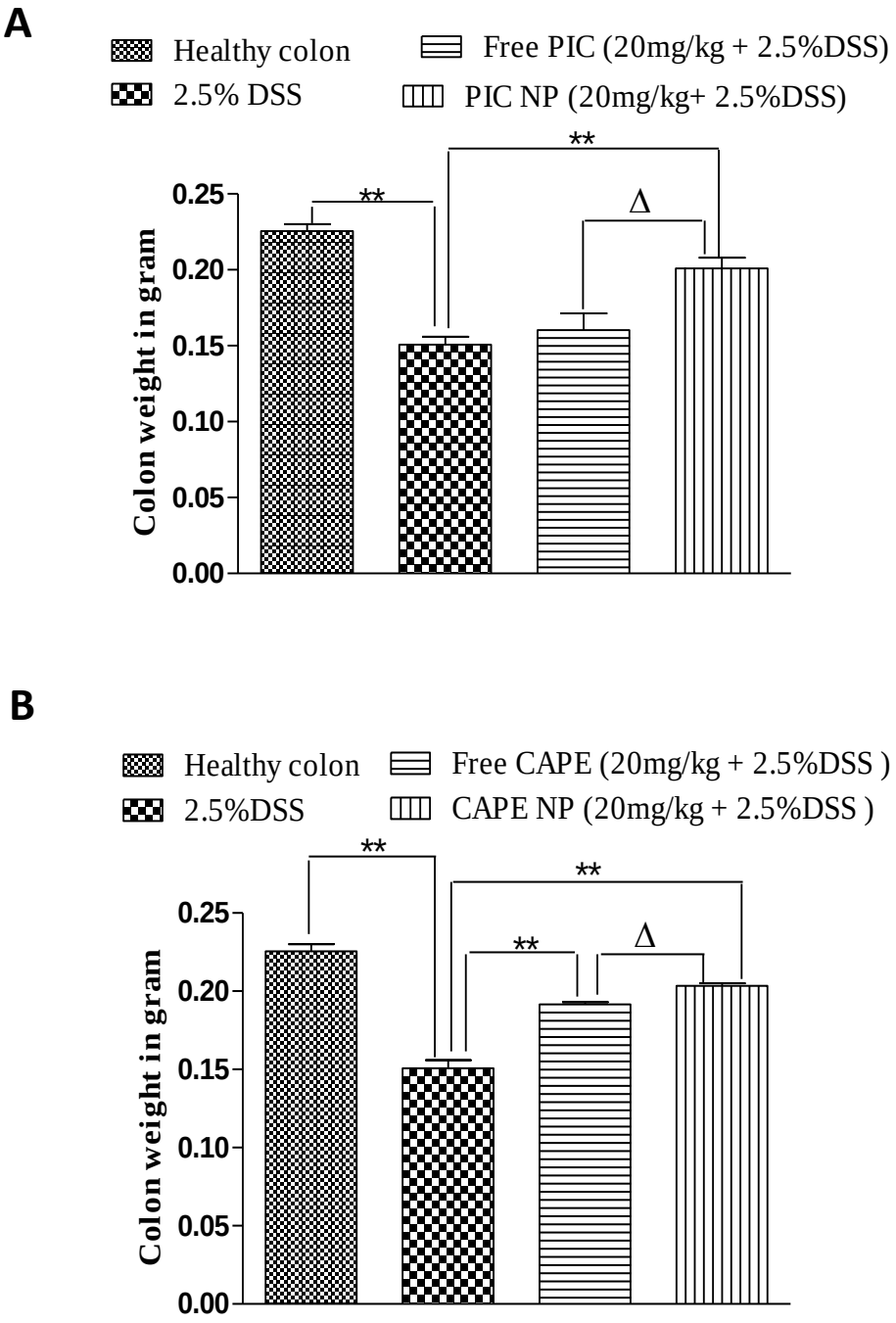

Figure 6.5: Less weight loss in colon treated with PIC (A) and CAPE-loaded albumin NP+DSS (B) as compared to DSS group and free PIC and CAPE group. Mice treated with PIC and CAPE-loaded albumin NP+DSS group showed the similar weight of colon than the free PIC and DSS group as shown in the Figure 6.5A and 6.5B. N = 5-6 mice per group. **P< 0.01. $^{\Delta}$P<0.05.

6.5.4.1 Histological investigation after treatment of PIC-loaded albumin NP

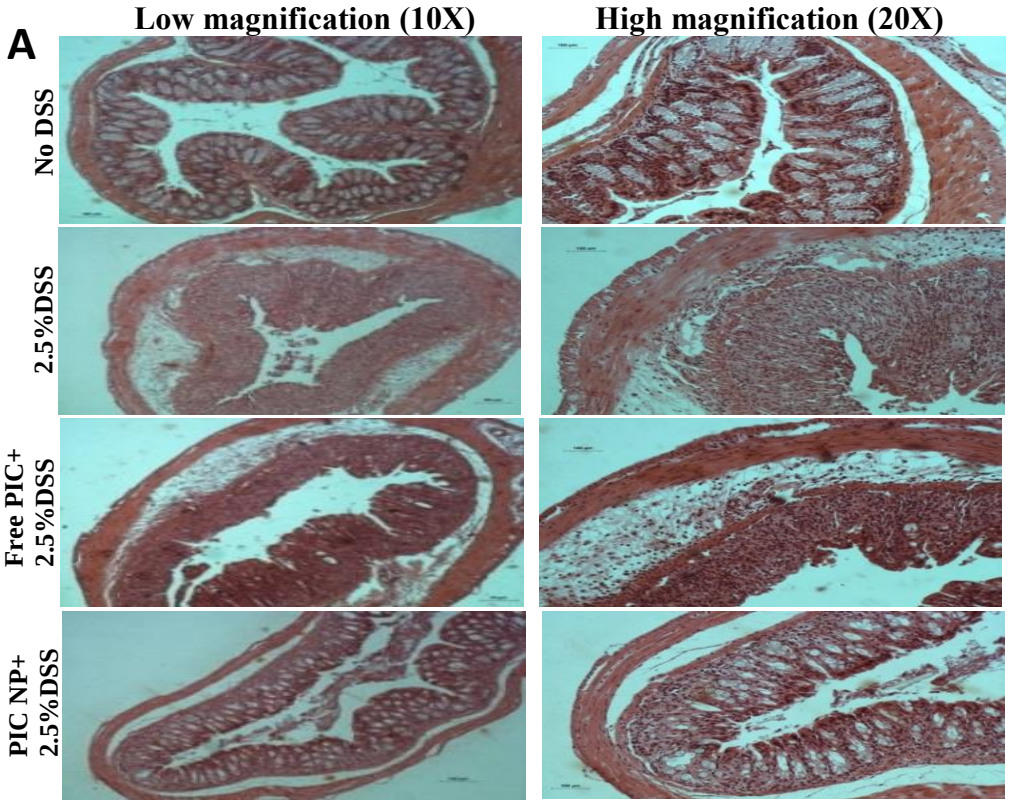

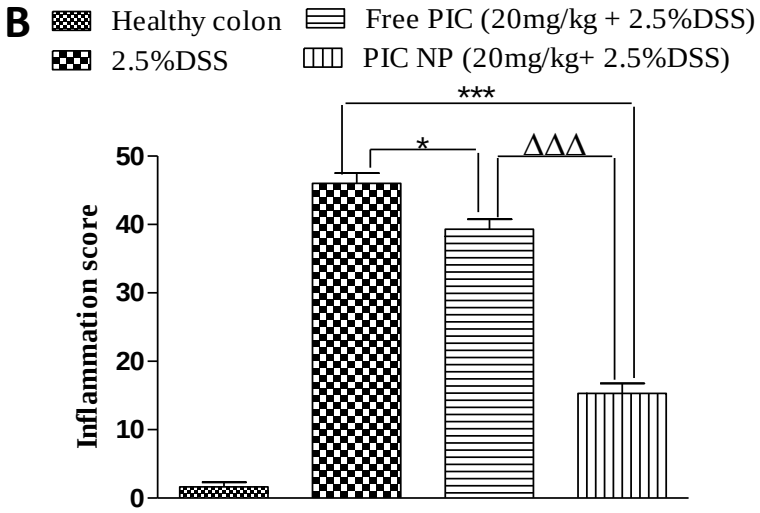

Figure 6.6: Improved colon histological outcome in mice treated with PIC (A) loaded albumin NP+DSS and lower rate of inflammation score PIC (B). The cryptic structure in the epithelial layer of healthy, PIC-loaded albumin NP group is identical as shown in the Figure 6.6A. However, infiltration of cytokines and the distorted epithelial layer can be recognized in the free PIC treated mice. DSS groups demonstrate similar trends of epithelial distortion as depicted in the Figure 6A. Significant ($^{\Delta\Delta\Delta}P<0.0001$) low inflammation was recorded in PIC-loaded albumin NP treated group as shown in the Figure 6.6B. N = 5-6 mice per group. *P<0.05 and ***P<0.001. . $^{\Delta\Delta\Delta}P<0.001$.

6.5.4.2 Histological investigation after treatment of CAPE-loaded albumin NP

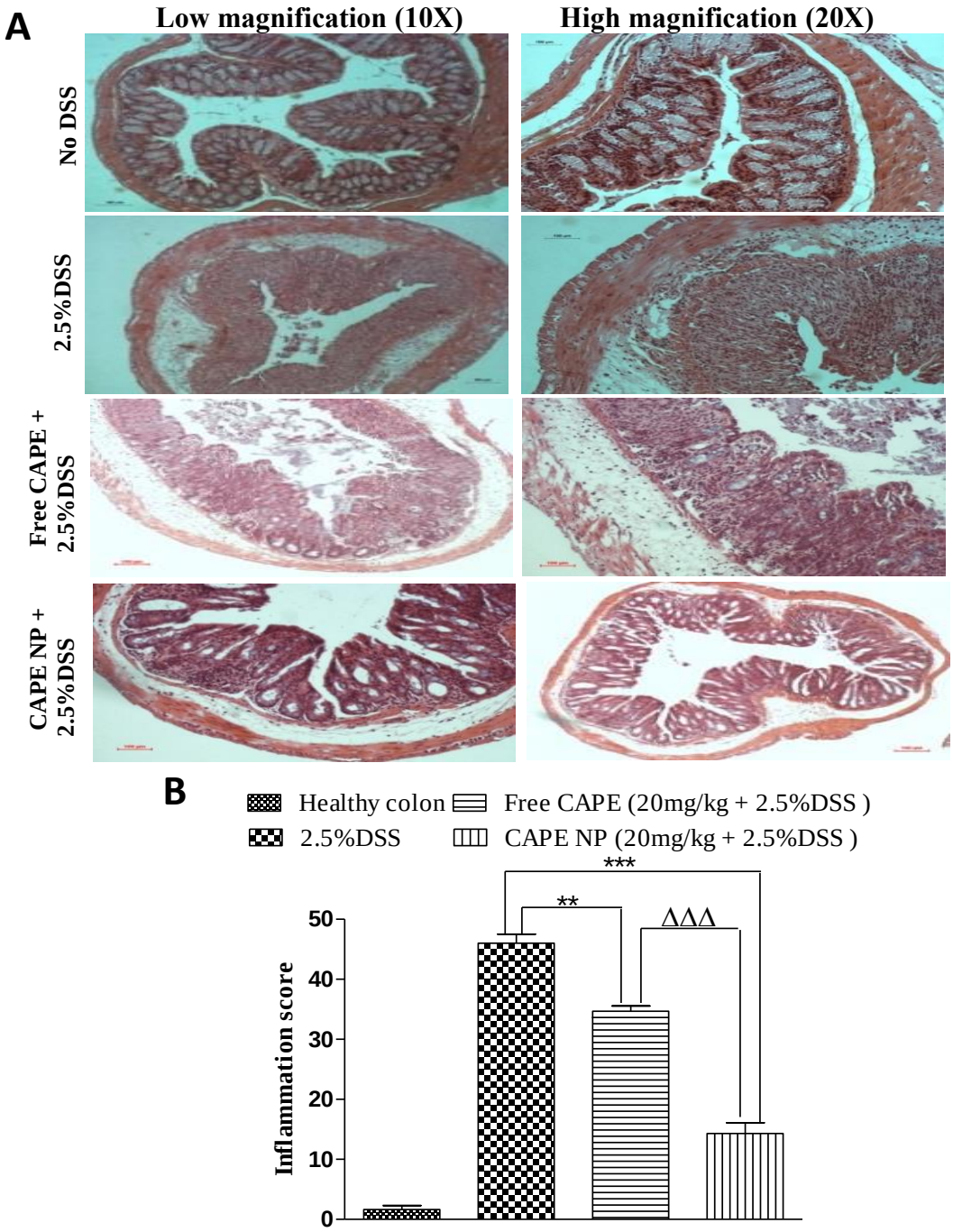

Figure 6.7: Improved colon histological outcome in mice treated with CAPE-loaded albumin NP+DSS (7A) and lower rate of inflammation score (7B). The cryptic structure in the epithelial layer of healthy, CAPE-loaded albumin NP group is identical as shown in the Figure 6.7A. However, infiltration of cytokines and the distorted epithelial layer can be recognized in the free CAPE treated mice. DSS groups demonstrate similar trends of epithelial distortion as depicted in the Figure 7A. The inflammation score graph was significantly ($^{\Delta\Delta\Delta}P<0.0001$) low in CAPE-loaded albumin NP treated group than free CAPE as shown in Figure 6.7B. N = 5-6 mice per group **P<0.001 and ***P<0.001. $^{\Delta\Delta\Delta}P<0.001$.

6.5.5 Level of p65 in PIC and CAPE-loaded albumin NP tissue

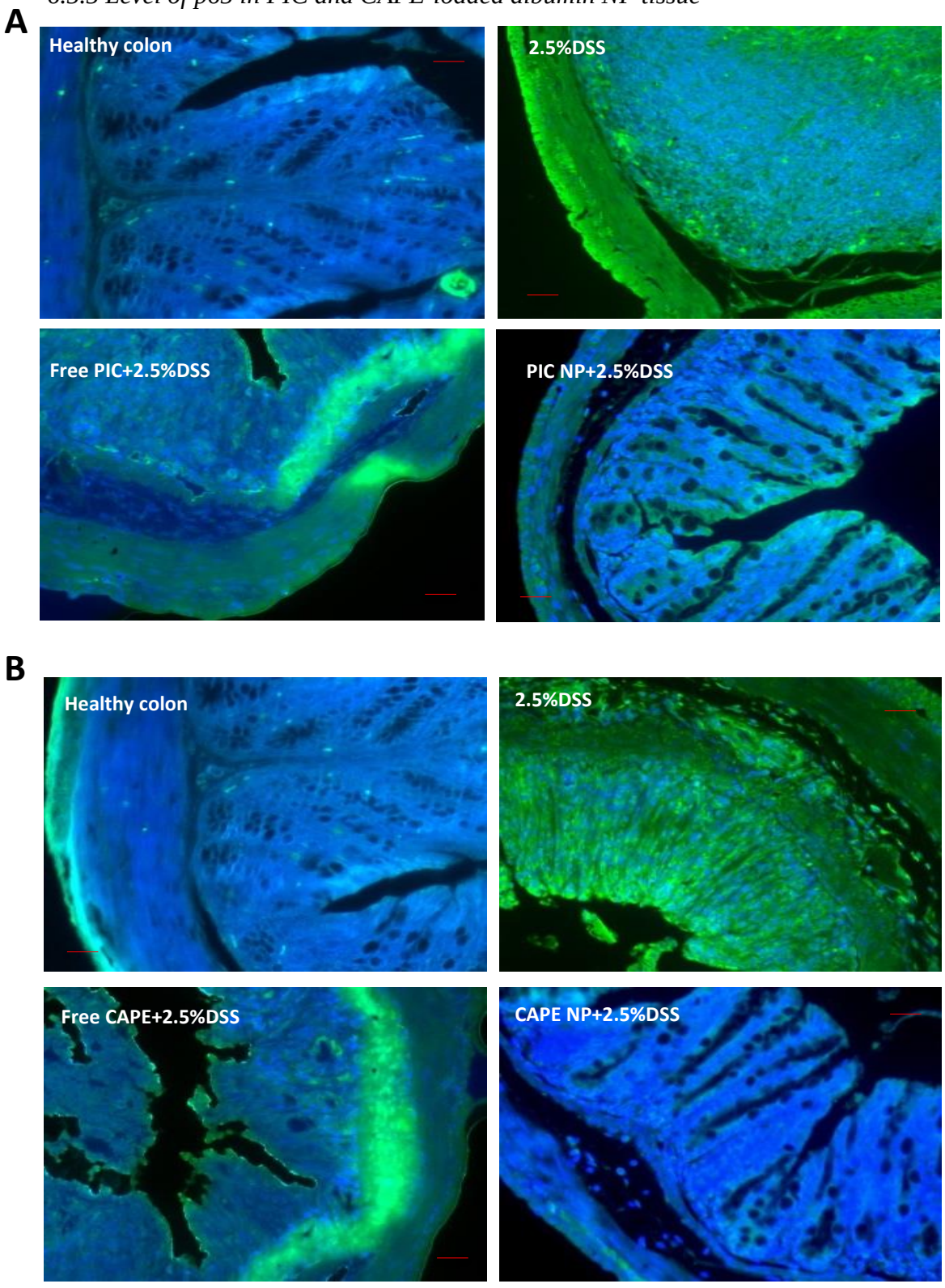

Figure 6.8: Low level of p65 in PIC (A) and CAPE-loaded albumin NP+DSS (B) treated group at 20X magnification. Low expression of p65 can be seen in colonic tissue of mice treated with PIC and CAPE-loaded albumin NP as evident in Figure 8A and 8B. However, these proteins are highly elevated in tissue of mice treated with free PIC, CAPE and DSS groups as demonstrated in Figure 6.8(A and B).

6.5.6 Level of HIF-1α in PIC and CAPE-loaded albumin NP treated tissue

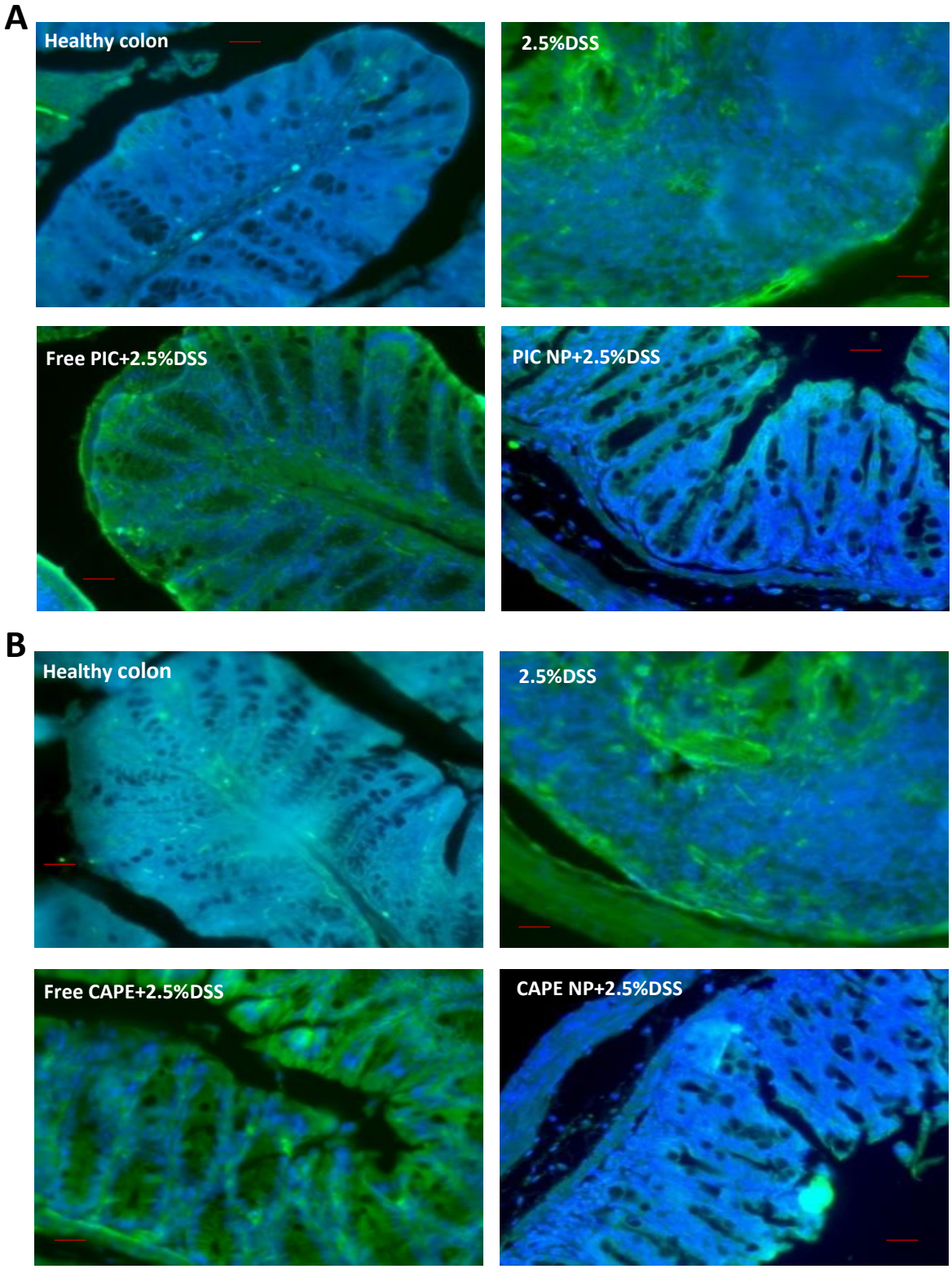

Figure 6.9: low level of HIF-1α in in PIC-loaded albumin NP+DSS (A) and CAPE-loaded albumin NP+DSS (B) treated group. Lower level of HIF-1α can be observed in colonic tissue of mice treated with PIC and CAPE-loaded albumin NP as evident in Figure 6.9A and 6.9B. However, these proteins are highly expressed in mice treated with free PIC, CAPE and DSS groups as illustrated in Figure 6.9(A and B).

6.6 Discussions

The anti-inflammatory potential of PIC and CAPE has been documented in the current work, high degree of anti-inflammatory therapeutics in nanoparticles form than the free PIC and CAPE in a mouse model of UC was reported. The early sign of UC such as weight loss, loose stool, diarrhoea and appearance of blood in stool confirm colitis in DSS groups as shown in Figure 1. However, these symptoms are absent in PIC and CAPE-loaded albumin NP. Though, free PIC and CAPE demonstrate these symptoms to some extent as depicted in the weight loss and DAI graph in Figure 6.1(A and B) and Figure 6.2(A and B).

After dissection of the colon, blood clot, loose stool and shorted colon length was reported in DSS, free PIC and CAPE treated group as shown in Figure 6.3A and Figure 6.4A. But PIC and CAPE-loaded albumin NP exhibit normal stool, no blood and the equivalent colon length as healthy group as depicted in the Figure 6.3A and Figure 6.4A. Figure 6.3B and Figure 6.4B demonstrate no significant difference in colon length as healthy group. The entire colon weight was recorded and colon of PIC and CAPE-loaded albumin NP treated mice illustrate no significant difference in weight as visible in the Figure 6.5(A and B).

Mucosal layer damage has been documented to be a major cause of colitis which can be noticed in colons of DSS treated group as shown in Figure 6.6A and Figure 6.7A. Moreover, free PIC and CAPE treated mice shows the same extent of colon damage as DSS group as evident from the Figure6.6A and Figure 6.7A. However, colon of mice treated with PIC and CAPE-loaded albumin NP do not display damage to the epithelial layer. Mucosal layer of mice treated with NPs appeared to be normal as in healthy group. The blinded histological inflammation score reveals that albumin

nanoparticles treated PIC and CAPE colon exhibits significant low inflammation score than free PIC and CAPE as shown in the Figure 6.6B and Figure 6.7B.

Overactivation of nuclear factor p65 was reported in UC which was confirmed in animal model of colitis as represented in ICH staining of colonic tissue from DSS group as shown in Figure 6.8 (A and B). Furthermore, free PIC and CAPE treated mice express the slightly low level of p65 in the colon as visible in Figure 6.8 (A and B). Although, PIC and CAPE-loaded albumin NP treated mice exhibit a very low level of this protein in colonic tissue as demonstrated in Figure 6.8(A and B). Similarly, level of HIF-1α was reduced after mice were treated with PIC and CAPE-loaded albumin NP compared to free PIC and CAPE as shown in Figure 6.9(A and B).

Therefore, the current work demonstrated the increased efficacy of PIC and CAPE in nanopaticulate form. It would be benefit to cure in UC patients over other novel and conventional treatments to amend mucosal barrier function, ceased progression of onset of disease and promote mucosal healing.

6.7 Conclusion

The finding of this chapter reveals a high degree of anti-inflammatory properties of the natural and novel PIC and CAPE compounds. Nanoparticles of these compounds refrained symptoms of colitis such as weight loss, loose stool, diarrhoea and blood in faces as to huger extent than free drug. The colon length and weight appear to be normal after treatment with nanoparticles of PIC and CAPE. However, colon length and weight of PIC and CAPE treated mice does not appear to resist the detrimental effects of DSS. Histological images of the colon from PIC and CAPE-loaded

albumin NP illustrate the effectiveness of PIC and CAPE in the form of nanoparticles. Whereas free drugs fails to produced therapeutic effects due to limited solubility. Nanoparticles of drugs such as PIC and CAPE inhibited the overstimulated level of p65 and HIF-1α significantly than free drug. Hence nanotechnology will play a pivotal role in improving solubility and bioavailability of low soluble natural compounds.

Chapter 7

General discussion and future work

7.1 General discussion

UC and colorectal cancer are interlinked with each other in terms of pathophysiology, symptoms and treatment (Kim and Chang, 2014). It is believed that UC and colorectal cancer bare the common etiology of the disease such as genetic alteration, life style, environment, overexpression of transcription protein and damage in the epithelial layer of colon (Kim and Chang, 2014). The current therapeutic practiced in these complication offers detrimental side effects such as immunity damage, oral ulcer, infertility and bone marrow depletion (Hofheinz et al., 2017). The life style and finical condition violates during management of these complication. Patients have to bare the pain of surgery to remove infected colon in chronic condition. Therefore, we have tested anti-inflammatory and anticancer activity of natural compounds such as PIC and CAPE in ulcerative model of colitis and colorectal cancer cell lines. The effectiveness of free drug was compared with albumin nanoparticles of these drugs because these natural compounds are low soluble in aqueous media. Therefore, albumin nanoparticles of these natural compounds were fabricated to optimise the physicochemical parameters and enhance the therapeutic activity in nanoparticle form. Albumin nanoparticles of PIC and CAPE were fabricated by desolvation method due to its simplicity robustness (D'Ignazio et al., 2017). This method has been used method for the formulation of nanoparticles of natural and synthetic compound used in ulcerative colitis and colorectal cancer.

Firstly, the anti-inflammatory activity of free CAPE was evaluated in animal model of ulcerative colitis. Where 30 mg/kg of free CAPE was given to mice with 2.5% DSS in drinking water and macroscopic parameter such as weight loss, DAI and rectal bleeding was monitored during the experiment. Parameters such as DAI, rectal

bleeding, shortening of colon length, weight of colon and alteration of epithelial layer of colon in DSS induce colitis were also accessed during testing of anti-inflammatory activity of natural compounds in (Algieri et al., 2014., Bereswill et al., 2010., Murakami et al., 2003., Islam et al., 2008). It was reported that percentage weight loss and disease activity index was less in mice after treatment with free molecule of CAPE. However, mice treated with DSS show weight loss and higher DAI during the experiment. After the mice were sacrificed appearance, length and weight of colon was reported. Mice treated with free CAPE molecules demonstrate significant higher colon length and normal faeces than DSS treated mice. Additionally the weight of colon of CAPE treated mice weigh significant more as compare to colon of mice treated with DSS.

It was stated that inflammatory markers results overstimulation of transcription protein such as NF-kβ and HIF-1α in UC and colorectal cancer and results into damage in architect of epithelial layer of colon (Kao et al., 2016., Simiantonaki et al., 2008., Han et al., 2016). Therefore, presence of inflammatory markers was detected in different group of mice colonic tissue lysate. It was observed that the expression of inflammatory markers such as interferons, interleukins and TNF-α was higher in mice treated DSS as compare mice treated with free molecule of CAPE. Moreover, the histological evolution of epithelia layer of colon does not show alteration in epithelial layer and infiltration of neutrophils when mice treated with CAPE. Whereas, mice treated with DSS only show damage in epithelial layer and permeation of neutrophils. The expression of transcription protein such as p65 and HIF-1α was also monitored in colon tissue of mice from different group and it was found that mice after treatment with free CAPE decrease the expression of these proteins.

Secondly, during optimisation study it was reported that increase in polymer albumin amount increases the particles size of PIC and CAPE which is due to increase in viscosity of polymer solution. Similar trend of increase in particle size due to increase in albumin concentration was also reported by June et al., 2001. Additionally, entrapment efficiency and percentage yield also increase as albumin concentration increase as demounted by Ganesh et al., 2015. The effect of increase concentration of crosslinking agent was studied and was reported that as amount of glutaraldehyde increases larger particles of PIC and CAPE was produced during formulation. Rajith and Ravindran, 2014 was also documented increase in particle size due to increase in glutaraldehyde. After solubility study as have been performed by Kim et al., 2011. It was observed that optimised batch of nanoparticles demonstrate noticeable increase in solubility as compare to free drugs in distilled water. SEM study also confirms formation of smooth, spherical and uniform nanoparticles which are localise under cancer cell lines such CaCo-2 and HT-29.

After optimisation and cellular uptake studies I performed *in-vitro* cytotoxic assay in cancer cell lines to observe and compare the cytotoxicity of nanoparticles and free drugs and it was found that nanoparticles illustrates higher cytotoxic action in cancer cell lines than free drugs. Zhang et al have monitored anticancer in colorectal cancer cell lines via migration, colony formation and invasion experiments. Therefore, anticancer potential of free PIC and CAPE was measured and compare with nanoparticles of these drugs in cancer cells via migration, colony formation and invasion assay. The result obtained from *in-vitro* anticancer experiment reveals that nanoparticle demonstrates significant higher anticancer activity that free drugs. Müller-Edenborn et al., 2015 and D'Ignazio et al., 2017 mentioned that inhibtion of p65 and HIF-1α mitigate disease condtion in colorectal cancer and UC. Hence

expression of transcription protein such as p65 and HIF-1α was evaluated by ICC and Invitrogen ELISA assay kit and it was shown that when cancer cells transfected with nanoparticle of natural compounds decrease the over induction of transcription protein significantly as compare to cell treated with free PIC and CAPE.

Lastly, after confirmation of anticancer activity of nanoparticles in colorectal cancer cell lines such as CaC-2 and HT-29 of PIC and CAPE and the anti-inflammatory activity was observed in animal model of UC. The data obtained from the experiment confirms that albumin nanoparticles of PIC and CAPE enhance the anti-inflammatory activity as compare to free molecules based on the weight loss, DAI, colon length, histology and expression of p65 and HIF-1α.

Therefore, formulation of nanoparticles of these natural agents PIC and CAPE enhances the anticancer and anti-inflammatory activities due to enhancement in physicochemical properties which leads to increase in solubility, morphology and cellular uptake. Additionally, albumin nanoparticles also inhibit overstated transcription proteins in colonic tissue of colitis induce mice and colorectal cancer cell lines. Therefore natural compound in nanoparticles form may provide better therapeutic effect in cancer and UC via modulating transcription factors as compare to free molecules.

7.2 Future work

Albumin nanoparticles of natural compound such as PIC and CAPE enhances the anti-inflammatory and anticancer at higher degree than free compounds as documented from the *in-vitro* and *in-vivo* studies in this work. The future work

would be to test expression of other transcription protein such as p52, RelA and RelB in colorectal cancer cell lines and colonic tissue of colitis induce mice after treatment with these nanoparticles. Additionally the anticancer potential of albumin nanoparticles would be tested animal model of colorectal cancer.

Chapter 8
Reference

A ALJUFFALI, I., FANG, C.-L., CHEN, C.-H. & FANG, J.-Y. 2016. Nanomedicine as a strategy for natural compound delivery to prevent and treat cancers. *Curr Pharm Des,* 22**,** 4219-4231.

AALDERS, K. C., TRYFONIDIS, K., SENKUS, E. & CARDOSO, F. 2017. Anti-angiogenic treatment in breast cancer: Facts, successes, failures and future perspectives. *Cancer Treatment Reviews,* 53**,** 98-110.

ABBASI, S., PAUL, A., SHAO, W. & PRAKASH, S. 2012. Cationic Albumin Nanoparticles for Enhanced Drug Delivery to Treat Breast Cancer: Preparation and *In Vitro* Assessment. *Journal of Drug Delivery,* 2012**,** 686108.

ABDALLA, M., LANDERHOLM, K., ANDERSSON, P., ANDERSSON, R. E. & MYRELID, P. 2017. Risk of Rectal Cancer After Colectomy for Patients With Ulcerative Colitis: A National Cohort Study. *Clinical Gastroenterology and Hepatology,* 15**,** 1055-1060.e2.

ABRAHAM, C. & CHO, J. H. 2009. IL-23 and autoimmunity: new insights into the pathogenesis of inflammatory bowel disease. *Annu Rev Med,* 60**,** 97-110.

ADAMI, H. O., BRETTHAUER, M., EMILSSON, L., HERNAN, M. A., KALAGER, M., LUDVIGSSON, J. F. & EKBOM, A. 2016. The continuing uncertainty about cancer risk in inflammatory bowel disease. *Gut,* 65**,** 889-93.

AGGARWAL, B. B. 2004. Nuclear factor-κB: The enemy within. *Cancer Cell,* 6**,** 203-208.

AGGARWAL, B. B., TAKADA, Y., SHISHODIA, S., GUTIERREZ, A. M., OOMMEN, O. V., ICHIKAWA, H., BABA, Y. & KUMAR, A. 2004. Nuclear transcription factor NF-kappa B: role in biology and medicine.

AKASH, M. S. H., REHMAN, K. & CHEN, S. 2016. Polymeric-based particulate systems for delivery of therapeutic proteins. *Pharmaceutical development and technology,* 21**,** 367-378.

AKYOL, S., OZTURK, G., GINIS, Z., ARMUTCU, F., YIGITOGLU, M. R. & AKYOL, O. 2013. In vivo and *in vitro* antineoplastic actions of caffeic acid phenethyl ester (CAPE): therapeutic perspectives. *Nutr Cancer,* 65**,** 515-26.

ALVES DE ALMEIDA, A. C., DE-FARIA, F. M., DUNDER, R. J., MANZO, L. P. B., SOUZA-BRITO, A. R. M. & LUIZ-FERREIRA, A. 2017. Recent Trends in Pharmacological Activity of Alkaloids in Animal Colitis: Potential Use for Inflammatory Bowel Disease. *Evidence-Based Complementary and Alternative Medicine,* 2017.

ANAND, P., NAIR, H. B., SUNG, B., KUNNUMAKKARA, A. B., YADAV, V. R., TEKMAL, R. R. & AGGARWAL, B. B. 2010. Design of curcumin-loaded PLGA nanoparticles formulation with enhanced cellular uptake, and increased bioactivity *in vitro* and superior bioavailability in vivo. *Biochem Pharmacol,* 79**,** 330-8.

ANANTHAKRISHNAN, A. N. 2015. Epidemiology and risk factors for IBD. *Nat Rev Gastroenterol Hepatol,* 12**,** 205-217.

ANDRESEN, L., JØRGENSEN, V. L., PERNER, A., HANSEN, A., EUGEN-OLSEN, J. & RASK-MADSEN, J. 2005. Activation of nuclear factor κB in colonic mucosa from patients with collagenous and ulcerative colitis. *Gut,* 54**,** 503-509.

ARDANI, H. K., IMAWAN, C., HANDAYANI, W., DJUHANA, D., HARMOKO, A. & FAUZIA, V. Enhancement of the stability of silver nanoparticles

synthesized using aqueous extract of Diospyros discolor Willd. leaves using polyvinyl alcohol. 2017. IOP Publishing, 012056.

ARDITE, E., PANES, J., MIRANDA, M., SALAS, A., ELIZALDE, J. I., SANS, M., ARCE, Y., BORDAS, J. M., FERNÁNDEZ-CHECA, J. C. & PIQUE, J. M. 1998. Effects of steroid treatment on activation of nuclear factor κB in patients with inflammatory bowel disease. *Br J Pharmacol,* 124**,** 431-433.

ARDIZZONE, S., MACONI, G., RUSSO, A., IMBESI, V., COLOMBO, E. & PORRO, G. B. 2006. Randomised controlled trial of azathioprine and 5-aminosalicylic acid for treatment of steroid dependent ulcerative colitis. *Gut,* 55**,** 47-53.

ATREYA, I., ATREYA, R. & NEURATH, M. F. 2008. NF-kappaB in inflammatory bowel disease. *J Intern Med,* 263**,** 591-6.

AUNE, D., CHAN, D. S. M., LAU, R., VIEIRA, R., GREENWOOD, D. C., KAMPMAN, E. & NORAT, T. 2011. Dietary fibre, whole grains, and risk of colorectal cancer: systematic review and dose-response meta-analysis of prospective studies. *BMJ,* 343.

AUNG, T. N., QU, Z., KORTSCHAK, R. D. & ADELSON, D. L. 2017. Understanding the Effectiveness of Natural Compound Mixtures in Cancer through Their Molecular Mode of Action. *Int J Mol Sci,* 18.

AZIZI, M., GHOURCHIAN, H., YAZDIAN, F., BAGHERIFAM, S., BEKHRADNIA, S. & NYSTRÖM, B. 2017. Anti-cancerous effect of albumin coated silver nanoparticles on MDA-MB 231 human breast cancer cell line. *Scientific Reports,* 7.

BAE, K. H., CHUNG, H. J. & PARK, T. G. 2011. Nanomaterials for Cancer Therapy and Imaging. *Molecules and Cells,* 31**,** 295-302.

BAETKE, S. C., LAMMERS, T. & KIESSLING, F. 2015. Applications of nanoparticles for diagnosis and therapy of cancer. *The British Journal of Radiology,* 88**,** 20150207.

BAIRD, A. C., MALLON, D., RADFORD-SMITH, G., BOYER, J., PICHE, T., PRESCOTT, S. L., LAWRANCE, I. C. & TULIC, M. K. 2016. Dysregulation of innate immunity in ulcerative colitis patients who fail anti-tumor necrosis factor therapy. *World Journal of Gastroenterology,* 22**,** 9104-9116.

BAKER, R. G., HAYDEN, M. S. & GHOSH, S. 2011. NF-κB, inflammation and metabolic disease. *Cell metabolism,* 13**,** 11-22.

BANDARRA, D. & ROCHA, S. 2013. Tale of two transcription factors: NF-κB and HIF crosstalk. *OA Mol Cell Biol,* 1**,** 6.

BEN-NERIAH, Y. & KARIN, M. 2011. Inflammation meets cancer, with NF-kappaB as the matchmaker. *Nat Immunol,* 12**,** 715-23.

BERGMANN, H., ROTH, S., PECHLOFF, K., KISS, E. A., KUHN, S., HEIKENWÄLDER, M., DIEFENBACH, A., GRETEN, F. R. & RULAND, J. 2017. Card9-dependent IL-1β regulates IL-22 production from group 3 innate lymphoid cells and promotes colitis-associated cancer. *Eur J Immunol*.

BEZERRA, R. M. N., VEIGA, L. F., CAETANO, A. C., ROSALEN, P. L., AMARAL, M. E. C., PALANCH, A. C. & DE ALENCAR, S. M. 2012. Caffeic acid phenethyl ester reduces the activation of the nuclear factor κB pathway by high-fat diet-induced obesity in mice. *Metabolism,* 61**,** 1606-1614.

BHARALI, D. J., SIDDIQUI, I. A., ADHAMI, V. M., CHAMCHEU, J. C., ALDAHMASH, A. M., MUKHTAR, H. & MOUSA, S. A. 2011.

Nanoparticle Delivery of Natural Products in the Prevention and Treatment of Cancers: Current Status and Future Prospects. *Cancers,* 3**,** 4024-4045.

BIDDLESTONE, J., BANDARRA, D. & ROCHA, S. 2015a. The role of hypoxia in inflammatory disease (Review). *International Journal of Molecular Medicine,* 35**,** 859-869.

BIDDLESTONE, J., BANDARRA, D. & ROCHA, S. 2015b. The role of hypoxia in inflammatory disease (review). *Int J Mol Med,* 35**,** 859-69.

BISHOP, J. L., ROBERTS, M. E., BEER, J. L., HUANG, M., CHEHAL, M. K., FAN, X., FOUSER, L. A., MA, H. L., BACANI, J. T. & HARDER, K. W. 2014. Lyn activity protects mice from DSS colitis and regulates the production of IL-22 from innate lymphoid cells. *Mucosal Immunol,* 7**,** 405-416.

BISHT, S., FELDMANN, G., SONI, S., RAVI, R., KARIKAR, C., MAITRA, A. & MAITRA, A. 2007. Polymeric nanoparticle-encapsulated curcumin ("nanocurcumin"): a novel strategy for human cancer therapy. *J Nanobiotechnology,* 5**,** 3.

BLONSKI, W. & LICHTENSTEIN, G. R. 2006. Safety of biologics in inflammatory bowel disease. *Curr Treat Options Gastroenterol,* 9**,** 221-33.

BOAL CARVALHO, P. & COTTER, J. 2017. Mucosal Healing in Ulcerative Colitis: A Comprehensive Review. *Drugs,* 77**,** 159-173.

BOBO, D., ROBINSON, K. J., ISLAM, J., THURECHT, K. J. & CORRIE, S. R. 2016. Nanoparticle-Based Medicines: A Review of FDA-Approved Materials and Clinical Trials to Date. *Pharm Res,* 33**,** 2373-87.

BONFERONI, M. C., ROSSI, S., SANDRI, G. & FERRARI, F. 2017. Nanoparticle formulations to enhance tumor targeting of poorly soluble polyphenols with potential anticancer properties. *Semin Cancer Biol*.

BORTHAKUR, A., SAKSENA, S., GILL, R. K., ALREFAI, W. A., RAMASWAMY, K. & DUDEJA, P. K. 2008. Regulation of Monocarboxylate Transporter 1 (MCT1) Promoter by Butyrate in Human Intestinal Epithelial Cells: Involvement of NF-κB Pathway. *J Cell Biochem,* 103**,** 1452-1463.

BRODERICK, P., DOBBINS, S. E., CHUBB, D., KINNERSLEY, B., DUNLOP, M. G., TOMLINSON, I. & HOULSTON, R. S. 2017. Validation of Recently Proposed Colorectal Cancer Susceptibility Gene Variants in an Analysis of Families and Patients—a Systematic Review. *Gastroenterology,* 152**,** 75-77.e4.

BUHRMANN, C., MOBASHERI, A., BUSCH, F., ALDINGER, C., STAHLMANN, R., MONTASERI, A. & SHAKIBAEI, M. 2011. Curcumin modulates nuclear factor kappaB (NF-kappaB)-mediated inflammation in human tenocytes *in vitro*: role of the phosphatidylinositol 3-kinase/Akt pathway. *J Biol Chem,* 286**,** 28556-66.

CAMPBELL, E. L., BRUYNINCKX, W. J., KELLY, C. J., GLOVER, L. E., MCNAMEE, E. N., BOWERS, B. E., BAYLESS, A. J., SCULLY, M., SAEEDI, B. J., GOLDEN-MASON, L., EHRENTRAUT, S. F., CURTIS, V. F., BURGESS, A., GARVEY, J. F., SORENSEN, A., NEMENOFF, R., JEDLICKA, P., TAYLOR, C. T., KOMINSKY, D. J. & COLGAN, S. P. 2014. Transmigrating neutrophils shape the mucosal microenvironment through localized oxygen depletion to influence resolution of inflammation. *Immunity,* 40**,** 66-77.

CAPALDO, C. T., POWELL, D. N. & KALMAN, D. 2017. Layered defense: how mucus and tight junctions seal the intestinal barrier. *J Mol Med,* 13**,** 017-1557.

CARRAT, F., SEKSIK, P., COLOMBEL, J. F., PEYRIN-BIROULET, L. & BEAUGERIE, L. 2017. The effects of aminosalicylates or thiopurines on the risk of colorectal cancer in inflammatory bowel disease. *Aliment Pharmacol Ther,* 45**,** 533-541.

CARTER, M., LOBO, A. & TRAVIS, S. 2004. Guidelines for the management of inflammatory bowel disease in adults. *Gut,* 53**,** v1-v16.

CASTAÑO-RODRÍGUEZ, N., KAAKOUSH, N. O., LEE, W. S. & MITCHELL, H. M. 2015. Dual role of Helicobacter and Campylobacter species in IBD: a systematic review and meta-analysis. *Gut*.

CHAN, H. C. & NG, S. C. 2017. Emerging biologics in inflammatory bowel disease. *J Gastroenterol,* 52**,** 141-150.

CHASSAING, B., AITKEN, J. D., MALLESHAPPA, M. & VIJAY-KUMAR, M. 2014a. Dextran Sulfate Sodium (DSS)-Induced Colitis in Mice. *Current protocols in immunology / edited by John E. Coligan ... [et al.],* 104**,** Unit-15.25.

CHASSAING, B., AITKEN, J. D., MALLESHAPPA, M. & VIJAY-KUMAR, M. 2014b. Dextran sulfate sodium (DSS)-induced colitis in mice. *Curr Protoc Immunol,* 104**,** Unit 15 25.

CHAUDARY, N. & HILL, R. P. 2007. Hypoxia and metastasis. *Clin Cancer Res,* 13**,** 1947-9.

CHAVANPATIL, M. D., PATIL, Y. & PANYAM, J. 2006. Susceptibility of nanoparticle-encapsulated paclitaxel to P-glycoprotein-mediated drug efflux. *Int J Pharm,* 320**,** 150-6.

CHEN, B., YANG, J.-Z., WANG, L.-F., ZHANG, Y.-J. & LIN, X.-J. 2015. Ifosfamide-loaded poly (lactic-co-glycolic acid) PLGA-dextran polymeric nanoparticles to improve the antitumor efficacy in Osteosarcoma. *BMC Cancer,* 15**,** 752.

CHEN, G., ROY, I., YANG, C. & PRASAD, P. N. 2016. Nanochemistry and Nanomedicine for Nanoparticle-based Diagnostics and Therapy. *Chem Rev,* 116**,** 2826-85.

CHEN, Q., SI, X., MA, L., MA, P., HOU, M., BAI, S., WU, X., WAN, Y., XIAO, B. & MERLIN, D. 2017. Oral delivery of curcumin via porous polymeric nanoparticles for effective ulcerative colitis therapy. *Journal of Materials Chemistry B*.

CHEN, Y., SI, J.-M., LIU, W.-L., CAI, J.-T., DU, Q., WANG, L.-J. & GAO, M. 2007. Induction of experimental acute ulcerative colitis in rats by administration of dextran sulfate sodium at low concentration followed by intracolonic administration of 30% ethanol. *Journal of Zhejiang University Science B,* 8**,** 632-637.

CHOI, D., HAN, J., LEE, Y., CHOI, J., HAN, S., HONG, S., JEON, H., KIM, Y. M. & JUNG, Y. 2010. Caffeic acid phenethyl ester is a potent inhibitor of HIF prolyl hydroxylase: structural analysis and pharmacological implication. *J Nutr Biochem,* 21**,** 809-17.

CHUMANEVICH, A. A., CHAPARALA, A., WITALISON, E. E., TASHKANDI, H., HOFSETH, A. B., LANE, C., PENA, E., LIU, P., PITTMAN, D. L., NAGARKATTI, P., NAGARKATTI, M., HOFSETH, L. J. &

CHUMANEVICH, A. A. 2017. Looking for the best anti-colitis medicine: A comparative analysis of current and prospective compounds. *Oncotarget,* 8**,** 228-237.

CLARKE, K. & REGUEIRO, M. 2012. Stopping immunomodulators and biologics in inflammatory bowel disease patients in remission. *Inflamm Bowel Dis,* 18**,** 174-9.

COHEN, R. D. & THOMAS, T. 2006. Economics of the use of biologics in the treatment of inflammatory bowel disease. *Gastroenterol Clin North Am,* 35**,** 867-82.

COLGAN, S. P. & TAYLOR, C. T. 2010. Hypoxia: an alarm signal during intestinal inflammation. *Nat Rev Gastroenterol Hepatol,* 7**,** 281-287.

COLOMBEL, J. F., LOFTUS, E. V., JR., TREMAINE, W. J., EGAN, L. J., HARMSEN, W. S., SCHLECK, C. D., ZINSMEISTER, A. R. & SANDBORN, W. J. 2004. The safety profile of infliximab in patients with Crohn's disease: the Mayo clinic experience in 500 patients. *Gastroenterology,* 126**,** 19-31.

COLOTTA, F., ALLAVENA, P., SICA, A., GARLANDA, C. & MANTOVANI, A. 2009a. Cancer-related inflammation, the seventh hallmark of cancer: links to genetic instability. *Carcinogenesis,* 30**,** 1073-81.

COLOTTA, F., ALLAVENA, P., SICA, A., GARLANDA, C. & MANTOVANI, A. 2009b. Cancer-related inflammation, the seventh hallmark of cancer: links to genetic instability. *Carcinogenesis,* 30**,** 1073-1081.

CONNELL, W. R., KAMM, M. A., RITCHIE, J. K., LENNARD-JONES, J. E., DICKSON, M. & BALKWILL, A. M. 1994. Long-term neoplasia risk after azathioprine treatment in inflammatory bowel disease. *The Lancet,* 343**,** 1249-1252.

CONRAD, K., ROGGENBUCK, D. & LAASS, M. W. 2014. Diagnosis and classification of ulcerative colitis. *Autoimmunity Reviews,* 13**,** 463-466.

COSTA, R., CARNEIRO, B. A., AGULNIK, M., RADEMAKER, A. W., PAI, S. G., VILLAFLOR, V. M., CRISTOFANILLI, M., SOSMAN, J. A. & GILES, F. J. 2017. Toxicity profile of approved anti-PD-1 monoclonal antibodies in solid tumors: a systematic review and meta-analysis of randomized clinical trials. *Oncotarget,* 8**,** 8910-8920.

CÔTÉ-DAIGNEAULT, J., BOUIN, M., LAHAIE, R., COLOMBEL, J.-F. & POITRAS, P. 2015. Biologics in inflammatory bowel disease: what are the data? *United European Gastroenterology Journal,* 3**,** 419-428.

CRAGG, G. M. & PEZZUTO, J. M. 2016. Natural Products as a Vital Source for the Discovery of Cancer Chemotherapeutic and Chemopreventive Agents. *Medical Principles and Practice,* 25(suppl 2)**,** 41-59.

CUHLS, H., MARINOVA, M., KAASA, S., STIEBER, C., CONRAD, R., RADBRUCH, L. & MÜCKE, M. 2017. A systematic review on the role of vitamins, minerals, proteins, and other supplements for the treatment of cachexia in cancer: a European Palliative Care Research Centre cachexia project. *Journal of cachexia, sarcopenia and muscle,* 8**,** 25-39.

CULVER, C., SUNDQVIST, A., MUDIE, S., MELVIN, A., XIRODIMAS, D. & ROCHA, S. 2010. Mechanism of hypoxia-induced NF-kappaB. *Mol Cell Biol,* 30**,** 4901-21.

CUMMINS, E. P., BERRA, E., COMERFORD, K. M., GINOUVES, A., FITZGERALD, K. T., SEEBALLUCK, F., GODSON, C., NIELSEN, J. E., MOYNAGH, P., POUYSSEGUR, J. & TAYLOR, C. T. 2006. Prolyl

hydroxylase-1 negatively regulates IκB kinase-β, giving insight into hypoxia-induced NFκB activity. *Proc Natl Acad Sci U S A,* 103**,** 18154-18159.

CUMMINS, E. P., SEEBALLUCK, F., KEELY, S. J., MANGAN, N. E., CALLANAN, J. J., FALLON, P. G. & TAYLOR, C. T. 2008. The hydroxylase inhibitor dimethyloxalylglycine is protective in a murine model of colitis. *Gastroenterology,* 134**,** 156-65.

D'HAENS, G., LEMMENS, L., GEBOES, K., VANDEPUTTE, L., VAN ACKER, F., MORTELMANS, L., PEETERS, M., VERMEIRE, S., PENNINCKX, F., NEVENS, F., HIELE, M. & RUTGEERTS, P. 2001. Intravenous cyclosporine versus intravenous corticosteroids as single therapy for severe attacks of ulcerative colitis. *Gastroenterology,* 120**,** 1323-9.

DAN, A., BOUTROS, M., NEDJAR, H., KOPYLOV, U., AFIF, W., KHALIL, M. A. & RAHME, E. 2017. Cost of Ulcerative Colitis in Quebec, Canada: A Retrospective Cohort Study. *Inflamm Bowel Dis*.

DANESE, S., BONOVAS, S. & PEYRIN-BIROULET, L. 2017. Budesonide MMX Add-on to 5-Aminosalicylic Acid Therapy in Mild-to-Moderate Ulcerative Colitis: A Favourable Risk-Benefit Profile. *J Crohns Colitis,* 21.

DANESE, S. & FIOCCHI, C. 2011. Ulcerative colitis. *N Engl J Med,* 365**,** 1713-25.

DANESE, S., SANS, M. & FIOCCHI, C. 2004. Inflammatory bowel disease: the role of environmental factors. *Autoimmunity Reviews,* 3**,** 394-400.

DANHIER, F., LECOUTURIER, N., VROMAN, B., JEROME, C., MARCHAND-BRYNAERT, J., FERON, O. & PREAT, V. 2009. Paclitaxel-loaded PEGylated PLGA-based nanoparticles: in vitro and *in vivo* evaluation. *J Control Release,* 133**,** 11-7.

DAVIES, S. E. C., INSERRA, C., POLITO, G., PANCIROLI, C., DRAGONETTI, M. M. & MINGHETTI, P. 2017. CP-227 Cost utility analyses of biological agents for refractory moderate to severe ulcerative colitis. British Medical Journal Publishing Group.

DE ABAJO, F. J., MONTERO, D., MADURGA, M. & GARCIA RODRIGUEZ, L. A. 2004. Acute and clinically relevant drug-induced liver injury: a population based case-control study. *Br J Clin Pharmacol,* 58**,** 71-80.

DE JONG, W. H. & BORM, P. J. A. 2008. Drug delivery and nanoparticles: Applications and hazards. *International Journal of Nanomedicine,* 3**,** 133-149.

DE, S. B. F. R., CARVALHO, A. T. P., DE, V. C. A. J., DE BARROS MOREIRA, A. M. H., MOREIRA, J. P. L., LUIZ, R. R. & DE SOUZA, H. S. 2017. The socio-economic impact of work disability due to inflammatory bowel disease in Brazil. *Eur J Health Econ,* 18**,** 017-0896.

DE SOUZA, H. S. P. & FIOCCHI, C. 2016. Immunopathogenesis of IBD: current state of the art. *Nat Rev Gastroenterol Hepatol,* 13**,** 13-27.

DEBNATH, T., KIM, D. H. & LIM, B. O. 2013. Natural products as a source of anti-inflammatory agents associated with inflammatory bowel disease. *Molecules,* 18**,** 7253-70.

DEDIEGO, M. L., NIETO-TORRES, J. L., REGLA-NAVA, J. A., JIMENEZ-GUARDEÑO, J. M., FERNANDEZ-DELGADO, R., FETT, C., CASTAÑO-RODRIGUEZ, C., PERLMAN, S. & ENJUANES, L. 2014. Inhibition of NF-κB-mediated inflammation in severe acute respiratory syndrome coronavirus-infected mice increases survival. *J Virol,* 88**,** 913-924.

DEIANA, S., GABBANI, T. & ANNESE, V. 2017. Biosimilars in inflammatory bowel disease: A review of post-marketing experience. *World Journal of Gastroenterology,* 23**,** 197-203.

DENLINGER, C. S. & BARSEVICK, A. M. 2009. The Challenges of Colorectal Cancer Survivorship. *Journal of the National Comprehensive Cancer Network : JNCCN,* 7**,** 883-894.

DENNIS, M. S., ZHANG, M., MENG, Y. G., KADKHODAYAN, M., KIRCHHOFER, D., COMBS, D. & DAMICO, L. A. 2002. Albumin binding as a general strategy for improving the pharmacokinetics of proteins. *J Biol Chem,* 277**,** 35035-43.

DIELEMAN, L. A., PALMEN, M. J. H. J., AKOL, H., BLOEMENA, E., PEÑA, A. S., MEUWISSEN, S. G. M. & VAN REES, E. P. 1998. Chronic experimental colitis induced by dextran sulphate sodium (DSS) is characterized by Th1 and Th2 cytokines. *Clinical and Experimental Immunology,* 114**,** 385-391.

DINARVAND, R., SEPEHRI, N., MANOOCHEHRI, S., ROUHANI, H. & ATYABI, F. 2011. Polylactide-co-glycolide nanoparticles for controlled delivery of anticancer agents. *International Journal of Nanomedicine,* 6**,** 877-895.

DOS REIS, S. A., DA CONCEIÇÃO, L. L., SIQUEIRA, N. P., ROSA, D. D., DA SILVA, L. L. & PELUZIO, M. D. C. G. 2017. Review of the mechanisms of probiotic actions in the prevention of colorectal cancer. *Nutrition Research,* 37**,** 1-19.

DOU, Q. P. & ZONDER, J. A. 2014. Overview of Proteasome Inhibitor-Based Anti-cancer Therapies: Perspective on Bortezomib and Second Generation Proteasome Inhibitors versus Future Generation Inhibitors of Ubiquitin-Proteasome System. *Current cancer drug targets,* 14**,** 517-536.

DUBINSKY, M. C., LAMOTHE, S., YANG, H. Y., TARGAN, S. R., SINNETT, D., THÉORÊT, Y. & SEIDMAN, E. G. 2000. Pharmacogenomics and metabolite measurement for 6-mercaptopurine therapy in inflammatory bowel disease. *Gastroenterology,* 118**,** 705-713.

DULAI, P. S., LEVESQUE, B. G., FEAGAN, B. G., D'HAENS, G. & SANDBORN, W. J. 2015. Assessment of mucosal healing in inflammatory bowel disease: review. *Gastrointest Endosc,* 82**,** 246-255.

EGGER, B., BAJAJ-ELLIOTT, M., MACDONALD, T. T., INGLIN, R., EYSSELEIN, V. E. & BUCHLER, M. W. 2000. Characterisation of acute murine dextran sodium sulphate colitis: cytokine profile and dose dependency. *Digestion,* 62**,** 240-8.

EISSA, N., HUSSEIN, H., KERMARREC, L., ELGAZZAR, O., METZ-BOUTIGUE, M.-H., BERNSTEIN, C. N. & GHIA, J.-E. 2017. Chromofungin (CHR: CHGA47-66) is downregulated in persons with active ulcerative colitis and suppresses pro-inflammatory macrophage function through the inhibition of NF-κB signaling. *Biochem Pharmacol*.

ELZOGHBY, A. O., SAMY, W. M. & ELGINDY, N. A. 2012a. Albumin-based nanoparticles as potential controlled release drug delivery systems. *J Control Release,* 157**,** 168-82.

ELZOGHBY, A. O., SAMY, W. M. & ELGINDY, N. A. 2012b. Protein-based nanocarriers as promising drug and gene delivery systems. *Journal of Controlled Release,* 161**,** 38-49.

ENGEL, M. A. & NEURATH, M. F. 2010. New pathophysiological insights and modern treatment of IBD. *Journal of Gastroenterology,* 45**,** 571-583.

ESPIN, J. C., GARCIA-CONESA, M. T. & TOMAS-BARBERAN, F. A. 2007. Nutraceuticals: facts and fiction. *Phytochemistry,* 68**,** 2986-3008.

FALLACARA, A. L., MANCINI, A., ZAMPERINI, C., DREASSI, E., MARIANELLI, S., CHIARIELLO, M., POZZI, G., SANTORO, F., BOTTA, M. & SCHENONE, S. 2017. Pyrazolo[3,4-d]pyrimidines-loaded human serum albumin (HSA) nanoparticles: Preparation, characterization and cytotoxicity evaluation against neuroblastoma cell line. *Bioorganic & Medicinal Chemistry Letters,* 27**,** 3196-3200.

FAN, G., JIANG, X., WU, X., FORDJOUR, P. A., MIAO, L., ZHANG, H., ZHU, Y. & GAO, X. 2016. Anti-Inflammatory Activity of Tanshinone IIA in LPS-Stimulated RAW264.7 Macrophages via miRNAs and TLR4-NF-kappaB Pathway. *Inflammation,* 39**,** 375-384.

FANG, J., SEKI, T., TSUKAMOTO, T., QIN, H., YIN, H., LIAO, L., NAKAMURA, H. & MAEDA, H. 2013. Protection from inflammatory bowel disease and colitis-associated carcinogenesis with 4-vinyl-2,6-dimethoxyphenol (canolol) involves suppression of oxidative stress and inflammatory cytokines. *Carcinogenesis,* 34**,** 2833-2841.

FAVORITI, P., CARBONE, G., GRECO, M., PIROZZI, F., PIROZZI, R. E. M. & CORCIONE, F. 2016. Worldwide burden of colorectal cancer: a review. *Updates in Surgery,* 68**,** 7-11.

FERRARI, D., SPECIALE, A., CRISTANI, M., FRATANTONIO, D., MOLONIA, M. S., RANALDI, G., SAIJA, A. & CIMINO, F. 2016a. Cyanidin-3-O-glucoside inhibits NF-kB signalling in intestinal epithelial cells exposed to TNF-α and exerts protective effects via Nrf2 pathway activation. *Toxicol Lett,* 264**,** 51-58.

FERRARI, L., KRANE, M. K. & FICHERA, A. 2016b. Inflammatory bowel disease surgery in the biologic era. *World Journal of Gastrointestinal Surgery,* 8**,** 363-370.

FIOCCHI, C. 1998. Inflammatory bowel disease: etiology and pathogenesis. *Gastroenterology,* 115**,** 182-205.

FISHER, E. M., KHAN, M., SALISBURY, R. & KUPPUSAMY, P. 2013. Noninvasive monitoring of small intestinal oxygen in a rat model of chronic mesenteric ischemia. *Cell biochemistry and biophysics,* 67**,** 10.1007/s12013-013-9611-y.

FITZPATRICK, L. R., WANG, J. & LE, T. 2001. Caffeic acid phenethyl ester, an inhibitor of nuclear factor-kappaB, attenuates bacterial peptidoglycan polysaccharide-induced colitis in rats. *J Pharmacol Exp Ther,* 299**,** 915-20.

FORD, A. C., SANDBORN, W. J., KHAN, K. J., HANAUER, S. B., TALLEY, N. J. & MOAYYEDI, P. 2011. Efficacy of biological therapies in inflammatory bowel disease: systematic review and meta-analysis. *Am J Gastroenterol,* 106**,** 644-59.

FRANCESCONE, R., HOU, V. & GRIVENNIKOV, S. I. 2015. Cytokines, IBD and colitis-associated cancer. *Inflamm Bowel Dis,* 21**,** 409-418.

FRASER, A. G. 2003. Methotrexate: first-line or second-line immunomodulator? *Eur J Gastroenterol Hepatol,* 15**,** 225-31.

FRASER, A. G., ORCHARD, T. R. & JEWELL, D. P. 2002. The efficacy of azathioprine for the treatment of inflammatory bowel disease: a 30 year review. *Gut,* 50**,** 485-9.

FRIEDL, P. & WOLF, K. 2003. Tumour-cell invasion and migration: diversity and escape mechanisms. *Nature reviews. Cancer,* 3**,** 362.

FRØSLIE, K. F., JAHNSEN, J., MOUM, B. A. & VATN, M. H. 2007. Mucosal Healing in Inflammatory Bowel Disease: Results From a Norwegian Population-Based Cohort. *Gastroenterology,* 133**,** 412-422.

FURUTA, G. T., TURNER, J. R., TAYLOR, C. T., HERSHBERG, R. M., COMERFORD, K., NARRAVULA, S., PODOLSKY, D. K. & COLGAN, S. P. 2001. Hypoxia-inducible factor 1-dependent induction of intestinal trefoil factor protects barrier function during hypoxia. *J Exp Med,* 193**,** 1027-34.

GADALETA, R. M., GARCIA-IRIGOYEN, O. & MOSCHETTA, A. 2017. Bile acids and colon cancer: Is FXR the solution of the conundrum? *Molecular Aspects of Medicine,* 56**,** 66-74.

GANESH, K., ARCHANA, D. & PREETI, K. 2015. Galactosylated Albumin Nanoparticles of Simvastatin. *Iranian Journal of Pharmaceutical Research : IJPR,* 14**,** 407-415.

GARG, S. K., AHUJA, V., SANKAR, M. J., KUMAR, A. & MOSS, A. C. 2012. Curcumin for maintenance of remission in ulcerative colitis. *The Cochrane database of systematic reviews,* 10**,** CD008424-CD008424.

GE, Y., CAO, X., WANG, D., SUN, W., SUN, H., HAN, B., CUI, J. & LIU, B. 2016. Overexpression of Livin promotes migration and invasion of colorectal cancer cells by induction of epithelial–mesenchymal transition via NF-κB activation. *OncoTargets and therapy,* 9**,** 1011-1021.

GECSE, K. B. & LAKATOS, P. L. 2017. IBD in 2016: Biologicals and biosimilars in IBD - the road to personalized treatment. *Nat Rev Gastroenterol Hepatol,* 14**,** 74-76.

GIATROMANOLAKI, A., SIVRIDIS, E., MALTEZOS, E., PAPAZOGLOU, D., SIMOPOULOS, C., GATTER, K. C., HARRIS, A. L. & KOUKOURAKIS, M. I. 2003. Hypoxia inducible factor 1alpha and 2alpha overexpression in inflammatory bowel disease. *J Clin Pathol,* 56**,** 209-13.

GÓMEZ-ESTACA, J., BALAGUER, M. P., LÓPEZ-CARBALLO, G., GAVARA, R. & HERNÁNDEZ-MUÑOZ, P. 2017. Improving antioxidant and antimicrobial properties of curcumin by means of encapsulation in gelatin through electrohydrodynamic atomization. *Food Hydrocolloids,* 70**,** 313-320.

GRIVENNIKOV, S. I. 2013. Inflammation and colorectal cancer: colitis-associated neoplasia. *Seminars in Immunopathology,* 35**,** 229-244.

GROSSER, T., RICCIOTTI, E. & FITZGERALD, G. A. 2017. The Cardiovascular Pharmacology of Nonsteroidal Anti-Inflammatory Drugs. *Trends in Pharmacological Sciences,* 38**,** 733-748.

GU, P., ZHU, L., LIU, Y., ZHANG, L., LIU, J. & SHEN, H. 2017. Protective effects of paeoniflorin on TNBS-induced ulcerative colitis through inhibiting NF-kappaB pathway and apoptosis in mice. *Int Immunopharmacol,* 50**,** 152-160.

GU, Y., LEE, H. M., NAPOLITANO, N., CLEMENS, M., ZHANG, Y., SORSA, T., JOHNSON, F. & GOLUB, L. M. 2013. 4-methoxycarbonyl curcumin: a unique inhibitor of both inflammatory mediators and periodontal inflammation. *Mediators Inflamm,* 329740**,** 24.

GUO, Y., SU, Z.-Y., ZHANG, C., GASPAR, J. M., WANG, R., HART, R. P., VERZI, M. P. & KONG, A.-N. T. 2017. Mechanisms of colitis-accelerated colon carcinogenesis and its prevention with the combination of aspirin and curcumin: Transcriptomic analysis using RNA-seq. *Biochem Pharmacol,* 135**,** 22-34.

GUPTA, S. C., KIM, J. H., PRASAD, S. & AGGARWAL, B. B. 2010a. Regulation of survival, proliferation, invasion, angiogenesis, and metastasis of tumor cells through modulation of inflammatory pathways by nutraceuticals. *Cancer Metastasis Rev,* 29**,** 405-34.

GUPTA, S. C., PATCHVA, S. & AGGARWAL, B. B. 2013. Therapeutic Roles of Curcumin: Lessons Learned from Clinical Trials. *The AAPS Journal,* 15**,** 195-218.

GUPTA, S. C., SUNDARAM, C., REUTER, S. & AGGARWAL, B. B. 2010b. Inhibiting NF-κB Activation by Small Molecules As a Therapeutic Strategy. *Biochim Biophys Acta,* 1799**,** 775-787.

GUSTAVSSON, B., CARLSSON, G., MACHOVER, D., PETRELLI, N., ROTH, A., SCHMOLL, H. J., TVEIT, K. M. & GIBSON, F. 2015. A review of the evolution of systemic chemotherapy in the management of colorectal cancer. *Clin Colorectal Cancer,* 14**,** 1-10.

HAGGAG, Y., ABDEL-WAHAB, Y., OJO, O., OSMAN, M., EL-GIZAWY, S., EL-TANANI, M., FAHEEM, A. & MCCARRON, P. 2016. Preparation and in vivo evaluation of insulin-loaded biodegradable nanoparticles prepared from diblock copolymers of PLGA and PEG. *International Journal of Pharmaceutics,* 499**,** 236-246.

HAGGAR, F. A. & BOUSHEY, R. P. 2009. Colorectal Cancer Epidemiology: Incidence, Mortality, Survival, and Risk Factors. *Clinics in Colon and Rectal Surgery,* 22**,** 191-197.

HAKANSSON, A., TORMO-BADIA, N., BARIDI, A., XU, J., MOLIN, G., HAGSLATT, M. L., KARLSSON, C., JEPPSSON, B., CILIO, C. M. & AHRNE, S. 2015. Immunological alteration and changes of gut microbiota after dextran sulfate sodium (DSS) administration in mice. *Clin Exp Med,* 15**,** 107-20.

HALAYQA, M. & DOMAŃSKA, U. 2014. PLGA Biodegradable Nanoparticles Containing Perphenazine or Chlorpromazine Hydrochloride: Effect of Formulation and Release. *Int J Mol Sci,* 15**,** 23909-23923.

HANS, M. L. & LOWMAN, A. M. 2002. Biodegradable nanoparticles for drug delivery and targeting. *Current Opinion in Solid State and Materials Science,* 6**,** 319-327.

HASSANZADEH, P. 2011. Colorectal cancer and NF-κB signaling pathway. *Gastroenterology and Hepatology from bed to bench,* 4**,** 127-132.

HE, Z. Y., SHI, C. B., WEN, H., LI, F. L., WANG, B. L. & WANG, J. 2011. Upregulation of p53 expression in patients with colorectal cancer by administration of curcumin. *Cancer Invest,* 29**,** 208-13.

HÉBUTERNE, X., LEMARIÉ, E., MICHALLET, M., DE MONTREUIL, C. B., SCHNEIDER, S. M. & GOLDWASSER, F. 2014. Prevalence of Malnutrition and Current Use of Nutrition Support in Patients With Cancer. *Journal of Parenteral and Enteral Nutrition,* 38**,** 196-204.

HEGAZY, S. K. & EL-BEDEWY, M. M. 2010. Effect of probiotics on pro-inflammatory cytokines and NF-kappaB activation in ulcerative colitis. *World J Gastroenterol,* 16**,** 4145-51.

HERFARTH, H., BRAND, K., RATH, H. C., ROGLER, G., SCHOLMERICH, J. & FALK, W. 2000. Nuclear factor-kappa B activity and intestinal inflammation in dextran sulphate sodium (DSS)-induced colitis in mice is suppressed by gliotoxin. *Clin Exp Immunol,* 120**,** 59-65.

HOCHWALD, S. N., LIND, D. S., MALATY, J., COPELAND, E. M., 3RD, MOLDAWER, L. L. & MACKAY, S. L. 2003. Antineoplastic therapy in colorectal cancer through proteasome inhibition. *Am Surg,* 69**,** 15-23.

HOESEL, B. & SCHMID, J. A. 2013. The complexity of NF-κB signaling in inflammation and cancer. *Molecular Cancer,* 12**,** 86-86.

HOFHEINZ, R.-D., SEGAERT, S., SAFONT, M. J., DEMONTY, G. & PRENEN, H. 2017a. Management of adverse events during treatment of gastrointestinal cancers with epidermal growth factor inhibitors. *Critical Reviews in Oncology/Hematology,* 114**,** 102-113.

HOFHEINZ, R.-D., SEGAERT, S., SAFONT, M. J., DEMONTY, G. & PRENEN, H. 2017b. Management of adverse events during treatment of gastrointestinal cancers with epidermal growth factor inhibitors. *Critical Reviews in Oncology/Hematology,* 114**,** 102-113.

HUANG, W. Y., CAI, Y. Z. & ZHANG, Y. 2010. Natural phenolic compounds from medicinal herbs and dietary plants: potential use for cancer prevention. *Nutr Cancer,* 62**,** 1-20.

INAGAKI, H., ITO, R., SETOGUCHI, Y., ORITANI, Y. & ITO, T. 2016. Administration of Piceatannol Complexed with alpha-Cyclodextrin Improves Its Absorption in Rats. *J Agric Food Chem,* 64**,** 3557-63.

JAFARI, S. M. & MCCLEMENTS, D. J. 2017. Chapter One - Nanotechnology Approaches for Increasing Nutrient Bioavailability. *In:* TOLDRÁ, F. (ed.) *Advances in Food and Nutrition Research.* Academic Press.

JAHANGIRIAN, H., LEMRASKI, E. G., WEBSTER, T. J., RAFIEE-MOGHADDAM, R. & ABDOLLAHI, Y. 2017. A review of drug delivery systems based on nanotechnology and green chemistry: green nanomedicine. *International Journal of Nanomedicine,* 12**,** 2957-2978.

JANA, A., KRETT, N. L., GUZMAN, G., KHALID, A., OZDEN, O., STAUDACHER, J. J., BAUER, J., BAIK, S. H., CARROLL, T., YAZICI, C. & JUNG, B. 2017. NFkB is essential for activin-induced colorectal cancer migration via upregulation of PI3K-MDM2 pathway. *Oncotarget,* 8**,** 37377-37393.

JANI, T. S., DEVECCHIO, J., MAZUMDAR, T., AGYEMAN, A. & HOUGHTON, J. A. 2010. Inhibition of NF-kappaB signaling by quinacrine is cytotoxic to human colon carcinoma cell lines and is synergistic in combination with tumor necrosis factor-related apoptosis-inducing ligand (TRAIL) or oxaliplatin. *J Biol Chem,* 285**,** 19162-72.

JANZ, T., LU, K., POVLOW, M. R. & URSO, B. 2016. A Review of Colorectal Cancer Detection Modalities, Stool DNA, and Fecal Immunochemistry Testing in Adults Over the Age of 50. *Cureus,* 8**,** e931.

JENITA, J. L., CHOCALINGAM, V. & WILSON, B. 2014. Albumin nanoparticles coated with polysorbate 80 as a novel drug carrier for the delivery of antiretroviral drug—Efavirenz. *International Journal of Pharmaceutical Investigation,* 4**,** 142-148.

JIANG, Y., WONG, S., CHEN, F., CHANG, T., LU, H. & STENZEL, M. H. 2017. Influencing Selectivity to Cancer Cells with Mixed Nanoparticles Prepared from Albumin–Polymer Conjugates and Block Copolymers. *Bioconjugate Chemistry,* 28**,** 979-985.

JORDAN, C., SIN, J., FEAR, N. T. & CHALDER, T. 2016. A systematic review of the psychological correlates of adjustment outcomes in adults with inflammatory bowel disease. *Clinical Psychology Review,* 47**,** 28-40.

JUN, J. Y., NGUYEN, H. H., PAIK, S.-Y.-R., CHUN, H. S., KANG, B.-C. & KO, S. 2011. Preparation of size-controlled bovine serum albumin (BSA) nanoparticles by a modified desolvation method. *Food Chemistry,* 127**,** 1892-1898.

JURJUS, A. R., KHOURY, N. N. & REIMUND, J. M. 2004. Animal models of inflammatory bowel disease. *J Pharmacol Toxicol Methods,* 50**,** 81-92.

KAELIN, W. G., JR. & RATCLIFFE, P. J. 2008. Oxygen sensing by metazoans: the central role of the HIF hydroxylase pathway. *Mol Cell,* 30**,** 393-402.

KAMATH, N., PAI, C. G. & DELTOMBE, T. 2016. Pure red cell aplasia due to azathioprine therapy for Crohn's disease. *Indian Journal of Pharmacology,* 48**,** 86-87.

KANE, S. V. 2006. Systematic review: adherence issues in the treatment of ulcerative colitis. *Aliment Pharmacol Ther,* 23**,** 577-85.

KANG, T., LI, F., BAIK, S., SHAO, W., LING, D. & HYEON, T. 2017. Surface design of magnetic nanoparticles for stimuli-responsive cancer imaging and therapy. *Biomaterials,* 136**,** 98-114.

KANNEGANTI, M., MINO-KENUDSON, M. & MIZOGUCHI, E. 2011. Animal models of colitis-associated carcinogenesis. *BioMed Research International,* 2011.

KAPLAN, G. G. 2015. The global burden of IBD: from 2015 to 2025. *Nat Rev Gastroenterol Hepatol,* 12**,** 720-727.

KARHAUSEN, J., FURUTA, G. T., TOMASZEWSKI, J. E., JOHNSON, R. S., COLGAN, S. P. & HAASE, V. H. 2004. Epithelial hypoxia-inducible factor-1 is protective in murine experimental colitis. *J Clin Invest,* 114**,** 1098-106.

KARIN, M. 2009. NF-kappaB as a critical link between inflammation and cancer. *Cold Spring Harb Perspect Biol,* 1.

KARREMAN, M. C., LUIME, J. J., HAZES, J. M. W. & WEEL, A. E. A. M. 2017. The Prevalence and Incidence of Axial and Peripheral Spondyloarthritis in Inflammatory Bowel Disease: A Systematic Review and Meta-analysis. *Journal of Crohn's and Colitis,* 11**,** 631-642.

KARUNAWEERA, N., RAJU, R., GYENGESI, E. & MÜNCH, G. 2015. Plant polyphenols as inhibitors of NF-κB induced cytokine production—a potential anti-inflammatory treatment for Alzheimer's disease? *Frontiers in Molecular Neuroscience,* 8**,** 24.

KEMP, J. A., SHIM, M. S., HEO, C. Y. & KWON, Y. J. 2016. "Combo" nanomedicine: Co-delivery of multi-modal therapeutics for efficient, targeted, and safe cancer therapy. *Advanced Drug Delivery Reviews,* 98**,** 3-18.

KETKAR, S., PAGIRE, S. K., GOUD, N. R., MAHADIK, K., NANGIA, A. & PARADKAR, A. 2016. Tracing the architecture of caffeic acid phenethyl ester cocrystals: studies on crystal structure, solubility, and bioavailability implications. *Crystal Growth & Design,* 16**,** 5710-5716.

KHAN, A. A., KHAN, Z., MALIK, A., KALAM, M. A., CASH, P., ASHRAF, M. T. & ALSHAMSAN, A. 2017a. Colorectal cancer-inflammatory bowel disease nexus and felony of Escherichia coli. *Life Sci,* 180**,** 60-67.

KHAN, A. A., MUDASSIR, J., MOHTAR, N. & DARWIS, Y. 2013. Advanced drug delivery to the lymphatic system: lipid-based nanoformulations. *International Journal of Nanomedicine,* 8**,** 2733-2744.

KHAN, I., GOTHWAL, A., SHARMA, A. K., KESHARWANI, P., GUPTA, L., IYER, A. K. & GUPTA, U. 2016. PLGA Nanoparticles and Their Versatile

Role in Anticancer Drug Delivery. *Crit Rev Ther Drug Carrier Syst,* 33**,** 159-93.

KHAN, K., CUNNINGHAM, D. & CHAU, I. 2017b. Targeting angiogenic pathways in colorectal cancer: complexities, challenges and future directions. *Curr Drug Targets,* 18**,** 56-71.

KHAN, M. N., LANE, M. E., MCCARRON, P. A. & TAMBUWALA, M. M. 2017c. Caffeic acid phenethyl ester is protective in experimental ulcerative colitis via reduction in levels of pro-inflammatory mediators and enhancement of epithelial barrier function. *Inflammopharmacology,* 20**,** 017-0364.

KIESLER, P., FUSS, I. J. & STROBER, W. 2015. Experimental Models of Inflammatory Bowel Diseases. *Cellular and molecular gastroenterology and hepatology,* 1**,** 154-170.

KıLıÇARSLAN, M. & BAYKARA, T. 2003. The effect of the drug/polymer ratio on the properties of the verapamil HCl loaded microspheres. *International Journal of Pharmaceutics,* 252**,** 99-109.

KILICAY, E., DEMIRBILEK, M., TURK, M., GUVEN, E., HAZER, B. & DENKBAS, E. B. 2011. Preparation and characterization of poly(3-hydroxybutyrate-co-3-hydroxyhexanoate) (PHBHHX) based nanoparticles for targeted cancer therapy. *Eur J Pharm Sci,* 44**,** 310-20.

KIM, E. R. & CHANG, D. K. 2014. Colorectal cancer in inflammatory bowel disease: The risk, pathogenesis, prevention and diagnosis. *World Journal of Gastroenterology : WJG,* 20**,** 9872-9881.

KIM, H., BANERJEE, N., SIRVEN, M. A., MINAMOTO, Y., MARKEL, M. E., SUCHODOLSKI, J. S., TALCOTT, S. T. & MERTENS-TALCOTT, S. U. 2017. Pomegranate polyphenolics reduce inflammation and ulceration in intestinal colitis—involvement of the miR-145/p70S6K1/HIF1α axis in vivo and in vitro. *The Journal of Nutritional Biochemistry,* 43**,** 107-115.

KIM, S. B., BOZEMAN, R., KAISANI, A., KIM, W., ZHANG, L., RICHARDSON, J. A., WRIGHT, W. E. & SHAY, J. W. 2016. Radiation Promotes Colorectal Cancer Initiation and Progression by Inducing Senescence-Associated Inflammatory Responses. *Oncogene,* 35**,** 3365-3375.

KIM, T. H., JIANG, H. H., YOUN, Y. S., PARK, C. W., TAK, K. K., LEE, S., KIM, H., JON, S., CHEN, X. & LEE, K. C. 2011. Preparation and characterization of water-soluble albumin-bound curcumin nanoparticles with improved antitumor activity. *Int J Pharm,* 403**,** 285-91.

KIMURA, H., WEISZ, A., KURASHIMA, Y., HASHIMOTO, K., OGURA, T., D'ACQUISTO, F., ADDEO, R., MAKUUCHI, M. & ESUMI, H. 2000. Hypoxia response element of the human vascular endothelial growth factor gene mediates transcriptional regulation by nitric oxide: control of hypoxia-inducible factor-1 activity by nitric oxide. *Blood,* 95**,** 189-97.

KINOSHITA, R., ISHIMA, Y., CHUANG, V. T. G., NAKAMURA, H., FANG, J., WATANABE, H., SHIMIZU, T., OKUHIRA, K., ISHIDA, T., MAEDA, H., OTAGIRI, M. & MARUYAMA, T. 2017. Improved anticancer effects of albumin-bound paclitaxel nanoparticle via augmentation of EPR effect and albumin-protein interactions using S-nitrosated human serum albumin dimer. *Biomaterials,* 140**,** 162-169.

KLAMPFER, L. 2011. CYTOKINES, INFLAMMATION AND COLON CANCER. *Current cancer drug targets,* 11**,** 451-464.

KLAVER, C. E. L., KAPPEN, T. M., BORSTLAP, W. A. A., BEMELMAN, W. A. & TANIS, P. J. 2017. Laparoscopic surgery for T4 colon cancer: a systematic review and meta-analysis. *Surg Endosc*.

KO, H. S., LEE, H. J., KIM, S. H. & LEE, E. O. 2012. Piceatannol suppresses breast cancer cell invasion through the inhibition of MMP-9: involvement of PI3K/AKT and NF-kappaB pathways. *J Agric Food Chem,* 60**,** 4083-9.

KOCAADAM, B. & ŞANLIER, N. 2017. Curcumin, an active component of turmeric (Curcuma longa), and its effects on health. *Critical reviews in food science and nutrition,* 57**,** 2889-2895.

KORNBLUTH, A. & SACHAR, D. B. 2010. Ulcerative colitis practice guidelines in adults: American College Of Gastroenterology, Practice Parameters Committee. *Am J Gastroenterol,* 105**,** 501-23.

KUMAR, A., TAKADA, Y., BORIEK, A. M. & AGGARWAL, B. B. 2004. Nuclear factor-κB: its role in health and disease. *Journal of Molecular Medicine,* 82**,** 434-448.

KUMAR, S. S., MAHESH, A., MAHADEVAN, S. & MANDAL, A. B. 2014. Synthesis and characterization of curcumin loaded polymer/lipid based nanoparticles and evaluation of their antitumor effects on MCF-7 cells. *Biochim Biophys Acta,* 1840**,** 1913-22.

KUMARI, A., YADAV, S. K. & YADAV, S. C. 2010a. Biodegradable polymeric nanoparticles based drug delivery systems. *Colloids Surf B Biointerfaces,* 75**,** 1-18.

KUMARI, A., YADAV, S. K. & YADAV, S. C. 2010b. Biodegradable polymeric nanoparticles based drug delivery systems. *Colloids and Surfaces B: Biointerfaces,* 75**,** 1-18.

KUNNUMAKKARA, A. B., BORDOLOI, D., HARSHA, C., BANIK, K., GUPTA, S. C. & AGGARWAL, B. B. 2017a. Curcumin mediates anticancer effects by modulating multiple cell signaling pathways. *Clin Sci,* 131**,** 1781-1799.

KUNNUMAKKARA, A. B., BORDOLOI, D., PADMAVATHI, G., MONISHA, J., ROY, N. K., PRASAD, S. & AGGARWAL, B. B. 2017b. Curcumin, the golden nutraceutical: multitargeting for multiple chronic diseases. *Br J Pharmacol,* 174**,** 1325-1348.

KUO, Y. Y., JIM, W. T., SU, L. C., CHUNG, C. J., LIN, C. Y., HUO, C., TSENG, J. C., HUANG, S. H., LAI, C. J., CHEN, B. C., WANG, B. J., CHAN, T. M., LIN, H. P., CHANG, W. S., CHANG, C. R. & CHUU, C. P. 2015. Caffeic Acid phenethyl ester is a potential therapeutic agent for oral cancer. *Int J Mol Sci,* 16**,** 10748-66.

KWON, J. Y., SEO, S. G., HEO, Y. S., YUE, S., CHENG, J. X., LEE, K. W. & KIM, K. H. 2012. Piceatannol, natural polyphenolic stilbene, inhibits adipogenesis via modulation of mitotic clonal expansion and insulin receptor-dependent insulin signaling in early phase of differentiation. *J Biol Chem,* 287**,** 11566-78.

LAASS, M. W., ROGGENBUCK, D. & CONRAD, K. 2014. Diagnosis and classification of Crohn's disease. *Autoimmunity Reviews,* 13**,** 467-471.

LAMICHHANE, S. P., ARYA, N., OJHA, N., KOHLER, E. & SHASTRI, V. P. 2015. Glycosaminoglycan-functionalized poly-lactide-co-glycolide nanoparticles: synthesis, characterization, cytocompatibility, and cellular uptake. *Int J Nanomedicine,* 10**,** 775-89.

LANE, E. R., ZISMAN, T. L. & SUSKIND, D. L. 2017. The microbiota in inflammatory bowel disease: current and therapeutic insights. *Journal of Inflammation Research,* 10**,** 63-73.

LANG, A., LAHAV, M., SAKHNINI, E., BARSHACK, I., FIDDER, H. H., AVIDAN, B., BARDAN, E., HERSHKOVIZ, R., BAR-MEIR, S. & CHOWERS, Y. 2004. Allicin inhibits spontaneous and TNF-α induced secretion of proinflammatory cytokines and chemokines from intestinal epithelial cells. *Clinical Nutrition,* 23**,** 1199-1208.

LANGER, K., BALTHASAR, S., VOGEL, V., DINAUER, N., VON BRIESEN, H. & SCHUBERT, D. 2003a. Optimization of the preparation process for human serum albumin (HSA) nanoparticles. *International Journal of Pharmaceutics,* 257**,** 169-180.

LANGER, K., BALTHASAR, S., VOGEL, V., DINAUER, N., VON BRIESEN, H. & SCHUBERT, D. 2003b. Optimization of the preparation process for human serum albumin (HSA) nanoparticles. *Int J Pharm,* 257**,** 169-80.

LARSEN, M. T., KUHLMANN, M., HVAM, M. L. & HOWARD, K. A. 2016. Albumin-based drug delivery: harnessing nature to cure disease. *Molecular and Cellular Therapies,* 4**,** 3.

LARUSSA, T., IMENEO, M. & LUZZA, F. 2017. Potential role of nutraceutical compounds in inflammatory bowel disease. *World Journal of Gastroenterology,* 23**,** 2483-2492.

LASRY, A., ZINGER, A. & BEN-NERIAH, Y. 2016. Inflammatory networks underlying colorectal cancer. *Nat Immunol,* 17**,** 230-240.

LAWRENCE, T. 2009. The nuclear factor NF-kappaB pathway in inflammation. *Cold Spring Harb Perspect Biol,* 1**,** 7.

LEE, K. W., KANG, N. J., KIM, J. H., LEE, K. M., LEE, D. E., HUR, H. J. & LEE, H. J. 2008. Caffeic acid phenethyl ester inhibits invasion and expression of matrix metalloproteinase in SK-Hep1 human hepatocellular carcinoma cells by targeting nuclear factor kappa B. *Genes & Nutrition,* 2**,** 319-322.

LEIVA, A., ESTEVA, M., LLOBERA, J., MACIÀ, F., PITA-FERNÁNDEZ, S., GONZÁLEZ-LUJÁN, L., SÁNCHEZ-CALAVERA, M. A. & RAMOS, M. 2017. Time to diagnosis and stage of symptomatic colorectal cancer determined by three different sources of information: A population based retrospective study. *Cancer Epidemiology,* 47**,** 48-55.

LEWIS, J. D., SCHWARTZ, J. S. & LICHTENSTEIN, G. R. 2000. Azathioprine for maintenance of remission in Crohn's disease: benefits outweigh the risk of lymphoma. *Gastroenterology,* 118**,** 1018-24.

LI, F.-Q., SU, H., WANG, J., LIU, J.-Y., ZHU, Q.-G., FEI, Y.-B., PAN, Y.-H. & HU, J.-H. 2008a. Preparation and characterization of sodium ferulate entrapped bovine serum albumin nanoparticles for liver targeting. *International Journal of Pharmaceutics,* 349**,** 274-282.

LI, F.-Q., SU, H., WANG, J., LIU, J.-Y., ZHU, Q.-G., FEI, Y.-B., PAN, Y.-H. & HU, J.-H. 2008b. Preparation and characterization of sodium ferulate entrapped bovine serum albumin nanoparticles for liver targeting. *International Journal of Pharmaceutics,* 349**,** 274-282.

LI, J., CHEN, T., DENG, F., WAN, J., TANG, Y., YUAN, P. & ZHANG, L. 2015a. Synthesis, characterization, and in vitro evaluation of curcumin-loaded albumin nanoparticles surface-functionalized with glycyrrhetinic acid. *Int J Nanomedicine,* 10**,** 5475-87.

LI, R., KIM, M.-H., SANDHU, A. K., GAO, C. & GU, L. 2017. Muscadine Grape (Vitis rotundifolia) or Wine Phytochemicals Reduce Intestinal Inflammation in Mice with Dextran Sulfate Sodium-Induced Colitis. *Journal of agricultural and food chemistry,* 65**,** 769-776.

LI, Z., JIANG, H., XU, C. & GU, L. 2015b. A review: Using nanoparticles to enhance absorption and bioavailability of phenolic phytochemicals. *Food Hydrocolloids,* 43**,** 153-164.

LIANG, C.-C., PARK, A. Y. & GUAN, J.-L. 2007. In vitro scratch assay: a convenient and inexpensive method for analysis of cell migration in vitro. *Nat. Protocols,* 2**,** 329-333.

LIAO, H. F., CHEN, Y. Y., LIU, J. J., HSU, M. L., SHIEH, H. J., LIAO, H. J., SHIEH, C. J., SHIAO, M. S. & CHEN, Y. J. 2003. Inhibitory effect of caffeic acid phenethyl ester on angiogenesis, tumor invasion, and metastasis. *J Agric Food Chem,* 51**,** 7907-12.

LIN, H. P., LIN, C. Y., LIU, C. C., SU, L. C., HUO, C., KUO, Y. Y., TSENG, J. C., HSU, J. M., CHEN, C. K. & CHUU, C. P. 2013. Caffeic Acid phenethyl ester as a potential treatment for advanced prostate cancer targeting akt signaling. *Int J Mol Sci,* 14**,** 5264-83.

LIU, L., BI, Y., ZHOU, M., CHEN, X., HE, X., ZHANG, Y., SUN, T., RUAN, C., CHEN, Q. & WANG, H. 2017. Biomimetic Human Serum Albumin Nanoparticle for Efficiently Targeting Therapy to Metastatic Breast Cancers. *ACS Applied Materials & Interfaces,* 9**,** 7424-7435.

LJUNG, T., KARLEN, P., SCHMIDT, D., HELLSTROM, P. M., LAPIDUS, A., JANCZEWSKA, I., SJOQVIST, U. & LOFBERG, R. 2004. Infliximab in inflammatory bowel disease: clinical outcome in a population based cohort from Stockholm County. *Gut,* 53**,** 849-53.

LOFTUS, E. V., JR., KANE, S. V. & BJORKMAN, D. 2004. Systematic review: short-term adverse effects of 5-aminosalicylic acid agents in the treatment of ulcerative colitis. *Aliment Pharmacol Ther,* 19**,** 179-89.

LOHCHAROENKAL, W., WANG, L., CHEN, Y. C. & ROJANASAKUL, Y. 2014. Protein nanoparticles as drug delivery carriers for cancer therapy. *BioMed Research International,* 2014.

LORUSSO, D., BRIA, E., COSTANTINI, A., DI MAIO, M., ROSTI, G. & MANCUSO, A. 2017. Patients' perception of chemotherapy side effects: Expectations, doctor–patient communication and impact on quality of life–An Italian survey. *European journal of cancer care,* 26.

LOUAGE, B., VAN STEENBERGEN, M. J., NUHN, L., RISSEEUW, M. D. P., KARALIC, I., WINNE, J., VAN CALENBERGH, S., HENNINK, W. E. & DE GEEST, B. G. 2017. Micellar Paclitaxel-Initiated RAFT Polymer Conjugates with Acid-Sensitive Behavior. *ACS Macro Letters,* 6**,** 272-276.

LOUIS, N. A., HAMILTON, K. E., KONG, T. & COLGAN, S. P. 2005. HIF-dependent induction of apical CD55 coordinates epithelial clearance of neutrophils. *FASEB J,* 19**,** 950-9.

LOUREIRO, J. A., ANDRADE, S., DUARTE, A., NEVES, A. R., QUEIROZ, J. F., NUNES, C., SEVIN, E., FENART, L., GOSSELET, F. & COELHO, M. A. N. 2017. Resveratrol and grape extract-loaded solid lipid nanoparticles for the treatment of Alzheimer's disease. *Molecules,* 22**,** 277.

LOW, D., NGUYEN, D. D. & MIZOGUCHI, E. 2013. Animal models of ulcerative colitis and their application in drug research. *Drug Design, Development and Therapy,* 7**,** 1341-1357.

LU, Y., WANG, A., SHI, P. & ZHANG, H. 2017. A Theoretical Study on the Antioxidant Activity of Piceatannol and Isorhapontigenin Scavenging Nitric Oxide and Nitrogen Dioxide Radicals. *PLoS One,* 12**,** e0169773.

LUNNEY, P. C. & LEONG, R. W. 2012. Review article: Ulcerative colitis, smoking and nicotine therapy. *Aliment Pharmacol Ther,* 36**,** 997-1008.

LYNCH, D. & MURPHY, A. 2016. The emerging role of immunotherapy in colorectal cancer. *Annals of Translational Medicine,* 4**,** 305.

MA, C., PANACCIONE, R., FEDORAK, R. N., PARKER, C. E., KHANNA, R., LEVESQUE, B. G., SANDBORN, W. J., FEAGAN, B. G. & JAIRATH, V. 2017a. Development of a core outcome set for clinical trials in inflammatory bowel disease: study protocol for a systematic review of the literature and identification of a core outcome set using a Delphi survey. *BMJ open,* 7**,** e016146.

MA, J., MI, C., WANG, K. S., LEE, J. J. & JIN, X. 2016. Zinc finger protein 91 (ZFP91) activates HIF-1alpha via NF-kappaB/p65 to promote proliferation and tumorigenesis of colon cancer. *Oncotarget,* 7**,** 36551-36562.

MA, X., MENG, Z., JIN, L., XIAO, Z., WANG, X., TSARK, W. M., DING, L., GU, Y., ZHANG, J., KIM, B., HE, M., GAN, X., SHIVELY, J. E., YU, H., XU, R. & HUANG, W. 2017b. CAMK2γ in Intestinal Epithelial Cells Modulates Colitis-Associated Colorectal Carcinogenesis via Enhancing STAT3 Activation. *Oncogene,* 36**,** 4060-4071.

MALICKI, S., WINIARSKI, M., MATLOK, M., KOSTARCZYK, W., GUZDEK, A. & KONTUREK, P. C. 2009. IL-6 and IL-8 responses of colorectal cancer in vivo and in vitro cancer cells subjected to simvastatin. *J Physiol Pharmacol,* 60**,** 141-6.

MANGAN, N. E., VAN ROOIJEN, N., MCKENZIE, A. N. & FALLON, P. G. 2006. Helminth-modified pulmonary immune response protects mice from allergen-induced airway hyperresponsiveness. *J Immunol,* 176**,** 138-47.

MANZAT-SAPLACAN, R. M., MIRCEA, P. A., BALACESCU, L., CHIRA, R. I., BERINDAN-NEAGOE, I. & BALACESCU, O. 2015. Can we change our microbiome to prevent colorectal cancer development? *Acta Oncol,* 54**,** 1085-95.

MARELLI, G., SICA, A., VANNUCCI, L. & ALLAVENA, P. 2017. Inflammation as target in cancer therapy. *Curr Opin Pharmacol,* 35**,** 57-65.

MARTELLI, L., OLIVERA, P., ROBLIN, X., ATTAR, A. & PEYRIN-BIROULET, L. 2017. Cost-effectiveness of drug monitoring of anti-TNF therapy in inflammatory bowel disease and rheumatoid arthritis: a systematic review. *Journal of Gastroenterology,* 52**,** 19-25.

MARTIN, J., HALM, E. A., TIRO, J. A., MERCHANT, Z., BALASUBRAMANIAN, B. A., MCCALLISTER, K., SANDERS, J. M., AHN, C., BISHOP, W. P. & SINGAL, A. G. 2017. Reasons for Lack of Diagnostic Colonoscopy After Positive Result on Fecal Immunochemical Test in a Safety-Net Health System. *Am J Med,* 130**,** 93.e1-93.e7.

MASTROPIETRO, G., TISCORNIA, I., PERELMUTER, K., ASTRADA, S. & BOLLATI-FOGOLÍN, M. 2015. HT-29 and Caco-2 Reporter Cell Lines for Functional Studies of Nuclear Factor Kappa B Activation. *Mediators Inflamm,* 2015**,** 860534.

MAXWELL, J. R., BROWN, W. A., SMITH, C. L., BYRNE, F. R. & VINEY, J. L. 2009. Methods of inducing inflammatory bowel disease in mice. *Curr Protoc Pharmacol,* 5.

MCCOLE, D. F. 2014. IBD Candidate Genes and Intestinal Barrier Regulation. *Inflamm Bowel Dis,* 20**,** 1829-1849.

MEIRA, L. B., BUGNI, J. M., GREEN, S. L., LEE, C. W., PANG, B., BORENSHTEIN, D., RICKMAN, B. H., ROGERS, A. B., MOROSKI-ERKUL, C. A., MCFALINE, J. L., SCHAUER, D. B., DEDON, P. C., FOX, J. G. & SAMSON, L. D. 2008. DNA damage induced by chronic inflammation contributes to colon carcinogenesis in mice. *J Clin Invest,* 118**,** 2516-25.

MELLEMKJAER, L., JOHANSEN, C., GRIDLEY, G., LINET, M. S., KJAER, S. K. & OLSEN, J. H. 2000. Crohn's disease and cancer risk (Denmark). *Cancer Causes Control,* 11**,** 145-50.

MIRNEZAMI, R., CHANG, G. J., DAS, P., CHANDRAKUMARAN, K., TEKKIS, P., DARZI, A. & MIRNEZAMI, A. H. 2013. Intraoperative radiotherapy in colorectal cancer: Systematic review and meta-analysis of techniques, long-term outcomes, and complications. *Surg Oncol,* 22**,** 22-35.

MISHRA, J., DROMUND, J., QUAZI, S. H., KARANKI, S. S., SHAW, J. J., CHEN, B. & KUMAR, N. 2013. Prospective of Colon Cancer Treatments and Scope for Combinatorial Approach to Enhanced Cancer Cell Apoptosis. *Critical Reviews in Oncology/Hematology,* 86**,** 232-250.

MITCHELL, E., MACDONALD, S., CAMPBELL, N. C., WELLER, D. & MACLEOD, U. 2008. Influences on pre-hospital delay in the diagnosis of colorectal cancer: a systematic review. *British Journal of Cancer,* 98**,** 60-70.

MITTAL, G., SAHANA, D. K., BHARDWAJ, V. & RAVI KUMAR, M. N. 2007. Estradiol loaded PLGA nanoparticles for oral administration: effect of polymer molecular weight and copolymer composition on release behavior in vitro and in vivo. *J Control Release,* 119**,** 77-85.

MIYATA, T. 2007. Pharmacological basis of traditional medicines and health supplements as curatives. *J Pharmacol Sci,* 103**,** 127-31.

MIZOGUCHI, A. 2012. Animal Models of Inflammatory Bowel Disease. *In:* CONN, P. M. (ed.) *Progress in Molecular Biology and Translational Science.* Academic Press.

MOĆKO, P., KAWALEC, P. & PILC, A. 2016. Safety Profile of Biologic Drugs in the Therapy of Ulcerative Colitis: A Systematic Review and Network Meta-Analysis. *Pharmacotherapy: The Journal of Human Pharmacology and Drug Therapy,* 36**,** 870-879.

MOLODECKY, N. A., SOON, I. S., RABI, D. M., GHALI, W. A., FERRIS, M., CHERNOFF, G., BENCHIMOL, E. I., PANACCIONE, R., GHOSH, S., BARKEMA, H. W. & KAPLAN, G. G. 2012. Increasing incidence and prevalence of the inflammatory bowel diseases with time, based on systematic review. *Gastroenterology,* 142**,** 46-54.

MORIARITY, A., O'SULLIVAN, J., KENNEDY, J., MEHIGAN, B. & MCCORMICK, P. 2016. Current targeted therapies in the treatment of advanced colorectal cancer: a review. *Ther Adv Med Oncol,* 8**,** 276-93.

MORIN, P., ST-COEUR, P. D., DOIRON, J. A., CORMIER, M., POITRAS, J. J., SURETTE, M. E. & TOUAIBIA, M. 2017. Substituted Caffeic and Ferulic Acid Phenethyl Esters: Synthesis, Leukotrienes Biosynthesis Inhibition, and Cytotoxic Activity. *Molecules,* 22.

MOURA, F. A., DE ANDRADE, K. Q., DOS SANTOS, J. C. F., ARAÚJO, O. R. P. & GOULART, M. O. F. 2015. Antioxidant therapy for treatment of inflammatory bowel disease: Does it work? *Redox Biol,* 6**,** 617-639.

MUKERJEE, A. & VISHWANATHA, J. K. 2009. Formulation, characterization and evaluation of curcumin-loaded PLGA nanospheres for cancer therapy. *Anticancer Res,* 29**,** 3867-75.

MULLER, R. H., SHEGOKAR, R. & KECK, C. M. 2011. 20 years of lipid nanoparticles (SLN and NLC): present state of development and industrial applications. *Curr Drug Discov Technol,* 8**,** 207-27.

MURTAZA, G., KARIM, S., AKRAM, M. R., KHAN, S. A., AZHAR, S., MUMTAZ, A. & BIN ASAD, M. H. H. 2014a. Caffeic Acid Phenethyl Ester and Therapeutic Potentials. *BioMed Research International,* 2014**,** 145342.

MURTAZA, G., KARIM, S., AKRAM, M. R., KHAN, S. A., AZHAR, S., MUMTAZ, A. & BIN ASAD, M. H. H. 2014b. Caffeic acid phenethyl ester and therapeutic potentials. *BioMed Research International,* 2014.

MURTAZA, G., SAJJAD, A., MEHMOOD, Z., SHAH, S. H. & SIDDIQI, A. R. 2015. Possible molecular targets for therapeutic applications of caffeic acid phenethyl ester in inflammation and cancer. *Journal of Food and Drug Analysis,* 23**,** 11-18.

MŰZES, G., MOLNÁR, B., TULASSAY, Z. & SIPOS, F. 2012. Changes of the cytokine profile in inflammatory bowel diseases. *World Journal of Gastroenterology : WJG,* 18**,** 5848-5861.

NAMDARI, M., EATEMADI, A., SOLEIMANINEJAD, M. & HAMMED, A. T. 2017. A brief review on the application of nanoparticle enclosed herbal medicine for the treatment of infective endocarditis. *Biomedicine & Pharmacotherapy,* 87**,** 321-331.

NATHKE, I. & ROCHA, S. 2011. Antagonistic crosstalk between APC and HIF-1alpha. *Cell Cycle,* 10**,** 1545-7.

NELSON, K. M., DAHLIN, J. L., BISSON, J., GRAHAM, J., PAULI, G. F. & WALTERS, M. A. 2017. The Essential Medicinal Chemistry of Curcumin. *J Med Chem,* 60**,** 1620-1637.

NENCI, A., BECKER, C., WULLAERT, A., GAREUS, R., VAN LOO, G., DANESE, S., HUTH, M., NIKOLAEV, A., NEUFERT, C., MADISON, B., GUMUCIO, D., NEURATH, M. F. & PASPARAKIS, M. 2007. Epithelial NEMO links innate immunity to chronic intestinal inflammation. *Nature,* 446**,** 557-61.

NEURATH, M. F. 2014a. Cytokines in inflammatory bowel disease. *Nat Rev Immunol,* 14**,** 329-42.

NEURATH, M. F. 2014b. Cytokines in inflammatory bowel disease. *Nature Reviews Immunology,* 14**,** 329-342.

NITZAN, O., ELIAS, M., PERETZ, A. & SALIBA, W. 2016. Role of antibiotics for treatment of inflammatory bowel disease. *World Journal of Gastroenterology,* 22**,** 1078-1087.

NUÑEZ-SÁNCHEZ, M. A., GONZÁLEZ-SARRÍAS, A., GARCÍA-VILLALBA, R., MONEDERO-SAIZ, T., GARCÍA-TALAVERA, N. V., GÓMEZ-SÁNCHEZ, M. B., SÁNCHEZ-ÁLVAREZ, C., GARCÍA-ALBERT, A. M., RODRÍGUEZ-GIL, F. J., RUIZ-MARÍN, M., PASTOR-QUIRANTE, F. A., MARTÍNEZ-DÍAZ, F., TOMÁS-BARBERÁN, F. A., ESPÍN, J. C. & GARCÍA-CONESA, M.-T. 2017. Gene expression changes in colon tissues from colorectal cancer patients following the intake of an ellagitannin-containing pomegranate extract: a randomized clinical trial. *The Journal of Nutritional Biochemistry,* 42**,** 126-133.

O'CONNOR, A., QASIM, A. & O'MORÁIN, C. A. 2010. The long-term risk of continuous immunosuppression using thioguanides in inflammatory bowel disease. *Therapeutic Advances in Chronic Disease,* 1**,** 7-16.

OGAWA, A., ANDOH, A., ARAKI, Y., BAMBA, T. & FUJIYAMA, Y. 2004. Neutralization of interleukin-17 aggravates dextran sulfate sodium-induced colitis in mice. *Clin Immunol,* 110**,** 55-62.

OKAYASU, I., HATAKEYAMA, S., YAMADA, M., OHKUSA, T., INAGAKI, Y. & NAKAYA, R. 1990. A novel method in the induction of reliable experimental acute and chronic ulcerative colitis in mice. *Gastroenterology,* 98**,** 694-702.

OKE, S. & MARTIN, A. 2017. Insights into the role of the intestinal microbiota in colon cancer. *Therapeutic Advances in Gastroenterology,* 10**,** 417-428.

OWCZAREK, K., HRABEC, E., FICHNA, J., SOSNOWSKA, D., KOZIOŁKIEWICZ, M., SZYMAŃSKI, J. & LEWANDOWSKA, U. 2017. Inhibition of nuclear factor-kappaB, cyclooxygenase-2, and metalloproteinase-9 expression by flavanols from evening primrose (Oenothera paradoxa) in human colon cancer SW-480 cells. *Journal of Functional Foods,* 37**,** 553-563.

OZTURK, G., GINIS, Z., AKYOL, S., ERDEN, G., GUREL, A. & AKYOL, O. 2012. The anticancer mechanism of caffeic acid phenethyl ester (CAPE): review of melanomas, lung and prostate cancers. *Eur Rev Med Pharmacol Sci,* 16**,** 2064-8.

PAL, S., BHATTACHARJEE, A., ALI, A., MANDAL, N. C., MANDAL, S. C. & PAL, M. 2014. Chronic inflammation and cancer: potential chemoprevention through nuclear factor kappa B and p53 mutual antagonism. *J Inflamm,* 11**,** 1476-9255.

PATEL, D., MADANI, S., PATEL, S. & GUGLANI, L. 2016. Review of pulmonary adverse effects of infliximab therapy in Crohn's disease. *Expert Opin Drug Saf,* 15**,** 769-75.

PATEL, V. B., MISRA, S., PATEL, B. B. & MAJUMDAR, A. P. N. 2010. Colorectal Cancer: Chemopreventive Role of Curcumin and Resveratrol. *Nutrition and Cancer,* 62**,** 10.1080/01635581.2010.510259.

PATIL, Y. B., TOTI, U. S., KHDAIR, A., MA, L. & PANYAM, J. 2009. Single-step surface functionalization of polymeric nanoparticles for targeted drug delivery. *Biomaterials,* 30**,** 859-66.

PAYTON, F., SANDUSKY, P. & ALWORTH, W. L. 2007. NMR study of the solution structure of curcumin. *J Nat Prod,* 70**,** 143-6.

PEKOW, J. 2015. Do I Have Crohn's Disease or Ulcerative Colitis? Identifying Factors That Distinguish CD from UC and Indeterminate Colitis. *In:* STEIN, D. J. & SHAKER, R. (eds.) *Inflammatory Bowel Disease: A Point of Care Clinical Guide.* Cham: Springer International Publishing.

PELTONEN, L., AITTA, J., HYVÖNEN, S., KARJALAINEN, M. & HIRVONEN, J. 2004. Improved entrapment efficiency of hydrophilic drug substance during nanoprecipitation of poly (I) lactide nanoparticles. *AAPS PharmSciTech,* 5**,** 115.

PEYRIN-BIROULET, L., LOFTUS, E. V., JR., COLOMBEL, J. F. & SANDBORN, W. J. 2010. The natural history of adult Crohn's disease in population-based cohorts. *Am J Gastroenterol,* 105**,** 289-97.

PICHAI, M. V. & FERGUSON, L. R. *Potential prospects of nanomedicine for targeted therapeutics in inflammatory bowel diseases,* World J Gastroenterol. 2012 Jun 21;18(23):2895-901. doi: 10.3748/wjg.v18.i23.2895.

PILERI, P., CAMPAGNOLI, S., GRANDI, A., PARRI, M., DE CAMILLI, E., SONG, C., GANFINI, L., LACOMBE, A., NALDI, I., SARMIENTOS, P., CINTI, C., JIN, B., GRANDI, G., VIALE, G., TERRACCIANO, L. & GRIFANTINI, R. 2016. FAT1: a potential target for monoclonal antibody therapy in colon cancer. *Br J Cancer,* 115**,** 40-51.

PIOTROWSKA, H., KUCINSKA, M. & MURIAS, M. 2012. Biological activity of piceatannol: Leaving the shadow of resveratrol. *Mutation Research/Reviews in Mutation Research,* 750**,** 60-82.

PONDER, A. & LONG, M. D. 2013. A clinical review of recent findings in the epidemiology of inflammatory bowel disease. *Clinical Epidemiology,* 5**,** 237-247.

PORTÉ, F., UPPARA, M., MALIETZIS, G., FAIZ, O., HALLIGAN, S., ATHANASIOU, T. & BURLING, D. 2017. CT colonography for surveillance of patients with colorectal cancer: Systematic review and meta-analysis of diagnostic efficacy. *European Radiology,* 27**,** 51-60.

PUGLIA, C., LAURO, M. R., TIRENDI, G. G., FASSARI, G. E., CARBONE, C., BONINA, F. & PUGLISI, G. 2017. Modern drug delivery strategies applied to natural active compounds. *Expert Opin Drug Deliv,* 14**,** 755-768.

QI, P., XU, M. D., NI, S. J., SHEN, X. H., WEI, P., HUANG, D., TAN, C., SHENG, W. Q., ZHOU, X. Y. & DU, X. 2015. Down-regulation of ncRAN, a long non-coding RNA, contributes to colorectal cancer cell migration and invasion and predicts poor overall survival for colorectal cancer patients. *Mol Carcinog,* 54**,** 742-50.

QIN, X. 2013. Why is damage limited to the mucosa in ulcerative colitis but transmural in Crohn's disease? *World Journal of Gastrointestinal Pathophysiology,* 4**,** 63-64.

QUEIMADA, A. J., MOTA, F. L., PINHO, S. P. & MACEDO, E. A. 2009. Solubilities of biologically active phenolic compounds: measurements and modeling. *J Phys Chem B,* 113**,** 3469-76.

RAFA, H., BENKHELIFA, S., AITYOUNES, S., SAOULA, H., BELHADEF, S., BELKHELFA, M., BOUKERCHA, A., TOUMI, R., SOUFLI, I., MORALES, O., DE LAUNOIT, Y., MAHFOUF, H., NAKMOUCHE, M., DELHEM, N. & TOUIL-BOUKOFFA, C. 2017. All-Trans Retinoic Acid Modulates TLR4/NF-kappaB Signaling Pathway Targeting TNF-alpha and Nitric Oxide Synthase 2 Expression in Colonic Mucosa during Ulcerative Colitis and Colitis Associated Cancer. *Mediators Inflamm,* 7353252**,** 20.

RAFIEI, P. & HADDADI, A. 2017. Docetaxel-loaded PLGA and PLGA-PEG nanoparticles for intravenous application: pharmacokinetics and biodistribution profile. *International Journal of Nanomedicine,* 12**,** 935-947.

RAJITH, B. & RAVINDRAN, A. 2014. BSA nanoparticle loaded atorvastatin calcium-a new facet for an old drug. *PLoS One,* 9**,** e86317.

RANDHAWA, P. K., SINGH, K., SINGH, N. & JAGGI, A. S. 2014. A Review on Chemical-Induced Inflammatory Bowel Disease Models in Rodents. *The Korean Journal of Physiology & Pharmacology : Official Journal of the Korean Physiological Society and the Korean Society of Pharmacology,* 18**,** 279-288.

RAO, J. P. & GECKELER, K. E. 2011. Polymer nanoparticles: Preparation techniques and size-control parameters. *Progress in Polymer Science,* 36**,** 887-913.

RASHIDIAN, A., MUHAMMADNEJAD, A., DEHPOUR, A. R., MEHR, S. E., AKHAVAN, M. M., SHIRKOOHI, R., CHAMANARA, M., MOUSAVI, S. E. & REZAYAT, S. M. 2016. Atorvastatin attenuates TNBS-induced rat colitis: the involvement of the TLR4/NF-kB signaling pathway. *Inflammopharmacology,* 24**,** 109-18.

REVIA, R. A. & ZHANG, M. 2016. Magnetite nanoparticles for cancer diagnosis, treatment, and treatment monitoring: recent advances. *Materials Today,* 19**,** 157-168.

ROBINSON, A., KEELY, S., KARHAUSEN, J., GERICH, M. E., FURUTA, G. T. & COLGAN, S. P. 2008. Mucosal protection by hypoxia-inducible factor prolyl hydroxylase inhibition. *Gastroenterology,* 134**,** 145-55.

RÖDEL, F., FREY, B., MULTHOFF, G. & GAIPL, U. 2015. Contribution of the immune system to bystander and non-targeted effects of ionizing radiation. *Cancer Letters,* 356**,** 105-113.

ROGLER, G. 2014. Chronic ulcerative colitis and colorectal cancer. *Cancer Letters,* 345**,** 235-241.

RUBIN, D. C., SHAKER, A. & LEVIN, M. S. 2012. Chronic intestinal inflammation: inflammatory bowel disease and colitis-associated colon cancer. *Front Immunol,* 3**,** 107.

RUBIN, R. 1994. Sulfasalazine-induced fulminant hepatic failure and necrotizing pancreatitis. *Am J Gastroenterol,* 89**,** 789-91.

SAHOO, S. K., PANYAM, J., PRABHA, S. & LABHASETWAR, V. 2002. Residual polyvinyl alcohol associated with poly (d,l-lactide-co-glycolide) nanoparticles affects their physical properties and cellular uptake. *Journal of Controlled Release,* 82**,** 105-114.

SAKAMOTO, K., MAEDA, S., HIKIBA, Y., NAKAGAWA, H., HAYAKAWA, Y., SHIBATA, W., YANAI, A., OGURA, K. & OMATA, M. 2009. Constitutive NF-kappaB activation in colorectal carcinoma plays a key role in angiogenesis, promoting tumor growth. *Clin Cancer Res,* 15**,** 2248-58.

SALATA, O. V. 2004. Applications of nanoparticles in biology and medicine. *Journal of Nanobiotechnology,* 2**,** 3-3.

SAMANT, R. S. & SHEVDE, L. A. 2011. Recent advances in anti-angiogenic therapy of cancer. *Oncotarget,* 2**,** 122-34.

SANCHEZ-MUÑOZ, F., DOMINGUEZ-LOPEZ, A. & YAMAMOTO-FURUSHO, J. K. 2008. Role of cytokines in inflammatory bowel disease. *World Journal of Gastroenterology : WJG,* 14**,** 4280-4288.

SAPIO, L., GALLO, M., ILLIANO, M., CHIOSI, E., NAVIGLIO, D., SPINA, A. & NAVIGLIO, S. 2017. The Natural cAMP Elevating Compound Forskolin in Cancer Therapy: Is It Time? *J Cell Physiol,* 232**,** 922-927.

SATHYANARAYANAN, V. & NEELAPU, S. S. 2015. Cancer immunotherapy: Strategies for personalization and combinatorial approaches. *Molecular Oncology,* 9**,** 2043-2053.

SAVANI, C., DEVANI, K., HAZRA, A., PATHAK, A., SHAH, H., PATEL, R., MISHRA, T., THAKORE, K., AMIN, A. & NARWAL, K. 2017. P-105 Inluence of Patient and Hospital Characteristics on Length of Stay and Cost of Care in Ulcerative Colitis Patients. *Inflamm Bowel Dis,* 23**,** S38-S39.

SAXENA, R., RIDA, P. C., KUCUK, O. & ANEJA, R. 2016. Ginger augmented chemotherapy: A novel multitarget nontoxic approach for cancer management. *Mol Nutr Food Res,* 60**,** 1364-73.

SCARPA, M., CASTAGLIUOLO, I., CASTORO, C., POZZA, A., SCARPA, M., KOTSAFTI, A. & ANGRIMAN, I. 2014a. Inflammatory colonic carcinogenesis: A review on pathogenesis and immunosurveillance mechanisms in ulcerative colitis. *World Journal of Gastroenterology : WJG,* 20**,** 6774-6785.

SCARPA, M., RUFFOLO, C., ERROI, F., FIOROT, A., BASATO, S., POZZA, A., CANAL, F., MASSANI, M., CAVALLIN, F. & ANTONIUTTI, M. 2014b. Obesity is a risk factor for multifocal disease and recurrence after colorectal cancer surgery: a case-control study. *Anticancer Res,* 34**,** 5735-5741.

SCHREIBER, S., NIKOLAUS, S. & HAMPE, J. 1998. Activation of nuclear factor kappa B inflammatory bowel disease. *Gut,* 42**,** 477-84.

SCHUSTER, R., ZEINDL, L., HOLZER, W., KHUMPIRAPANG, N., OKONOGI, S., VIERNSTEIN, H. & MUELLER, M. 2017. Eulophia macrobulbon – an orchid with significant anti-inflammatory and antioxidant effect and anticancerogenic potential exerted by its root extract. *Phytomedicine,* 24**,** 157-165.

SEBAK, S., MIRZAEI, M., MALHOTRA, M., KULAMARVA, A. & PRAKASH, S. 2010. Human serum albumin nanoparticles as an efficient noscapine drug delivery system for potential use in breast cancer: preparation and in vitro analysis. *International Journal of Nanomedicine,* 5**,** 525-532.

SEMENZA, G. L. 2012. Hypoxia-Inducible Factors in Physiology and Medicine. *Cell,* 148**,** 399-408.

SERASANAMBATI, M. & CHILAKAPATI, S. R. 2016. Function of Nuclear Factor kappa B (NF-kB) in human diseases-A Review. *South Indian Journal of Biological Sciences,* 2**,** 368-387.

SERRA, G., DEIANA, M., SPENCER, J. P. E. & CORONA, G. 2017. Olive Oil Phenolics Prevent Oxysterol-Induced Pro-Inflammatory Cytokine Secretion and ROS Production in Human PBMCs, Through Modulation of p38 and JNK Pathways. *Molecular Nutrition & Food Research*.

SEYED, M. A., JANTAN, I., BUKHARI, S. N. & VIJAYARAGHAVAN, K. 2016. A Comprehensive Review on the Chemotherapeutic Potential of Piceatannol for Cancer Treatment, with Mechanistic Insights. *J Agric Food Chem,* 64**,** 725-37.

SHAH, Y. M. 2016. The role of hypoxia in intestinal inflammation. *Molecular and Cellular Pediatrics,* 3**,** 1.

SHARMA, N., MADAN, P. & LIN, S. 2016. Effect of process and formulation variables on the preparation of parenteral paclitaxel-loaded biodegradable polymeric nanoparticles: A co-surfactant study. *Asian Journal of Pharmaceutical Sciences,* 11**,** 404-416.

SHEIKHOLESLAMI, Z. S., SALIMI-KENARI, H., IMANI, M., ATAI, M. & NODEHI, A. 2017. Exploring the effect of formulation parameters on the particle size of carboxymethyl chitosan nanoparticles prepared via reverse micellar crosslinking. *J Microencapsul,* 34**,** 270-279.

SHEN, P., YUE, Y., SUN, Q., KASIREDDY, N., KIM, K. H. & PARK, Y. 2017. Piceatannol extends the lifespan of Caenorhabditis elegans via DAF-16. *Biofactors*.

SHEPHERD, C., GIACOMIN, P., NAVARRO, S., MILLER, C., LOUKAS, A. & WANGCHUK, P. 2018. A medicinal plant compound, capnoidine, prevents the onset of inflammation in a mouse model of colitis. *J Ethnopharmacol,* 211**,** 17-28.

SHI, J., KANTOFF, P. W., WOOSTER, R. & FAROKHZAD, O. C. 2017. Cancer nanomedicine: progress, challenges and opportunities. *Nat Rev Cancer,* 17**,** 20-37.

SHIH, R.-H., WANG, C.-Y. & YANG, C.-M. 2015. NF-kappaB Signaling Pathways in Neurological Inflammation: A Mini Review. *Frontiers in Molecular Neuroscience,* 8**,** 77.

SIEGEL, R. L., MILLER, K. D., FEDEWA, S. A., AHNEN, D. J., MEESTER, R. G. S., BARZI, A. & JEMAL, A. 2017. Colorectal cancer statistics, 2017. *CA: a cancer journal for clinicians,* 67**,** 177-193.

SINGH, P., ANANTHAKRISHNAN, A. & AHUJA, V. 2017a. Pivot to Asia: inflammatory bowel disease burden. *Intestinal research,* 15**,** 138-141.

SINGH, P., KIM, Y. J., SINGH, H., AHN, S., CASTRO-ACEITUNO, V. & YANG, D. C. 2017b. In situ preparation of water-soluble ginsenoside Rh2-entrapped bovine serum albumin nanoparticles: in vitro cytocompatibility studies. *International Journal of Nanomedicine,* 12**,** 4073.

SINGH, P., KIM, Y. J., SINGH, H., AHN, S., CASTRO-ACEITUNO, V. & YANG, D. C. 2017c. In situ preparation of water-soluble ginsenoside Rh2-entrapped bovine serum albumin nanoparticles: in vitro cytocompatibility studies. *International Journal of Nanomedicine,* 12**,** 4073-4084.

SINGH, P., KUMAR, S. & BAST, F. 2017d. Natural Compounds Are Smart Players in Context to Anticancer Potential of Receptor Tyrosine Kinases: An In Silico and In Vitro Advancement. *Translational Bioinformatics and Its Application.* Springer.

SINGH, R. & LILLARD, J. W. 2009. Nanoparticle-based targeted drug delivery. *Experimental and molecular pathology,* 86**,** 215-223.

SONG, H., JUNG, J. I., CHO, H. J., HER, S., KWON, S.-H., YU, R., KANG, Y.-H., LEE, K. W. & PARK, J. H. Y. 2015. Inhibition of tumor progression by oral piceatannol in mouse 4T1 mammary cancer is associated with decreased angiogenesis and macrophage infiltration. *The Journal of Nutritional Biochemistry,* 26**,** 1368-1378.

SOPPIMATH, K. S., AMINABHAVI, T. M., KULKARNI, A. R. & RUDZINSKI, W. E. 2001. Biodegradable polymeric nanoparticles as drug delivery devices. *Journal of Controlled Release,* 70**,** 1-20.

SREEDHAR, R., ARUMUGAM, S., THANDAVARAYAN, R. A., KARUPPAGOUNDER, V. & WATANABE, K. 2016. Curcumin as a therapeutic agent in the chemoprevention of inflammatory bowel disease. *Drug Discov Today,* 21**,** 843-849.

STAFF, N. P., GRISOLD, A., GRISOLD, W. & WINDEBANK, A. J. 2017. Chemotherapy-Induced Peripheral Neuropathy: A Current Review. *Annals of Neurology*.

STANIĆ, Z. 2017. Curcumin, a Compound from Natural Sources, a True Scientific Challenge – A Review. *Plant Foods for Human Nutrition,* 72**,** 1-12.

STROBER, W., FUSS, I. & MANNON, P. 2007. The fundamental basis of inflammatory bowel disease. *Journal of Clinical Investigation,* 117**,** 514-521.

SUBRAMANIAN, S., EKBOM, A. & RHODES, J. M. 2017. Recent advances in clinical practice: a systematic review of isolated colonic Crohn's disease: the third IBD? *Gut,* 66**,** 362-381.

SULLIVAN, K. J., WEI, M., CHERNETSOVA, E., HALLANI, S., DE NANASSY, J., BENCHIMOL, E. I., MACK, D. R., NASR, A. & EL DEMELLAWY, D. 2017. Value of upper endoscopic biopsies in predicting medical refractoriness in pediatric patients with ulcerative colitis. *Human Pathology*.

SUTHERLAND, L. R., MARTIN, F., GREER, S., ROBINSON, M., GREENBERGER, N., SAIBIL, F., MARTIN, T., SPARR, J., PROKIPCHUK, E. & BORGEN, L. 1987. 5-Aminosalicylic acid enema in the treatment of distal ulcerative colitis, proctosigmoiditis, and proctitis. *Gastroenterology,* 92**,** 1894-8.

SYNNESTVEDT, K., FURUTA, G. T., COMERFORD, K. M., LOUIS, N., KARHAUSEN, J., ELTZSCHIG, H. K., HANSEN, K. R., THOMPSON, L. F. & COLGAN, S. P. 2002. Ecto-5'-nucleotidase (CD73) regulation by hypoxia-inducible factor-1 mediates permeability changes in intestinal epithelia. *J Clin Invest,* 110**,** 993-1002.

TAGHIPOUR, N., MOLAEI, M., MOSAFFA, N., ROSTAMI-NEJAD, M., ASADZADEH AGHDAEI, H., ANISSIAN, A., AZIMZADEH, P. & ZALI, M. R. 2016. An experimental model of colitis induced by dextran sulfate sodium from acute progresses to chronicity in C57BL/6: correlation between conditions of mice and the environment. *Gastroenterology and Hepatology from bed to bench,* 9**,** 45-52.

TAK, P. P. & FIRESTEIN, G. S. 2001. NF-kappaB: a key role in inflammatory diseases. *J Clin Invest,* 107**,** 7-11.

TAMBUWALA, M. M. 2016. Natural Nuclear Factor Kappa Beta Inhibitors: Safe Therapeutic Options for Inflammatory Bowel Disease. *Inflamm Bowel Dis,* 22**,** 719-23.

TAMBUWALA, M. M., CUMMINS, E. P., LENIHAN, C. R., KISS, J., STAUCH, M., SCHOLZ, C. C., FRAISL, P., LASITSCHKA, F., MOLLENHAUER, M., SAUNDERS, S. P., MAXWELL, P. H., CARMELIET, P., FALLON, P. G., SCHNEIDER, M. & TAYLOR, C. T. 2010. Loss of prolyl hydroxylase-1 protects against colitis through reduced epithelial cell apoptosis and increased barrier function. *Gastroenterology,* 139**,** 2093-101.

TAMBUWALA, M. M., MANRESA, M. C., CUMMINS, E. P., AVERSA, V., COULTER, I. S. & TAYLOR, C. T. 2015. Targeted delivery of the hydroxylase inhibitor DMOG provides enhanced efficacy with reduced systemic exposure in a murine model of colitis. *J Control Release,* 217**,** 221-7.

TAMMALI, R., SAXENA, A., SRIVASTAVA, S. K. & RAMANA, K. V. 2011. Aldose Reductase Inhibition Prevents Hypoxia-induced Increase in Hypoxia-inducible Factor-1α (HIF-1α) and Vascular Endothelial Growth Factor (VEGF) by Regulating 26 S Proteasome-mediated Protein Degradation in Human Colon Cancer Cells. *J Biol Chem,* 286**,** 24089-24100.

TAN, M. C., EL-SERAG, H. B. & HOU, J. K. 2017a. Determinants of Healthcare Utilization Among Veterans with Inflammatory Bowel Disease. *Dig Dis Sci,* 62**,** 607-614.

TAN, Z., HUANG, Q., ZANG, J., TENG, S.-F., CHEN, T.-R., WEI, H.-F., SONG, D.-W., LIU, T.-L., YANG, X.-H., FU, C.-G., HU, Z.-Q., ZHOU, W., YAN,

W.-J. & XIAO, J.-R. 2017b. HIF-1α activates hypoxia-induced BCL-9 expression in human colorectal cancer cells. *Oncotarget,* 8**,** 25885-25896.

TANAKA, T., KOHNO, H., SUZUKI, R., HATA, K., SUGIE, S., NIHO, N., SAKANO, K., TAKAHASHI, M. & WAKABAYASHI, K. 2006. Dextran sodium sulfate strongly promotes colorectal carcinogenesis in Apc(Min/+) mice: inflammatory stimuli by dextran sodium sulfate results in development of multiple colonic neoplasms. *Int J Cancer,* 118**,** 25-34.

TANG, Y. L. & CHAN, S. W. 2014. A review of the pharmacological effects of piceatannol on cardiovascular diseases. *Phytother Res,* 28**,** 1581-8.

TARGAN, S. R. 2006. Current limitations of IBD treatment: where do we go from here? *Ann N Y Acad Sci,* 1072**,** 1-8.

TARHINI, M., GREIGE-GERGES, H. & ELAISSARI, A. 2017. Protein-based nanoparticles: From preparation to encapsulation of active molecules. *International Journal of Pharmaceutics,* 522**,** 172-197.

TARIQ, K. & GHIAS, K. 2016. Colorectal cancer carcinogenesis: a review of mechanisms. *Cancer Biol Med,* 13**,** 120-35.

TAYLOR, C. T. & COLGAN, S. P. 2007. Hypoxia and gastrointestinal disease. *J Mol Med,* 85**,** 1295-300.

TAYLOR, C. T. & CUMMINS, E. P. 2009. The role of NF-kappaB in hypoxia-induced gene expression. *Ann N Y Acad Sci*.

TAYLOR, K. & GIBSON, P. R. 2017. Conventional Therapy of Ulcerative Colitis: Corticosteroids. *Crohn's Disease and Ulcerative Colitis.* Springer.

TAYLOR, R. A. & LEONARD, M. C. 2011. Curcumin for inflammatory bowel disease: a review of human studies. *Altern Med Rev,* 16**,** 152-6.

TE, H. S., SCHIANO, T. D., KUAN, S. F., HANAUER, S. B., CONJEEVARAM, H. S. & BAKER, A. L. 2000. Hepatic effects of long-term methotrexate use in the treatment of inflammatory bowel disease. *Am J Gastroenterol,* 95**,** 3150-6.

TOLBA, M. F., OMAR, H. A., AZAB, S. S., KHALIFA, A. E., ABDEL-NAIM, A. B. & ABDEL-RAHMAN, S. Z. 2016a. Caffeic Acid Phenethyl Ester: A Review of Its Antioxidant Activity, Protective Effects against Ischemia-reperfusion Injury and Drug Adverse Reactions. *Crit Rev Food Sci Nutr,* 56**,** 2183-90.

TOLBA, M. F., OMAR, H. A., AZAB, S. S., KHALIFA, A. E., ABDEL-NAIM, A. B. & ABDEL-RAHMAN, S. Z. 2016b. Caffeic acid phenethyl ester: a review of its antioxidant activity, protective effects against ischemia-reperfusion injury and drug adverse reactions. *Critical reviews in food science and nutrition,* 56**,** 2183-2190.

TORRICE, M. 2016. Does Nanomedicine Have a Delivery Problem? *ACS Central Science,* 2**,** 434-437.

TOSI, F., MAGNI, E., AMATU, A., MAURI, G., BENCARDINO, K., TRUINI, M., VERONESE, S., DE CARLIS, L., FERRARI, G., NICHELATTI, M., SARTORE-BIANCHI, A. & SIENA, S. 2017. Effect of KRAS and BRAF Mutations on Survival of Metastatic Colorectal Cancer After Liver Resection: A Systematic Review and Meta-Analysis. *Clinical Colorectal Cancer,* 16**,** e153-e163.

TOYODA, T., TSUKAMOTO, T., TAKASU, S., SHI, L., HIRANO, N., BAN, H., KUMAGAI, T. & TATEMATSU, M. 2009. Anti-inflammatory effects of caffeic acid phenethyl ester (CAPE), a nuclear factor-κB inhibitor, on

Helicobacter pylori-induced gastritis in Mongolian gerbils. *International journal of cancer,* 125**,** 1786-1795.

TRIANTAFILLIDIS, J. K., NASIOULAS, G. & KOSMIDIS, P. A. 2009. Colorectal cancer and inflammatory bowel disease: epidemiology, risk factors, mechanisms of carcinogenesis and prevention strategies. *Anticancer Res,* 29**,** 2727-37.

TURNER, N. D. & LLOYD, S. K. 2017. Association between red meat consumption and colon cancer: A systematic review of experimental results. *Experimental Biology and Medicine,* 242**,** 813-839.

VAN ASSCHE, G., D'HAENS, G., NOMAN, M., VERMEIRE, S., HIELE, M., ASNONG, K., ARTS, J., D'HOORE, A., PENNINCKX, F. & RUTGEERTS, P. 2003. Randomized, double-blind comparison of 4 mg/kg versus 2 mg/kg intravenous cyclosporine in severe ulcerative colitis. *Gastroenterology,* 125**,** 1025-31.

VAN STAA, T. P., TRAVIS, S., LEUFKENS, H. G. & LOGAN, R. F. 2004. 5-aminosalicylic acids and the risk of renal disease: a large British epidemiologic study. *Gastroenterology,* 126**,** 1733-9.

VÁRADI, J., HARAZIN, A., FENYVESI, F., RÉTI-NAGY, K., GOGOLÁK, P., VÁMOSI, G., BÁCSKAY, I., FEHÉR, P., UJHELYI, Z. & VASVÁRI, G. 2017. Alpha-Melanocyte Stimulating Hormone Protects against Cytokine-Induced Barrier Damage in Caco-2 Intestinal Epithelial Monolayers. *PLoS One,* 12**,** e0170537.

VERGNOLLE, N. 2016. Protease inhibition as new therapeutic strategy for GI diseases. *Gut,* 65**,** 1215-1224.

VEZZA, T., RODRÍGUEZ-NOGALES, A., ALGIERI, F., UTRILLA, M. P., RODRIGUEZ-CABEZAS, M. E. & GALVEZ, J. 2016. Flavonoids in Inflammatory Bowel Disease: A Review. *Nutrients,* 8**,** 211.

VIENNOIS, E., CHEN, F. & MERLIN, D. 2013. NF-κB pathway in colitis-associated cancers. *Translational gastrointestinal cancer,* 2**,** 21-29.

VOBORIL, R. & WEBEROVA-VOBORILOVA, J. 2006. Constitutive NF-kappaB activity in colorectal cancer cells: impact on radiation-induced NF-kappaB activity, radiosensitivity, and apoptosis. *Neoplasma,* 53**,** 518-23.

WALLIS, C. J. D., MAHAR, A. L., CHOO, R., HERSCHORN, S., KODAMA, R. T., SHAH, P. S., DANJOUX, C., NAROD, S. A. & NAM, R. K. 2016. Second malignancies after radiotherapy for prostate cancer: systematic review and meta-analysis. *BMJ : British Medical Journal,* 352**,** i851.

WANG, L., HUANG, J., CHEN, H., WU, H., XU, Y., LI, Y., YI, H., WANG, Y. A., YANG, L. & MAO, H. 2017. Exerting Enhanced Permeability and Retention Effect Driven Delivery by Ultrafine Iron Oxide Nanoparticles with T1-T2 Switchable Magnetic Resonance Imaging Contrast. *ACS Nano,* 11**,** 4582-4592.

WANG, L. C., CHU, K. H., LIANG, Y. C., LIN, Y. L. & CHIANG, B. L. 2010a. Caffeic acid phenethyl ester inhibits nuclear factor-kappaB and protein kinase B signalling pathways and induces caspase-3 expression in primary human CD4+ T cells. *Clin Exp Immunol,* 160**,** 223-32.

WANG, L. C., CHU, K. H., LIANG, Y. C., LIN, Y. L. & CHIANG, B. L. 2010b. Caffeic acid phenethyl ester inhibits nuclear factor-κB and protein kinase B signalling pathways and induces caspase-3 expression in primary human CD4(+) T cells. *Clinical and Experimental Immunology,* 160**,** 223-232.

WANG, S., SU, R., NIE, S., SUN, M., ZHANG, J., WU, D. & MOUSTAID-MOUSSA, N. 2014. Application of nanotechnology in improving bioavailability and bioactivity of diet-derived phytochemicals. *The Journal of Nutritional Biochemistry,* 25**,** 363-376.

WATKINS, R., WU, L., ZHANG, C., DAVIS, R. M. & XU, B. 2015a. Natural product-based nanomedicine: recent advances and issues. *Int J Nanomedicine,* 10**,** 6055-74.

WATKINS, R., WU, L., ZHANG, C., DAVIS, R. M. & XU, B. 2015b. Natural product-based nanomedicine: recent advances and issues. *International Journal of Nanomedicine,* 10**,** 6055-6074.

WEBER, C. K., LIPTAY, S., WIRTH, T., ADLER, G. & SCHMID, R. M. 2000. Suppression of NF-kappaB activity by sulfasalazine is mediated by direct inhibition of IkappaB kinases alpha and beta. *Gastroenterology,* 119**,** 1209-18.

WEI, J. & FENG, J. 2010. Signaling pathways associated with inflammatory bowel disease. *Recent Pat Inflamm Allergy Drug Discov,* 4**,** 105-17.

WILSON, M. R., BERGMAN, A., CHEVROU-SEVERAC, H., SELBY, R., SMYTH, M. & KERRIGAN, M. C. 2017. Cost-effectiveness of vedolizumab compared with infliximab, adalimumab, and golimumab in patients with ulcerative colitis in the United Kingdom. *The European Journal of Health Economics*.

WILSON, W. R. & HAY, M. P. 2011. Targeting hypoxia in cancer therapy. *Nat Rev Cancer,* 11**,** 393-410.

WIRTZ, S., NEUFERT, C., WEIGMANN, B. & NEURATH, M. F. 2007. Chemically induced mouse models of intestinal inflammation. *Nat Protoc,* 2**,** 541-6.

WLODARSKA, M., KOSTIC, ALEKSANDAR D. & XAVIER, RAMNIK J. 2015. An Integrative View of Microbiome-Host Interactions in Inflammatory Bowel Diseases. *Cell Host Microbe,* 17**,** 577-591.

XAVIER, R. J. & PODOLSKY, D. K. 2007a. Unravelling the pathogenesis of inflammatory bowel disease. *Nature,* 448**,** 427-434.

XAVIER, R. J. & PODOLSKY, D. K. 2007b. Unravelling the pathogenesis of inflammatory bowel disease. *Nature,* 448**,** 427-34.

XIAO, B., XU, Z., VIENNOIS, E., ZHANG, Y., ZHANG, Z., ZHANG, M., HAN, M. K., KANG, Y. & MERLIN, D. 2017. Orally Targeted Delivery of Tripeptide KPV via Hyaluronic Acid-Functionalized Nanoparticles Efficiently Alleviates Ulcerative Colitis. *Molecular Therapy,* 25**,** 1628-1640.

XIAO, Z., MORRIS-NATSCHKE, S. L. & LEE, K. H. 2016. Strategies for the Optimization of Natural Leads to Anticancer Drugs or Drug Candidates. *Med Res Rev,* 36**,** 32-91.

YALLAPU, M. M., GUPTA, B. K., JAGGI, M. & CHAUHAN, S. C. 2010. Fabrication of curcumin encapsulated PLGA nanoparticles for improved therapeutic effects in metastatic cancer cells. *J Colloid Interface Sci,* 351**,** 19-29.

YAMAMOTO, Y. & GAYNOR, R. B. 2001. Therapeutic potential of inhibition of the NF-κB pathway in the treatment of inflammation and cancer. *Journal of Clinical Investigation,* 107**,** 135-142.

YAMEEN, B., CHOI, W. I., VILOS, C., SWAMI, A., SHI, J. & FAROKHZAD, O. C. 2014. Insight into nanoparticle cellular uptake and intracellular targeting.

Journal of controlled release : official journal of the Controlled Release Society, 190**,** 485-499.

YAN, Y., KOLACHALA, V., DALMASSO, G., NGUYEN, H., LAROUI, H., SITARAMAN, S. V. & MERLIN, D. 2009. Temporal and spatial analysis of clinical and molecular parameters in dextran sodium sulfate induced colitis. *PLoS One,* 4**,** 0006073.

YANG, N., SHI, J.-J., WU, F.-P., LI, M., ZHANG, X., LI, Y.-P., ZHAI, S., JIA, X.-L. & DANG, S.-S. 2017. Caffeic acid phenethyl ester up-regulates antioxidant levels in hepatic stellate cell line T6 via an Nrf2-mediated mitogen activated protein kinases pathway. *World Journal of Gastroenterology,* 23**,** 1203-1214.

YEUNG, T. M., GANDHI, S. C., WILDING, J. L., MUSCHEL, R. & BODMER, W. F. 2010. Cancer stem cells from colorectal cancer-derived cell lines. *Proc Natl Acad Sci U S A,* 107**,** 3722-3727.

YUEN, H. F., GUNASEKHARAN, V. K., CHAN, K. K., ZHANG, S. D., PLATT-HIGGINS, A., GATELY, K., O'BYRNE, K., FENNELL, D. A., JOHNSTON, P. G., RUDLAND, P. S. & EL-TANANI, M. 2013. RanGTPase: a candidate for Myc-mediated cancer progression. *J Natl Cancer Inst,* 105**,** 475-88.

YUM, S., JEONG, S., LEE, S., NAM, J., KIM, W., YOO, J.-W., KIM, M.-S., LEE, B. L. & JUNG, Y. 2015. Colon-targeted delivery of piceatannol enhances anti-colitic effects of the natural product: potential molecular mechanisms for therapeutic enhancement. *Drug Design, Development and Therapy,* 9**,** 4247-4258.

ZAMAN, M., AHMAD, E., QADEER, A., RABBANI, G. & KHAN, R. H. 2014. Nanoparticles in relation to peptide and protein aggregation. *International Journal of Nanomedicine,* 9**,** 899-912.

ZAPH, C., TROY, A. E., TAYLOR, B. C., BERMAN-BOOTY, L. D., GUILD, K. J., DU, Y., YOST, E. A., GRUBER, A. D., MAY, M. J., GRETEN, F. R., ECKMANN, L., KARIN, M. & ARTIS, D. 2007. Epithelial-cell-intrinsic IKK-beta expression regulates intestinal immune homeostasis. *Nature,* 446**,** 552-6.

ZEITOUNI, N. E., CHOTIKATUM, S., VON KÖCKRITZ-BLICKWEDE, M. & NAIM, H. Y. 2016. The impact of hypoxia on intestinal epithelial cell functions: consequences for invasion by bacterial pathogens. *Molecular and Cellular Pediatrics,* 3**,** 14.

ZENG, M. Y., INOHARA, N. & NUNEZ, G. 2017. Mechanisms of inflammation-driven bacterial dysbiosis in the gut. *Mucosal Immunol,* 10**,** 18-26.

ZHANG, H., JIA, R., WANG, C., HU, T. & WANG, F. 2014. Piceatannol promotes apoptosis via up-regulation of microRNA-129 expression in colorectal cancer cell lines. *Biochem Biophys Res Commun,* 452**,** 775-781.

ZHANG, H. & SUN, S.-C. 2015. NF-κB in inflammation and renal diseases. *Cell & Bioscience,* 5**,** 63.

ZHANG, Y.-Z. & LI, Y.-Y. 2014. Inflammatory bowel disease: Pathogenesis. *World Journal of Gastroenterology : WJG,* 20**,** 91-99.

ZHAO, P., YIN, W., WU, A., TANG, Y., WANG, J., PAN, Z., LIN, T., ZHANG, M., CHEN, B. & DUAN, Y. 2017. Dual-Targeting to Cancer Cells and M2 Macrophages via Biomimetic Delivery of Mannosylated Albumin Nanoparticles for Drug-Resistant Cancer Therapy. *Advanced Functional Materials*.

ZIELLO, J. E., JOVIN, I. S. & HUANG, Y. 2007. Hypoxia-Inducible Factor (HIF)-1 Regulatory Pathway and its Potential for Therapeutic Intervention in Malignancy and Ischemia. *The Yale Journal of Biology and Medicine,* 80**,** 51-60.

Appendix

Formulation of cur-loaded PLGA NP and evaluation of anti-cancer activity using breast and lung cancer cell line model

1.1 Introduction

Curcumin is a well-known anticancer agent found in the rhizomes of the perennial herb *Curcuma longa*. It has a long history of use in traditional medicine, covering a broad spectrum of conditions, from various cancer, diabetes, inflammation and Alzheimer's disease (Naksuriya et al., 2014., Prasad et al., 2014). The FDA has endorsed its status as a safe home-based remedy. In more structured and rigorous evaluations, comprising of more than 65 clinical trials, benefit from life-threatening diseases has been demonstrated (Yallapu et al., 2013). In relation to inflammatory and cancerous disorders, therapeutic action are attributed to its ability via modulation of nuclear factor kappa-beta (NF-kβ) transcriptional factor (Thangapazham et al., 2013., Tambuwala, 2016) and hypoxia inducible factor (HIF) (Birner et al., 2000., Bae et al., 2006). Moreover, an elevated level of HIF-1α and NF-kβ has been documented in human colitis (Ma et al., 2016).

Free curcumin and curcumin nanoparticles have been reported to be of therapeutic value in almost all cancer types (Bisht et al., 2007a., Xing et al., 2014., Kamble et al., 2016., Bondi et al., 2017) . However, the molecular mechanism of action involved in the treatment of cancer under pathophysiological hypoxic tumour microenvironment is not clearly understood. This could be one of the major factors limiting the clinical use of curcumin as cancer therapeutic.

The over activation NF-kβ and HIF pathways, due to hypoxic tumour microenvironment, have been reported extensively in almost cancers (Redell and Tweardy, 2005., Tafani et al., 2013). This hypoxic micro-environment has been blamed for metabolic adaption of cancer cells which result in tumour development, progression and reduced effectiveness of cancer therapeutics (Eales et al., 2016).

Among all cancer types, breast cancer has been reported as the major cause of death among elderly women in Europe and the United States (Chakravarty et al.) (Malvezzi et al., 2016). Paclitaxel, 5-fluorouracil, cyclosporine, doxorubicin are most commonly prescribed as treatment options for breast and lung cancer (Gladkov et al., 2015., Del Mastro et al., 2016., Zhong et al., 2016). However, these conventional chemo-therapeutics result in serious side-effects, such as constipation, nausea, alopecia, neuronal damage, bone marrow depletion and heart failure (Lancellotti et al., 2015., Hanai et al., 2016). Similarly, lung cancer is reported as the major cause of cancer-related death in males from developing countries, which contributes approximately 18.2% of the total cancer death statistic (Ridge et al., 2013). Furthermore, tiredness, skin reaction, loss of appetite, neurotoxicity and hair loss are some of the general side effects associated with conventional therapeutics (Landesman-Milo et al., 2015). Patients suffering from breast and lung cancers usually have to undergo surgery and radiation-based treatments in addition to chemotherapy. Furthermore, these therapies are not site-specific and cause extensive damage to healthy tissue (Pouw et al., 2015). In addition, these interventions interfere with the menopause and fertility (Recio-Saucedo et al., 2016). Hence, there is a pressing need to develop safer and effective alternatives for treatment of cancer.

The therapeutic value of curcumin in the treatment of breast and lung cancer have been reported, in *in-vitro*, *in-vivo* and clinical studies (Coleman et al., 2015., Kang et al., 2015). However, these findings highlight solubility issue of curcumin, which results in low systemic bioavailability, poor pharmacokinetic profile and sub-optimal delivery to the target cells (Ireson et al., 2001., Ireson et al., 2002). Thus the first objective of the present work was to use pharmaceutical technology to formulate a drug delivery system for curcumin with improved solubility and intra-cellular

delivery properties. Nano-encapsulation of drugs in PLGA matrices has been reported to enhance therapeutic efficacy/targeting capabilities (Danhier et al., 2012), protect from degradation (Kumari et al., 2010b) and improve aqueous solubility of poorly water-soluble drugs (Zhong et al., 2016., Brigger et al., 2002., Haggag and Faheem, 2015). Since curcumin is practically insoluble in water, it makes an ideal model drug candidate for current investigation (Yallapu et al., 2010). Nano-encapsulation is also known to enhance cellular permeability and retention effects, which are proposed as mechanisms to target and enhance drug accumulation in solid tumour masses (Reddy, 2005). Since hypoxia plays a critical role in tumour development and progression, the primary objective of the work was to investigate the molecular mechanism of action of free curcumin and nano-encapsulated curcumin towards the expression of the two master transcriptional regulators HIF-1α and p65 (Rel A), which are known to be expressed in response to hypoxia and are positively associated with almost all cancers (Vaughan et al., 1966., Weichert et al., 2007).

It is hypothesize that nano-encapsulation of curcumin will enhance its solubility and facilitate intra-cellular delivery of the drug resulting in improved bioavailability and anticancer activity via modulation of the over activated NF-kβ and HIF pathways in lung and breast cancer cells under hypoxic condition. Thus, resulting in stabilization of a tumour and preventing the further development of cancer. In this study, solvent evaporation method was employed, using sonication to homogenize the emulsion phases, and poly (vinyl alcohol) (PVA) to stabilize and control particle size (Sahoo et al., 2002). Optimisations of PLGA and PVA content were carried out to select optimum settings during the formulation of curcumin-loaded PLGA NP (cur-PLGA-NP). The nanoparticle formulation exhibiting superior cellular uptake, retention and

in-vitro release was selected for further assessment of anticancer and anti-metastatic activity of curcumin in the highly metastatic breast (MDA-MB231) and lung cancer (A549) cell lines.

1.2 Summary

Therefore, due to seriousness and side effects linked with current treatment in lung and breast cancer, there is compelling need to formulate nanoparticles of the natural compound and study the pathways involved in lung and breast cancer. Therapeutic potential of curcumins has been documented by researchers. It has low solubility in aqueous media which can be improved by nanotechnology. Encapsulation of curcumin with PLGA will protect it from stomach degradation and will offer control release. As curcumin also modulates transcription factors, therefore, it will also assist to study pathways involved in tumour development.

1.3 Hypothesis

In the current chapter, we hypothesize that reduction of particle size of the natural compound will improve the anticancer property of curcumin at a higher extent than free curcumin.

1.4 Aims and objectives

- Formulation of Cur- loaded PLGA nanoparticles
- Optimisation of Cur- loaded PLGA nanoparticles

- Evaluation of anticancer properties of Cur- loaded PLGA nanoparticles

in MDA-MB-231 and A549

2 Result

2.1 Calibration curve

Calibration curve of PIC was plotted in methanol (1:9) and absorbance was measured at 430 nm.

2.2 Effect of PLGA concentration

Three different batches nanoparticles were formulated by solvent evaporation techniques as described in section 2.2 with different amount of PLGA and an equal amount of curcumin. The effect of an increase in the mass of polymer on physicochemical properties of cur-PLGA-NP is shown in Figure 2. It was found that particle size increased significantly from 265 nm to 606 nm ($P<0.001$) as the quantity of PLGA increased (Figure 2A). This increase in size is due to increase in the viscosity of polymer solution and formation of larger disperses droplets (Cui et al., 2005., Haggag et al., 2016b). It was also observed that increasing the amount of polymer increased the zeta potential significantly from –13.7 mV (F1) to -3.1 mV (Figure 2B; $P<0.01$). This is due to the accumulation of ionised carboxylic groups on the nanoparticles as result of increasing amount the polymer. Entrapment efficiency increased significantly, as the ratio of PLGA increased (Figure 2C). Similar results were reported by (Derman, 2015), along with others, proposes that the increase in PLGA in the organic phase increases the viscosity in this phase and slows unwanted diffusivity to the water phase (Cun et al., 2010).

2.3 Effect of surfactant concentration

The amount of surfactant plays an important role in stabilization of emulsion and prevents the coalescence by lowering the free energy at the interface of nanodroplets (Kwon et al., 2001). Insufficient amount of emulsifier may cause aggregation of nanoparticles. Particle size significantly ($P<0.001$) increases from 308 nm to 721 nm as the PVA concentration increases to 3.5% as illustrated in the Figure 3A. A similar finding was also reported by (Kwon et al., 2001). However, zeta potential fluctuates as the PVA concentration increase as shown in Figure 3 (graph B). Figure 3 (graph C) depicts that increases in PVA concentration lead to increase in entrapment efficiency significantly ($P<0.001$). It increases from 73% to 89% with an increase in PVA concentration. Increase concentration of PVA may be responsible for increase viscosity of aqueous phase which results in higher entrapment efficiency and larger particle size. A similar finding was documented by (Song et al., 2008).

The initial burst release was reported around 32%, 20% and 18% for 1.5 %, 2.5% and 3.5% batches respectively (graph D). The percentage release for batches formulated with 1.5%, 2.5% and 3.5% was found to be 89%, 80%and 75% respectively after 168 hours. Therefore, increase in the concentration of PVA may slow down the diffusion of the drug. It has been also documented by (Sahoo et al., 2002) where increase concentration of PVA affect diffusion of the drug from nanoparticles.

2.4 Effect of drug concentration

The physicochemical properties such as particle size, zeta potential, entrapment efficiency and *in-vitro* release studies of cur-PLGA-NP were evaluated as shown

Figure 4. The average particle size of nanoparticles fabricated with 25 mg, 50 mg and 75 mg of curcumin was found to be 233 nm 292 nm and 510 nm, respectively as visible in the Figure 4A. This increase in particle size may be due to increase in the curcumin concentration which increases the size of nanodroplets in the emulsion (Krishnamachari et al., 2007). Cur-PLGA-NP in the graph 4B shows negative zeta potential (-6mV, -13mV and -7mV) due to the ionized terminal carboxylic groups of PLGA present on the surface of the nanoparticles. Entrapment efficiency of batches containing 25 mg and 50 mg (4C) were found to be 64% and 78%, respectively. The initial burst release was found to be around 25%, 14% and 13% for batch formulated with 25 mg, 50 mg and 75 mg of curcumin, respectively (graph D). The percentage release for batches formulated with 25 mg, 50 mg and 75 mg of curcumin was found to be 88%, 86%and 81% respectively after 168 hours. Therefore, increase in drug amount decreases the release of the drug due to increase in viscosity of drug solution.

2.5 NMR spectra of cur-PLGA-NP

The H NMR study of cur-PLGA-NP was performed as per section 2.5. The 1H NMR spectrum of curcumin revealed the signals due to six aromatic protons [7.13 ppm (d, 2H, J = 8.1 Hz, B), 7.04 ppm (s, 2H, C) and 6.93 ppm (d, 2H, J = 8.1 Hz, D)], a trans trans double bond [7.58 ppm (d, 2H, J = 16 Hz, A) and 6.47 ppm (d, 2H, J = 16 Hz, E)], one methylene group [around 5.8 ppm (s, 2H, F)] and methoxy group [3.94 ppm (s, 6H, OCH3]. These data confirmed the structure of curcumin in nanoparticles as shown in Figure 5.

2.6 Solubility of cur-PLGA-NP and free curcumin

The solubility of cur-PLGA-NP and free curcumin was determined by the method given in section 2.9. The apparent water solubility of curcumin in both free and nano-encapsulated form was determined by UV- spectroscopy at 430 nm. The vials in Figure 6AI give a visual representation of the enhanced solubility of curcumin when formulated as cur-PLGA-NP vs free curcumin in water. It is evident that cur-PLGA-NP produce a uniform dispersion, whereas free curcumin (6AII) was sparingly soluble in water. The solubility of free curcumin was found to be 0.3446µg/ml, whereas that of cur-PLGA-NP was 3.5128µg/ml. These results indicate an approximate ten-fold increase in aqueous solubility of cur-PLGA-NP as compared to free curcumin.

2.7 Scanning Electron Microscopy

The sample for SEM was prepared by the method mentioned in the section 2.10. Figure 7 shows SEM images of F1, F2, and F3 formulated with 30 mg, 60 mg and 90 mg of polymer with equal amounts of curcumin and PVA. F1 exhibited a monodisperse appearance, with the smallest particle size. SEM images of cur-PLGA-NP suggest that an increase in the polymer (PLGA) concentration not only leads to an increase in particle size but also results in non-spherical particles. Thus, batch F1 batch was selected for intracellular delivery due to smaller size (De Jong and Borm, 2008).

2.8 Cellular uptake of cur-PLGA-NP

The MDA-MB231 and A549 cell were incubated with cur-PLGA-NP as described in the section 2.12. The nuclei of MDA-MB231 and A549 cells were stained with DAPI and Nile red-tagged cur-PLGA-NP were observed under fluorescent microscopy as shown in Figure 8. Cellular uptake of cur-PLGA-NP labelled with Nile red, in MDA-MB231 and A549 cells were visualized by overlaying images obtained by fluorescent microscopy. Nile red-coated cur-PLGA-NP can be seen within the MDA-MB231 and A549 cells as depicted in the Figure 8A and 8B. Cur-PLGA-NP in MDA- The result indicates that formulation F1 NP facilitates cellular uptake of curcumin, which could result in enhanced therapeutic activity as compared vto free curcumin.

2.9 In-vitro cytotoxicity assay

The cytotoxicity study was performed as described in the section 2.13. The cytotoxic action of cur-PLGA-NP on the MDA-MB-231 Figure (9 A) and A549 (9B) cell lines was evaluated by MTT assay after 24, 48, 72 and 96 hours of treatment at 3.68 µg/ml, 7.36 µg/ml and 11.05 µg/ml of cur-PLGA-NP and an equivalent amount of free curcumin. The results showed that blank NP had no cytotoxicity on breast and lung cancer cells within the concentrations used. Free curcumin and cur-PLGA-NP showed a dose response cytotoxic effect. Free curcumin exhibited its cytotoxic action during the first 24 hours in both cell lines. The cell viability started to increase after the first day due to the diminished cytotoxic action of the free drug. The MDA-MB-231 and A549 cell viability decreased to approximately 60% after 96 h treatment with 11.05 µg/ml of free curcumin. Cur-PLGA-NP reduced cell viability

and sustained cytotoxic action was achieved up to four days after treatment Based on the values depicted in the graph A and B, it is clear that cur-PLGA-NP showed significantly higher cytotoxic action and lower cell viability in both cell lines. Cur-PLGA-NP sustained the cytotoxic action of the free drug due to the enhanced penetration and retention effect inside the cancer cells (Patil et al., 2009., Chavanpatil et al., 2006) also due to improving its solubility, and bioavailability (Mittal et al., 2007., Anand et al., 2010). The achieved lower cell viability and greater cytotoxicity compared to free curcumin was clear after 96 hours of treatment.

2.10 Migration assay

The migration study was carried out in MDA-MB-231 and A549 as stated in the section 2.14. A scratch assay was conducted on both cell lines in this work to investigate doses response of free curcumin and cur-PLGA-NP on the migration capability of MDA-MB-231 (Figure 10A) and A549 (Figure 10B) cells. Migration of cancer cells from the primary tumour site to other sites is a predominant feature of metastatic breast and lung cancer cells (Palmer et al., 2011). Figure 10 shows the graphical quantification of the degree of wound closure when breast and lung cancer cell treated with cur-PLGA-NP and equivalent dose of free curcumin (3.68 µg/ml, 7.36 µg/ml and 11.05 µg/ml). Treatment with free curcumin resulted in a mild decrease in closure for all concentrations in both cell lines however, cur-PLGA-NP extensively enhanced reduction in the degree of wound closure compared to the free curcumin after 72 hours of using the same concentrations curcumin (Figure 10A and B). These results demonstrated that cur-PLGA-NP have the superior anti-migration capability as compared to free curcumin.

2.11 Colony formation assay

The colony formation assay was performed as the procedure mentioned in the section 2.15. Colony formation assay has been used to study the long-term anticancer activity of curcumin . The number of colonies formed after 7 days was quantified for MDA-MB-231 (Figure 11A) and A549 (Figure 11B) cells treated with blank PLGA-NP as control, along with three different concentrations of free curcumin and cur-PLGA-NP curcumin (3.68 µg/ml, 7.36 µg/ml and 11.05 µg/ml). Treatment with cur-PLGA-NP resulted in significantly lower numbers of colonies compared to free curcumin as shown Figure 11A and B.

2.12 Invasion assay

The protocol for invasion assay was given in the 2.16. Invasion assay was conducted to investigate the effect of free curcumin and cur-PLGA-NP on the invasion capability of MDA-MB-231 (Figure 12A) and A549 (Figure 12B) cells. Dissemination of tumour cells from the primary site to distant locations starts with cell detachment followed by the local invasion of the normal tissues adjacent to a tumour which then can infiltration through the lymphatic drainage (Palmer et al., 2011). Treatment with cur-PLGA-NP (3.68 µg/ml, 7.36 µg/ml and 11.05 µg/ml) resulted in a significant decrease in cell invasion compared to free curcumin for all concentrations in both cell lines as shown in Figure 12. These results suggest that Cur-PLGA-NP can significantly inhibit the invasion capability of invasive lung and breast cancer cells when compared to free curcumin. This enhanced anti-invasive effect imparted to curcumin by nano-encapsulation is critical to inhibit metastasis of highly invasive breast and lung cancer cells.

2.13 Assessment of p65 and HIF-1α levels

The protocol followed was described in section 2.18. Having assessed the physical parameters, aqueous solubility, intracellular uptake and anticancer potential of cur-PLGA-NP versus free curcumin, we need to investigate the molecular mechanism for the improved anticancer potential of curcumin when formulated as PLGA nanoparticles. Recent research indicates that metastatic human cancer tumours are hypoxic and these cells could have elevated levels HIF-1α and NF-kβ/p65 (Rel A) which may result tumour development and progression of cancer (Zhang et al., 2015., Liu et al., 2015., Chaturvedi et al., 2014., Patel and Simon, 2008., Shukla et al., 2004). Hence, to investigate if curcumin treatment has an effect on these transcription factors we used whole cell lysates from metastatic breast (MDA-MB231) and lung (A549) cancer cells treated blank NP, cur-PLGA-NP and free curcumin under hypoxic condition (10% O2) to quantify the levels of HIF-1α and p65 (Rel A) using ELISA assay. The results from the ELISA assay indicated that free curcumin had no significant effect on the levels of HIF-1α and p65 (Rel A) as compared to blank NP however, there was a significant reduction in the levels of HIF-1α (Figure 13: panel A) and p65 (Rel A) (Figure 13: panel B) in both breast and lung cancer cells treated with cur-PLGA-NP (Figure 13; ($P<0.001 – 0.01$). This result indicates that curcumin can suppress the cellular levels of HIF-1α and p65 (Rel A) only when delivered as nanoparticles.

2.1 Calibration curve

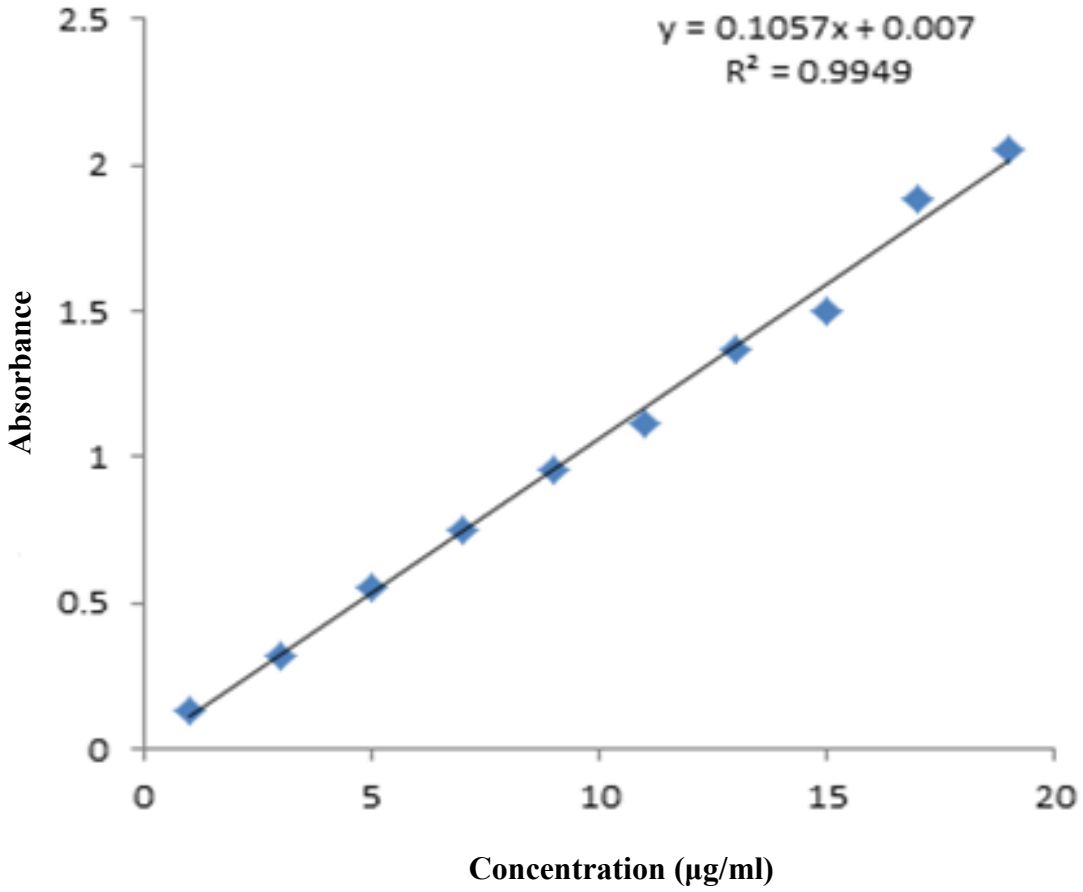

Figure 1: Calibration curve of curcumin

2.2 Effect of PLGA concentration

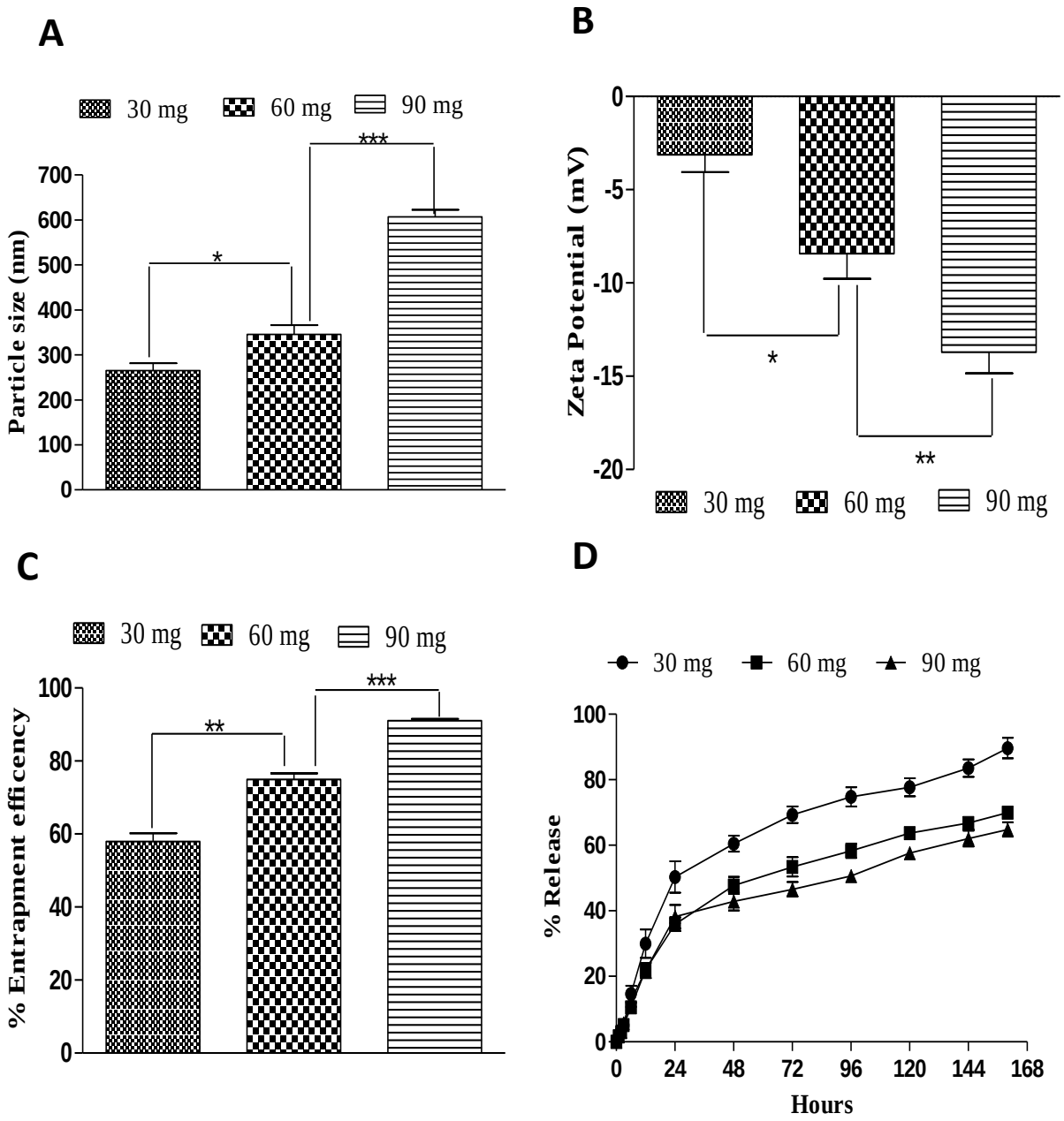

Figure 2: Effect of polymer amount on particle size (A), zeta potential (B), entrapment efficiency (C) and in vitro release (D). The particle size of nanoparticles increases significantly as the polymer amount increases from 30 mg to 90 mg (A). Zeta potential decreases significantly upon increasing the polymer amount from 30 mg to 90 mg (B). Entrapment efficiency increases with increase in PLGA amount (C). The release profile depicts initial burst release after 24 hours. Nanoparticles formulated using 60 mg PLGA shows the highest percentage release of curcumin (D). Values are mean ± SEM (n = 3). *P<0.05, **P<0.01 and ***P<0.001 compared with 30 mg PLGA.

2.3 Effect of surfactant concentration

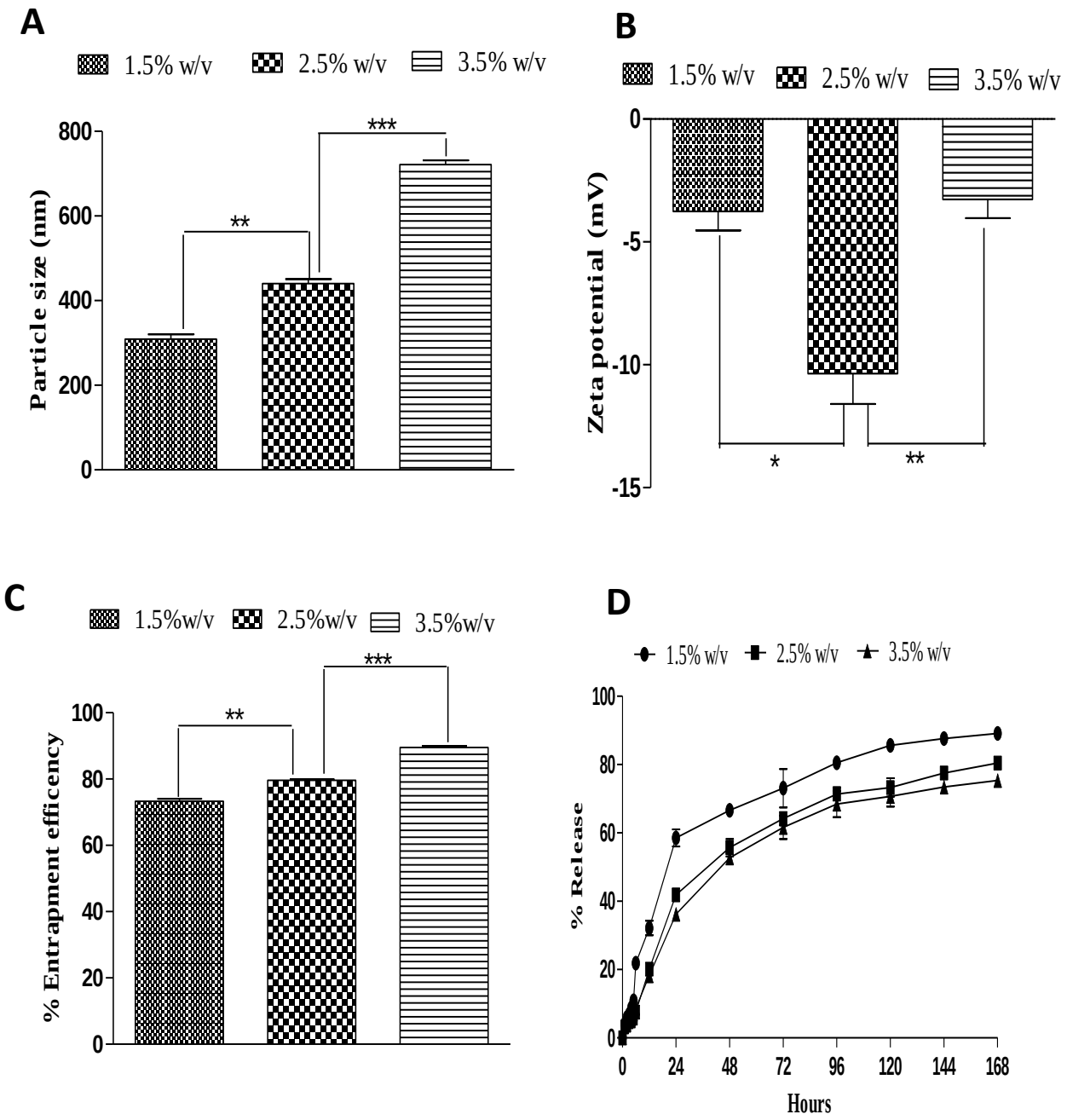

Figure 3: Effect of PVA concentration on particle size (A), zeta potential (B), entrapment efficiency (C) and in vitro release (D). The particle size of nanoparticles significantly increases as the PVA concentration increases from 1.5% to 3% (A). Zeta potential decreases significantly upon increasing the PVA concentration but it increases on further increase in PVA concentration. Entrapment efficiency shows significant increase with an increase in PVA concentration (C). The release profile depicts initial burst release after 24 hours. Nanoparticles formulated with1.5% PVA shows the highest percentage release of curcumin (D). Values are mean ± SEM (n = 3). *P<0.05, **P<0.01 and ***P<0.001 compared with 30 mg PLGA

2.4 Effect of drug concentration

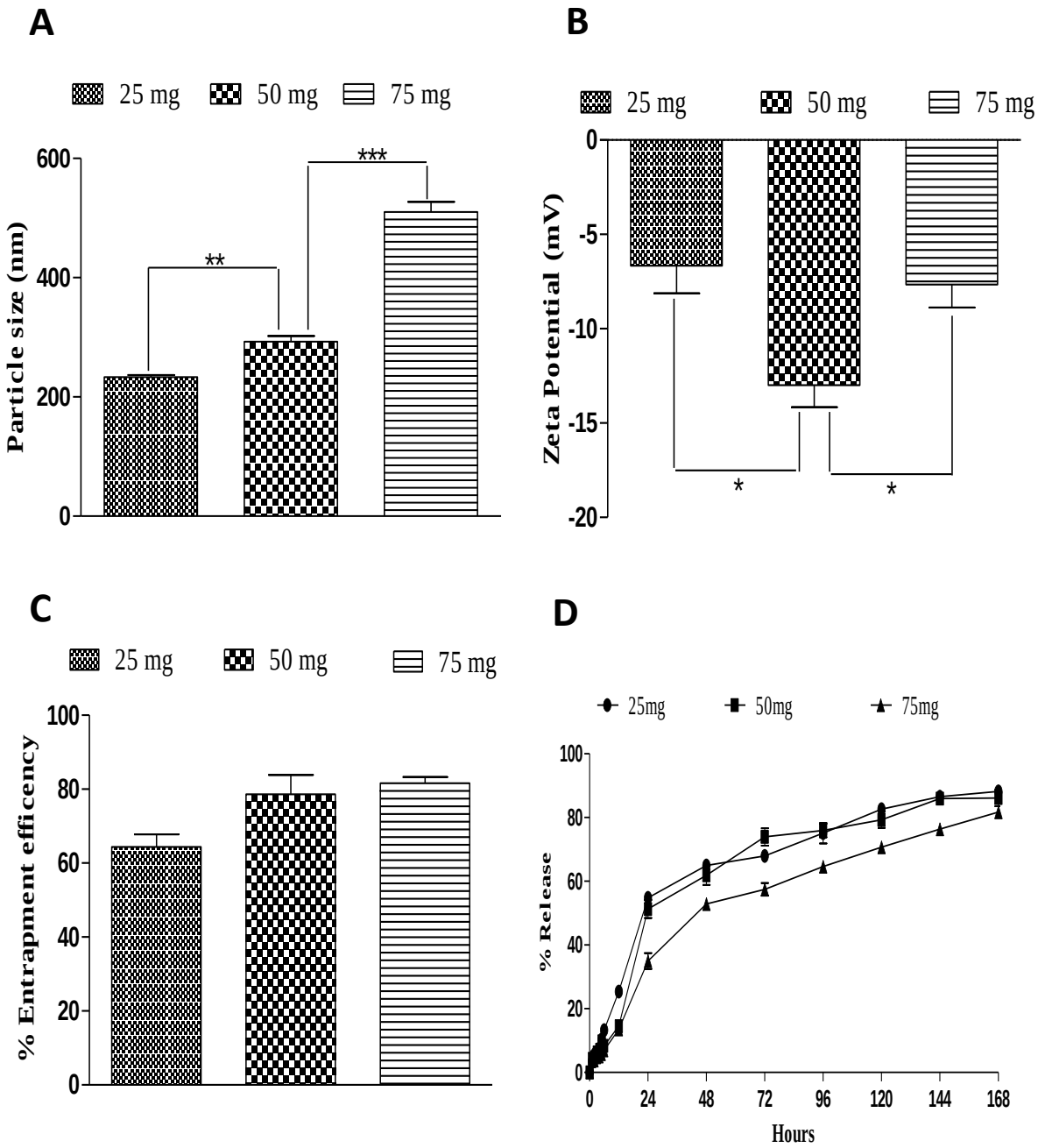

Figure 4: Effect of drug amount on particle size (A), zeta potential (B), entrapment efficiency (C) and in vitro release (D). Increase in drug amount significantly increases the particle size of nanoparticles from 25 mg to 75 mg (A). Zeta potential does not have any significant effect as the amount of curcumin increases (B). Entrapment efficiency shows a significant increase with an increase in drug amount (C). The release profile depicts initial burst release after 24 hours. Nanoparticles formulated with125 mg of curcumin shows the highest percentage release of curcumin (D). Values are mean ± SEM (n = 3). *$p < 0.05$, **$P<0.01$ and ***$P<0.001$ compared with 30 mg PLGA.

2.5 NMR spectra of cur-PLGA-NP

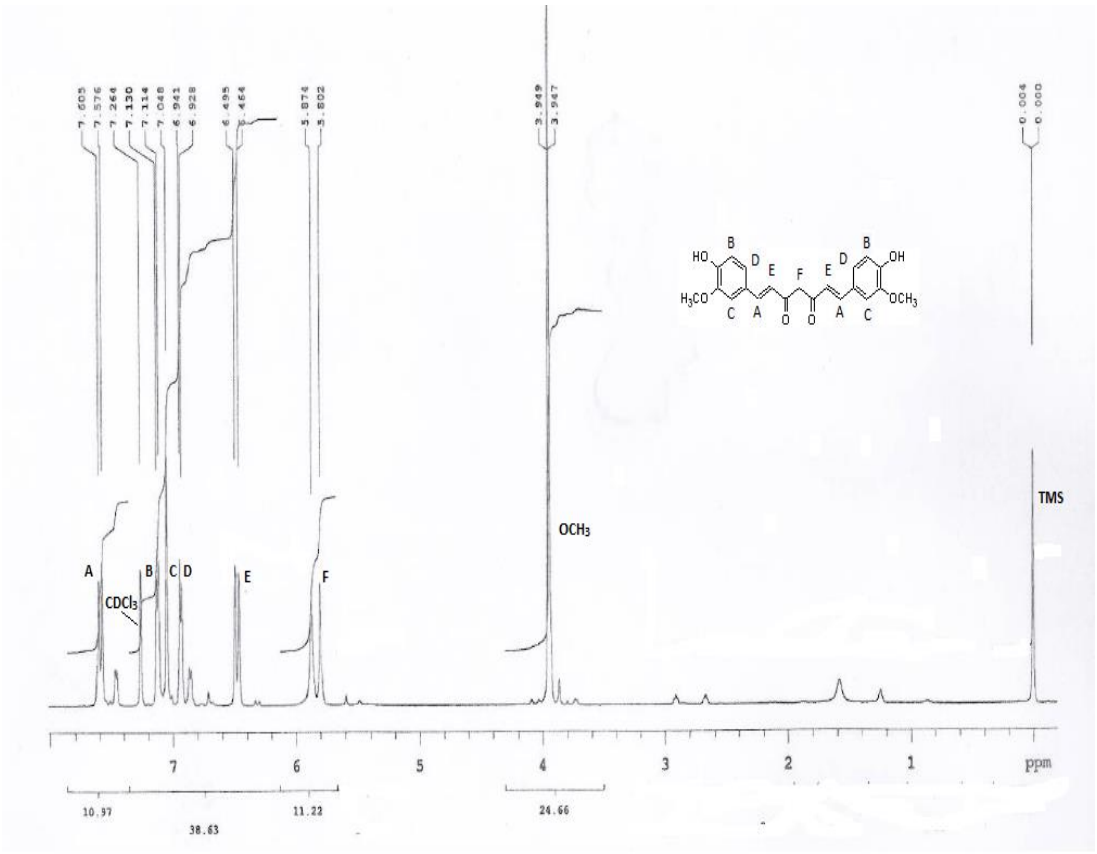

Figure 5: H NMR of curcumin in PLGA nanoparticles. The above H NMR confirms the curcumin stucture in the nanoparticle form.

2.6 Solubility of cur-PLGA-NP and free curcumin

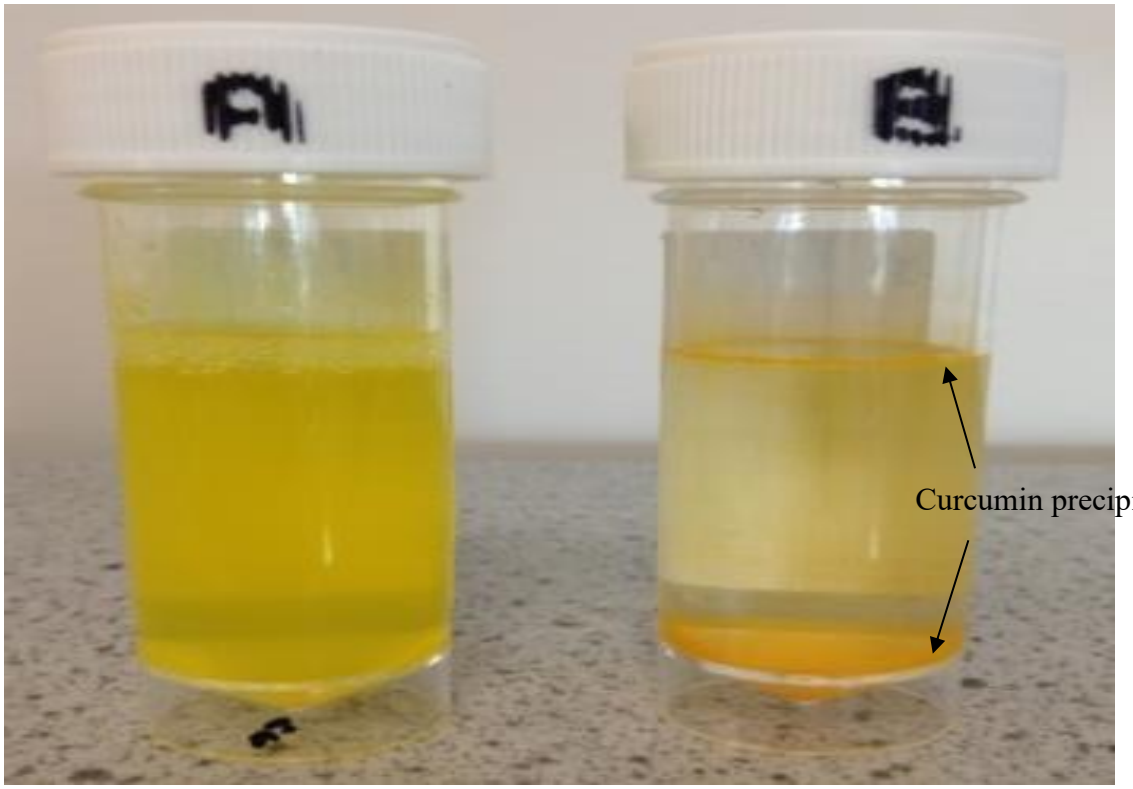

Figure 6: Water solubility of cur-PLGA-NP (A) and free curcumin (B). The vials in figures shows the solubility of cur-PLGA-NP (A) and free curcumin (B) respectively. The free curcumin precipitates and settles down whereas cur-PLGA-NP shows uniform dispersion throughout the vial.

2.7 Scanning Electron Microscopy

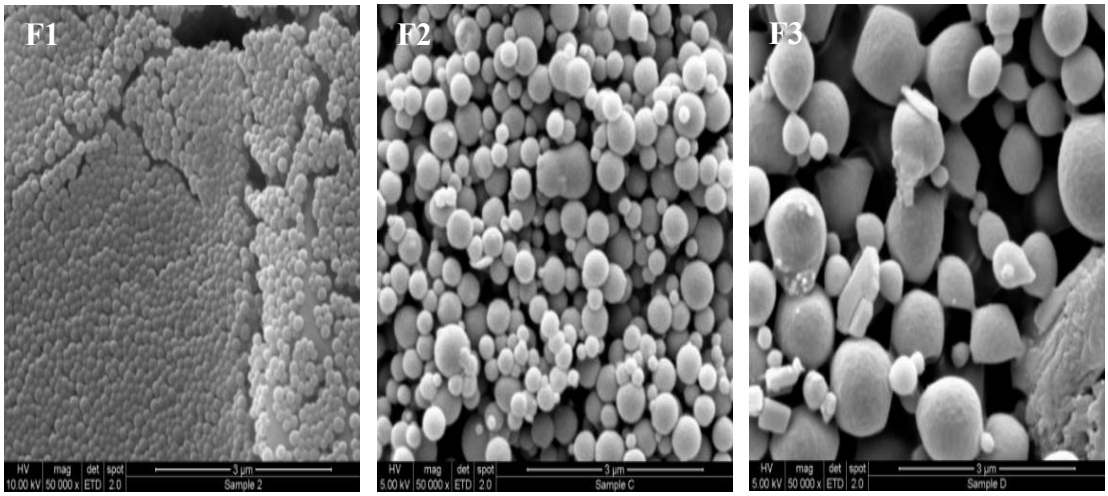

Figure 7: Scanning Electron Microscopy of cur-PLGA-NP F1, F2, and F3 containing 30 mg, 60 mg and 90 mg of PLGA polymer respectively. Scanning electron microscopic images of F1, F2 and F3 batches containing 30 mg, 60 mg and 90 mg of PLGA demonstrate an increase in particle size. F1 has smaller and uniform particle size as compared to F2 and F3. SEM images confirm that increase in polymer amount leads to increase in particle size and distortion of particle shape.

2.8 Cellular uptake of cur-PLGA-NP

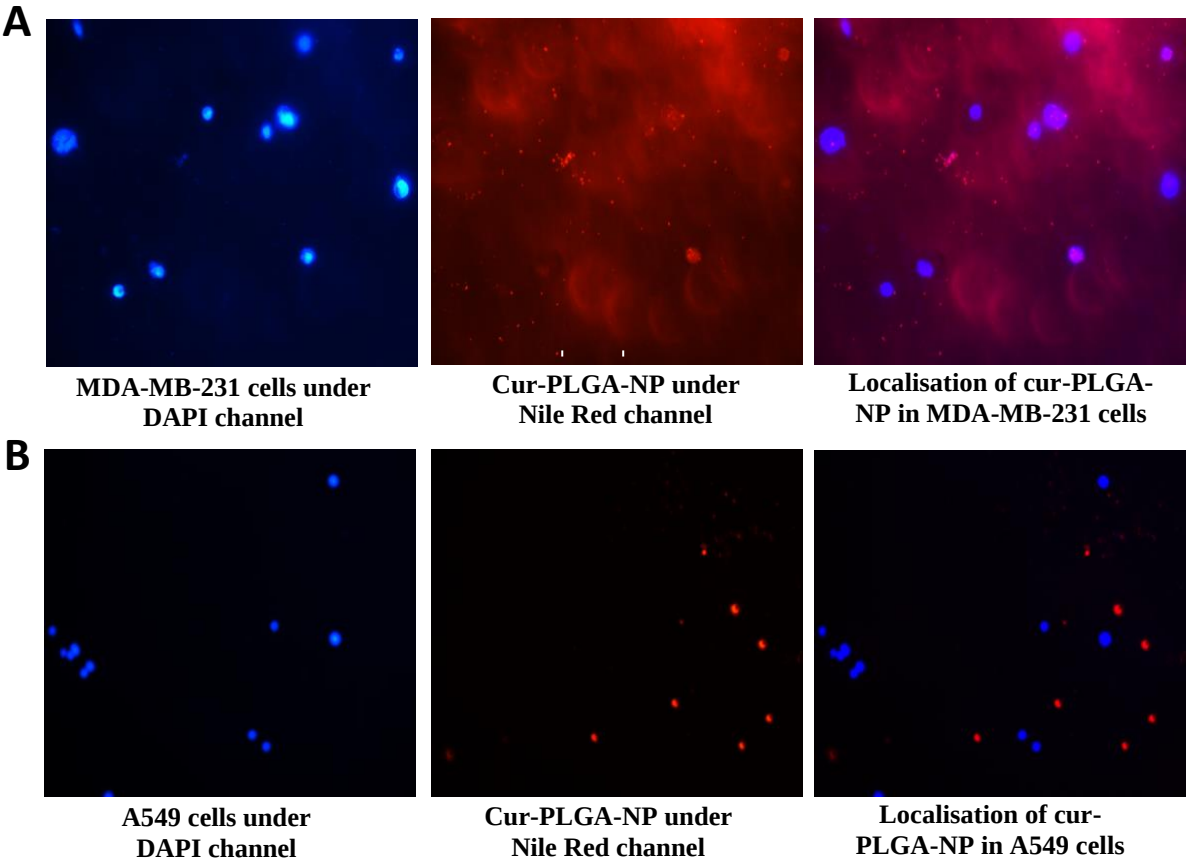

Figure 8: Cellular uptake of cur-PLGA-NP in MDA-MB231 and A549 at 20X. Cellular localization of Nile red-coated cur-PLGA-NP was observed in MDA-MB231 (A) and A549 (B) and visualized by overlapping under fluorescent microscopy. Figure A shows that nanoparticles are present in the cytoplasm and nucleus of the MDA-MB231 cells. Curcumin nanoparticles were observed only in the cytoplasm of A549 cells (B).

2.9 In-vitro cytotoxicity assay

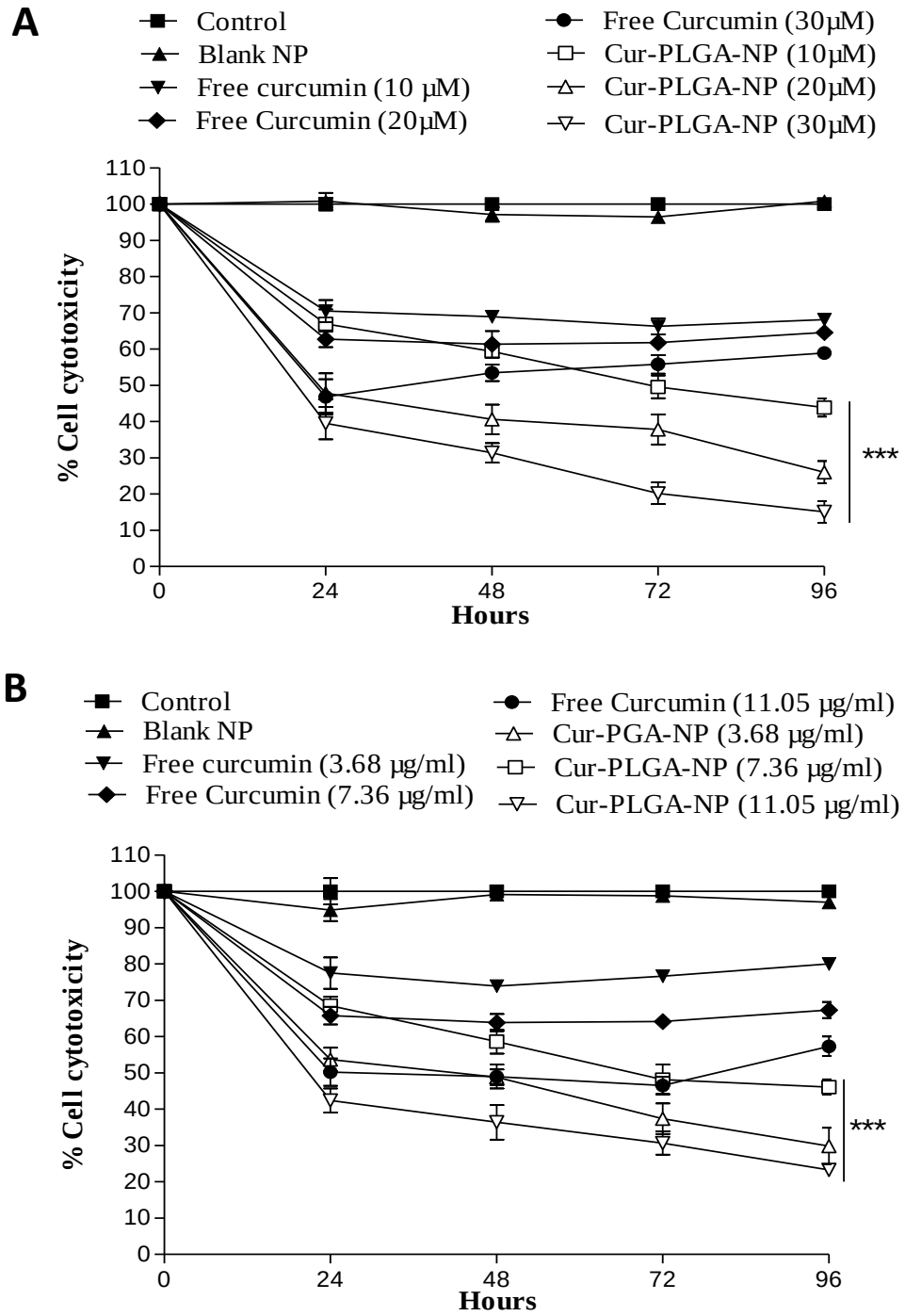

Figure 9: Effect of cur-PLGA-NP and free curcumin on cytotoxicity of MDA-MB-231 and A549 cell lines. Dose dependent response was observed in cytotoxicity assay on MDA-MB-231 (A) and A549 (B) cell lines. However, of cur-PLGA-N demonstrate higher toxicity than free curcumin in both cell lines. Values are mean ± SEM (n = 3). ***P<0.001 compared with same amount of free drug.

2.10 Migration assay

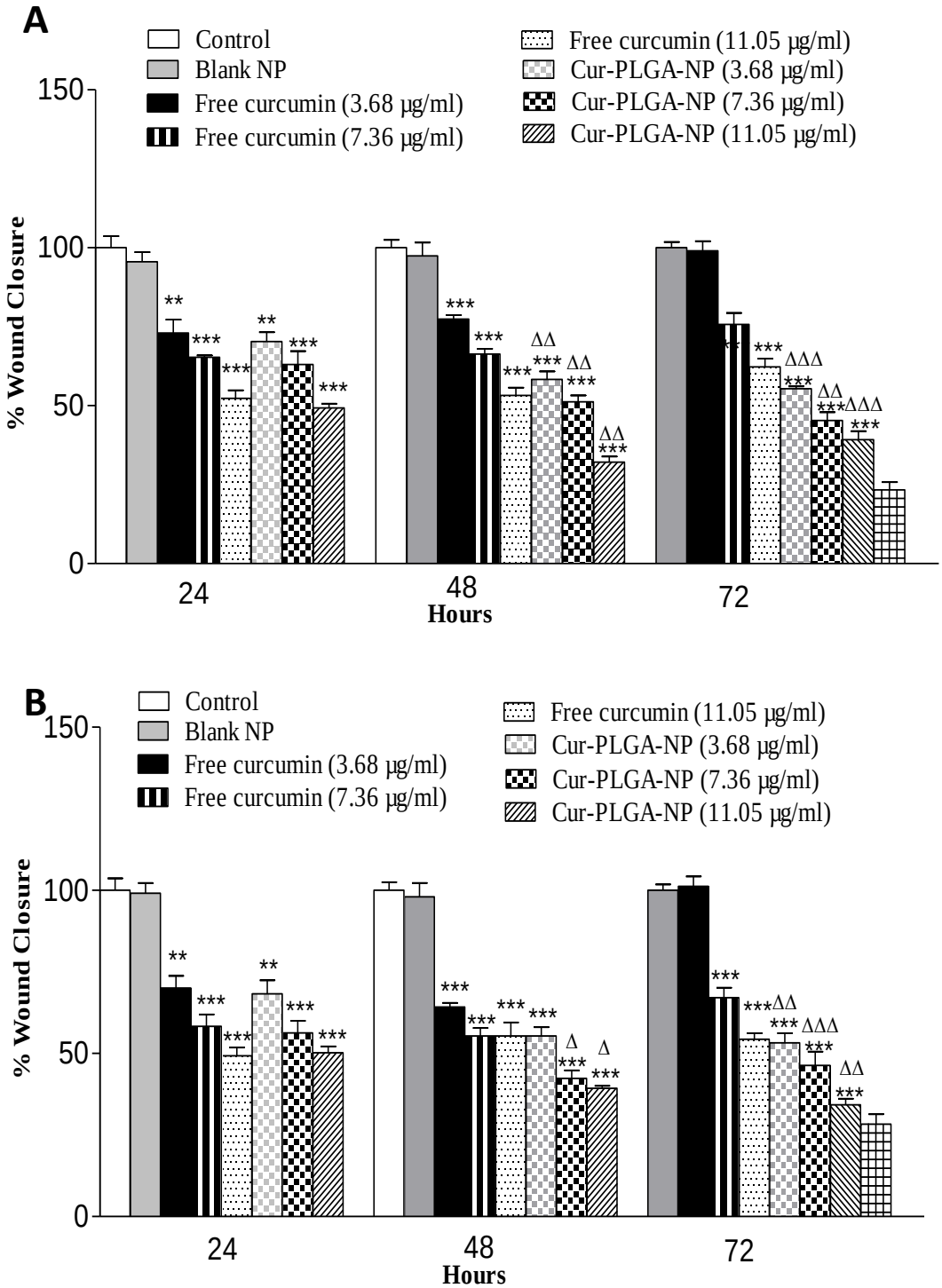

Figure 10: Effect of cur-PLGA-NP and free curcumin on migration of MDA-MB231 and A549 cell lines. The effect of cur-PLGA-NP and free curcumin on migration capacity of MDA-MB231 (A) and A549 (B) cell lines were evaluated. Cur-PLGA-NP shows a significant reduction in migration capability of both cell lines as compared to free curcumin. Values are mean ± SEM with n=3. *P<0.05, **P<0.01, ***P<0.001 compared with control (blank NP). $^{\Delta}$P<0.05, $^{\Delta\Delta}$ P<0.01, $^{\Delta\Delta\Delta}$P<0.001 compared with the same dose of free curcumin.

2.11 Colony formation assay

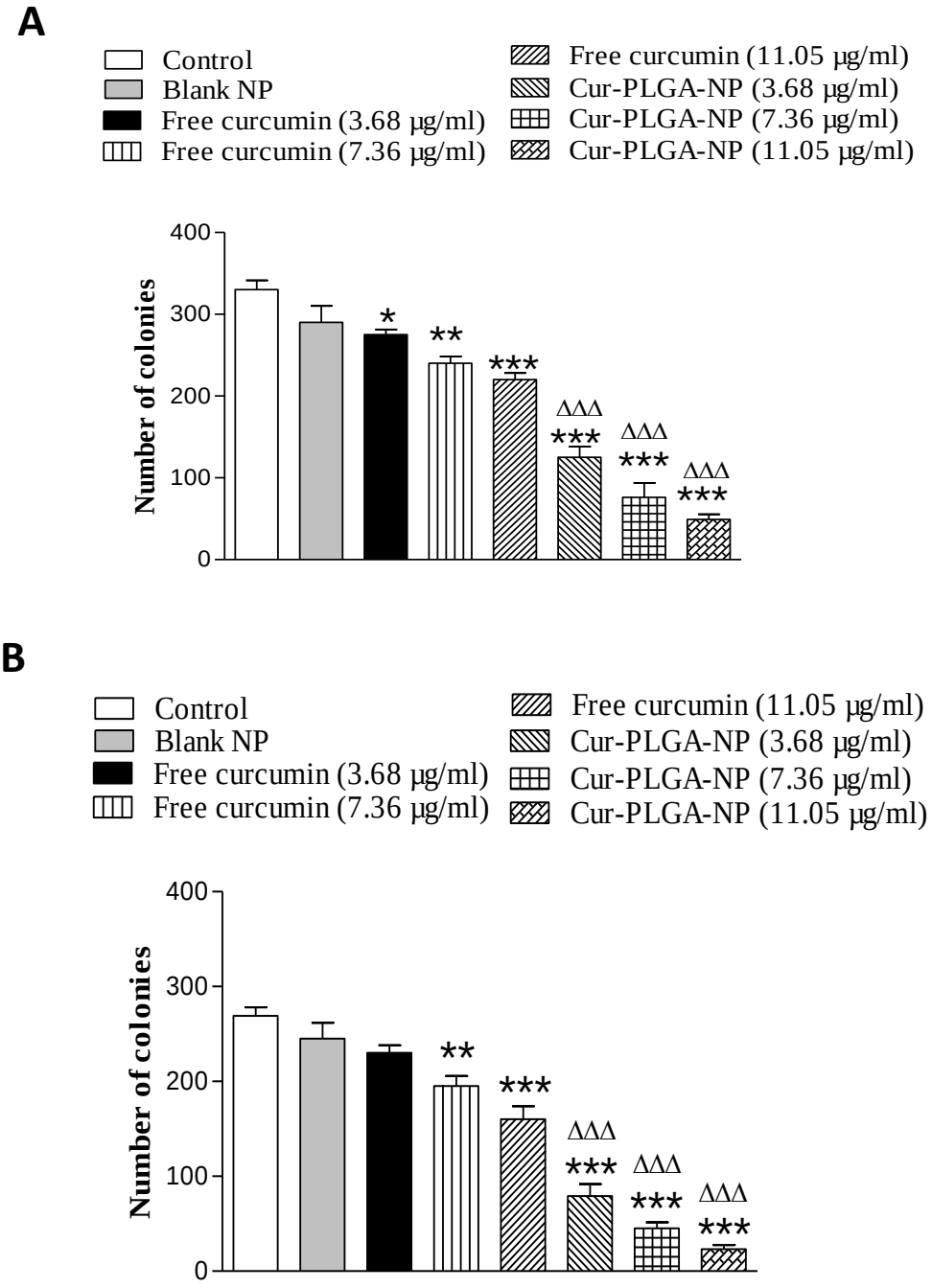

Figure 11: Effect of cur-PLGA-NP and free curcumin on colony formation ability of MDA-MB231 and A549 cell lines. Cur-PLGA-NP significantly reduces the colony formation ability of both MDA-MB231 (A) and A549 (B) cell lines. Cur-PLGA-NP shows a significant reduction in colony formation capability of both cell lines as compared to free curcumin. Values are mean ± SEM with n=3. *P<0.05, **P<0.01, ***P<0.001 compared with control (blank NP). $^{\Delta}$P<0.05, $^{\Delta\Delta}$P<0.01, $^{\Delta\Delta\Delta}$P<0.001 compared with the same dose of free curcumin.

2.12 Invasion assay

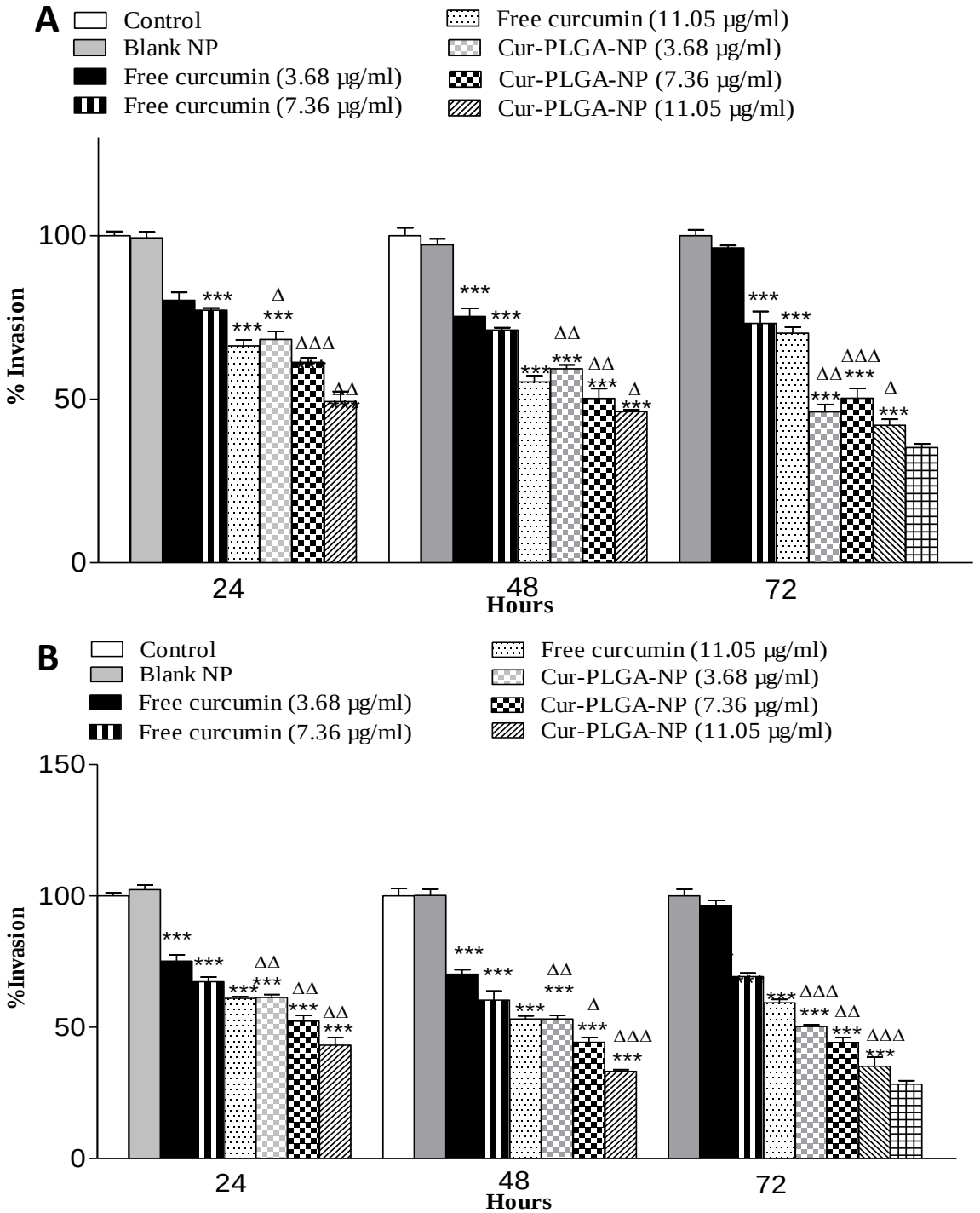

Figure 12: Effect of cur-PLGA-NP and free curcumin on invasion of MDA-MB231 and A549 cell lines. The effect of cur-PLGA-NP and free curcumin on invasion capability of MDA-MB231 (A) and A549 (B) cell lines was observed. Cur-PLGA-NP shows a significant reduction in invasion capability of both cell lines as compared to free curcumin. Values are mean ± SEM with n=3. *P<0.05, **P<0.01, ***P<0.001 compared with control (blank NP). $^{\Delta}$P<0.05, $^{\Delta\Delta}$P<0.01, $^{\Delta\Delta\Delta}$P<0.001 compared with the same dose of free curcumin.

2.13 Assessment of p65 and HIF-1α levels

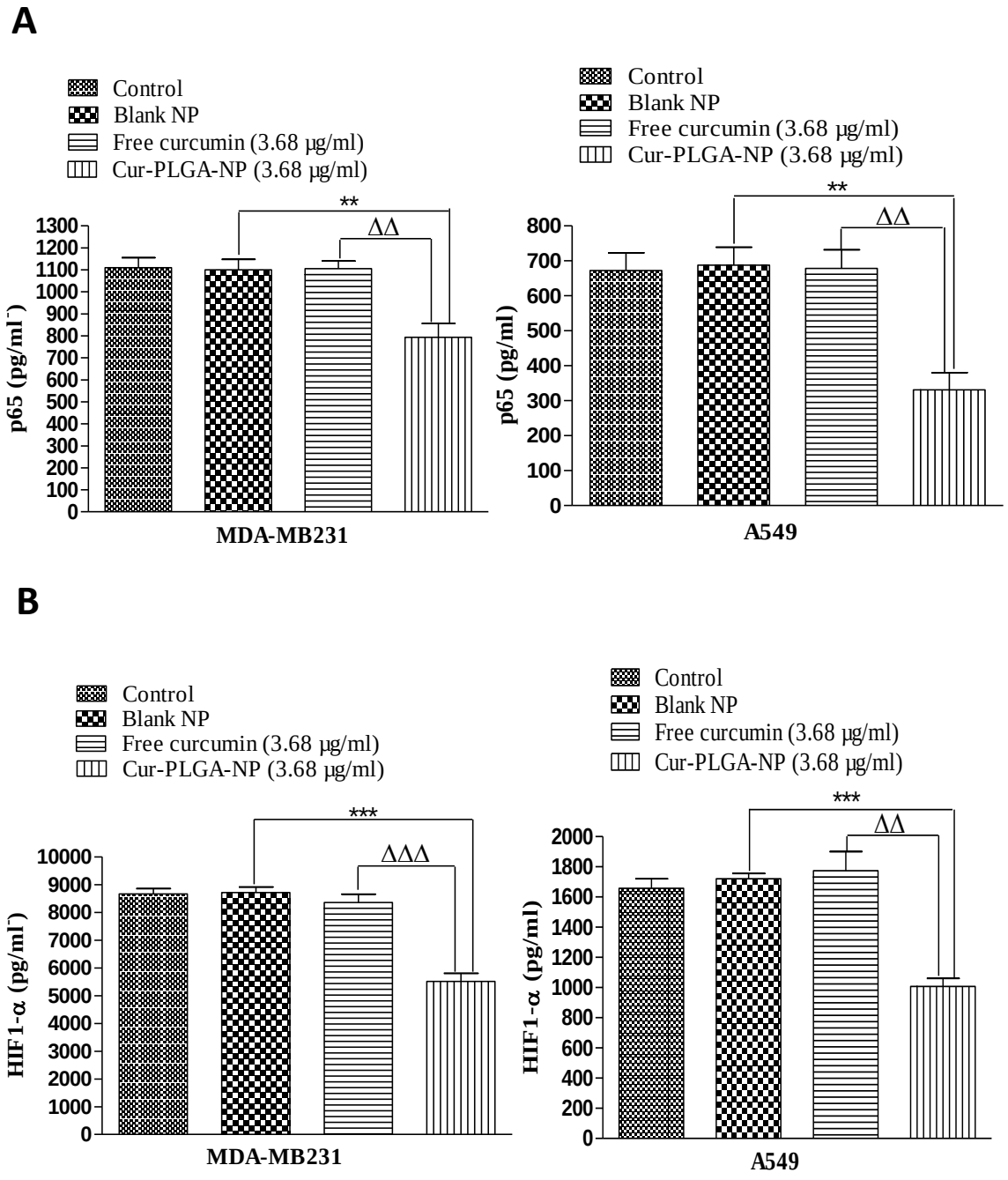

Figure 13: Effect of cur-PLGA-NP and free curcumin on expression of cellular levels of p65 (Rel A) and HIF-1α. Cur-PLGA-NP significantly reduces the levels of p65 (A) and HIF-1α (B) in both MDA-MB231 and A549 cell lines. Values are mean ± SEM with n=4. **P<0.01, ***P<0.001 compared with blank NP. $^{\Delta\Delta}$P<0.01, $^{\Delta\Delta\Delta}$P<0.001 compared with the same dose of free curcumin treatment for 24 hours.

3.1 Discussion

Curcumin has received considerable attention as a potent anticancer (Bollu et al., 2016) and an anti-inflammatory agent. However, it is not currently used as a clinical medicine for treating inflammation or cancer. Our work has demonstrated the effect of increase amount of PLGA on particle size, zeta potential, entrapment efficiency and *in-vitro* release. These findings are in agreement with previously published data (Pandit et al., 2015). Figure 2 shows that increase in PLGA amount increases the particle size, zeta potential and entrapment efficiency significantly. However, percentage release decrease with increase in PLGA amount. This may be due to increase in the viscosity of polymer solution Similarly, increase in PVA concentration also leads to increase in particle size, entrapment efficiency and *in-vitro* release significantly as shown in Figure 3. However, increase in PVA concentration does not have any significant effect zeta potential. Furthermore, increase in drug amount cause increase in particles size, entrapment efficiency and *in-vitro* release but it does not produce any significant result on zeta potential as visible in Figure 4. NMR spectroscopy confirms the purity of curcumin in nanoparticles forms as depicted in Figure 5.

We also observed a ten-fold increase in curcumin solubility when formulated as PLGA nanoparticles (Figure 6) this increased solubility can increase the bioavailability of curcumin and intra-cellular delivery (Tiwari et al., 2014).

SEM images from the batches F1, F2 and F3 as shown in Figure 7 demonstrate that increase in PLGA amount not only leads to increase in particle size but also distorts the spherical structure of the nanoparticles.

Current work indicates that curcumin uptake by cancer cells is achieved when it is formulated as PLGA nanoparticles (Figure 8), and cytotoxicity study demonstrate that curcumin nanoparticles have higher anti-proliferation action than free curcumin as noticed in Figure 9. This evidence of cellular uptake and cytotoxic study of curcumin nanoparticles forms the basis of our further findings indicating reduce migration (Figure 10), colony formation (Figure 11) and decrease invasion power (Figure 12) of the breast and lung cancer cells. Similar findings related to the anticancer potential of curcumin and curcumin nanoparticles have been reported by several researchers (Yallapu et al., 2014., Anitha et al., 2014., Chang et al., 2013., Verderio et al., 2013).

However, there is no study till date reporting the action of curcumin and/or curcumin nanoparticles on elevated levels HIF-1α and p65 (Rel A) in breast and lung cancer cells under a tumour hypoxic condition. Thus the most important findings of current work indicate that nano-encapsulation of curcumin is capable of downregulating the expression of HIF-1α and p65 (Rel A) levels in breast and lung cancer cells when exposed to hypoxia (10% O2) (Figure 13). This finding suggests that the increased therapeutic value of the natural anticancer agent curcumin could be via suppression of over activated HIF and NF-kβ pathways, which are predominately responsible for adaptation of hypoxic tumours resulting in the development and spread of cancer in our body.

Hence, the findings from this work conclude that nanotechnology based drug delivery system could be an effective tool to enhance the anticancer activity of several natural and/or novel anticancer compounds, which are currently not in clinical use due to their low solubility and/or poor bioavailability. Future work will

involve functionalizing these PLGA-NP using salic acid to selectively target cancer tumour cells in in vivo models of lung and breast cancer.

3.2 Conclusion

The data from this chapter demonstrate that PLGA nanoparticles loaded with curcumin can be successfully fabricated by a solvent evaporation method. For *in-vitro* characterization, such as cell viability and cellular uptake were carried out after optimization process. The cell toxicity experiment demonstrates a dose dependent relationship with cell viability in A549 and MDA-MB-231. This implies that Cur-loaded PLGA NP is more efficacious that free curcumin towards cancer cell toxicity. PLGA nanoparticles loaded with curcumin show higher efficiency in controlling tumour growth than free curcumin which can be illustrated by migration, colony formation and invasion assays. The reduced level of p65 and HIF-1α has been depicted in A549and MDA-MB-231 after transfection with curcumin nanoparticles. Therefore, polymeric delivery of curcumin nanoparticles may provide therapeutic cure to lung and breast cancer based on the above data.